Final report

Prepared for: Van Oord, WL| Delft Hydraulics, Delft University of Technology

Morphological analysis and optimization of Dubai nourishments

M.D. van Dijk
MSc Thesis

July 15, 2005

TU Delft Van Oord WL | delft hydraulics

Prepared for: Van Oord, WL| Delft Hydraulics, Delft University of Technology

Morphological analysis and optimization of Dubai nourishments

Graduation committee:

Prof. Dr. Ir. M.J.F. Stive	DUT
Dr. Ir. J. van de Graaff	DUT
Drs. P. Dankers	DUT
Ir. H. de Vroeg	WL | Delft Hydraulics
Dr. Ir. A. Hibma	Van Oord
Ir. G.B.H. Spaan	Van Oord

M.D. van Dijk
MSc Thesis

July 15, 2005

TU Delft Van Oord WL | delft hydraulics

Preface

This report is the result of my master thesis project of the study Civil Engineering at the Delft University of Technology. The research was carried out at WL | Delft Hydraulics in Delft in cooperation with Van Oord between September 2004 and July 2005.

This research was performed within the scope of studies by WL | Delft Hydraulics and Van Oord. While this Dutch marine contractor is constructing large land reclamations in Dubai it also carries out nourishments on the existing beaches. Furthermore, since these were emergency solutions, future nourishment will be necessary. More insight is required in the morphologic behaviour of these beaches. The question is raised whether the possibility exists of optimization of nourishment.

I would like to thank Van Oord and WL | Delft Hydraulics for making this research possible. Ir. H. de Vroeg for the fact that his door was always open for valuable advice. A. Hibma and G. Spaan for their support and enthusiasm: Furthermore everybody of MCI and especially B. Hofland for my nice room and nice environment: And my fellow students at WL for the entertaining lunches and coffee breaks. Finally, I want to thank Prof. Dr. Ir. M.J.F. Stive, Dr. Ir. J. van de Graaff and Drs. P. Dankers for their advice.

With this thesis I hope to complete my studies in Delft. Therefore I would like to take this opportunity to also thank my family and friends in Delft, The Hague and the rest of the world for the great time and their support.

Merijn van Dijk,

Delft, 15 July 2005

Contents

List of Figures

List of Tables

List of Tables

List of Symbols

List of Symbols	Unit	description
Latin symbols		
A	$\mathbf{m^{1/3}}$	1. shape parameter
	$\mathbf{m^2}$	2. roller area
B'	**[-]**	dimensionless berm height = B/h_*
B	**m**	1. berm height
	[-]	2. coefficient used in the BIJKER transport formula in UNIBEST-CL+ for the criterion deep water and shallow water
C	**m/s**	1. wave celerity
	$\mathbf{m^{1/2}/s}$	2. Chézy friction coefficient
C_D	**[-]**	drag coefficient
C_g	**m/s**	group velocity of waves
C_r	**[-]**	correlation coefficient bound long waves
c_1,c_2	**[-]**	coefficients for the determination of the $Q_s(\theta)$ function in UNIBEST-LT
D_x	**m**	sand particle diameter of which x% has a smaller diameter
D_b	$\mathbf{W/m^2}$	dissipation of wave energy due to wave breaking
D_f	$\mathbf{W/m^2}$	dissipation of wave energy due to bottom friction
D_w	$\mathbf{W/m^2}$	dissipation of organised wave energy
DISS	$\mathbf{W/m^2}$	dissipation of roller energy
E	$\mathbf{J/m^2}$	wave energy per unit surface area
E_r	$\mathbf{J/m^2}$	roller energy
F	**W/m**	mean energy transfer in wave direction
f_w	**[-]**	coefficient for bottom friction
g	$\mathbf{m/s^2}$	acceleration of gravity
H_D	**m**	diffracted wave height
H_e	**m**	significant wave height exceeded 12 hr/ yr
H_i	**m**	incident wave height
H_m	**m**	depth limited wave height
H_{RMS}	**m**	root-mean-square wave height
H_s	**m**	significant wave height
h	**m**	water depth
h_o	**m**	still water depth
h_c	**m**	closure depth
h_p	**m**	active profile height (berm and closure depth)
I_1,I_2	**[-]**	Einstein integrals used in Bijker transport formula
K_D	**[-]**	diffraction coefficient (H_D/H_i)
k	$\mathbf{m^{-1}}$	wave number $=2\pi/L$
k_b	**m**	bottom roughness in Chézy friction coefficient (KB)
k_s	**m**	roughness height (RKVAL)

List of Symbols	Unit	description
L	**m**	1. wavelength
		2. length of the roller
M_φ	**[-]**	mean grain diameter in phi units
n	**[-]**	ratio of group velocity to wave velocity = C_g/C
p	**[-]**	coefficient for porosity of sediment
Q_s	**m^3/s**	total sediment transport
Q_b	**[-]**	local fraction of breaking waves
q_b	**$m^3/m/s$**	sediment source or sink
Re	**[-]**	Reynolds number
R_i	**N/m^2**	pressure gradient forcing, assumed to be depth independent
S	**$m^3/m/s$**	total sediment transport, including pores
S_b	**$m^3/m/s$**	bottom sediment transport
S_s	**$m^3/m/s$**	suspended sediment transport
S_{xx}	**N/m**	radiation stress component in cross-shore direction
S_{xy}	**N/m**	longshore radiation stress component
s_0	**[-]**	deep water wave steepness
s_1	**[$m^3/m/s$]**	variation of transport as function of the coastline rotation
tan (φ)	**[-]**	angle of natural repose
T	**s**	wave period
T_e	**s**	peak period exceeded 12 hr/ yr
T_p	**s**	peak period
T_z	**s**	zero crossing period
T*	**[-]**	relative wave period (TDRY)
t	**s**	time
U_{RMS}	**m/s**	amplitude of the wave orbital velocity
V'	**[-]**	dimensionless fill volume =V/(BW*)
V	**m/s**	alongshore velocity
w_s	**m/s**	sediment fall speed (WS)
W_*	**m**	width of the breaker zone corresponding with the closure depth and shape parameter
x	**m**	1. coordinate parallel to shore or baseline
y	**m**	1. Coordinate perpendicular to the shore positive in offshore direction.
		2. Coastline position
y'_0	**[-]**	dimensionless dry-beach width = y_o/W_*
Greek symbols		
α_c	**[-]**	coefficient of wave breaking (ALFA)
β	**[-]**	slope of the wave front (BETD)
γ	**[-]**	breaking index (GAMMA)
Δ	**[-]**	relative density = $(\rho_s-\rho)/\rho$

List of Symbols	Unit	description
δ	**[m]**	thickness of the wave boundary layer
η	**m**	wave set-up
θ	**0**	1. coastline orientation with respect to the x-axis
	0	2. angle between the point of interest and the diffraction point and the incident wave angle
θ_e	**0**	equilibrium angle for which $Q_s(\theta)$ is zero
θ_n	**0**	resultant of $\theta - \theta_w$
θ_r	**0**	resultant of $\theta - \theta_e$
θ_w	**0**	wave angle with respect to the coastal normal
μ	**[-]**	ripple factor = $(C/C_{90})^{3.2}$
ν	**m^2/s**	viscosity
ξ	**-**	Bijker parameter
ρ_s	**kg/m^3**	sand density
ρ_w	**kg/m^3**	water density
σ_x	**Depends**	Standard deviation of a parameter x
τ	**N/m^2**	shear stress
τ_{cw}	**N/m^2**	bed shear stress due to waves and currents
φ_x	**[-]**	x^{th} percentile in phi units. Larger values of phi denote finer material, $\varphi=^{-2}\log(D)$
ω	**s^{-1}**	peak wave frequency
ω_r	**s^{-1}**	relative wave peak frequency

Summary

Background

Dubai's coastline is continuously under influence of human implemented changes. While constructing large projects as the World and the Palm Islands, but also prior to their construction, erosion problems occurred on the existing coastline between Palm Island Jumeirah and Port Rashid. To mitigate erosion along the Dubai coastline, at several locations nourishment have been carried out in the recent past. By the end of 2003, Van Oord carried out nourishments on six locations *(Figure 1.D)*. For these locations survey data is available including the sand characteristics.

Since these were emergency solutions, future nourishment will be necessary. In September 2004, WL| Delft Hydraulics in cooperation with Van Oord indicated their interested in more detailed research. More insight is required in the morphologic behaviour of the beaches and especially the nourished areas. The question is raised whether the possibility exists of optimization of the nourishments at these locations.

Objectives and approach

The main objective of this thesis is to gain insight into the morphological behaviour of the nourished areas along the Jumeirah beaches and optimize possible future nourishments. An additional objective was to obtain insight in the performance of UNIBEST-CL+ for the prediction of such nourishments.

In order to reach this objective the morphologic behaviour of the coast and nourished areas of the Jumeirah beaches were analysed and a suitable study location was selected. For this location the hydrodynamic conditions and sand characteristics as well as a detailed analysis of the survey data was carried out. Based on this information a morphodynamic model in UNIBEST-CL+ was created, calibrated and verified. With this model optimization and suggestions for future nourishments were made. Finally, cross-shore modelling was carried out to gain insight into cross-shore processes.

Analysis of morphologic behaviour of the coast and nourished areas

It was seen that the coastline of Dubai consists of a large number of coastal protection works and marinas. Separated by the breakwaters of Port Rashid and Palm Jumeirah. These have a large impact on the behaviour of the beaches and cause that each beach can be seen as separate cell. At the beaches north of the Chicago beach area a northward directed transport takes place (Italian, Glass Palace, Jumeirah 1 and 2) causing accretion on the north side and severe erosion on the south side of the different cells. Nourishments were required at these locations. South of the Chicago beach area (Madinat Jumeirah), transport was in the southern direction, due to the influence of Palm Jumeirah.

Based on the available data, indications of sediment transport and suitability of modelling Italian beach was selected as study location (Table 3.2).

Detailed analysis of the survey data of Italian beach

Analysis of the survey data of Italian beach showed that after the nourishments erosion immediately started, a reaction of the nourished area to several storm events. After this erosion was slower. Overall an erosive trend was seen and the volume of eroded sand was about 30,000 to 40,000 m^3 in the period from January to August 2004 (Figure 5.2).

The shoreline retreat in time was mainly due to transport of sand from above CD to lower parts. Most severe regression was approx. 40 m *(Figure 5.B)*. The sediment balance *(Figure 5.A)* did not show large sand loss over the whole width of the nourished area. This leads to the conclusion that cross-shore processes determined for a large part the behaviour of dry-beach width.

Modelling of the nourished area

A coastline model was set-up and verified that predicts the behaviour of the nourishment. It was shown that a good similarity between the survey data and the model was obtained in a section of 500 m near the marina, based on the comparison of sediment balances *(Figure 6.A)*. The correspondence 200 m further down drift was less well. The conclusion is that with the Italian beach model volume computations can be made for Italian beach with satisfactory results. But in this short period of 8 month cross-shore processes are dominant over longshore processes for the prediction of the dry-beach width *(Figure 5.B)*.

Optimization

Three cases were tested with this model for optimization, placement in triangular, rectangular and undulation shape. All three cases improved the critical section of 300 m near the marina, relative to the reference case ("as placed in the past"). However further down drift more erosion occurs *(Figure 7.C.1)*. It has to be decided if this is acceptable or not.

Cross-shore modelling

A model was created in UNIBEST-TC to simulate cross-shore effects, the result is presented in *Figure 8.A*. Instability of the dune was seen for computations with grain sizes coarser than 400 μm. Also waves with $H_{rms} < 0.75$ m caused instability. This calibration makes the results less reliable. Above MSL some instability of the profile was seen. This is the influence of the seawall boundary. Around MSL to CD -2 m the model has very good results. This shows that the model can predict the dry beach width with good results. Below CD too much accretion is computed. This is probably because part of the material was transported alongshore and to deeper depths.

Recommendations

Most surveys were carried out until 400 m offshore to about CD – 5 m. In some profiles this was too short and significant transport took place to deeper parts of the cross-shore profile. It is recommended to survey to a minimal depth of CD –7 m, about 650 m. Regarding the modelling with UNIBEST: A more state-of-the-art model taking into account flow calculations, sediment concentrations, time records of waves, water elevations and current, might give better result for the prediction of the dry-beach width. This can be used for the

optimization and then it can be decided if the erosion down drift of the critical area near the marina is acceptable or not.

1 Introduction

1.1 Introduction

In this chapter the introduction of the thesis will be presented. In Section 1.2 some general information on beach nourishment is presented. Section 1.3 gives some information on Dubai. Subsequently in Section 1.4 a description is given of the coast where the Van Oord nourishment locations are situated. In Section 1.5 the main and sub-objectives are presented. Section 1.6 explains how the coordinate system is used. And finally in Section 1.7 the approach of the research and this report are described.

1.2 Beach nourishment

Around the world many sandy beaches are suffering from erosion. Coastal shoreline recession and erosion can be caused by a relative rise in sea level, or by cross or longshore transport when the volume of sediment removed exceeds the volume supplied to the beach. Human modifications or actions can also contribute or accelerate localized coastal erosion.

A range of techniques are available to counteract erosion. As opposed to permanent hard-type structures to protect the shore (e.g. groynes and breakwaters), also less intrusive techniques are available such as beach nourishment or beach fill. Sand from offshore or onshore sources is placed on the eroding beach setting back the time. Beach nourishment can be used to build additional recreational area and to provide storm protection. An optimization in beach nourishment is found when the lifetime of the nourishment is extended and when losses of sand compared to the initial nourished volume costs are minimized. A variety of things can be investigated; among these are sand volume, location of the placement, grain size and execution methods.

The subject of this thesis is to study and optimize the behaviour of nourishment. For this aim Van Oord, a Dutch marine contractor presented several study locations in Dubai. The coastal stretch considered in this thesis is a 20 km long coast, which is bordered on the southwest side by Palm Island Jumeirah and on the northeast side by the Dubai Dry Docks and Port Rashid.

A lot of development takes place on this coastline, with the aim to stimulate tourism. But to improve the existing beaches or create new beaches, nourishment on a frequent basis is required. Six beaches on this coast were nourished in the period from December 2003 until September 2004. For these beaches, data is available on wave climate, sand characteristics and bathymetry. This makes it a good location for study.

1.3 Dubai

Originally a small fishing settlement, Dubai was taken over in about 1830 by a branch of the Bani Yas tribe, led by the Maktoum family, who still rule the emirate today.

Commercial success allied to the liberal attitudes of Dubai's rulers, made the emirate attractive to traders from India and Iran, who began to settle in the growing town. But, while trade developed, Dubai remained politically a protectorate of Britain. On the British withdrawal in 1971, Dubai came together with Abu Dhabi, Sharjah, Ajman, Umm Al Quwain, Fujairah and (in 1972) Ras Al Khaimah to create the federation of the United Arab Emirates.

This was shortly after the discovery of oil in 1966, which transformed the emirate and its way of life. Dubai's first oil exports in 1969 were followed by a period of rapid development that laid the foundations for today's modern society. The late Ruler, HH Sheikh Rashid bin Saeed Al Maktoum, ensured that Dubai's oil revenues, despite being relatively modest by the standards of the region, were deployed to maximum effect. His work has been continued by the present Ruler, HH Sheikh Maktoum bin Rashid Al Maktoum.

With only modest oil reserves, Dubai Emirate has undertaken a range of diversification efforts to establish itself as tourism, ICT, re-export and financial hub. Taking full advantage of its position near the head of the Gulf, it has become an important region. Dubai has developed prestige hotels, massive port facilities and a range of free trade zones to attract both manufacturing and services industries.

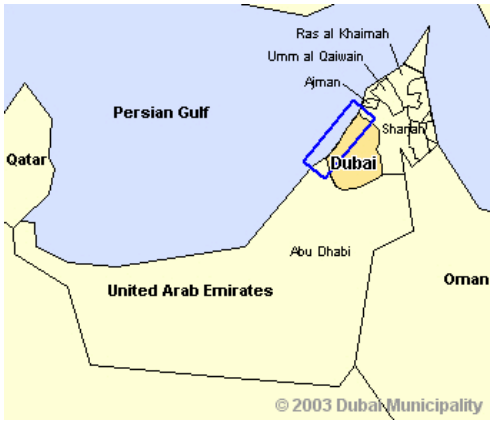

Figure 1-1 Map of the United Arabic Emirates

Figure 1-2 Satellite image of the coast of Dubai

1.4 Description of the Dubai coast

1.4.1 Recent coastal developments

Dubai has done a lot of developments on its coastline in order to become a centre for tourism. Among these are completely reclaimed islands with diameters of several kilometres. A few examples of the projects are presented in *Figure 1.A (in the back of this report)*:

Palm Island 1 or Palm Jumeirah was the first major development. This artificial island has the shape of a palm tree with a diameter of 5 km in front of Jumeirah beach. In total, up to 70 million m^3 of sand was supplied. The reclamation works and breakwater were completed in December 2003. In May 2005 the infrastructure and housing are still under construction.

Palm Island 2, also referred to as the Palm Jebel Ali is the second island in the shape of a palm tree. This palm tree is about 50% larger than the Palm Jumeirah. The location is outside the study area, near Mina Jebel Ali, about 20 km south of Palm Island Jumeirah. The reclamation is scheduled to finish towards the end of 2005.

Another prestigious project is the World Archipelago; this project consists of the reclamation of 300 artificial islands, 10 km in front of Jumeirah beach. The islands form together the map of the World with Dubai in the centre. A breakwater of 25 km, requiring 20 million ton of rock protects the islands for which 300 million m^3 of sand will be used. The project started in October 2003 and will be finished in 2007.

In order to build the Dubai Maritime City, a land reclamation project near Port Rashid is initiated for which 30 million m^3 of sand will be used. The project began in November 2003 and will be finished in the second half of 2005.

These projects prove that Dubai's coastline is continuously under the influence of human implemented changes. While constructing these large projects, also smaller beach nourishments have been carried out on the coastline. This is done to prevent further erosion and improve the beach. By the end of 2003, Van Oord carried out several nourishments on beach areas that suffer from erosion or where even no beach is present.

1.4.2 Coastal features from southwest to northeast

The sandy coast considered within this thesis stretches out from the Palm Jumeirah to Port Rashid and is about 20 km *(Figure 1.B)*. In this report, this part of the coast of Dubai is referred to as the Jumeirah beaches.

The description of the coastal features on this part of the coast is made on the basis of satellite images of the coast, made between 1980 and 2003 and a previous study by WL| Delft Hydraulics (2002) on the morphology of the entire Dubai coast. *Figure 1.B* shows the coastline between Palm Island Jumeirah and the Dubai Dry docks. The names of the beaches (as used by Van Oord), the marinas and breakwaters are included. *Figure 1.C* shows satellite images of the six beaches, where nourishments have been carried out.

The first main feature at the southwest side border of the area is Palm Island Jumeirah. This artificial island has the shape of a palm tree with a trunk and leaves, Figure 1.3 (in the text). An 11 km long crescent protects the island. The island extends up to 4.5 km offshore and its projection on the coast is about 4.5 km. A 300 m long bridge is the connection to the main land. The Palm has influence on the northern beaches. It blocks all waves from western direction. Study (WL| Delft Hydraulics, 2002) indicates that this influence on the wave climate extends to approx. 5 km along the shore up to Chicago beach.

Between the Palm and the coast lie two artificial islands. These islands have the shape of the logo of the Dubai Emirate, hence the name Logo Islands. In the southeast corner of the Palm Jumeirah also lie the Sheikh Mohammed Marina and the Sheik Ahmed Marina. In this area not a lot of sand is present. But on the north side of the Ahmed Marina, some accretion is observed.

The beach northeast of these marinas is called Madinat Jumeirah. It runs from the Sheik Ahmed Marina to the Madinat groyne. The Madinat groyne is constructed in 2003 to detain more sediment in the area. From the satellite images *(Figure 1.C)* it is observed that the structures on the land are very close to the sea and hardly any beach is present. Begin 2004 the groyne is extended in northwest direction, Figure 1.4 shows that sediment is detained in its leeside (upper right corner).

Figure 1-3 Satellite image of Palm Island, Logo islands, and marinas

Figure 1-4 Image from Burj Al Arab hotel in southern direction with Mina A'Salam beach in front and Madinat Jumeirah beach in the back (Dubai Municipality, Sept. 2004)

The beach between the Madinat breakwater and the Chicago beach area is called Mina A'salam. In this area recreational facilities are well developed. The famous Burj Al Arab hotel is built on an artificial island (Figure 1.5). The construction of this island and marina began in 1994, the hotel opened in the end of 1999. The connection to the land is formed by a 280m long bridge. Sand is kept in this area, and a salient is shaped behind the island. Accretion to the Umm as Suqaym II Marina is also visible.

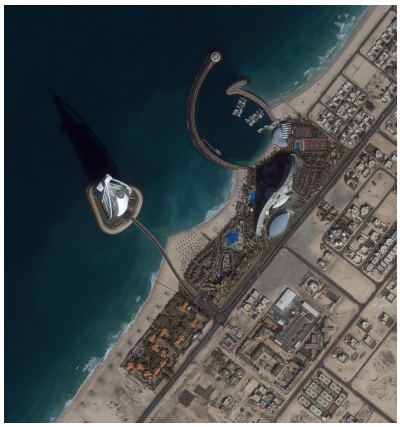

Figure 1-5 Satellite image Burj Al Arab hotel and Chicago beach area

Figure 1-6 Image from Burj Al Arab hotel in northern direction with Italian beach in the back (Dubai Municipality, Sept. 2004)

Italian beach is located between the Umm as Suqaym II Marina and the Umm as Suqaym I Marina (Figure 1.6). In 1980 these marinas were already present, but later an extra groyne in northwest direction was constructed. At the leeside of the Suqaym II Marina hardly any

beach is present. The beach gradually widens up further north and a reorientation of the coastline is visible. At the Suqaym I Marina, the same pattern is seen.

The beach northeast of Italian beach is referred to as Glass Palace beach. It runs from the Umm Suqaym I Marina to the Al Rais breakwater. This breakwater was constructed sometime between 1980 and 2001 (unknown to the author). Revetments, groynes and offshore breakwaters protect this beach. In August 2004, two more offshore breakwaters were completed. These defence works protect expensive houses closely built to the sea. Satellite images show that before 2003 hardly any sand is present in this area. Up north at the Al Rais breakwater, some more sediment is detained and a small beach is seen.

Jumeirah beach 2, north of the Glass Palace beach, is situated between the Al Rais breakwater and the Jumeirah Fishing Harbour, this fishing harbour was already present in 1980. It shows a pocket beach with a slight reorientation to the north.

North of the Jumeirah Fishing Harbour at Jumeirah beach 1 a revetment was built and groynes protect the area. In front of this revetment hardly any beach was present. This revetment stretches out to the Jumeirah beach protection works, consisting of a detached breakwater, a T- groyne and a curved groyne. At these protection works sand has remained forming a curved beach.

After these works, the large breakwaters of the Dubai Dry Dock and Port Rashid completely block the littoral drift. These breakwaters extend several kilometres into the sea. Some accretion is seen at the breakwater.

1.5 Objective of this thesis

1.5.1 Problem description

From the previous description it was seen that the coastline of Dubai consists of a large number of coastal engineering works. Revetments, groynes, offshore breakwaters and marinas have a large impact on the formation of the beaches. These beaches have an important function as protection of structures on the land and for recreation and tourism. All these beaches have a general trend of reorientation between existing marinas. The beaches gradually widen in down drift direction, and leave a large beach on the updrift side of marinas and groynes.

Erosion problems are found at the leeside of these structures. While plans are being developed to mitigate erosion problems along the Dubai coastline in the future. Emergency measures have been carried out on some locations to counteract these problems. The location of these measures is presented in *Figure 1.D*. The emphasis is on soft-type solutions in the form of beach nourishments, because of the rapid developments on the coast of Dubai. After the completion of these nourishments in 2004, a survey program took place to monitor the bathymetry.

But, since these were emergency solutions, future nourishment will be necessary. In September 2004, WL| Delft Hydraulics in cooperation with Van Oord is interested in more detailed research to obtain more insight in the morphologic behaviour of the beaches and

especially the nourished areas. The question is raised whether the possibility exists of optimization of the nourishment at these locations.

A numerical morphologic model can be used for the study of the morphological developments with the available survey data. The UNIBEST package is presented and selected. This model is widely applied in long-term morphological studies (years or decades), but uncertainty exists in the performance of this package for short-term predictions.

1.5.2 Main objective

The main objective of this thesis is to gain insight in the morphological behaviour at the nourishment locations along the Jumeirah beaches. Therefore the survey data will be analysed, and a model will be made in the morphologic package UNIBEST for a selected location on the Jumeirah beaches. Once validated with the data, this model will be used as a tool to make suggestions for optimization of possible future nourishment.

1.5.3 Sub objectives

Several sub objectives are defined in order to reach this objective:

- Analysis of morphologic behaviour of the coast and nourished areas of the Jumeirah beaches and determination of a suitable study location
- Analysis of the hydrodynamic conditions and sand characteristics for this location.
- Detailed analysis of the survey data for this location
- Set-up, calibration and verification of a morphodynamic model in UNIBEST.
- Analysis of the UNIBEST software package, definition of its capability to make short-term predictions
- Optimization and suggestions for future nourishments with the UNIBEST model

1.6 Approach of the thesis and structure of the report

The approach of the thesis is represented in Figure 1.7.

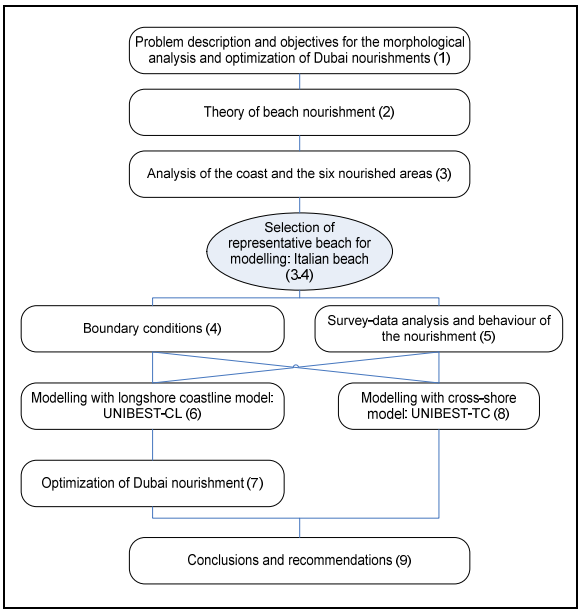

Figure 1-7 Approach of the thesis. The numbers is brackets refer to the relevant chapter

In Chapter 2 some background theory regarding the morphologic behaviour and modelling of beach nourishments is given. In Chapter 3 an analysis of the coast and of the six nourished areas is performed and a selection is made for further analysis and modelling. In Chapter 4 the boundary conditions for this location are presented and in Chapter 5 a detailed study of the survey data of this location is carried out. A numerical model to simulate longshore processes will be calibrated and verified in Chapter 6. With this model an attempt to optimize the nourished area is carried out in Chapter 7. In Chapter 8 a numerical model to simulate cross-shore processes will be described. Finally in Chapter 9 conclusions and recommendations of the thesis research will be presented.

2 Beach nourishment and design

2.1 Introduction

The goal of this chapter is to present a review of available theories on beach nourishments. This is presented to gain insight in all aspects of beach nourishment. Not all of this theory will be used for the analysis and modelling of the Dubai beach nourishments. Important are Section 2.2.2, where the behaviour of nourishment after the placement is described, and Section 2.3.2 in which the single-line theory of Pelnard-Considère is presented that will be used for modelling. Other sections serve to gain insight in how designing and modelling of nourishment is usually carried out.

Nourishment in general will be described in Section 2.2. Methods to design beach nourishment both by hand calculations and by numerical models are presented in respectively Section 2.3 and 2.4. Finally, in Section 2.5 the conclusions of the review will be presented.

2.2 Nourishment in general

2.2.1 Benefits of nourishment

Primary objectives of nourishment are (Coastal Engineering Manual, 2002):

- Provide improved protection to upland structures and infrastructure from the effect of storms.
- Stimulate recreational benefits.

The benefits of beach nourishment can include storm damage reduction, recreational and environmental enhancement (Dean, 2002). Sometimes sandy beach is desired where no beach is present. A wide beach serves as both an effective energy absorber during periods of elevated water levels and storm waves and also provides a reservoir of sand which can be transported and deposited offshore as a bar on which the larger waves break, thereby further reducing the wave energy which reaches the shore. Tourists are attracted to beaches and a wide recreational beach can result in a significant increase in tourist related income to resort areas.

Nourishment is a soft-type solution, since it has no permanent impact on the coast. It is generally applied because of flexibility, harmony with nature and the spreading of costs (Manual on Artificial Beach Nourishment, 1987). Nowadays the decision to apply beach nourishment as method for shore protection and stabilization is made more and more often by coastal authorities.

A significant problem associated with beach nourishments design is predicting the lifetime of a project. Usually a beach that is nourished is eroding and the placement of sand is simply a means of turning back time, since the erosion mechanisms are still taking place.

Regarding the beaches in Dubai, these trends are also seen (Section 1.3). Although sediment is placed, on most locations the erosion process continues. So it is mere to set-back of the limits of time, but an optimization could possibly be made. Therefore, it is very interesting to study the beach nourishments in Dubai and to investigate on what aspects of nourishment an optimization might be realizable.

2.2.2 Behaviour of a nourishment

Of most nourishment projects, the beach berm is the primary feature. A nourishment project usually involves widening the berm to create a wider sand buffer for dissipating storm energy. For practical and economical reasons, the total nourishment volume required to advance the berm to the desired width, is placed on the visible part of the beach. This construction method enables the economic use of standard earth-moving equipment for the distribution of the nourishment and minimizes the relocation of discharge point. The result of this technique is a beach berm that is considerably wider than the target design width.

After the placement, the nourishment will begin to respond to the conditions. In beach nourishment, sand is usually placed on the beach at a slope steeper than its equilibrium profile, so in the profile the beach is out of equilibrium. Also in planform the beach is out of equilibrium. The waves will begin the restore equilibrium both in profile and in planform. The progress of shoreline changes consists of three stages (Dean and Dalrymple, 2002).

1. The profile equilibration, this process generally results in a cross-shore transfer of sand from the upper to lower parts of the profile and, thus, a shoreline regression. This is not a transfer of sand out of the profile (Figure 2.2)
2. The spreading process, this is a transfer of sand along the beach and a result of the placement of the nourishment. (Figure 2.1)
3. The background shoreline erosion, this is due to the ongoing morphologic processes before the project was placed. (Figure 2.1)

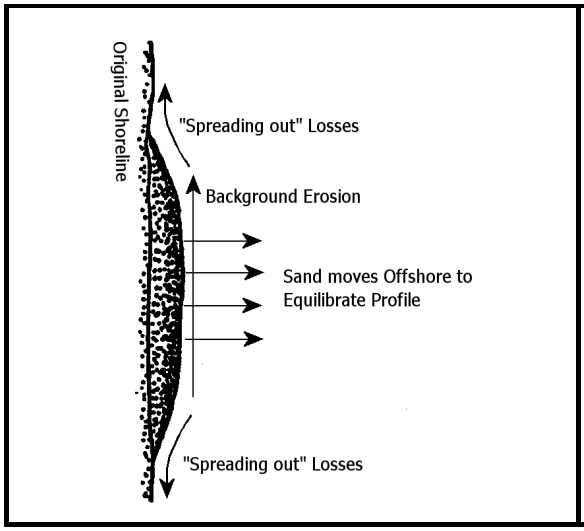

Figure 2-1 Plan view, showing "spreading out" losses, background erosion and sand moving to equilibrate profile (Dean, 2002)

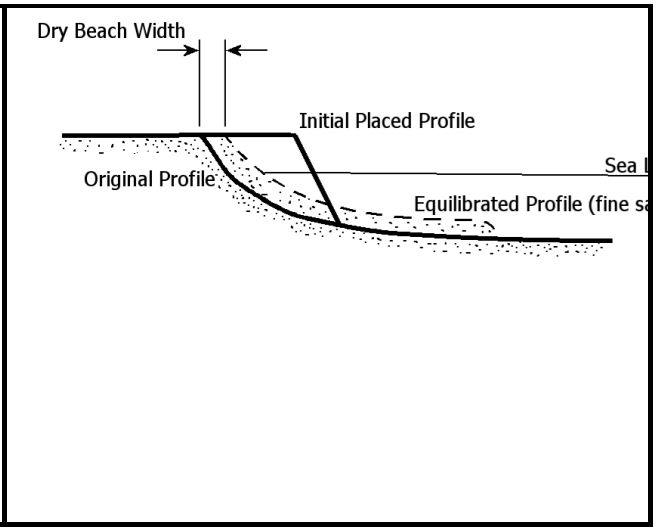

Figure 2-2 Cross view, showing the equilibrated profile as result of the placement of a nourishment with fine sand (Dean, 2002)

These three components of change are operative simultaneously. However they usually have somewhat different time scales. Profile equilibration typically dominates on time scales on the order of a year, whereas longshore diffusion losses generally occur on the order of decades. Usually it is assumed that the background erosion losses continue at the same rate as before the project. Thus their effect is the same for each year.

Figure 2.3 qualitatively illustrates the shoreline changes for each of the three effects and their sum for two background erosion rates.

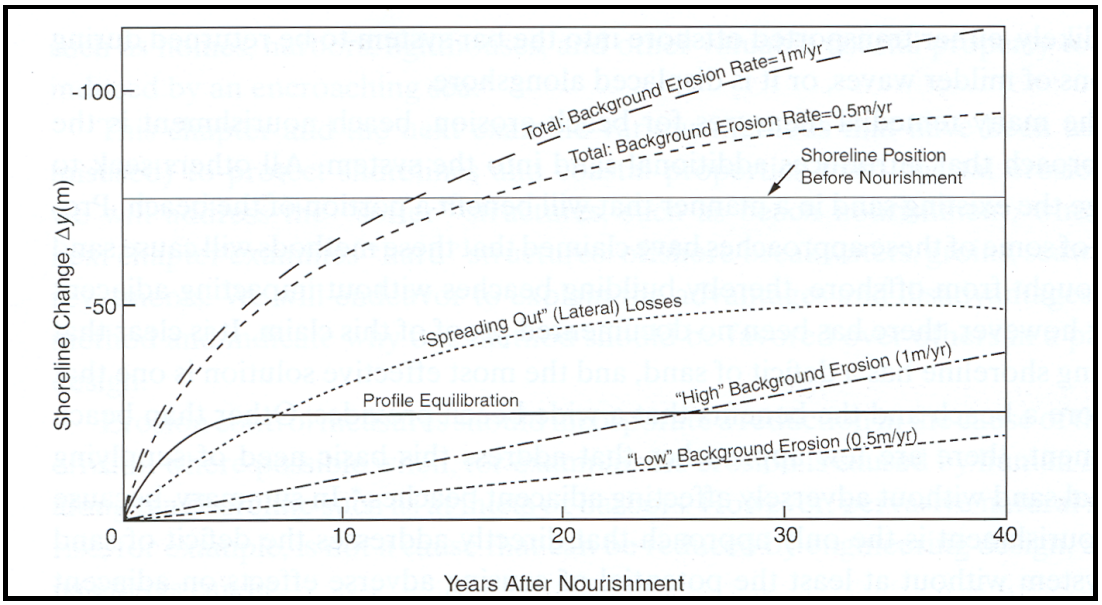

Figure 2-3 Development of a initial nourishment width of 75 m in time as a result of the three components of shoreline regression (Dean and Dalrymple, 2002)

These three processes determined the morphologic behaviour at the Dubai nourishments. In the analysis of the nourishment, these processes will be investigated.

2.2.3 Placement strategies

The placement of the sand is mostly done hydraulically. At the borrow sites, which are usually offshore, the sand is lifted from the bottom by hydraulic dredges and then is taken with either floating lines, hopper barges or hopper dredgers to the fill site, where it is discharged to the beach. At the fill site, the borrow sand can be placed in a variety of positions; offshore of the beach, on the foreshore, on the back beach, or the dunes. Planform options are to spread the fill material over the beach.

The sediment can be placed in a variety of positions and this should be considered in the design process of the nourishment. There are various positions possible in the profile but also in the planform. Various combinations for the placement can be possible, depending on the objectives of the project, requirements and the availability of material. Table 2.1 presents possible options.

Cross-shore position	**Alongshore position**
At the back or on top of the dunes	Direct placement of the sand where it is needed
At the face of the dunes	A stockpile of sand
On the beach	Continuous nourishment in time at one or two points
In the offshore zone	

Table 2-1 Options for placement within the profile and in planform (Manual on Artificial Beach Nourishment, 1987)

At the Dubai nourishments the sand was placed on the beach and on the foreshore. The placement in a longshore position was directly where it was needed.

2.3 Design of beach nourishment

The methods described in this section are used to obtain insight in how a relatively simple estimation of the required volume of nourishment could be made, based on the behaviour of the nourished sand as a response to the original sand (before the placement), or as a response to longshore processes. It shows the importance of certain aspects in the designing process. But no computations with this theory were made in this study.

The desired additional beach width is determined based on:

- The desired level of storm protection
- The persistent long-term erosion trends
- The target renourishment interval

When designing a beach nourishment protection the primary objective is to understand the ongoing sediment transport processes of the system. After that, the required volume of nourishment can be estimated by hand using certain simple methods which can be separated in methods for cross-shore and longshore response. The cross-shore methods are mostly based on the behaviour of the nourished sand as a response to the original sand. The longshore methods are based on other factors, such as the wave climate. The methods are described in the following Sub-sections.

2.3.1 Beach fill design in cross-shore response

The methods described in this section are used to obtain insight in how a relatively simple estimation of the required volume of nourishment could be made, based on the behaviour of the nourished sand as a response to the original sand.

To determine the necessary volume in the cross section for a required location several methods are available, the CEM (2003) presents two methods:

- Using the overfill factor R_A (James, 1975)
- Equilibrium profile design methods (Dean, 1991)

Overfill and renourishment factor design method

The grain-size distribution of the borrow material will affect the cross-shore shape of the nourished beach profile, the rate at which nourishment material is eroded and how the beach will respond to storms. The borrow material will not exactly match the native beach. An analysis is required to assess the compatibility of the borrow material with the native beach, from a functional perspective.

Early research into the compatibility of borrow material developed a factor, indicating how much nourishment material is required. Many researchers assumed that borrow material placed on the beach will undergo sorting as a result of the coastal processes; and given enough time, will approach the native grain-size distribution. The portion of borrow material that does not match the native sediment grain distribution is assumed to be lost. James developed this concept into a method to calculate an overfill factor R_A and a renourishment factor, R_J, in which the use of the renourishment factor is no longer recommended in beach fill design calculations (CEM, 2003).

These models only take into account the effect of a possible difference between the properties of the native and borrow sand (Manual on Artificial Beach Nourishment, 1987). The overfill factor, the volume of sand used to maintain 1 m^3 of beach, can be obtained graphically from Figure A.1 in Appendix A.1.

Equilibrium profile design methods

Recent research and experience have questioned the continued use of these grain based overfill and renourishment factors to estimate the performance of nourishment (Dean, 2000). They recommend design based on equilibrium beach profile concepts; an assessment of storm induced erosion; and an assessment of wave driven longshore transport losses.

The equilibrium beach profile concept is an important aspect in the study of morphologic behaviour of nourishment and is explained in Appendix A.2.1. It states that the shape of the natural beach profile depends on a parameter, A, function of the energy dissipation and indirectly the grain size of the beach. So when a volume of sand is added to the native beach it will eventually equilibrate to form $h=A\ y^{2/3}$. Depending on the native and the borrowed sediment scale parameters the nourished beach profile can be intersecting, non-intersecting, *(Formula A.2)*. Or non-intersecting, but emerged or submerged *(Formula A.4)*. With this knowledge, the volume of nourished sand can be calculated.

The process to design the required nourishment volume with the equilibrium based methods is described in Appendix A.2.2.

Discussion

These methods treat sediment characteristics using a single grain size parameter, the median grain diameter. Equilibrium method has the advantage over the “overfill and renourishment method” because it includes the effects of the forces that shape the natural and altered beach profiles.

These methods provide valuable insight regarding the implications of using nourishment material with different grain characteristics, but are not recommended for final volume computations. The equilibrium profile methods do not account for a sediment deficit in the pre-project beach profile.

2.3.2 Beach planform design (single-line theory)

The method described in this section is used to obtain insight in how a relatively simple estimation of the required volume of nourishment could be made, based on longshore processes. The single-line theory is an important tool for study of morphologic behaviour and is used in the UNIBEST-CL+ model.

To estimate a volume needed in the lateral direction, other conditions than the role of the grains are usually considered. In this the effect of wave-driven longshore sand transport processes in combination with the local morphology are the major factors for determining the required volume of nourishment. Also the project itself causes a perturbation in shoreline and beach orientation and at last coastal structures can have a large influence on the loss of sand in longshore direction.

Methods exist to predict the rate of alongshore spreading and include the length of nourishment length, the effect of wave climate and the effect of background shoreline regression.

For example the single-line theory of Pelnard-Considère can be used. With the classical one-dimensional diffusion equation (Equation 2.1) one can derive several relatively simple analytical solutions. The derivation of the equation and an explanation of theory of the single-line theory are presented in Appendix A.3.1. This theory is also used in UNIBEST-CL+.

$$\frac{\partial y}{\partial t} = \frac{s_1}{h_p}\frac{\partial^2 y}{\partial x^2} \tag{2.1}$$

In which:			
	y	coastline position	[m]
	s_1	variation of the transport as a function of coastline rotation	[m^3/m·s]
	h_p	active profile height (closure depth and berm height)	[m]
	x	position alongshore	[m]

Several approximations for s_1 exist. Some well known longshore transport formulae are the formula of CERC (1984) and BIJKER (1971). The longshore transport formulae are based on different principles, and apply for different situations.

Several analytical solutions have been obtained. E.g. the accretion at a breakwater and a rectangular beach fill. However beach erosion is often caused by gradients in longshore transport, while the original coastline is mostly not straight. Also in these cases the one-line coast model can be applied, but, because of the more complicated boundary conditions, a numerical model is needed.

2.3.3 Comments

Usually the methods presented in this section to estimate a beach fill are not satisfactory because the boundary conditions at the project area are much more complicated. Therefore they are not used to design and analyse the Dubai nourishments. These methods can be used to give an indication of the amount of beach nourishment, and moreover provide valuable insight in the processes. These methods show also that it is very complex to estimate the lifespan of a beach nourishment project and simple calculations are very often not possible.

Therefore to make proper estimations for the loss of sand in a complex system, more detailed methods are required and the help of numerical models is in most cases necessary. In this study the UNIBEST package for cross-shore and longshore modelling will be used.

2.4 Numerical modelling of beaches and shorelines

For the numerical modelling of morphologic behaviour of beaches, also this separation in cross-shore and longshore response is seen. An appropriate model should be selected according to which phenomena are likely to occur or which phenomena are of interest to simulate. In this section three types of modelling are presented.

2.4.1 Profile modelling

Profile modelling is used to study the evaluation of the profile in cross-shore direction in time. It can be used to evaluate the impact of a storm, with elevated storm tides and wave

heights on the beach and dunes. Second application can be to predict the profile evolution of a beach nourishment project that is placed on a steeper slope than the equilibrium profile. This application could be of interest for the modelling of the Dubai nourishments.

Examples of numerical model are E-DUNE (Kriebel and Dean) and UNIBEST-TC (WL| Delft Hydraulics). The last can be used to assess coastal profile developments due to wave action. By choosing UNIBEST-TC one implicitly assumes that the nourishment profile is uniform in longshore direction and profile changes are a result of cross-shore sediment transport processes.

2.4.2 Planform modelling

With the use of contour line models the shoreline behaviour can be studied. In general planform models make use of the single-line theory (as described in Section 2.3.2), because the offshore profile is usually considered to remain constant in form and to move landward or seaward with the monitored contour and vertically with the water level.

The model is based on a numerical solution of the transport and continuity equation. The most appropriate grid is one in which the transport quantities are specified at the grid lines and the coastline position is computed at the grid midpoints. The equation may be solved by explicit or implicit methods.

Examples of models are: UNIBEST-CL+ (WL| Delft Hydraulics) and GENESIS (Hanson).

2.4.3 Coastal morphodynamic models

Coastal morphodynamic models examine the behaviour of the bathymetry by calculating the sediment transport locally and using the conservation of sand to determine the local depth change over some unit of time. These types of models have the advantage of being able to deal with non monotonic beach profiles and deal with both cross-shore and longshore processes. A disadvantage of these models is the difficulty to operate.

An example of a morphodynamic model is Delft 3D (WL| Delft Hydraulics).

2.5 Conclusions

Three processes play a role when looking at the behaviour of the nourished area after placement. These can be separated in three processes:

- profile equilibration (cross-shore process)
- spreading (longshore process)
- background erosion (longshore process)

Different methods exist to design a beach nourishment scheme. Simple calculations by hand are also separated in cross-shore and longshore design. When applying numerical models more complex calculations can be carried out. Models exist for profile modelling, planform modelling and morphodynamic modelling (both profile and planform).

In this thesis research two types of modelling will be performed: Planform modelling with the use of the single-line theory (Chapter 6), and cross-shore modelling (Chapter 8). An optimisation will be made with the planform model of the nourished area (Chapter 7).

3 Analysis of the coast

3.1 Introduction

Several nourishments took place on the coast between Palm Jumeirah and the Dubai Dry-docks. Goal of this chapter is to describe the morphologic behaviour of these nourished beaches and to make a selection for a location to model. The analysis is based on photos, satellite images made between 1980 and 2003 and available survey data of Van Oord.

Section 3.2 describes the available data for the morphologic analysis and how these data were obtained. The analysis of the morphologic behaviour of the nourished area and the Jumeirah beaches will be described in Section 3.3. Subsequently, in Section 3.4 the most suitable location for modelling of nourishment in Dubai will be selected. Finally, in Section 3.5 the conclusions of the analysis will be drawn.

3.2 Coordinate system

In this report a coordinate system is used that was defined by Van Oord:

Each nourished area uses a separate coordinate system in which the x-axis runs on a baseline, which can be a revetment or a selected angle more or less parallel to the shoreline. Positive on this baseline is from northeast to southwest. *Figure 1.C* shows the baseline for each nourished area. The y-axis is rotated 90 degrees clockwise, relative to the x-axis, positive in seaward direction. The z-axis is the bottom height relative to Chart Datum (CD), perpendicular to the x-and y-axis positive in upward direction.

3.3 Available data

Van Oord presented survey data of bathymetry at the six nourishment locations in the period from December 2003 to May 2004. These surveys consisted of a hydrographical and a land part. These surveys are linked to each other to determine the bathymetry of the beaches. The survey carried out just before the nourishment is called the Pre-survey, the survey directly after the placement is called the Post-survey.

The equipment used on land and shore is called Real Time Kinetic – Global Position System (RTK-GPS). The system contains of two units. One is a base station on a benchmark. The other one is mobile and used to collect data.

The base station will generate corrections between the known benchmark co-ordinates and the co-ordinates that are calculated by triangulation between the GPS satellites that the base station receives. Due to interference in the stratosphere and ionosphere a normal GPS will be generating coordinates within 25 m accuracy horizontal and 50 m vertical, this difference in accuracy is caused by the triangulation from the satellites which are too close to make an optimal calculation. The distance is measured by means of atomic clocks that are controlled from 3 base stations around the world. Via a radio link the second unit will receive these

differential corrections. That is called Differential Global Positioning System (DGPS). The used units will receive every second new corrections and the unit can "predict" certain values, it becomes RTK. These units will provide coordinates accurate within 3 cm horizontally and 5 cm vertically.

For the hydrographical data collection an echo sounder was mounted on a boat. To determine the water depth with respect to Chart Datum (CD), a correction for the tide, wave action and increasing water depth was applied and that decreased the accuracy of the vertical measurements to about 15 cm.

Profiles with an absolute length of 250 m were presented by Van Oord and were used to analyse the cross-shore behaviour of the nourishments. The profiles reach a depth ranging between MSL -5 m and -7 m (MSL is 1.1m above CD , see Section 4.4).

Sediment balances were used in order to analyse the nourishment in a quantitative way. They present the volume of eroded or accreted sand in a profile compared to the Post-survey. The area difference was calculated for profiles for every 25 m, and the volume by multiplying this by the width of the section that it represents. A negative number indicates that sediment was being transported to an unsurveyed area (further offshore than 250 m or alongside the coast). Sediment balances w.r.t. the Post-survey of February and May 2004 were available.

The analysis of the morphologic behaviour of the beaches in this chapter was made based on this information, on satellite images between 1980 and 2003 and on photos from the Dubai Municipality (later referred to as: DM).

3.4 Behaviour of the beaches and the nourishments

The objective of this section is to perform an analysis of the survey data and morphological processes of the nourished areas along the Jumeirah beaches. In the study area, six beaches are present where nourishment was carried out. The observed morphologic behaviour of the beaches and the nourishments are analysed in the next Sub-sections. The location of these beaches was shown in *Figure 1.B*. Satellite images of the six beaches made in October 2003 were presented in *Figure 1.C.*. In the following the nourishments are discussed.

3.4.1 Madinat Jumeirah beach

In the end of 2003 an existing groyne was extended into sea to CD -5 m. A seawall backs Madinat Jumeirah beach. The beach has a total length of 2600 m and the nourished area covered 800 m southwest of the groyne. The nourishment started on 17 December 2003 and amounts 154,000 m^3.

Photos from the Burj Al Arab hotel show that sediment was detained in the south side of the groyne. The satellite image (*Figure 1.C*) shows that some accretion occurred at the Sheik Ahmed Marina.

Sediment balances of Madinat Jumeirah beach of February and May 2004 are available (*Figure 3.A)*. A sediment balance presents the volume of sediment loss or accretion with respect to Post-survey in a representative profile of 25 m width. Moreover it presents the

location of the loss or accretion, and with multiple surveys it shows the behaviour in time. On the x-axis is the coordinate of the profile (as defined in *Figure 1.C*). On the y-axis is the volume loss of sand with respect to the Post-survey.

The accretion found near the groyne (Section 200-300) was due to the spreading of the nourishment, and was detained in the period from February to May due to the local diffraction due to the groyne. Erosion took place in the south side of the groyne due to the blocking of updrift sediments by the Madinat groyne (Section 300-700). The wave climate for the region was changed locally because of Palm Island Jumeirah. This caused transport of sediment in southern direction. This process continued, since the stored volume decreased from February to May. Accretion occurred in Section 700-1025. This was probably sediment from updrift. The total volume that disappeared from 7 January 2004 to 10 May 2004 was approx. 12,900 m^3. This was 8% of the nourishment.

The profiles in *Figure 3.B* show that down drift of the groyne no underwater berm was shaped (Profile 400). Above CD the slopes became steeper in time up to 1:3. Under water milder slopes were shaped, around 1:25. Profile equilibration, a cross-shore transfer of sand from upper to lower parts of the profile did not take place until a distance of 750 m down drift of the breakwater. All profiles show that in time almost all erosion was in the upper part of the profile (between CD and CD +4 m). In profile 750 the sediment from the upper parts was distributed under water and generated very mild slopes to CD -1 m (1:100) and 1:25 (from CD -1 m to -5 m). Profile 750 showed accumulation above MSL, the regression of the part above MSL between the Pre and Post-survey is remarkable.

To see whether cross-shore transport loss took place, the profiles have to reach a closure depth. Theory relates this depth to the local wave height. The closure depth will be further discussed in Section 4.8, but theory presents a closure depth of approx. 4.7 m (Section 4.8). The profiles reach a depth of CD -6.0 m and because all profiles coincided at this depth and the waves hardly exceed a H_s of 2 m, it is assumed that the transport over this depth was limited, so the sediment that disappeared from this section was transported alongshore.

3.4.2 Mina A'Salam beach

No bathymetric information was available of Mina A'Salam. The nourishment started on 17 December 2003 and covered 1000 m coastline.

From pictures no considerable change in coastline position is seen at the north side of the Madinat groyne. At the Burj el Arab hotel and Umm as Suqaym II Marina some accretion occurred. This nourishment remained after the placement. The influence of the Palm Jumeirah on the wave climate was probably more limited than on Madinat, so the main wave direction was changing from the south to north on this beach.

3.4.3 Italian beach

Italian beach with a length of approx. 2450 m is located between the Umm as Suqaym II Marina and the Umm as Suqaym I Marina. The beach is backed by a seawall. The Umm Suqaym II Marina consists of two breakwaters that mark the entrance. The outer one reaches to 300 m from the coast, to a water depth of approx. CD -5 m. The inner one is 150 m and

advances to CD -2 m. The Umm as Suqaym I Marina is similar shaped. Starting 10 December 2003 a total volume of 114,000 m^3 of sand was nourished on an area of 675 m, located in the leeside of Umm as Suqaym II.

Photos and satellite images *(Figure 1.C)* show erosion at the north side of both marinas; hardly any beach area was left in August 2004. This resulted in a new nourishment. In northern direction the beach gradually widened, and large accretion on the south side of both marinas was observed. This was the reason that on the southern side of the breakwaters of the marinas an extra groyne was constructed (before 2001). This groyne collects sand, to prevent bypass and siltation of the marinas. The coastline reoriented to the local wave climate. This caused sediment transport in northern direction. This reorientation also took place before the construction of the Palm, so it showed that the influence on the wave climate was limited at Italian beach.

In the end of 2002 a techno reef barrier was constructed north of the Umm as Suqaym II Marina with a length of approx. 450 m. The reef consists of small, loose, relatively open elements placed at CD – 2 m to 2.5 m. After the nourishments they were covered with sand. So it is stated that the function was very limited. This conclusion was supported by an investigation by WL| Delft Hydraulics (2003) that also stated the influence negligible.

The sediment balance of Italian beach indicates where sediment eroded or accreted in a profile or section (*Figure 3.A*). For Italian beach only a sediment balance was available for the period between 1 January and 9 May. In the leeside of the Umm as Suqaym II (Section 125-675) the volume of sediment decreased. This was caused by longshore drift in northern direction. The sediment was spread in northern direction along the beach. Here accretion was observed (Section 25-125). The total volume that disappeared in the section until May 2004 was approx. 25,500 m^3. This was 25% of the total nourished sand at this moment.

The profiles of the Section 200-600 had a similar pattern. Profile 450 (*Figure 3.C*) shows that the nourishment was constructed with a slope of about 1:20. And became steeper above CD to about 1:6 and retreated with this slope. Around CD almost horizontal slopes were seen. Part of the material that was eroded above the waterline was placed under water at a water depth between CD -0.5 m and CD -4 m. Since the total volume decreased and the profiles coincided considerably at the toe; it is supposed that the sediment was transported in southern direction.

Profile 50 (*Figure 3.C*) is located in an accreting section. It shows that above CD +2 m the profile accreted. Between CD +2 m and CD (tidal range) the profile eroded. Around CD almost horizontal slopes were seen. And from CD to CD -4 m accretion took place with milder slopes (to 1:60) than the original profile. Also at the toe accretion took place, the depth became shallower (approx. 0.5 m). Maybe at water depths deeper than this transport took place.

3.4.4 Glass Palace beach

The beach northeast of Italian beach is referred to as Glass Palace beach. Revetments, groynes and an offshore breakwater protect this beach. In August 2004 a second and third offshore breakwater were completed. The location of the first two breakwaters is included in green in *Figure 1.C.* The beach has a length of approx. 4000 m. In Section 1375-2050 five

(short) groynes are situated (indicated in green). Multiple nourishments took place in this period. The first started on 28 December 2003 and the second on 24 January 2004. In total 489,690 m^3 sand was supplied. More nourishment started on 27 May 2004, data of this was not available.

The satellite images were made before the construction of the offshore breakwaters. It shows that hardly any beach was present in the area *(Figure 1.C)*. Some sand was detained in the leeside of Umm Suqaym I, due to the sheltering effect of the marina for waves from south and western direction. Towards the Al Rais breakwater, the beach reoriented, caused by wave induced transport in northern direction.

The analysis of the sediment balance *(Figure 3.A)* shows a pattern of accretion and erosion. The beach protection works were partly responsible for this pattern. In Section 2100-2800 accretion took place. What was remarkable in this period was that accretion took place (approx. 7,500 m^3) on this whole section, while a more or less neutral sediment balance was expected. A natural bypass along the harbour could have been influential as well, but the increase was not found at the toe of the profiles *(Figure 3.D, profile 2300)* but around CD and on the dry-beach. The profiles show that the Post-survey was about 80 cm lower than all other surveys and around CD the Pre-survey is higher than the Post-survey. So another explanation could have been that unreported maintenance was carried out in this period, or errors are made in the surveys. The conclusion is that a more detailed study is necessary to explain these phenomena. In Section 1600-2100 erosion was observed. The erosion continued from February to May 2004 and was caused by longshore transport in northern direction. In Section 1000-1600 again accretion took place. The offshore breakwater reduced the wave action behind it, inducing tombolo formation. The volume increased between February and May. In Section 750-1000 some erosion was seen. This area is between the two offshore breakwaters. So the wave climate here was less reduced, which caused more transport. Accretion occurred behind the next offshore breakwater (Section 400-750). In the last section (Section 0-475); large erosion occurred due to two effects: The spreading of the nourishment and the interruption of the longshore sediment drift in northern direction by the offshore breakwaters. The total volume of sand accreted from the end of January to 9 May 2004, with 12,000 m^3. This accretion could have been due to bypass transport, or unreported maintenance (especially in the Section 2100-2800). But it remained uncertain, due to inconsistencies in the data. Therefore, to determine the shoreline trends with complete certainty, more data should have been available.

Profile 1700 *(Figure 3.D)* was situated in an erosive area. The profile above CD became steeper in February (1:6) but later hardly moved. Around CD milder slopes are generated and accretion was seen up to a depth of CD- 3 m. The surveys deeper coincide, indicating less transport. The sediment balance as well as the profile showed that a clear equilibrium process: The sediment was transported from above CD to below CD and remained relatively stable after.

Profile 600 *(Figure 3.D)* is located behind the offshore breakwater. The original slope under MSL was around 1:30. At the waterline a particularly large increase was seen. A salient was shaped due to longshore processes. A very large berm at the toe of the profile in the 12 Feb-survey is seen. The width of this berm was almost 50 m and approaches to CD -1 m (Profile 600). This area was not surveyed after February, so this is probably part of the offshore breakwater.

3.4.5 Jumeirah beach 2

Between the Al Rais and the Jumeirah fishing harbour, the beach is referred to as Jumeirah beach 2. The total length of the beach is approx. 750 m. On 21 April 2004, Van Oord started the nourishment of a total of 174,900 m^3 sand.

The satellite image *(Figure 1.C)* made in October 2003, shows a very small beach at the Al Rais Breakwater and a wide beach at the Jumeirah Fishing Harbour. This re-orientation was due to wave induced longshore transports in northern direction.

Van Oord presented only survey data of the pre-survey of 23 April and the Post-survey of 21 May 2004, so no comments could be made about the behaviour of the nourishment.

3.4.6 Jumeirah beach 1

The total length of the beach is approx. 3,000 m and stretches out from the Jumeirah Fishing harbour to the Jumeirah beach protection works. This beach is referred to as Jumeirah beach 1. North of Jumeirah Fishing harbour a revetment and two short groynes were present (indicated in green in *Figure 1.C*). Protection works consisting of an offshore breakwater, a T-groyne and a curved groyne, protect the northern part of the beach. Nourishment was carried out on 1,800 m of this beach in February, March and April 2004 with a total volume of 478,000 m^3.

Satellite images *(Figure 1.C)* show that no beach was present up to the protection works. At the unnourished section down drift; at the offshore breakwater a salient was shaped. The image shows that accretion took place at the T-groyne, and a small pocket beach between the T- and the curved-groyne. The works were able to detain the sand.

Only one survey was carried out after the nourishment and unfortunately no volume computations of the surveys were available. From observations of profiles it was seen that in Section 1700-1800 some small accretion took place, probably due to spreading of the nourishment and the sheltering effect of the harbour. In Section 600-1700, sediment was lost above MSL but no berm was shaped. No bed movement was seen at the bottom of the profiles and the profiles reach a depth deeper than the estimated closure depth. From this it can be concluded that the sand was transported in northern direction towards the protection works. In Section 600-300 the volume in the profiles also decreased, but some profile adjustment and berm-shaping was seen. In Section 0-300 the offshore breakwater stimulated the accretion of the salient.

3.4.7 Conclusions on the behaviour of the nourishments

All beaches lie between existing marinas and harbour. At the beaches north of the Chicago beach area a northward directed transport took place (Italian, Glass Palace, Jumeirah 1 and 2). This caused that on the north side the beach accreted and on the south side hardly any beach remained. Nourishments were required at these locations. At Glass Palace a scheme of hard-type solutions was implemented to counteract this tendency. From the analysis of the available data it is concluded that this scheme had a positive result, although some

inconsistency was found in the data. South of the Chicago beach area at Madinat Jumeirah. Recently the net transport has reversed due to the presence of Palm Jumeirah.

From these observations it could be concluded that north from the Chicago area, the dominant longshore sediment transport was directed in northern direction. South of this area the sediment transport was in southern direction.

Sediment balances of the nourished areas were used to determine on which parts erosion and accretion took place. They showed that the coastal structures had a large impact on the morphologic behaviour. The total stored volume of sand volume in the nourished areas are listed in Table 3.1.

Location	Nourished volume [m^3]	Length [m]	Volume change [m^3]
Madinat Jumeirah	150,000	800	-12,900
Italian beach	115,000	675	-25,600
Glass palace	508,000	2450	12,300

Table 3-1 Stored volume of sand in May 2004 after the Post-survey

Profiles show the cross-shore development in time. In general near structures, the erosion took place over the whole height of the profile. This indicates dominancy of longshore transport near structures. On locations further from these structures, the trend was that the profile adjusted with slightly steeper slopes above MSL and increase of sediment under water. This berm-formation was found to a depth of CD -4 m. Accretion in the profiles was found below CD.

3.5 Choice of study location

Due to the limited time and to meet the objectives of the thesis, not all nourished beaches will be modelled. The three locations for which data for a relative long period is available are Madinat beach, Italian beach and Glass Palace beach. Of the other locations less data was available.

Between these three locations, a choice was made based on:

- Availability of data
- Indications of sediment transport and erosion
- Suitability for modelling

Remarks regarding these three criteria are schematized in Table 3.2.

Location	Remarks about the suitability of modelling
Madinat Jumeirah	- Reliable data - Longshore sediment transport in southwestern direction - Extension of the Madinat groyne in the period January-May 2004 - Large influence of Palm Jumeirah on the wave climate
Italian beach	- Reliable data - Sediment transport in northeast direction - Little/no influence of Palm Jumeirah on the wave climate
Glass Palace beach	- Inconsistency in the data - Presence of hard structures makes modelling case-sensitive and will cause the focus to shift on the modelling of these structures instead of the nourishment. - Construction of a second and third offshore breakwater in the period May-August 2004

Table 3-2 Progress of six nourishments

As can be concluded from Table 3.2 both the Madinat Jumeirah and Italian beach nourishment showed indications of sediment transport and erosion. The Glass Palace nourishment had a more complex morphologic behaviour due to a large scheme of beach protection works: this would make modelling very complex and not relevant for this study. Another disadvantage to model the nourishment of Madinat beach was that in this period the groyne was extended, which will affect the morphologic behaviour, making it less reliable to model. This was also the case for Glass Palace where two offshore breakwaters were constructed.

Based on these criteria and in consultation with the graduation committee, Italian beach was chosen as study location. This beach had visible longshore trends, which were also seen on other parts of the coast. This made it interesting for the modelling in UNIBEST. Furthermore sufficient data was available. In Chapter 5, a detailed study of the nourishment will be presented.

3.6 Conclusions

Van Oord nourished at six locations between Palm Jumeirah and the Dubai Dry-Docks in the period from December 2003 to May 2004. These beaches were surveyed in this period and this survey data was used to analyse the behaviour of the nourishment in time.

Satellite images and photos were used for the analysis of the whole beaches. The conclusions of this analysis for each beach are summarized below.

Madinat Jumeirah

Nourishment of approx. 150,000 m^3 was started on 17 December 2003. Placement was on 600 m coastline south of the extended Madinat groyne. The nourishment spread out after the

placement of the nourishment in southern direction. Some sand was detained in the leeside of the extended groyne. Cross-shore effects led to berm-formation and were found at 600 m south of the groyne. The total volume of sand that was disappeared in this section was 12,900 m^3.

Mina A'Salam

The nourishment started on 17 December 2003. Placement was on 1000 m coastline north of the extended Madinat groyne. In this section accretion occurred at the north at the Burj al Arab hotel, while in the south the coastline remained in place. No signs of erosion were seen, so the beach was stable after the nourishment.

Italian beach

Nourishment of approx. 115,000 m^3 was started on 10 December 2003. Placement is on 675 m coastline north of the Umm as Suqaym II Marina. Spreading of the nourishment was seen and longshore transport took place in northern direction. Also cross-shore effects and accretion below CD was observed. The total volume of eroded sand until May is 25,000 m^3.

Glass palace beach

Nourishment of approx. 489,690 m^3 was started between 28 December 2003 and 24 January 2004. Placement was on the coast north of the Umm as Suqaym I Marina to the offshore breakwater, over 2300 m. A pattern of erosion and accretion was seen, influenced by groynes and offshore breakwaters. The volume of sand increased in the period with approx. 12,000 m^3.

Jumeirah beach 2

Nourishment of approx. 175,000 m^3 started on 21 April 2004. Placement was on 600 m beach north of the Al Rais Breakwater. The satellite image shows that some reorientation of the beach had occurred.

Jumeirah beach 1

Nourishment of approx. 478,000 m^3 was carried out between February and April 2004. Placement was on 1500 m coastline north of the Jumeirah Fishing harbour. Before the nourishment no beach was present. An offshore breakwater, a T-groyne and a curved groyne detain the beach in the north part of the beach.

Selection of location for modelling

Based on the available data, indications of sediment transport, suitability of modelling and in consultation with the advisors Italian beach was chosen as study location. This beach had visible morphologic trends that were also seen on other parts of the coast. Furthermore sufficient data was available. In Chapter 4, the boundary conditions will be presented for this location. In Chapter 5, a more detailed analysis of the morphologic behaviour of the nourished area at this beach will be presented.

4 Boundary conditions Italian beach

4.1 Introduction

In the previous chapter the choice was made to model Italian beach. In this chapter the boundary conditions for Italian beach will be presented. The period to model is between the first and the second nourishment from January until August 2004. The boundary conditions consist of bathymetry, hydrodynamic conditions and sediment characteristics.

The sources of the available data for the boundary conditions will be described in Section 4.2. Subsequently, in Section 4.3 information on bathymetry is presented. In Section 4.4, 4.5, 4.6 and 4.7 respectively the water levels, currents, wave climate and wind are discussed. Section 4.8 gives an estimate for the closure depth. Section 4.9 the sediment characteristics and finally, conclusions are drawn in Section 4.10.

4.2 Available data

Hydrodynamic data are available from the Dubai Coastal Zone Monitoring Program. The Marine Works Unit of the DM runs the program that started in 1997 when a baseline bathymetric and topographic survey of the Jumeirah coastline was undertaken. It uses an Acoustic Doppler Current Profiler (ADCP) and a pressure transducer to measure on tide, currents and waves.

The ADCP is mounted in frames on the seabed 500 m in front of Jumeirah beach at MLS -10 m. The instrument measures currents throughout the water column using the return echo of an acoustic signal transmitted by the instrument. This system is used to calculate current speed and direction. These data together with instantaneous water depth data from the integral pressure transducer provide directional wave data. Unfortunately, the data was not available in digital format, so the handling is done by estimations from graphs derived from the website www.dubaicoast.org.

From the British Admiralty information on bathymetry, tidal levels and current velocities is obtained.

Van Oord presented data concerning grain sizes and distributions for all beaches, bathymetric data, and a model to simulate the wave climate at an appointed location called World Waves (further referred to as: WW).

4.3 Bathymetry

Bathymetry is the description of the variation in the bed level of an area relative to a certain datum. On charts for navigation purposes the seabed level is defined relative to CD.

The beach is characterized by more or less parallel depth contour lines, with slopes until the CD -5 m depth contour line of about 1:60. Further offshore very gentle slopes are observed with the CD -10 m between 3 and 4 km offshore.

Two data sources are available for bathymetry:

- Surveys by Van Oord, January – August 2004, profiles can be made from these surveys.
- Admiralty Charts, 1994

4.3.1 Profiles Van Oord

Input files are six DGPS surveys carried out by Van Oord between January and August, creating a XYZ file. The way the surveys were carried out was described in Section 3.2. From these surveys Van Oord made profiles and calculated volume differences for sections of 25 m.

The surveys are presented in *Figure 4.A* in which blue points represent a location where a bottom height was measured. Profiles with a length of 675 m were added in the figure (red). It shows that not for every point of the profile a near survey point was available.

The profiles presented by Van Oord have a length of 250 m and reach a depth between CD -5 m and -7 m. The surveys were made only for the nourished area of the beach. In Chapter 5 a method is presented to obtain profiles from the surveys.

4.3.2 Admiralty Charts

The Admiralty Charts are used for the north part of the beach, where no survey was carried out. The following Admiralty Charts (1994) are used:

- Nr. 3176
- Nr. 3412
- Nr. 3739

Depth lines from the Admiralty Chart are presented in Table 4.1. The distance is positively from the Umm as Suqaym II Marina (reverse of the coordinate system in the nourished area). The length is the offshore distance perpendicular to the baseline. E.g. at the location on the baseline situated 1000 m from the Marina is the CD -5 m, 300 m from baseline.

Contour line	**Location profile at Italian beach**			
	1000	1500	2000	2450
CD -5 m	300 [m]	300 [m]	200 [m]	175 [m]
CD -7.5 m	1500 [m]	1200 [m]	1000 [m]	1500 [m]
CD -10 m	3400 [m]	3150 [m]	2850 [m]	2500 [m]

Table 4-1 Offshore distance from baseline to depth contour line (British Admiralty, 1994)

4.4 Water levels

Short-term water level variation is caused by the astronomic tide, and can be expected due to onshore winds and/or low atmospheric pressure. The extreme water levels for Italian beach occur as a result of tide and storm. Highest water levels occur in this area when the coast is attacked by the Shamal, which is a yearly recurrent storm event, developing over the northwest part of the Gulf and then moving southeast in the course of a few days.

4.4.1 Tide

The astronomical tide along the coast of Dubai is a mixed tide. It is mainly semidiurnal with a strong diurnal component leading to a difference of up to 0.5 m between the two daily high waters (WL| Delft Hydraulics, 2002).

The British Admiralty Tide Tables (1979) and the DM (2004) present data of tidal levels. A discussion on tidal levels is presented in Appendix B.1 and summarized in Table 4.2.

Location	**Tidal levels**						
Italian beach (relative to CD)	LAT	MLLW	MHLW	MSL	MLHW	MHHW	HAT
	0.1	0.5	0.9	1.1	1.4	1.7	2.2

Table 4-2 Tidal levels at Jebel Ali Port (British Admiralty 1979; DM, 2004)

CD in this thesis is 0.1 m under the lowest astronomic tide level (LAT) in the Dubai region. MSL is selected as CD +1.1 m.

4.4.2 Storm surges

Variations in wind and air pressure can cause some difference in the water level, especially in the Shamal season from December to May. High waters levels are expected as a result of these events.

DM presents no data concerning extreme surges. The surge levels are determined by WL| Delft Hydraulics (2001) based on historic events. The extreme water level with a return period of one year is approx. 0.9 m (w.r.t. MSL) and with a return period of ten years around 1.1 m (w.r.t. MSL). They are presented here for completeness, but are not used for sediment computations in the thesis.

4.5 Currents

The currents in the region around Italian beach are produced by various factors. The principal sources and types of currents are:

- Tidal currents
- Wind induced currents
- Wave induced currents

Tidal currents are produced by the tide. Wind induced currents result from local differences in wind and wave transport. Wave induced current originate due the effect of non-oblique wave attack.

The Admiralty Charts indicate current velocities of max 0.5 m/s at a distance of 60 km offshore.

From DM no data concerning current velocity and directions are derived since this was impossible to obtain from graphs. What is seen is that flood induces currents in southwest direction and ebb in northeast direction.

WL| Delft Hydraulics presents current velocities computed with the use of a FLOW model in an 18 day cycle in September 1992 (without the World). This location is approx. 3 km of Italian beach and is marked in Figure 4.1. The water depth at this location is approx. CD – 15 m. The depth averaged velocities are smaller than 0.3 m/s (Figure 4.1).

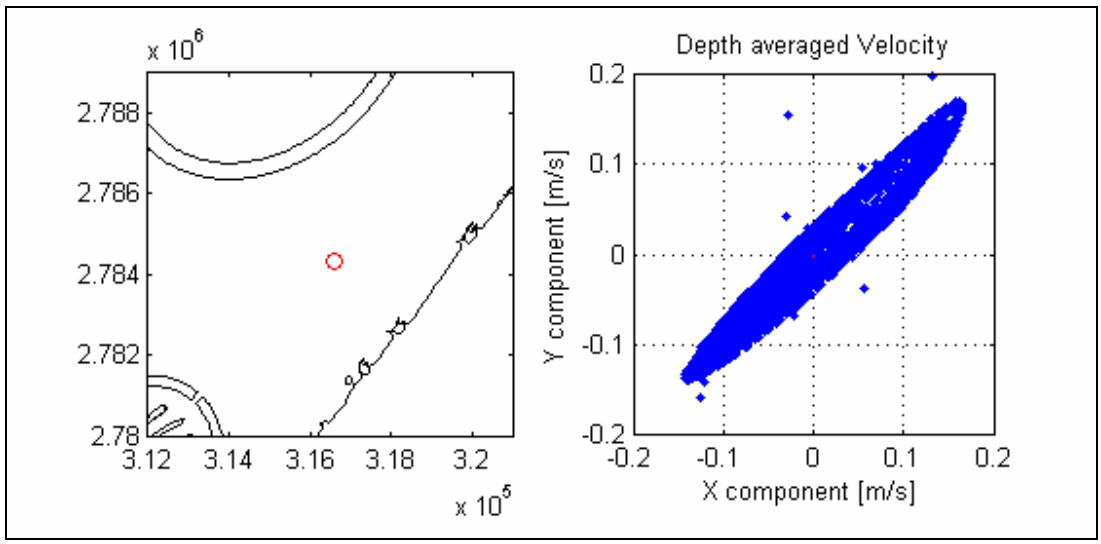

Figure 4-1 location of the current computed point, and depth averaged velocity at this location (WL| Delft Hydraulics, 2004)

4.6 Wave climate at Italian beach

4.6.1 Sources

A normal wave climate consists of sea and swell waves. A wave field under influence of local winds is called “sea”, one not generated by local winds is known as “swell”. As the wave field approaches the coast it is subjected to a transformation due to reduced water depth and coastal forms, changing in height and direction. These phenomena are called refraction, shoaling. Diffraction occurs due to non-uniform beaches and coastal structures.

Two sources are selected for the wave climate at Italian beach. These sources were costless available and contain a time record of the concerning period from January to August 2004, while other sources were averaged over several years. One climate is from the DM Measurement Program. The other is from the program WW.

From these two sources a wave climate for Italian beach must be derived to use for the morphological modelling. A comparison between these sources is made to determine the reliability of the climates.

The DM measures waves 200 m seaward of the T-groyne at Jumeirah beach 2 at MSL -10 m. The position of the measurement point is indicated in *Figure 4.B*. DM presents the occurred significant wave height (H_s), peak period (T_p) and corresponding direction (*Dir*) for every hour (www.dubaicoast.org). Accuracy was lost in these data, because the data was only available in graphical form, instead of a digital record. It was derived by hand for every 12 hours, creating a wave record of 491 observations, representing the period of January to August 2004. Especially the direction of waves lower than 0.5 m was difficult to determine. The direction of higher waves was more accurate, since the graphs had less scatter. The waves at this location were influenced by the Dry-Docks and it lies in the shelter of the World which was under construction in the considered period (the parts above water in May 2004 are shaded in *Figure 4.B*). Difference between the wave climate at Italian beach and at the DM measurement location will therefore exist. An easy adaptation of the DM climate for Italian beach is therefore not possible, but since this is real-occurred data of the considered period, it remains an important source.

The second source is WW. It provides a deep-water wave database of hindcasted time-series from the European Centre for Medium-Range Weather Forecasts (ECMWF) archive and is calibrated by FUGRO oceanor using global satellite and in-situ data. It consists of a 10-year time record of measurements for every 6 hours until May 2004. With the use of SWAN and bathymetry charts, the deep-water wave climate *(three red dots in Figure 4.C)* is transformed to a near shore wave climate at Italian beach at a depth of MSL -10 m *(yellow dot in Figure 4.C)*. The bathymetry at this point and at the DM measurement point is similar. The outcome of the WW model would have been equal as when computed at the DM measurement point since the main coastal features (World and the Dubai Dry-Docks) were not in the WW bathymetry. WW is two times more detailed (derived for every six hours), and has a digital format, but no data are available for the period June-August 2004.

4.6.2 Comparison of the sources

In this section we want to determine the reliability of both climates to use for sediment computations at Italian beach. The climates are considered reliable when the data on the wave height, period and direction correspond reasonably. To make a comparison the data is presented in graphs in *Figure 4.D,* and *Figure 4.E* and analysed in the next Sub-sections. For DM the measured data at MSL -10 m and for WW the data transformed with SWAN to MSL -10 m at Italian beach are compared.

4.6.2.1 Wave records

The records for both climates of the wave height (H_s), Peak period (T_p) and peak direction (*Dir*) *(Figure 4.D.1,2 and 3)* show a good corresponding trend, but some small distinctions were observed.

The record of H_s (*Figure 4.D.1*) shows that the DM peaks were generally higher than the WW peaks in January, while in February the peaks became equal and from March the peaks of the WW were higher than the DM. The low waves (smaller than 0.5m) of the WW data were generally higher than the DM waves.

The time record of T_p (*Figure 4.D.2*) shows that the records of the DM and the WW data corresponded well. Occasionally peaks were measured in the DM climate that not occurred in the WW climate. This could have been local waves that were not measured at the deep water locations of the WW program.

The record of *Dir* (*Figure 4.D.3*) shows deviations in the data. Especially for waves lower than 0.5 m the WW had more scatter than the DM. The lines coincided at waves higher than 1.0 m, in the range between 280 and 300^0.

Above proves that both climates corresponded reasonable. Some deviation was seen for waves lower than 0.5 m. Waves higher than 0.5 m showed good correspondence in height, period and direction.

4.6.2.2 H_s against *Dir* and T_p

Figure 4.E shows H_s against *Dir* and T_p for the DM and the WW climate. What is seen is that for waves higher than 0.5 m the direction and significant wave height coincided well for both climates. For waves lower than 0.5 m the direction of the WW were more scattered, this seems realistic since the direction was scattered in the DM climate too and was difficult to estimate by hand. Other reason was the effect of the Dry-Docks on the data of the DM in the region 0 to 53^0. At Italian beach the Dry-Docks have a limited effect. WW shows that waves from this direction had small heights (<0.5 m). This is according to expectations, since high waves are due to the Shamal that develops in the northwest part of the Gulf.

If we look at *(Figure 4.E.2)* the relation between the wave period and the wave height (wave steepness), we distinguish similar slopes between H_s and T_p. The DM data has a tendency to follow a somewhat steeper slope than the WW data. Waves between 1.0 and 2.0 m have a lower period for the DM waves. This is an indication that the wave steepness of the WW climate is slightly higher. This difference was only minor. Overall the results show good similarity.

4.6.2.3 Energy considerations

Sediment transport is related to wave energy and direction. Wave energy is important for calculations of sediment transport. Both climates are divided into classes of 45^0. The amount of wave energy from each class is presented in *Figure 4.F*. Wave energy can be calculated with Equation 4.1 and 4.2.

$$E = \frac{1}{8}\rho g H_s^2 \tag{4.1}$$

$$F = E \cdot C_g \quad \text{,with } C_g = \frac{1}{2}\left[1 + \frac{4\pi h / L}{\sinh(4\pi h / L)}\right] \cdot C \quad \text{and } C = \frac{L}{T} \tag{4.2}$$

In which:	E	Total mean wave energy per unit area	[J/m^2]
	F	Total mean wave energy transfer in wave direction per unit time and width	[W/m]
	C_g	Group velocity of the wave field	[m/s]
	h	waterdepth	[m]
	L	wavelength	[m]
	C	wave celerity	

Equation (4.1) was used for the comparison of both climates. In *Figure 4.F.1* similarity between both climates is seen. The main driving force was waves from class 270-315^0. The figure shows that the total energy of the WW climate was higher. In the wave records for the wave height it was seen that from March the wave heights of the WW climate became larger than the DM climate. An explanation for this is that due to the influence of the World the measured wave heights at the DM point were reduced.

Equation (4.2) includes the effect of the period (in the wave celerity of the wave field). If the periods of both climates were equal, then the also a difference should have been found for the computations. But, because the periods in the DM climate were overall slightly higher than the WW. No difference in *F* between both climates was seen.

4.6.2.4 Influence of the World

The location of the World and the coastline is presented in *Figure 4.B*. The position of the World was obtained from WL| Delft Hydraulics (2004). The finished part (above MSL) on 31 May 2004 was shaded in this figure (Van Oord). The measurement locations of WW and DM are indicated. Furthermore the mean of wave class 270-315^0 was added. It shows that for this class the DM measurement point is in the direct shadow of the World. So it is reasonable to assume that the World had influence on the wave climate at Italian beach.

Difficulties exist to estimate the influence of the World on the measurements because:

- The influence is different at Italian beach than at DM measurement point.
- Gradual progress of the project in the period
- A wave that approaches the coast will bend around the World and change both wave height and direction before arriving at Italian beach
- Inaccuracy as a consequence of the schematization in the DM climate makes a comparison between the WW and the DM less reliable

Methods to estimate the influence of the World:

- Select a couple of waves of the offshore climate. Assume a relation between wave energy and direction. Compare these waves, with the waves of the WW and DM near

shore. Determine the difference and attribute this to the World. Use this to re-compute the climate at Italian beach.
- Simulations with WW with the World in the bathymetry of the model.
- Factor for H_s for the influence of the World, based on energy considerations

Because of the complexity and inaccuracy of the schematized DM climate, the first option was not carried out, the second neither because the bathymetry of the progress of the World was not available. Therefore the last option was selected. The energy development of the wave-records of the climates was compared. From March to May 30% less energy was present in the DM climate. This will be attributed to the World and will be used as a factor on wave-classes influenced by the World as discussed below. The assumption is that wave direction was not changed.

4.6.3 Wave climate at Italian beach

The DM and WW climates show similarity in H_s, T_p and direction. The World influenced the DM measurements and was likely to influence the wave climate at Italian beach. Highest waves were from direction 270-300^0. The influence of the World at Italian beach for these waves is less than at the DM measurement point. Therefore the WW climate is selected for sediment computations in this research. These data are also more accurate, since they are digitally available and of every 6 hour instead of 12 hour, but not available for the whole period.

A reduction factor of 30 % from March will be used for the influence of the World for class 315-360^0 and 0-45^0. Since wave energy is related to wave height to the second power, the waves of the WW climate from class 315-360^0 and 0-45^0 will be modified according to(4.3):

$$H_{s,Italian} = 1/\sqrt{1.3} \cdot H_{s,WW,nearshore} \qquad \text{for } 315<\text{Dir}(H_s)<45 \qquad (4.3)$$

Figure 4.E.1 shows that waves from these classes were small and had low occurrence. So although the assumption is rough the influence on sediment computations is likely to be minimal.

The WW climate was not available for the months June to August, so the DM climate was selected for these months. The DM measurement point lies in the shadow of the World for waves from class 225-270^0 and 270-315^0. The measured wave height at the DM for these classes will be modified according to(4.4):

$$H_{s,Italian} = \sqrt{1.3} \cdot H_{s,DM} \qquad \text{for } 270<\text{Dir}(H_s)<315 \qquad (4.4)$$

The DM measurement point also lies in the shadow of the Dry-Docks for waves from class 0-45^0, while Italian beach was not. The WW-data in the period from 1997 to 2003 was analysed for this period. It showed that for this region the wave height does not exceed 0.5 m and had very low occurrence. Since no more data was available, waves from this class are neglected for this period (June-August). The assumption is used that waves from class 315-360^0 were not influenced by the World.

DM presents the peak period. This is the inverse of the frequency at which the peak energy in the wave spectrum occurs. The relation between the peak period and the mean period is

based on the shape of the spectra of the wave climate. It goes beyond the scope of this thesis to investigate this shape. But assuming a JONSWAP spectral shape, the relation between the peak and the zero-crossing period (T_z or T_m) is presented in Equation 4.5 (Soulsby, 1997). The WW climate also presents mean wave periods, as used in the computations.

$$T_z = T_m = 0.781 \cdot T_p \tag{4.5}$$

4.6.4 Summary

Good similarity was found in H_s, T_p and direction for both climates for waves higher than 0.5 m. This was seen from:

- Time records January to May 2004 *(Figure 4.D)*
- H_s against T_p and direction *(Figure 4.E)*
- Energy distribution in wave classes of 45^0 *(Figure 4.F)*

The difference of H_s between the climates becomes larger in time, where from March the peaks of the WW record became significantly higher. This was also seen in the energy distribution and is subscribed to the World.

The wave climate at Italian beach between the nourishments will be represented by the wave climate described in Table 4.4. The modifications are based on energy considerations and will be applied to H_s. It is assumed that T_m and direction were not influenced by the World.

Class	January –February	March to May	June to August
$225\text{-}270^0$	WW	WW	DM$\cdot\sqrt{1.3}$
$270\text{-}315^0$	WW	WW	DM$\cdot\sqrt{1.3}$
$315\text{-}360^0$	WW	WW/$\sqrt{1.3}$	DM/$\sqrt{1.3}$
$0\text{-}45^0$	WW	WW/$\sqrt{1.3}$	-

Table 4-3 Wave climate at Italian beach

4.7 Wind

Wind information is derived from DM and of WL| Delft Hydraulics (2002). It can cause currents, water level differences and aeolian sediment transport on the dry-beach. At Italian beach hardly any dry-beach width was present; therefore this information will not be used for computations, but will be presented for the sake of completeness.

From observation from data, a few trends are distinguished:

- A land-sea breeze pattern, the wind was directed seaward in the night (around 135^0), and landward during the day (around 300^0).
- Wind speeds were around 7 m/s during day and 2 m/s at night.
- Maximal wind speeds (storms) reached up to 11 m/s and often lasted for three days, these are storm events.
- Storm events took place on 20 January, 07 February, 15 Mar, 1 Apr, 18 Apr, 05 May and 29 May 2004.
- These storms came from a direction between 225-300^o and are locally referred to as Shamal events.
- Wind speeds higher than 15 m/s were not recorded in the period from January to August 2004.

4.8 Closure depth

The seaward limit of effective profile fluctuation over long-term (seasonal or multi-year) time scales is referred to as the "closure depth," denoted by h_c. Although the waves can move sediment seaward of this depth, the net transport does not result in significant changes in mean water depth (Dean 2000).

The closure depth (h_c) can be determined based on:
- Visual observations based on bathymetric.
- Empiric approaches based on the wave climate.

The bathymetric data of the Italian, Madinat Jumeirah and Glass Palace beach was analysed. The conclusion is that the offshore closure depth of the 6 beach profiles between January 2004 and May 2004 is approx. CD - 6.0 m.

Based on the Shields parameter Hallermeier (1981) defined a condition for sediment motion resulting from relatively rare wave conditions (Equation 4.6).

$$h_c = 2.28 \cdot H_e - 68.5\left(\frac{H_e^2}{gT_e^2}\right) \qquad (4.6)$$

In which:			
	h_c	closure depth	[m]
	H_e	Effective significant wave height exceeded only 12 hr per year	[m]
	T_e	Effective significant wave period exceeded only 12 hr per year	[s]

Birkemeier (1985) evaluated the Hallermeier relationship and approximated the closure depth:

$$h_c = 1.57 H_e \qquad (4.7)$$

The corresponding closure depth is presented in Table 4.5. The effective wave height and period exceeded only 12 hr/yr was calculated by computing the wave climate of Italian beach over a period from January-August 2004, of which the 12 hr/yr exceedance chance is determined as in *Figure 4.G.*

Method	Result h_c [m]
Hallermeier	5.0
Birkemeier	3.8

Table 4-4 Results closure depth computations, (H_e; 2.4 m, T_e; 9.2 s)

From above the conclusion is drawn that the closure depth is between CD – 3.8 m and CD - 5 m. But because movement was observed deeper, a closure depth of CD – 6.0 m is assumed in this thesis. This will be tested with numerical modelling of the cross-shore transport, with UNIBEST-TC (Chapter 9).

4.9 Sediment characteristics

Van Oord took sand samples at Italian beach after finishing the nourishment one sample on 28 December 2003 and samples 1 to 9 on 12 April 2004. Van Oord took sand samples with a 75 cm sampling-tube as far inshore as possible at low tide, usually at the plunge point. This is according to the guidelines described in CUR 130, Manual on Artificial Nourishment. Sieve curves are made of the samples showing the percentage of sand that passes a certain sieve size. These curves are presented in *Figure 4.H.*

Information on the location of the December sample was not available. The location of the other 9 samples is shown in Appendix B.2. Samples one to five were taken on the nourished and six to nine on the unnourished area.

Smaller particles will be transported more easily than the coarser under the influence of attack. So a location under attack of erosion has its fine sediments washed away and transported with the longshore current further updrift, while the coarser parts remain at the erosion site.

This pattern was seen in the unnourished section *(Table B.3)*, sample 7 is the most coarse and after that respectively 8, 6 and 9. In the nourished section samples 1 to 5 show difference. Sample 3 is the coarsest (D_{50}; 810 µm) and sample 4 the finest (D_{50}; 350 µm). Sample 1, 2 and 5 become respectively finer, with a D_{50} around 550 µm. So on a local scale, more phenomena have to be taken into account (i.e. coastline orientation). This can partly explain the distribution, but also uncertainties in collection and interpretation of the samples have to be taken into account.

The mean size that is passed by 50 percent of the particles ranges between 250 µm and 900 µm. The median size of all samples can be considered as representative for the whole beach and the nourished section and is presented in Table 4.5. Grading in all samples between D_{50} and D_{90} is about 1:2. Different approaches exist to calculate the fall velocity of the sediment. These approaches are described in Appendix B.2.2 the velocity used in this thesis is listed in Table 4.5.

Sample	D_{10} [µm]	D_{50} [µm]	D_{90}[µm]	w_s [m/s]
Mean	260	550	1100	0.09

Table 4-5 Distribution of the representative sediment distribution (source: Van Oord and CEM)

4.10 Conclusions

There is a lot of reliable information available for the boundary conditions of Italian beach. Bathymetry is derived from surveys of the nourished area and nautical charts. The tide is semi-diurnal, with CD at lowest astronomical tide and MSL at CD + 1.1 m. Normal amplitude of the tide is about 0.6 m. Currents have small velocities and up to 0.3 m/s at CD –15 m. The wave climate for January to August 2004 at Italian beach is derived from the program World Waves and verified with measurement by the Dubai Municipality. The closure depth is assumed at CD –6.0 m. Information from samples on sediment characteristics varied, a D_{50} of 550 µm will be adopted for Italian beach. In addition, information on wind and storm surges was presented for completeness.

5 Analysis of the survey data of Italian beach

5.1 Introduction

In this chapter a detailed analysis of Italian beach will be presented. The brief analysis in Section 3.3.3 was based on processed data of Van Oord. For the study more data became available.

In Section 5.2 the method of placement is described. In Section 5.3 some remarks about the surveys are made. In Section 5.4 the total volume difference of sand is calculated based on the Van Oord calculations and a method is presented to obtain deeper profiles out of the surveys and a new analysis of the data is performed. In Section 5.5 the movement of the coastline in time is discussed. In Section 5.6 six representative profiles in the nourished area are analysed. Finally, Section 5.7 presents conclusions of the analysis of the survey data of Italian beach.

5.2 Placement

The placement of the sand at Italian beach was done hydraulically. At the borrow site, which is a few kilometres offshore, the sand was lifted from the bottom by a trailing hopper suction dredger and sailed to the near shore. Here the ship is connected to a floating line that becomes a sinker line, with which it was discharged to the beach. This started on Dec 20th 2003. Earth moving equipment spread the sand along the beach. The total volume of nourished sand was approx. 114,000 m^3. The placement was on the beach and on the foreshore.

5.3 Surveys

The surveys are presented in *Figure 4.A*. It shows that in the Post- and February-survey a large area near the marina (Section 625-675) was not surveyed. Van Oord calculated the bottom height here by interpolation between existing points in the profile. In *Figure 3.C* it was seen that not every profile (with a length of 250 m form the baseline) coincided at the toe. This was an indication that transport had taken place deeper. Longer profiles can be made using the GPS-data to investigate this. The maximal lengths of profiles that can be obtained from the GPS-surveys are listed in Table 5.1. All 6 surveys have limited points at the land side in Section 25-125

	1 Jan	**11 Feb**	**4 Mar**	**27 Mar**	**9 May**	**6 Aug**
Length from baseline [m]	650	450	375	300	400	400

Table 5-1 Length of the surveyed area perpendicular to the baseline

The equipment for the onshore survey had a vertical accuracy of 5 cm and the hydrographical part a vertical accuracy of 15 cm (source: Chief surveyor Van Oord). This was due to the use of a single beam to measure bathymetry, and correction methods for the

reference level (CD), increasing water depths, and wave action. A measurement was made for every 10 m^2 (26,000 points available in an area of approx. 700 m by 400 m).

5.4 Volume change

5.4.1 Van Oord calculations

The volume calculations made by Van Oord were based on the 27 profiles of the beach with a length of 250 m. Of each profile the area difference w.r.t. the Post-survey was calculated. This area was multiplied with the width of the cross section that it represented (25 m or 12.5 m). This gave the volume difference with respect to the Post-survey (1 January 2004). When cumulating all 27 profiles, the total volume that disappeared with respect to the Post-survey is acquired. The result is listed in Table 5.2 in which post is referred to the survey carried out directly after the placement.

	Post, 1 Jan	**11 Feb**	**4 Mar**	**27 Mar**	**9 May**	**6 Aug**
Volume w.r.t. post (m^3)	0	-16,100	-26,000	-48,400	-25,600	-36,800

Table 5-2 Volume difference in the nourished area with respect to the Post-survey (profile lengths of 250 m)

5.4.2 Method for further analysis

It was seen that the results of the Van Oord calculations showed inconsistencies. Deeper profiles are required to make volume computations for Italian beach. Moreover more insight is required in the way that these volumes were calculated. Therefore a method is made to obtain profiles from the surveys as described below:

- On the baseline 27 profiles are defined with a mutual distance of 25 m. Profile 25 is most downstream (north) and profile 675 is at the marina. Within the profile a x- and y-coordinates are defined for every 5 m
- To find the bottom height of these points, the nearest point in the GPS survey within a certain distance (*D*) is searched and its bottom height adopted
- If no nearest point is present in the survey data, then the bottom height is obtained through linear interpolation between existing points.

The selected distance from within the z-value is adopted is 2.5 m. The volume differences are within 2%, for *D* is 2 m. Too few GPS survey points for *D* is 1.0 m were found and therefore the profiles were not representative. With this script the sediment balances can be made in the same method as Van Oord (Section 3.2).

The profiles presented by Van Oord show that the land section of the 27 March survey is about 1 m lower than all other surveys (incl. Post and Aug-survey), also some discontinuity in the connection between land and sea was seen. After review it is concluded that the survey of 27 March was probably not carried out correctly and therefore will not be further used. This was confirmed by the chief surveyor of Van Oord. The other surveys were correct.

5.4.3 Volume computations

Table 5.3 presents the values for the volumes of sand that was eroded since the Post-survey. This is done for three different profile lengths; 250 m, 400 m and 450 m, because as seen in Section 5.3 no survey was carried out further offshore.

Profile length	1 Jan [m^3]	11 Feb [m^3]	4 mar [m^3]	9 May [m^3]	6 Aug [m^3]
250 [m]	0	-16,600	-30,800	-30,400	-39,900
400 [m]	0	-11,200	-28,500	-18,600	-31,300
450 [m]	0	-8,600	-28,500	-16,200	-29,900

Table 5-3 Volume difference in the nourished area between the post and the survey (profile lengths of 250, 400 and 450 m)

The calculations by Van Oord for 250 m profiles (Table 5.2) did not differ substantially from the above 250 m profiles (Table 5.3), only the 4 March and 9 May volumes were slightly higher. Increasing the length of the profiles led to different results: The volumes in all surveys decreased. This means that in reality transport took indeed place to lower parts that is not in the Van Oord calculations.

For the computations a 400 m profile will be selected, because all surveys have sufficient measurement points within this length.

What is striking about these results is that in the period from 4 March to 9 May no erosion (as expected) had occurred. The waterline is defined as the distance from a base point, calculated as the area between MSL +0.5 m and MSL -0.5 m in the profile, divided by the height difference (is 1.0 m). If we look at the land and underwater part separately, then the following results are obtained:

Part	1 Jan [m^3]	11 Feb [m^3]	4 Mar [m^3]	9 May [m^3]	6 Aug [m^3]
Above waterline	0	-9,000	-9,600	-14,700	-14,700
Below waterline	0	-2,200	-19,000	-3,900	-16,600

Table 5-4 Volume difference in the nourished section between the Post-survey above and below the waterline

These result shows that in the part above the waterline more material eroded in time, but came to a halt between May and August. It also shows that not taking the underwater part near the marina into account in February has a large influence on the result. It shows that the increase between March and May was in the part under water.

Possible explanations for the accretion in the under water part between March and May are:
- Increased wave action from northern direction
- Bypass, natural or artificial
- Uncertainties in Section 25-125 and 625-675
- Uncertainties or errors in the surveys

Increased wave action from the north:

This period was still in the Shamal season, with waves from the direction northwest. The amount of wave energy was slightly less in March than in February, April and May. The direction from all waves in this period higher than 1.0 m that contain this energy was from the region between 290^0 and 300^0 (Figure 5.1). The highest wave from a more northern direction is smaller than 1.0 m, and had a very low occurrence. The coastline orientation is 305^0, measured as the direction of the seaward directed coast-normal clockwise relatively to the North (Source: Admiralty Charts, Satellite images, WL| Delft Hydraulics 2003). So a northward transport and consequently erosion was expected in stead of accretion.

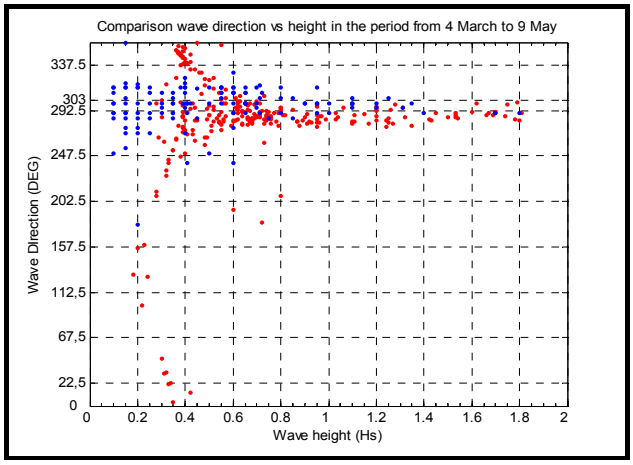

Figure 5-1 Waves heights and directions of the WW and DM climate between 4 and 27 March

Bypass

No artificial bypass has occurred in this period. Natural bypass along the updrift marina might have been the case. Natural bypass occurs during very high waves, and has a local effect on bathymetry. This has to be kept in mind, when looking for natural bypass.

Uncertainties in Section 25-125 and Section 625-675

When only points are compared that are present in all sections, the land part in Section 25-125 and under water near the marina (Section 600-675) will not be taken into account. The results are presented in Table 5.4.

Profile length	1 Jan [m^3]	11 Feb [m^3]	4 Mar [m^3]	9 May [m^3]	6 Aug [m^3]
400 [m]	0	-11,800	-20,100	-8,400	-22,300

Table 5-5 Difference volume in the nourished area between the post and the survey (profile lengths of 400 m where points are present in all surveys)

This proves that the results are partly influenced by the unsurveyed area. Especially Section 600-675 had a large influence and led to a difference of about 10,000 m^3 in March, May and August. But we expect erosion in this section and therefore continue to take this into account in the calculations (through interpolation between existing points).

Uncertainties or errors in the surveys
A measurement error of 10 cm leads to a volume difference of 27,000 m^3. So measurement uncertainties have to be kept in mind when looking at these data.

5.4.4 Sediment balance of the nourished area

A sediment balance for each profile provide insight in the way that these volumes are calculated. The discussion of the sediment balance in Section 3.3.3 was based on the Van Oord material. Now, more data is available and profiles have a length of 400 m (maximum length for which sufficient bottom height data could be obtained from the surveys). The sediment balance is presented in *Figure 5.A*. On the x-axis is the profile number, with 675 at the marina and 25 most downstream. On the y-axis is the volume of eroded or accreted sand per 25 m. The lines indicate the volume difference w.r.t. the Post-survey.

What is seen in the sediment balance is that in the period from 1 January to 11 February a large change immediately settled in. This was the reaction of the nourished area to several storm events in January and the beginning of February. After this period it is seen that all sections had a slower erosive trend. In the 11 Feb-survey a trend of erosion at the marina and accretion down drift is seen. These trends are present in all surveys. Some accretion in Section 25-250 occurred. Based on the available material it is assumed that this was still in the nourished area. This was probably sand that was transported from the area near the marina.

In the 4 Mar-survey similar trends as in the Feb-survey are seen *(Figure 5.A)*. Only in Section 625-675 more erosion is computed, this is because in this survey the area near the marina was surveyed. Over the whole width of the beach more erosion took place. In profile 150 all surveys meet, in this point no erosion has occurred in the whole period.

The volume of sand increased between the 4 Mar- and 9 May-survey. If we suppose some natural bypass from the marina, then this sand was likely to be found in Section 575-675. The sediment balance *(Figure 5.A)* shows that more sand was lost here in this period. In the rest of the beach in Section 25-575 the May survey had structural less erosion and more accretion. So no specific sections can be distinguished for the increase; it was structural in the May-survey over the whole nourished area.

The total volume of eroded sand in the survey on 6 August was slightly more than the survey on 4 March. The sediment balance *(Figure 5.A)* shows that this increase was found in Section 625-675. In Section 250-625 the erosion was slightly less than the 4 Mar-survey, indicating some accretion. The increase of material in section 0-250 was less than before indicating erosion of this section.

5.4.5 Conclusions

The sediment balance in *Figure 5.A* showed how the material was distributed over the nourished beach. Over the whole period it showed an erosive trend. This trend was disturbed in the 9 May survey. This increase was not likely due to the physical processes as bypass, or increased wave action from northern direction. Another explanation could be that this was due to transport further offshore than 400 m. But, this was not likely since the profiles

generally coincide at the toe and were deeper than the estimated closure depth. If we assumed by-pass, then we expect to see increase at the toe of the profiles. This was not seen, but in the next section some profiles will be further analysed.

Computations were made:
- Parts of the beach
- The underwater area
- Different interpolation methods

But all computations showed a similar result (an increase between March and May). Another possibility could be uncertainties in the measurements. An inaccuracy of 15 cm in the hydrographical survey leads already to a volume difference in one profile of 3,000 m^3. Some scatter in the results can therefore be expected.

But when looking at the volume differences still an erosive trend is discovered. When adding a trend line (Figure 5.2), we see that the total volume decreases with 30,000 m^3 to 40,000 m^3 in the period January to August 2004.

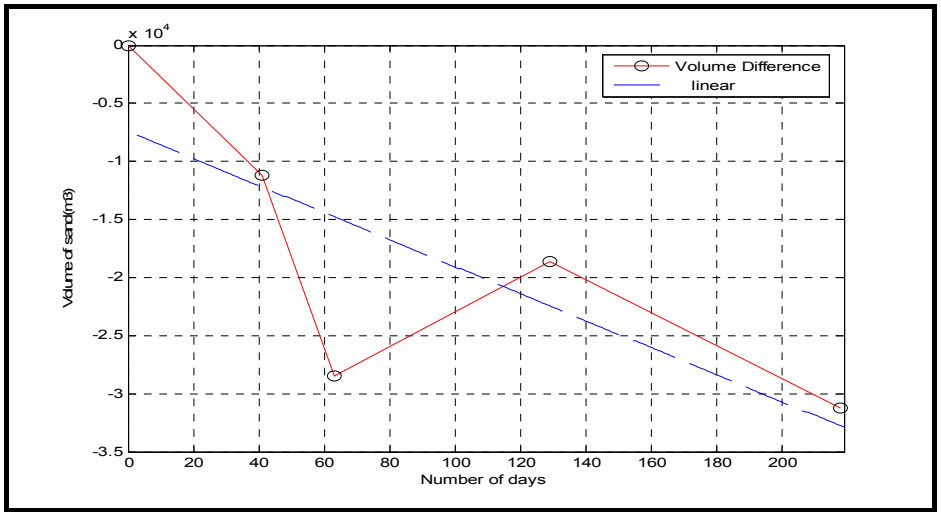

Figure 5-2 Volume difference development with respect to the Post-survey

5.5 Shoreline regression

Shoreline regression is also an indication of the behaviour of the nourishment, where the shoreline is defined as MSL. Uncertainties in measurement of water depths have less impact on the results. In *Figure 5.B*, the shoreline position of the surveys is presented. On the x-axis is the profile number and on the y-axis the position of the coastline. What is seen is that the coastline gradually retreats in the time. This is according to expectations.

The 1 Jan-survey (Post-survey) was made directly after the nourishment. It shows that the beach width was extended up to 50 m. Between January and February the shoreline retreated very fast. The nourishment was constructed steeper than the natural equilibrium slope of the sand for this beach, so redistribution took place from above to under water. This caused the shoreline to retreat, while no volume is lost. This phenomenon is also seen in the

profiles, and discussed in the next section. Remarkable is that in Section 25-100 the beach had temporally slightly accreted.

Redistribution within the profile continued up to August. Background erosion due to longshore processes had also effect on the shoreline position. Directly at the marina some regression occurred but here still a substantial beach width remained. Most severe regression of approx. 40 m was in Section 200-600. The sediment balance did not show most erosion outside Section 500-675. This leads to the conclusion that cross-shore processes also influence the beach width.

5.6 Profiles

In this section six profiles are analysed. The selected profiles represent the areas. These are, Profile: 50, 200, 300, 450, 550 and 650. Profile 650 is located nearest to the marina. On the basis of the discussion of these profiles several trends about slopes and behaviour of the nourishment are derived in Sub-section 5.6.7.

5.6.1 Discussion of the profiles

Profile 50

Profile 50 (*Figure 5.C*) is located 650 m updrift from the marina. The original nourished slope of the part above MSL was 1:16; it is seen in this profile that although the nourishment was constructed above MSL it had spread out under water to CD -2 m. The Feb-survey shows that accretion took place above water as well as under water. Above water a somewhat milder slope was created, after February this became steeper to about 1:7 and retreated in time with this slope. Around CD mild slopes were created in time to resist wave action and this part was in May even further retreated than before the nourishment. Below CD a large increase took place in February, mostly sediment from near the marina. After February not much movement below CD is seen. The under water slope was about 1:30. The profiles coincided well at CD -5 m.

Profile 200

A similar pattern as in profile 50 is seen in this profile (*Figure 5.D*). Above CD material was transported away while under water accretion took place. The slope of the nourishment was 1:20 and became steeper above MSL to 1:7 in February. After this, the part above CD gradually retreats in time with this slope. Around CD steeper slopes as in other profiles (1:50) were created and further below CD a slope of about 1:20 is seen. The surveys coincided at the toe at a depth of CD -4 m. The accretion under water was less than in Profile 50.

Profile 300

In profile 300 (*Figure 5.E*), erosion took place above CD. The initial slope of the nourishment above MSL was 1:15. In February this became steeper to 1:5. After February the shore retreated in time with this slope. Around CD milder slope were generated, in May

and August the mildest slopes are seen (1:70). Accretion under water occurred, but was not very large. Under water at CD -5 m a small berm was created in February that was not present in the January profile, caused by cross-shore transport from higher parts. This berm was also seen in profile 200, but not in the Post-survey of profile 300. In time only very small movement under water is seen. The profiles coincided at CD -6 m.

Profile 450

In profile 450 (*Figure 5.F*), the initial slope of the nourishment above MSL was 1:12. In March this steepened to 1:5. After March the shore retreated in time with this slope. Around CD large movement occurred: A small berm was created in March as also seen in profile 550. This berm disappeared after March. Below CD sediment was transported from the upper part. It is seen that the profile accreted here with respect to the Post-survey. The under water slope became approx. 1:20. Accretion also occurred at the toe of the profiles. The developments in time under water were small. The profiles coincided at CD -6.0 m.

Profile 550

In profile 550 (*Figure 5.G*), the initial slope of the nourishment above MSL was 1:16. In March this became steeper to 1:5. After March the shore retreated in time with this slope. The erosion of the nourishment in this profile was almost over the full length of the profile, so not only limited to the zone above CD as in the profiles more down drift. Slightly under water some very small accretion occurred, this was probably some transport from the upper part. Further under water to a depth of about CD -6 m the initial profile eroded. In February, the slope was about 1:18. At the toe of the profile at CD -6 m the profiles did not coincide, and some more accretion is expected here.

Profile 650

This profile (*Figure 5.H*) is located 50 m from the marina. The nourishment retreated in time over the whole length of the profile, but the Post-survey was interpolated between CD and CD -5 m.. The nourishment was constructed with a slope of 1:30. Above CD the slope became steeper in March, 1:7. The part above MSL retreated in time with this slope. Around CD in other profiles milder slopes are seen but here neither. From CD to CD -6 m the slope was about 1:35. The profiles coincided at 400 m, but the profiles have a different slope at the toe. The possibility exists that the hole between 400 m and 600 m was filled with material from the upper section. This can not be proved, since no survey was carried out in this area.

5.6.2 General trends

General trends in these profiles are that above CD the slope of the nourishment was constructed with a slope of about 1:20 until CD –2 m. After the nourishment this slope became rapidly steeper in time until in March it reached a slope around 1:6 and the sand was redistributed to a depth of CD –4 m. After March it retreated gradually in time with this slope. Erosion was seen in all profiles above CD.

After the placement no slope difference of the profile around CD was seen. But after the placement the slopes became much milder around CD: The natural reaction of the beach to resist wave action. It had a large variation in time; sometimes even a small berm was created. (i.e. profile 50). This behaviour was seen in all profiles except for profile 650.

Downstream in Section 50-450, an increase of material was seen between CD and CD -4 m. This was sediment from above CD and from upstream. The nourishment was constructed with a slope around 1:25. This became also steeper in time to around 1:20 in August. In Section 50-550 at CD - 4 m a berm was shaped. In Section 550-650 no increase under water was seen. Here all material was transported away.

5.7 Conclusions

It was concluded that the survey of 27 March was not carried out correctly. Moreover the volume computations by Van Oord were based on a length of 250 m with an insufficient depth to CD -5 m, while transport took place at deeper depths.

A method was made to make profiles with a longer length of 400 m, because the surveyed area was to about 400 m offshore. The toe of these profiles coincide better. From these profiles volume differences w.r.t the Post-survey were calculated. Between 4 March and 9 May the volume did not have erosion. Several possibilities were investigated, but no indications were found to explain this physically. Overall an erosive trend was seen and the volume of eroded sand was about 30,000 to 40,000 m^3 in the period from January to August 2004.

As expected the shoreline retreated in time, this regression was initialised by the transportation of sediment from above CD to lower parts, the equilibrium process. The profiles show that the nourishment was constructed with a slope of 1:25 above CD and became steeper to 1:6. Around CD very mild slopes were created, and if accretion occurred within a profile, this took place below CD.

6 Italian beach model

6.1 Introduction

In this chapter it is explained how Italian beach is modelled. Section 6.2 describes which software package was selected, the objectives and stages of the modelling. Furthermore an overview of how simulations are made is presented. Section 6.3 describes the input- and parameter-settings. In Section 6.4 the model will be calibrated, based on stored volumes and equilibrium angles. The calibrated model will be verified in Section 6.5 and subjected to a sensitivity analysis in Section 6.6. Finally in Section 6.7 the conclusions and recommendation will be presented.

6.2 Set up of the model

6.2.1 Introduction

Various software packages are available for numerical modelling of nourishment. The selection of the most suitable package depends on the objectives of the study. Three types of packages are available (Section 2.4).

For this study, it was decided to use the UNIBEST software package. UNIBEST-CL+ (UNIform BEach Sediment Transport) is a coastline model that can be used to model longshore processes. The reasons to use this package are:

- The availability of this package and the wide experience in the application for various morphologic studies
- Interest of the participating parties (WL| Delft Hydraulics, Van Oord) to determine the strong and weak points of this model for short-term predictions

6.2.2 Objectives

The model has the following objectives:
- Hindcast of the nourished area at Italian beach for the period January to August 2004
- Analysis of the UNIBEST-CL+ software package: Assessment of the performance to make short-term predictions with a coastline model
- Optimization and suggestions for future nourishments

6.2.3 Model overview

The UNIBEST-CL+ consists of two integrated sub-modules:
- The Longshore Transport module (LT-module)
- The CoastLine module (CL-module)

The required longshore sediment transports are computed with the LT-module. These transports are used by the CL-module to perform coastline evolution simulations.

In LT-module approximates the change of the transport rate due to a reorientation of the coastline by computing the volume transport *(Qs)* for a number of coast angles, an S-φ-curve. This is based on the offshore wave climate, parameter settings and cross-shore profiles. Thus the transport rate becomes a function of which the values depend on the actual orientation of the coastline.

In the CL-calculations the functions from the LT-calculations are used to compute coastline changes due to longshore sediment transport gradients. The transport rates on the user-defined grid points are calculated as a result of the coastline orientation. Gradients in these rates cause erosion or accretion. The erosion or accretion causes progression or regression of the coastline with a rate based on the active profile height (defined in the LT-calculations). In the next time step, the new coastline orientation is calculated with the accompanied rates, stored volume, and corresponding coastline position.

The full overview of the formulations and mathematical descriptions of the UNIBEST-CL+ software package are presented in Appendix C.

6.2.4 Stages of modelling

A number of stages have to be executed when UNIBEST-CL+ is applied, each important for the quality of the results. These stages are presented in the schematisation of Figure 6.1. In this figure a loop is added, marking the iterative process of the modelling. When the model has satisfactory results, the optimization process can be started.

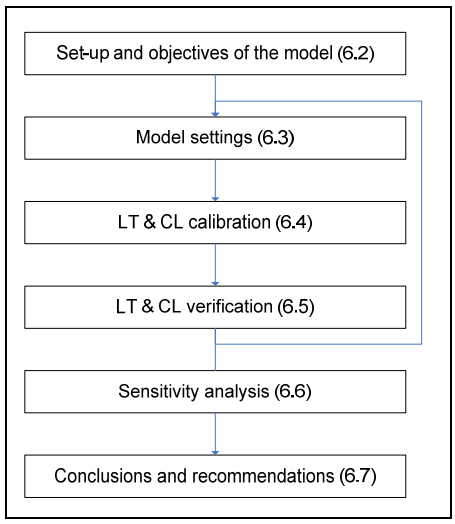

Figure 6-1 Stages of modelling including backward loop marking the iterative process of the modelling

The Post-model is the model where the coastline position and profiles in the nourished area was obtained from the Post-Survey (1 Jan 2004). This model is used for calibration and verification.

6.3 Post-model settings

6.3.1 Basic Model

Figures 6.2 and 6.3 present the Post-model. The model runs from the Umm as Suqaym II Marina to the Umm as Suqaym I Marina. The beach has a length of 2450 m. The baseline is the seawall of the beach and has an angle of 310^0N, measured as the direction of the seaward directed coast-normal clockwise relatively to the North. It is the same as used by Van Oord and in the data-analysis, but extended over the whole beach. Points are selected on this baseline, where the coastline is defined. The coastline is MSL of the Post-survey. In the unnourished area it is derived from satellite images of 2000, 2001 and 2003.

On the baseline is the revetment (marked with green dots) with a length of 700 m behind the nourished area.

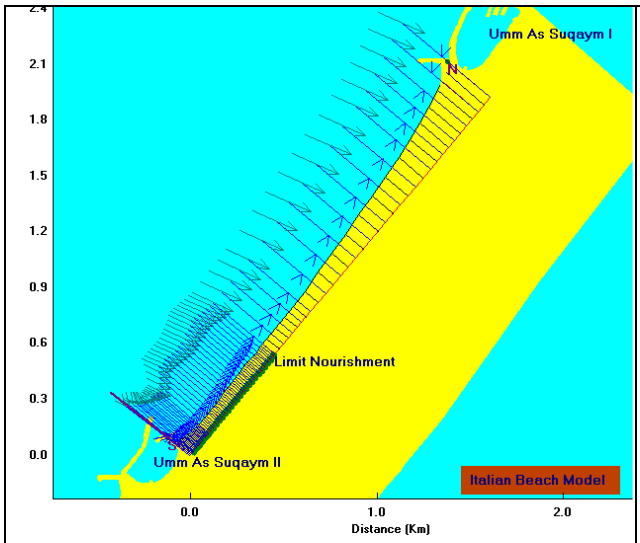

Figure 6-2 Graphic Overview Post-model

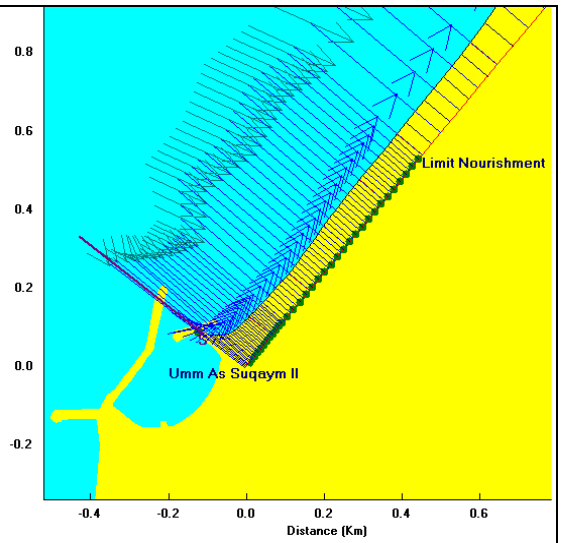

Figure 6-3 Nourished area in the Post-model

A boundary condition can be implied on the left border or right border of the model. For Italian beach this is defined at the left border with an incoming transport (Q_s) of zero (m^3/ yr). Possible sedimentation of the marina is not taken into account.

The total simulation time is 215 days, from 1 January to 6 August 2004.

6.3.2 Wave and Current scenario

The input for the LT-calculations is the wave climate at Italian beach, defined in Section 4.5. This wave climate is based on the measured climate of the DM and the verified climate of WW and includes the effect of the World. The adjusted wave climate is implemented at the sea boundary at a depth of MSL -10 m.

This wave record from January to August 2004 is categorized in classes of 0.25 m *(H_s)*, with corresponding mean period *(T_z)*, and directions (classes of 45^0). This accompanied with a percentage of occurrences (in days).

The effect of the Umm Suqaym II Marina is taken into account by applying a diffraction scheme around a structure, derived from Kamphuis (1992). This scheme is presented in Appendix C.4. This scheme is applied on the 1 km coast near this Marina. The non-diffracted climate is selected for the rest of the beach, since the effect of the marina became very small. The Umm as Suqaym I Marina is not taken into account in the modelling, since main interest is in the behaviour around the nourished area.

Current velocities are very small (within a margin of 0.2 m/s at a depth of CD -15 m, Chapter 4) and no significant asymmetry was found between currents during high and low tide. Although currents might have a local effect at the marina, it is not taken into account in this model. This influence is investigated in the sensitivity analysis (Section 6.6).

The water level is selected constant with CD +1.1 m.

6.3.3 Cross-shore profiles

The selected profiles are derived from the Post-survey. In the nourished section eight profiles are defined, with a mutual distance between 25 and 150 m. For these profiles the diffracted wave climate is calculated. Outside the nourished area a profile is selected for every 500 m.

The ‘dynamic area’ is the ‘active part’ of the profile. It is defined as the horizontal distance from baseline to closure depth per unit width. The sediment area (truncation transport) is the same. The active profile height is the height within accretion or erosion will be computed (height between closure depth and top of the dune). The selected closure depth is CD - 6 m, where hardly any bottom movement was seen in the data. The berm height varied around CD +4 m. So an active profile height of 10 m was selected.

For every defined profile a transport ray is calculated in UNIBEST-LT for a coast orientation of 305^0N (Baseline is the seawall with a orientation of 310^0N). This orientation is found in the middle of Italian beach (Source: satellite images and WL| Delft Hydraulics, 2003).

6.3.4 Parameter settings

There are two types of parameters that are used in UNIBEST-CL+, wave and transport parameters. To calculate the volume of sediment transport, the method of Bijker (1971) is adopted (Appendix C.3.3). This is a reliable and widely applied method.

For all parameters default values were used. Only the coefficient of wave breaking is 0.7 (See Appendix C.5) and the sediment characteristics are changed(presented in Section 4.9).

The parameter settings of Table 6.1 will be used for calibration.

Type	Input parameter	*Symbol*	Value	
Wave	Coefficient for wave breaking	γ	0.7	-
	Coefficient for wave breaking	α	1	-
	Coefficient for bottom friction	f_w	0.01	-
	Value of the bottom roughness	k_b	0.1	m
Transport	Median grain diameter	D_{50}	550	µm
	90% grain diameter	D_{90}	1100	µm
	Bottom roughness	k_b	0.1	m
	Sediment fall velocity	w_s	0.09	m/s
	Criterion deep water	H_s/h	0.07	-
	Coefficient deep water	b	2	-
	Criterion shallow water	H_s/h	0.6	-
	Coefficient shallow water	b	5	-

Table 6-1 Parameter settings of the calibration stage

6.4 Calibration of the Post-model

6.4.1 LT-calibration of the Post-Model

For the sections the transport capacities and equilibrium angles are presented in Table 6.2. In contradiction to normal reference, point zero is located at the marina. Point 25 is situated on the baseline, 25 m from point zero etc.

Points	Transport capacity Q_s [m^3/yr]	Equilibrium angle [^{0}N]
0	-5,400	325.28
25	-3,800	314.84
50	800	303.64
100	20,500	294.93
150	27,000	294.66
250	35,800	294.42
400	43,700	294.21
550	48,800	294.24
650	50,900	294.24
700	50,900	294.24
1000	53,100	294.21
Undisturbed	58,000	294.07

Table 6-2 Results LT-calibration

The calculated values in Table 6.2 have the same order of magnitude as the survey data where at the border a transport of (7/12 * 50,900 m^3 ≈ 30,000 m^3) is transported. From the data is was 30,000 to 40,000 m^3 in 7 months was found. It is seen that behind the inner breakwater of the marina (Points 0 and 25) the transport is directed in southern direction (negative). The further downstream of the marina the more the transport capacity increases, because of the diminishing influence of the marina on the wave climate.

An equilibrium angle is an angle with respect to the coastline orientation, for which the net longshore transport is zero. The calculated equilibrium angle for the undisturbed situation is about 294 ^{0}N. This equilibrium angle should also be found near the Umm as Suqaym I Marina. This equilibrium angle is added in the satellite images of 2001, January and October 2003 (Figure 6.4). In the first image also the 305 ^{0}N coastline is presented.

Figure 6-4 Equilibrium angles at Marina Umm as Suqaym I (in order: 2001, Jan 2003, Oct 2003)

Near the spur, the equilibrium angle is larger because of local diffraction and sheltering. But Figure 6.4 proves that slightly updrift this angle could be found. This also proves that bypass is most probably limited at the marinas. But this method is not very accurate and therefore no conclusions are drawn based on this angle. But satisfactory results are obtained and the calculated equilibrium angles of the model are acceptable.

Conclusions of the LT-calibration of the Post-model are:
- Same order of magnitude of transport capacity as the data.
- Similar equilibrium angle for the undisturbed beach as the satellite images

6.4.2 CL-calibration of the Post-Model

Goal of the CL-calibration is to find transport volumes comparable with the volumes calculated in the data analysis. The volume of sand in the nourished area decreased approx. 32,000 m^3 in the period for January to August 2004 (Section 5.5.3).

With above parameter settings the volume loss in the nourished area was 38,000 m^3. To obtain the same volume as in the data analysis, calibration is needed to decrease this loss with 6,000 m^3. The UNIBEST-CL+ manual (1994) suggests calibration on the basis of the bottom roughness. The bottom roughness (*KB*) is related to the under water ripple height, which is difficult to measure and to estimate. Instead of the default value of 0.1 m, *KB* is increased to 0.18 m. The stored volume becomes -31,900 m^3.

Another method of calibration is with the equilibrium angles in the S-φ curves. Small adjustments of the equilibrium angles are possible, since the direction of the mean energy of each wave class is probably not equal to the mean angle of the wave class. Here, they are decreased by two degrees. This gives with the same original coastline less transport for all rays. The total stored volume becomes -34,700 m^3. So by adjusting also the equilibrium angles better results are obtained (the difference will be discussed in the next Section).

6.5 Verification of the Post-model

Verification of the model will be carried out based on two aspects. The first aspect is the distribution of the stored volume of sediment after the nourishment. In Chapter 3 and 5 sediment balances are used to analyse this distribution. In the verification stage sediment balances of the Post-model will be compared with the sediment balance from the measured data on 6 August 2004.

The second is the coastline regression. In UNIBEST-CL+ a relation exists between the stored volume of sand in the profile and the coastline position. This relation is in the profile height, defined as the height of the profile where transport takes place (Section 6.3.3).

6.5.1 Sediment balance

Figure 6.A presents the volume difference of the 6 Aug-survey w.r.t. the Post-survey as well as the results of the Post-model. On the x-axis is the profile nr. and on the y-axis the stored volume in the profile (m^3/ 25 m).

The analysis of the sediment balance shows that both methods of calibration have a similar result (KB = 0.18 m, or decrease of the equilibrium angles with two degrees). So from this the conclusion is drawn that both calibration methods can be used.

The volume of eroded material in Section 500-675 in the Post-model is less than in the survey data. Profile 625 and 650 in the data had a peak that was not seen in the model results. But this was probably an overestimation, since a large part of these profiles was obtained by interpolation between existing points in the profile. In the model, the erosion increased to profile 600 and from there diminishes, this trend agrees with the surveyed data. In Section 275-500 similarity is seen both in volume as in erosive trend in the Post-model and the survey data. The conclusion is that for Section 225-675, good correspondence between the data and the model was obtained.

In Section 25-225 the results of the Post-model and the survey data deviate. In the data accretion was observed, while the model calculates erosion. In Chapter 4 it was stated that the accretion in this section was sand from up drift. Then material from the area near the marina was transported to this area by littoral transport, a process that UNIBEST-CL+ is capable of modelling. Since this is not seen in the Post-model, other explanations have to be found. This will be done in the sensitivity analysis in Section 6.6.

6.5.2 Waterline position

Figure 6.A also presents the position of the waterline in the Post-, Feb- and Aug-survey. Added is the development of the coastline from the Post-model in August. It is immediately seen that the model results and the surveyed waterline not correspond well.

The most critical zone of the model is at Profile 600. If we look at the fundamentals of the model, this is no surprise: The most erosion was computed here, so by using the single-line theory, the model also computes the most coastline regression here. The sediment balance showed that the sand was not lost, but redistributed within the profile. This proves that cross-shore processes had large influence on the position of the waterline. This is the reason that although the sediment balance corresponds, the waterline positions do not.

In short-term modelling of nourishment the position of the waterline is mainly determined by cross-shore processes. In the model the effect of cross-shore transports is not included. In the data accretion took place in Section 25-225, while the waterline in the data retreated. This is a situation that is impossible to model with a model based on the single-line theory.

6.5.3 Balanced coastline

The waterlines of the model and the data do not correspond. But the choice to compare the waterlines influences the results. Figure 6.5 shows that MSL (CD +1.1 m) has large regression, while CD -2 m accretes. To compare the results of the model with the data, a “balanced coastline” will be used.

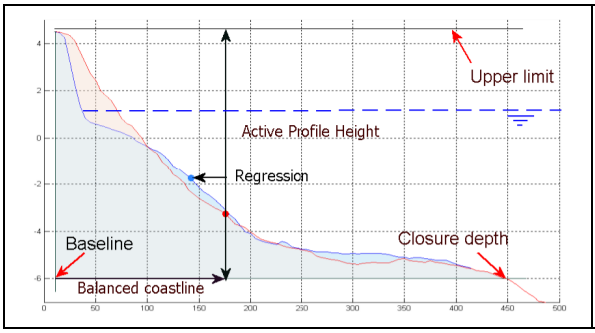

Figure 6-5 Schematization balanced coastline of the survey data

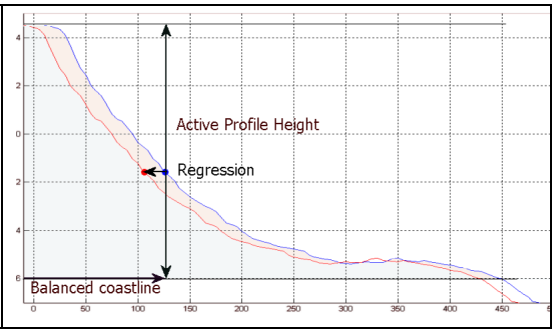

Figure 6-6 Schematization balanced coastline UNIBEST

Figure 6.5 explains how the balanced coastline is defined. This is the distance from the baseline; calculated by dividing the area of the profile between baseline, closure depth and upper limit, by the active profile height. In this way a distance is obtained independent of cross-shore processes. This can be calculated for different profiles and regression is the difference. Figure 6.6 explains how the Post-model calculates shoreline regression. In the model, the regression is also computed as the area of the profile, divided by the active profile height. But the profile moves uniform in shape, so the regression is equal at any bottom height within the active profile. With this distance the model results and the data can be compared.

The balanced coastline is determined from the baseline between the top of the beach (approx. CD + 4 m) and CD -6 m. The comparison is presented above in *Figure 6.B*. Correspondence between the sediment balance and the balanced coastline is seen. This is not surprising since this balanced coastline and the sediment balance are based on the same principle. The maximal regression is about 30 m. This proves that the selection of active profile height gives coastline regression similar as for the survey data. It also proves that the longshore processes are more influential for the position of the waterline near the marina than down drift. As in the sediment balance the correspondence in Section 25-225 is not well.

6.5.4 Development in time

Another difference between the model and the survey data is the development in time. *Figure 6.B* shows the development of the sediment balance of the model in time. The sediment balance in the data survey showed a large immediate response of the coast after the placement and little fluctuations after *(Figure 5.A)*. In reality the beach will respond to every wave condition this causes a difference between the model and the reality. The Post-model uses an averaged, categorized wave climate over a period of 8 months. And therefore the model will respond more gradual to the imposed wave climate.

6.6 Sensitivity analysis

Section 225-500 and Section 500-700 of the verified model corresponded reasonable, but the correspondence in Section 25-225 was less good. A physical reason for the accretion in this section was difficult, assuming this still in the nourished area. In Section 6.6.1 various processes are modelled in order to determine the sensitivity of the model to the model-settings. Special emphasis in this is the correspondence of Section 25-225.

Section 6.6.2 describes the sensitivity of the model to the wave parameters, while the sensitivity for the transport parameters are discussed in Section 6.6.3. The sensitivity to the boundary conditions is discussed in Section 6.6.4.

6.6.1 Model-settings

Assumptions in the Post-model that might have influenced the results are listed in Table 6.3. In this section attempts to simulate the influence of these assumptions on the whole model will be discussed.

Nr.	Assumption	Section
1.	Neglecting the equilibrium process	6.6.1.1
2.	Neglecting different sand distribution (non-uniform over the beach)	6.6.1.2
3.	Position of the coastline up drift of the nourished area (retreated/ extended)	6.6.1.3
4.	Use of balanced coastline	6.6.1.4
5.	The wave diffraction scheme (improper modelling)	6.6.1.5
6.	Neglecting currents or sand bypass	6.6.1.6

Table 6-3 Assumptions in the Post-model

6.6.1.1 Equilibrium process

As discussed in the data-analysis (Chapter 5) and theory (Section 2.2.2) the cross-shore processes had large influence on the position of the coastline. Sand was redistributed within the profile. At some locations (i.e. profile 450) the profile had small volume loss, but large decrease of the dry-beach width.

Here, an attempt is made to investigate the influence of neglecting cross-shore processes with the assumption that in February the profiles were more in equilibrium and after the position of the coastline changed more due to longshore transport. The February profiles and position of the coastline are selected.

This selection had small influence for transport capacities and equilibrium angles (results LT-computations). The sediment balance (transports compared w.r.t. the February survey) is presented together with the sediment balance from August in *Figure 6.C*. It shows that the model results correspond less with the survey.

An explanation is that with this model-settings the coastline was more advanced in Section 25-200 than after the post-survey. The model spreads this hump out because the coastline orientation is more out of equilibrium (causing larger transports). As a consequence accretion is computed in the Section 200-400 (upstream) and large erosion in this section.

The Feb-model can also not be used for waterline predictions (not presented). The balanced coastline *(Figure 6.C)* gives comparable results as the sediment balance.

Conclusions

- Selection of the February coastline position and profiles did not lead to better correspondence with the survey data, but an explanation for accretion in the model was found.
- The waterline can not be better predicted with the February coastline position and profiles.
- Using (partly) equilibrated profiles and coastline position does not improve the results in Section 25-225

6.6.1.2 Sand distribution

The Post-model uses uniform sand-characteristics for the whole beach. The sand samples showed a varied range of sediment distribution (Section 4.9). It was seen that at the limit of the nourished area coarser material was present (D_{50} of 900 μm). For Section 0-50 and down drift, sediment with a median diameter of 900 μm is selected, with corresponding fall velocity of 0.15 cm/s (Vanoni, 1975).

The results are presented in *Figure 6.D*. It shows that almost similar results as with the post-model were found. Erosion in Section 225-675 was slightly more. The erosion in Section 25-225 was slightly less, due to the increased sediment size and fall velocity. This trend corresponds slightly better with the data survey. But still, no accretion is found in the down drift section.

Conclusions

- With coarser sediment, the transport capacity locally decreases, causing less transport
- Coarser sediment in the end and down drift of the nourished area, leads to slightly less erosion in Section 25-225, but still not gives satisfactory results

6.6.1.3 Coastline down drift of the nourishment

The position of the coastline down drift of the nourishment is another aspect that might have influenced the model results. The nourishment extended the coastline further offshore and formed an impact on the existing coastline. As a consequence a transition zone was present at the limit of the nourishment with erosion in the nourished and accretion in the unnourished area. This was also seen in the result of the Post-model, but not in the survey data, where the accretion was already within the nourished section.

The coastline position in Section 700-2450 was obtained from several satellite images between 2000 and 2003. Water levels were unknown and more information was not available. So the possibility exists that in reality the down drift coastline position was more advanced than modelled.

The coastline in the model down drift was adjusted from 75 m to 100 m. And profile 1000 was adjusted from 87 m to 120 m. This is a large adjustment of the original coastline of the model, and therefore not likely (Figure 6.7).

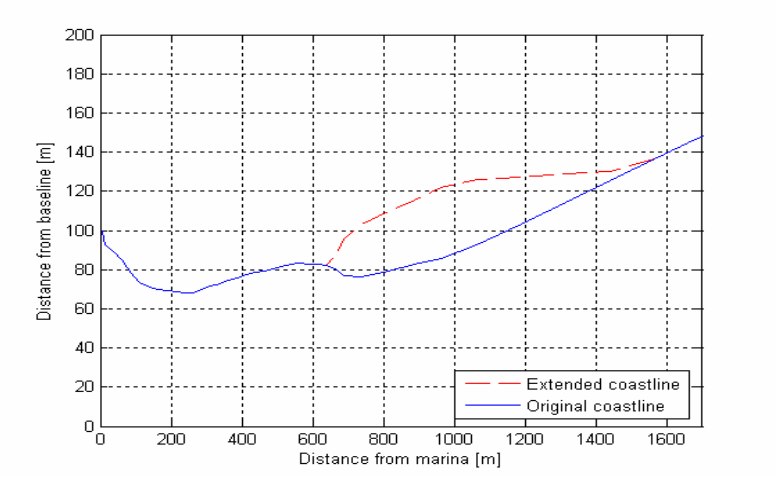

Figure 6-7 Extension of the coastline down drift of the nourished area

The resulting sediment balance is shown in *Figure 6.D*. It shows that the accretion in Section 25-225 is similar as in the data survey. Section 225-675 also corresponds with the data survey. This is caused by the fact that the coastline from 700 m to 1500 m from the marina is out of equilibrium. To come to a more equilibrated coastline it transports sediment up (Section 25-225) and down drift (1500 m to 2450 m from the marina). Thus accretion in Section 25-225 is obtained.

Conclusions:

- Adjustment of the coastline position down drift of Section 25-225, gives satisfactory results and a more accurate prediction of the coastline down drift of the nourished area might improve the results
- But normally the nourishment itself extends the coastline offshore. Therefore the adopted situation is unrealistic and will not be used to adjust the Post-model

6.6.1.4 Use of balanced coastline

The principle of the balanced coastline was explained in Section 6.5.3. The beach was extended with the nourishment with a certain volume up to a certain depth. T0his increased the dry-beach width and advanced the waterline. But this spreads out over the total active height. By dividing the advancement over the active profile height (as UNIBEST-CL+ does) another method to determine the coastline is used. The position of the coastline with this method w.r.t. the Pre-survey is presented in Figure 6.8. It shows that for Section 25-225 less material was nourished than for Section 225-675. There was some kind of a transition zone that was not seen in the Post-model.

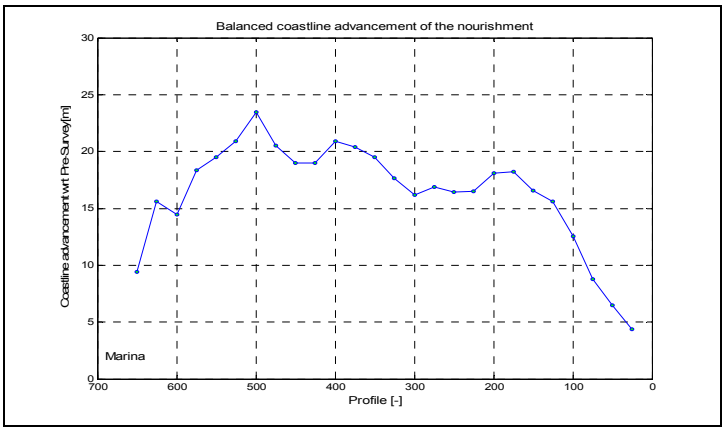

Figure 6-8 Balanced coastline progression w.r.t. the Pre-survey

Now a new model is introduced. The Pre-model; based on the coastline position of the waterline in the Pre-survey data with addition of the balanced coastline as in Figure 6.8. Thus the coastline of *Figure 6.E* is obtained. In this figure the red line is the position of the Pre-survey and the blue line of the position of the coastline used in this simulation.

With the balanced coastline less erosion was computed in Section 200-500 than the Post-model and even some accretion in Section 125-200. This is good correspondence with the survey data, but Section 25-125 shows a more erosive trend. Overall worse correspondence with the survey data was found. This leads to the conclusion that the position of the waterline is the best resemblance for the coastline in the model.

6.6.1.5 Modelling of wave diffraction

The wave climate was based on computations with the WW and is calibrated with the measurements of the DM. Adjustments were made to introduce the effect of the 'World' on the wave climate. A discussion of this climate was found in Chapter 4. For the modelling it is assumed that this was schematized correct.

Modifications on the model are made for the effect of wave diffraction by using a diffraction scheme of Kamphuis (1992). This scheme has influence on the wave climate near the marina. The diffraction scheme of Wiegel (1967) is used to compute another wave climate. *Figure 6.F* presents the resulting sediment balance of both schemes. It is seen that the erosion is slightly higher with the Wiegel scheme, but down drift in Section 25-150 the influence of the scheme is reduced and the eroded material from near the marina is settled at the coast further down drift and not in Section 25-225.

6.6.1.6 Currents and by-pass

Figure 6.G illustrates the bottom contours of the Italian beach model. What is seen in the bottom contour lines is that near the beach parallel uniform depth contour lines are present. These lines are fairly parallel until a depth of CD -4 m. Down drift of the marina (in northern direction) a bank is seen at CD -5, -6 -7 and -8 m. Since this bank is out of the breaker zone, this can be attributed to tidal currents. The marina disrupts the propagation of the tide. The current velocity increases near the marina, which causes steeper profiles.

The Post-model has the possibility of implementing tidal currents. Tidal current velocities and direction are very small for this area with maximal velocities of 0.2 m/s (Section 4.5). *Figure 6.G* illustrates the impact of a constant 0.2 m/s current. It is seen that even with this unrealistic situation, it has a very small impact on the results of the Post-model and therefore it can be concluded that currents have a small influence on the results of the model.

The border of the land part of a profile is the revetment, so no bypass occurs from here. But not every profile coincides at the toe. So cross-shore transport from deeper areas remains possible. This cross-shore transport can be some bypass from the marina. But no large movements are seen in the bottom contours so this is not likely. Cross-shore transport at the bottom of the profile can be modelled in UNIBEST-CL+ with the use of a sink. But since in the data analysis no clear point of accretion was found and quantities are unknown this possibility becomes so uncertain, that it is not seen as a realistic method to use in the Post-model to create an increase in Section 25-225.

6.6.2 Wave parameters

The wave parameters influence the wave propagation and decay and the wave-induced cross-shore water level set-up (Appendix C.5.1) as described by Equations C.3, C.4 and C.5. And influence the longshore current distribution (Appendix C.5.2) by Equation C.13.

Table 6.4 is used to classify the influence of the parameters to the model results. The sediment balances will be analysed, in which the default values of the parameters in the Post-model will be compared with modified values.

Classification	Description	Amount
Small	change in quantity	< 100 m^3 /25 m
Considerable	change in quantity	< 1000 m^3 /25 m
Large	change in quantity and change in trend	> 1000 m^3 /25 m

Table 6-4 Classification for sensitivity analysis

6.6.2.1 Coefficient of wave breaking (ALFA and GAMMA)

ALFA [-] and GAMMA [-] both influence the energy dissipation due to wave breaking (D_b) defined in the wave propagation and the wave decay model (ENDEC). Equation C.8 shows that (D_b) varies linear with *ALFA*.

The variation of (D_b) with GAMMA is not straightforward. Equation C.10 shows that a decrease of *GAMMA* leads to a decrease of (H_m) and thus of (D_b) to the second power, while Equation C.9 shows that the local fraction of breaking waves (Q_B) increases.

Lower values of the energy dissipation due to bottom friction (D_f) lead to higher values of energy dissipation due to wave breaking (D_b).

The resulting sediment balances are shown in *Figure 6.H*

Observations

- Variation of *ALFA* is possible within the domain [0.8-1.2]. The default value was 1.0, variation shows that *ALFA* had almost no influence on the resulting sediment balance.
- Variation of *GAMMA* is possible within the domain [0.4-0.9]. The used value was 0.7, variation shows that *GAMMA* had small influence on the resulting sediment balance.
- The setting of GAMMA had considerable influence in profile 650 where for all values of *GAMMA* the volume difference decreased, but a straightforward relation between GAMMA and the volume difference was not seen.

6.6.2.2 Coefficient of bottom friction (FW)

FW [-] influences the energy dissipation due to bottom friction *(Df)* defined in the wave propagation and decay model. Equation C.11 shows that D_f varies linear with *FW*.

The resulting sediment balances are presented in *Figure 6.I.*

Observations

- Variation of *FW* is possible within the domain [0-0.2]. The default value was 0.01. Variation shows that *FW* had small influence on the resulting sediment balance of the model.
- Neglecting *FW* lead to decrease of volume difference in profile 650. In other profiles the influence was small and no straightforward relation between *FW* and the total stored volume was seen.

6.6.2.3 Coefficient of bottom roughness (KB)

Equation C.17 shows that *KB* [-] influences the Chézy friction coefficient that is used in the momentum equation alongshore that describes the longshore current distribution (Equation C.14). As *KB* increases, the longshore current velocity *(V)* decreases; hence the total sediment transport decreases. (Van der Velden, 2000). *KB* is also used in the longshore transport formula of Bijker, but although physically the same parameter; in the program both parameters have to be set separately.

The resulting sediment balances are presented in *Figure 6.I:*

Observations

- Variation of *KB* is possible within the domain [0.05-0.5 m]. The default value was 0.10 m. Variation shows that *KB* has considerable influence on the resulting sediment balance of the model.
- Increase of *KB* lead to a decrease of volume difference (less erosion) in all sections.

6.6.3 Transport parameters

The transport parameters influence the longshore transports (Appendix C.5.3) as described by Equations C.18, C.19 and C.22.

6.6.3.1 Sediment characteristics (D50, D90, ws)

The sediment characteristics D_{50} [m], D_{90} [m] and W_S [m] are discussed simultaneously because correlation exists between these parameters. Table 6.5 presents the sediment characteristics for the sensitivity analysis. A grading between D_{50} and D_{90} of 200 % was used (Section 4.9). Fall velocity was obtained from Vanoni (1975).

Nr	D_{50} [µm]	D_{90} [µm]	W_S [m/s]
1	250	500	0.04
2	400	800	0.07
Default	550	1100	0.09
3	650	1300	0.11

Table 6-5 Sediment characteristics used for the sensitivity analysis

Increasing the bottom material grain size decreases the total sediment transport. D_{50} has a linear relationship in the Bijker equation for bottom transport (Equation C.19), but also influences the fall velocity (for the suspended load transport) and even the ripple factor. Furthermore it appears in the numerator of the exponent of the bed transport. An increase of D_{50} causes a decrease in transport. (Van der Velden, 2000). D_{90} influences the bottom transport indirectly through the ripple factor (µ). W_s influences the suspended transport (S_s). Increase of W_s leads to decrease of suspended sediment transport.

The resulting sediment balances are presented in *Figure 6.J.*

Observations

- Variation of D_{50}, D_{90} and W_S is possible. The default value was: (550 µm, 1100 µm, 0.09 m/s). Variation shows that the sediment characteristics have considerable influence on the resulting sediment balance of the model.
- D_{50} of 250 µm increased the volume difference (more erosion) in all sections.
- A value of D_{50} of 400 µm and 650 µm had only small influence on the results.

6.6.3.2 Bottom roughness (KB)

Equation C.17 shows that *KB* [-] influences the Chézy friction coefficient *(C)*, used in the Bijker formula. *KB* influences the current velocity calculated previously (Section 6.6.2.3). But here (in the program) it is only used for the Bijker calculations and as *KB* increases, *(C)* decreases, (S_b) and hence the total transport increases.

The resulting sediment balances are presented in *Figure 6.J.*

Observations

- Variation of *KB* is possible within the domain [0.01-0.1]. Variation shows that *KB* had considerable influence on the resulting sediment balance of the model.
- Increase of *KB* lead to an increase of volume difference (more erosion) in all sections.

6.6.3.3 Deep water criterion and coefficient (B)

Equation C.19 shows the relationship between *B* and *(S_b)*. The coefficient for deep water (1) will be applied for waves where H_s/h<0.07. A decrease of the criterion leads to more waves that are considered as deep water, which leads to lower total transport.

The resulting sediment balances are presented in *Figure 6.K*.

Observations

- Variation of *Hsig/h* is possible within the domain [0.01-0.2]. The default value was 0.07. Variation shows that *Hsig/h* had small influence on the resulting sediment balance of the model.
- Variation of B is possible within the domain [1-3]. The default value was 2. Variation shows that B has small influence on the resulting sediment balance of the model.
- Variation shows small differences in Section 600-650. In other sections the differences were minimal. No straightforward relation between the criterion, *B* and the total stored volume was seen.

6.6.3.4 Criterion shallow water and coefficient (B)

Equation C.19 shows the relationship between the coefficient for deep and shallow water *(B)* and *(S_b)*. The coefficient for shallow water (5) will be applied for waves where H_s/h<0.6. An increase of the coefficient leads to an increase of transport.

The resulting sediment balances are presented in *Figure 6.K*.

Observations

- Variation of H_s/h is possible within the domain [0.3-0.9]. The default value was 0.6. Variation shows that H_s/h had considerable influence on the resulting sediment balance of the model.
- Variation of *B* (shallow water) is possible within the domain [4-6]. The default value was 5. Variation shows that *B* had considerable influence on the resulting sediment balance of the model.
- Increase of the criterion lead to decrease of the volume differences (less erosion)
- Increase of *B* leads to increase of volume differences (more erosion)..

6.6.4 Boundary conditions

6.6.4.1 Dynamic area and active profile height

The dynamic area and the active profile height are discussed simultaneously because both are determined by the closure depth.

The ‘dynamic area’ is the ‘active part’ of the profile, defined as the horizontal distance from baseline to the closure depth per unit width. The depth contours in this area react in the model like the coastline itself. The sediment area (truncation transport) can be determined by the user too, but is generally the same. The active profile height is the height within the model computes accretion or erosion (height between closure depth and top of the dune).

The resulting sediment balances are presented in *Figure 6.L.*

Observations

- Variation of the dynamic area is possible within the domain [0-700]. The default value was on CD -6 m; the dynamic area varied between 200 and 350 m. Variation shows considerable influence on the resulting sediment balance of the model.
- Default value is 10 m (closure depth at CD -6 m and dune of CD +4 m). This value has some influence on the results of the Post-model. In the whole model differences were observed.
- Increasing the active profile height leads to an increase of volume differences.

6.6.4.2 Boundary condition

Instead of using the boundary condition that *Qs* at the left border is zero, the income of sediment is increased. *Figure 6.L* shows that in Section 625-675 small difference occurs. The model runs to profile 700. As observed in the data, this is the position of the breakwater. Section 675-700 was necessary for a good resemblance of the coastline orientation in the boundary of the model. Therefore no comparison was made and this section was not presented in the results. The results of the model with no sediment input, show erosion in this section and a more or less stable point at profile 675. By increasing the sediment input at the left boundary, the erosion in Section 675-700 decreases and the sediment input of the boundary condition is detained in this section. This is not a very good resemblance of reality, because an increase in this boundary, due to i.g bypass, is likely to spread along the nourished area. So the results are influenced by adjusting the boundary condition and a more detailed study is needed for a more realistic resemblance when adding sediment input in section 675-700.

6.7 Conclusions

6.7.1 Conclusions of the verification of the Post-model

The calibration was based on the total of eroded sand in the nourished area, where a good agreement between the survey data and the model was obtained. The computed equilibrium angle at which no net longshore transport takes place was around 294 ^{0}N and verified with the use of satellite images.

The conclusions of the verified model are presented in Table 6.6.

Section	Correspondence	Comment
500-675	Good	Details of pattern reproduced; overall trend reproduced. Erosion less in the model
225-500	Good	Details of pattern reproduced; overall trend reproduced. Data shows more scatter
25- 225	Bad	Measurements and model uncorrelated; erosion computed while accretion is measured

Table 6-6 Verification of the model

From the above it can be concluded that model can partly predict the behaviour of the nourishment. It was seen that for a *KB* of 0.18 m a good similarity between the data and the model was obtained in Section 225-675. This similarity was based on the comparison of stored volume in the profiles *(Balance in Figure 6.A)* and on the balanced coastline *(Figure 6.B)*. Less reliable results were obtained on the prediction of the waterline position (expected since cross-shore effect are not modelled) and the development in time (caused by the use of a schematized wave climate). The correspondence between the survey data and the model results in Section 25-225 was less well. An increase of material was seen while the model predicts erosion in this section.

The coastline position of the model *(Figure 6.A)* proves that the cross-shore effects cannot be neglected to compute the dry width beach although the sediment balance shows that sand was not lost, but redistributed within the profile. If UNIBEST-CL+ is applied then an interpretation of the results for the prediction of the waterline that includes cross-shore redistribution is required.

6.7.2 Conclusions of the sensitivity of the Post-model

The results of the Post-model correspond well with the data in Section 225-675, but deviate in Section 25-225. In Sub-section 6.6.1 possible scenarios were investigated.

- The assumption that in February a part of the equilibration was completed and therefore leads to better results was tested, but the sediment balance corresponded less well as with the verified Post-model.
- With coarser sands down drift of the nourishment less erosion was computed but no accretion occurred. The results were slightly better but still unsatisfactory.
- Extending the shoreline down drift of the nourishment gives satisfactory results. But this requires un-realistic extension of the beach down drift of the nourishment. This leads to the conclusion that a more accurate prediction of the coastline down drift of the nourished area might improve the results.
- The use of a balanced coastline progression did not improve the correspondence in Section 25-225.
- More erosion was seen with another wave diffraction scheme. But this had only small influence on the sediment balance.
- The influence of currents was limited to Section 300-675.
- Sediment bypass can be imposed in the model at any given location and could improve the result but is not considered as a valid option to obtain better results.

These scenarios were investigated and it can be concluded that the increase in Section 25-225 can be modelled in the Post-model, but requires unrealistic means and some uncertainty related to the cause of accretion at this end of the nourished area remains.

Table 6.7 indicates the sensitivity of the Post-model to the parameters:

Type	**Parameter**	**Sensitivity**			
		no	small	considerable	large
Wave	Coefficient of wave breaking (ALFA)	x			
	Coefficient of wave breaking (GAMMA)		x		
	Coefficient of bottom friction (FW)		x		
	Coefficient of bottom roughness (KB)			x	
Transport	Sediment characteristics (D50, D90, ws)			x	
	Bottom roughness (KB)			x	
	Deep water criterion and coefficient (B)	x			
	Criterion shallow water and coefficient (B)			x	
Boundary	Dynamic area and active profile height			x	
	Boundary condition			x	

Table 6-7 Sensitivity of the Post-model to the parameter settings and boundary conditions

6.7.3 General conclusions

Objective nr. 1: Hindcast simulation of the nourishment at Italian beach for the period January to August 2004

A hindcast simulation of the nourished area at Italian beach for the period January to August 2004 was performed using the software package UNIBEST-CL+. With this package a model was created which was capable to predict the sediment distribution within this period.

Objective nr. 2: Performance of UNIBEST-CL+ software package to make short-term predictions

The conclusion is that with the Italian beach model volume computations can be made for Italian beach with satisfactory results. For the prediction of the position of the waterline it was less effective. This is expected since UNIBEST-CL+ does not take into account the effects of cross-shore redistribution of sand on the waterline. It is concluded that in this short period the cross-shore processes are dominant over longshore processes for the position of the waterline at Italian beach. In general, these cross-shore effects will largely depend on the slope with which the nourishment is placed.

Objective nr 3. Optimization and suggestions for future nourishments

Optimization and suggestions for future nourishments, based on volume considerations can be made with the Italian beach model. A resulting sediment balance can be obtained of which the volume can be optimized.

7 Optimization of nourishment

7.1 Introduction

In this chapter the optimization of the nourished area is investigated with the Post-model of Italian beach from the previous chapter. Section 7.2 describes the objectives of the optimization. Three different shapes are simulated and discussed in Section 7.3, based on a redistribution of the waterline advancement. Section 7.4 describes a more realistic situation where the advancement is profile dependant. Finally, in Section 7.5 conclusions regarding the optimization are drawn.

7.2 Objectives

Several aspects can be investigated for the optimization of nourishment, such as:

- Cross-shore position
- Alongshore position
- Borrowed sand characteristics

In this thesis only the alongshore position will be investigated. The hypothesis is used that a better distribution of sand within the nourished area can improve the life span of the nourishment. The life span is determined by the time that it takes that no dry-beach width remains.

Italian beach is used for the optimization. In reality, a revetment borders the coast of the beach, and the entrance of the Marina requires a sufficient depth for the entrance of ships: lack of space is often an important boundary condition when designing a nourishment. But since this beach serves as case for all beaches in Dubai, this is not taken into account. The assumption is used that the hydrodynamic conditions are not influenced by the different alongshore placement of the nourishment.

The possibilities of shapes that can be investigated and optimized are almost infinite. In this research three shapes are used for optimization that will be discussed in the next Sub-sections,

- Case 1: Triangular
- Case 2: Rectangle
- Case 3: Two undulations

The criteria to judge the effectiveness of the optimized placement are:

- Total volume of eroded sand in one year
- The position of the coastline after one year
- The time that the nourishment crosses a critical boundary

The critical boundary is defined as the minimal width in August of the Post-model in the most critical area: Section 400-700. With the last two criteria question marks have to be

placed, since in the Chapter 6 it was concluded that the model was not able to predict the waterline in this short time interval. But in a coastline model, this waterline is a result of volume differences in the profile. Therefore it can be used for optimization of volume. Moreover the erosion can be translated into critical conditions and compared with other situations.

Optimization will be based on two concepts: area and volume. In the area concept, the obtained area of the nourishment is redistributed in another shape (independent of the water depth) in Section 7.3. In the volume concept, the total volume of 103,000 m^3 will be redistributed with increasing water depth (Section 7.4). The situation and development of the in reality executed placement will be referred to as the reference case.

7.3 Optimization based on area

With this method the area of advancement will be redistributed over the nourished area *(Figure 7.A)*. E.g. when the original coastline advancement in a profile was 30 m, than an advancement of 60 m requires twice as much of sand. This is a simplification of reality, but it is interesting for modelling to see what the consequences are in the model and if better results can be obtained. Since the advancement is less based on the shape of the profile it makes the results less case-sensitive.

7.3.1 Case 1: Triangular shape

For this case a 300 m shortening of the width of the nourished area is selected. The original volume over 675 m will now be placed with triangular shape in the most critical zone near the marina. The triangular shape is presented in *Figure 7.A*, added in the figure are the original Pre- and Post-survey waterline positions. As seen by redistribution of the area a large advancement near the marina can be obtained.

Figure 7.B (above right) shows the evolution of the coastline in a year time. In Section 400-675 the initial coastline is placed with a large advancement w.r.t. the original placement. It shows that initial retreat and erosion is fast, but after one year still a considerable increase of coastline remains in this section compared with the reference case *(Figure 7.B above left)*.

In Section 100-400 less or no sand is placed. This section accretes in time, so the placement near the marina is beneficial for this section. But the position of the coastline is still more retreated than in the reference case. This makes the beach here under-protected for storm-events. In Section 0-100 and further down drift more erosion occurs. The coastline here retreats, and depending on the beach authorities it can be stated if the remaining beach width here is acceptable or not.

The critical line is defined as the minimal distance of the waterline in August of the reference case in Section 400-675. This minimal width at T=0.6 yr was 57 m from the baseline. The time that it takes the triangular case to reach this is 1.6 yr. This means an extension of the life span of the project of 1 yr (neglecting cross-shore processes).

7.3.2 Case 2: Rectangular shape

The rectangular shape is presented in *Figure 7.A*, added in the figure are the original Pre- and Post-survey waterline positions. The nourishment will now be placed in a rectangular shape in 400 m at the marina. For stability and resemblance of reality the limit of this shape approaches the original coastline in 125 m. As seen in the figure a large advancement near the marina can be obtained.

Figure 7.B (left below) shows the evolution of the coastline in a year time. It shows that the retreat is less fast as compared with the triangular shape and after one year still more coastline remains as the reference case. The time that it takes the triangular case to reach the critical line in this section is 1.49 yr. This means an extension of the life span of the project of 0.9 yr (neglecting cross-shore).

On Section 100-400 less sand is placed. It shows that this section accretes after one year. So the placement of sands near the marina is beneficial for this section. But when looking at the position of the coastline it is still more retreated than in the post-survey. In Section 0-100 and further downstream some erosion occurs. It is seen that the coastline here retreats.

The time that it takes the triangular case to reach the critical line is 1.5 yr. This means an extension of the life span of the project of 0.9 yr (neglecting cross-shore).

7.3.3 Case 3: Two undulations

For this case the initial area is replaced in two undulations with amplitude of 40 m *(Figure 7.A)*. When looking at the development in one year *(Figure 7.B)* it is seen that the undulation height retreats fast and the coastline moves to an equilibrated shape. The troughs are filled with sediment from the peaks. It is also seen that the second undulation erodes faster than the first. With this shape the life span of the critical area will be 0.48 yr extended. With placement in this shape the coastline is more advanced in a large part of the area, but the erosion in the down drift area is slightly more. It was seen that the advancement in Section 500-700 was less. Erosion took place down drift.

7.3.4 Conclusions

In *Figure 7.C.1* the advancement of the coastline after one year as computed by the model compared with the reference case is presented. This figure shows that all three cases have better results in the critical Section 500-675. But it also shows that in Section 100-500 to approximately 500 m down drift the coastline is more retreated and more erosion is computed. This figure also shows that the triangular case has to most improvement in the critical section, but also most erosion down drift.

This model can not be used to predict the exact dry-beach width and the waterline computed by the model is a measure of volume. Thus above results can not be translated in real advancement and retreat. So with this model it can not be said if the erosion is acceptable or not.

The critical line is defined as the minimal width in August of the Post-model in Section 400-675. This minimal width at T=0.6 yr was 57 m form the baseline. When looking at the minimal width of the critical line in Section 400-675, the triangular shape gives the longest life span. If we look at the minimal width in the whole nourished area than the undulation shape has the best results. Table 7.1 present the extension of the life span of the critical section, based on a comparison with the reference situation:

	Reference	Triangular	Rectangular	Undulations
Life span [yr]	0.6	1.6	1.5	1.1

Table 7-1 Life span of the critical zone based on area advancement of three cases: triangular, rectangular and 2 undulations

If we look at the volume change of the nourished area *(Figure 7.C.2)* it is seen that the least volume is eroded after 1 year in the rectangular case. After this the triangular shape is better. And the case with the undulations is the least good. The results prove that with an optimized shape more volume can be remained within the nourished area.

Remarks:

- Cross-shore processes play a dominant role in the determination of life span. With the triangular and rectangular shape a smaller buffer is available for protection in Section 0-400, which makes it more vulnerable for storm-events
- Accretion occurs mostly under water and gives not more dry-beach width
- In reality these shapes are difficult to achieve because lack of space in the area and because during construction the longshore process already takes place
- Increased depth leads to larger volumes at deeper depths, therefore in the next section this will be taken into account

7.4 Optimization based on volume

In this Sub-section the new coastline positions are calculated on the base of the volume that it requires for protrusion of the waterline. Figure 7.1 illustrates that this does not relate linear with the required volume when the profile slope is steep. E.g. when the original coastline advancement in a profile was 30 m, then for an advancement of 60 m much more than two times the volume of sand is required.

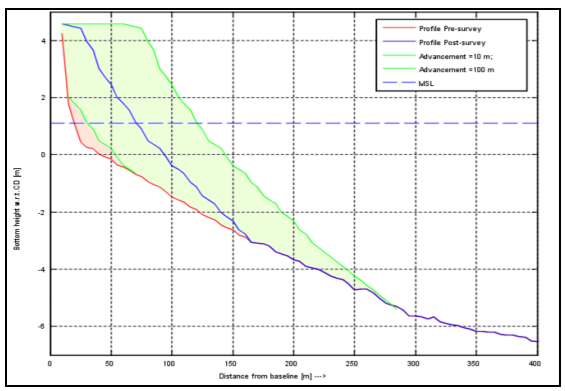

Figure 7-1 Advancement of the waterline

Assuming that the cross-shore profile has the same shape as in the Post-survey, q volume of 103,000 m^3 is redistributed in the area. For the nourishment at Italian beach a slope of 1:20, with 1:30 at the toe is a good resemblance (Section 5.6.2). For the optimization based on these volumes, the same three cases are considered as in the former sub-section. The positioning of the redistributed coastline is presented in *Figure 7.D.*

7.4.1 Triangular shape

The protrusion of the waterline near the marina is less than the former optimization. This is because more volume is required to obtain deeper depths. After simulation of 1 year the result is that in Section 450-675 still more coastline remains as in the reference case *(Figure 7.E, above right)*. In Section 0-450 the coastline is less than in the reference case. Erosion also occurred down drift of the nourished area. The critical line was passed after 1.08 yr. This means an extension of the life span of 0.48 yr.

7.4.2 Rectangular shape

The difference between this protrusion and the optimization based on area is large. The most seaward point at the marina is located about 30 m more inshore. What is seen after the simulation of 1 year is that in Section 400-675 still more width of the coastline remained compared with the reference case *(Figure 7.E, below left)*. In Section 0-400 the coastline is more retreated than the original situation. Erosion occurred down drift of the nourished area. The critical line was passed after 1.12 yr, an extension of the life span of 0.52 yr.

7.4.3 Two undulation

Figure 7.E shows the development of the case of the two undulations after 1 yr. The coastline position is about 10 m less advanced by using the replacement by volume. The coastline responds to this shape by equilibrating the undulations, this process is faster in the second undulation, because it is more exposed *(Figure 7.E, below right)*. It shows that for the whole nourished area a better coastline position is obtained by placement in this shape. The critical line in Section 450-675 is passed at 0.88 yr, an extension of the life span of 0.28 yr.

7.4.4 Conclusions

With the placement based on volumes a better correspondence with reality is obtained. But this makes the case dependent on the shape of the nourished profile to calculate the volume required for the advancement of the waterline. This profile shape is partly dependent of the grain characteristics and the hydrodynamic circumstances. This differs for every location and makes the optimization very case-sensitive.

In *Figure 7.F.1* the advancement of the coastline as computed by the model compared with the reference case is presented. This figure shows that all three cases have better results in the critical Section 500-675. But the results are less than in the optimization based on area. It also shows that in Section 100-500 to approximately 500 m down drift the coastline is more retreated and more erosion is computed. This figure also shows that the triangular case

has most improvement in the critical section, but also most erosion down drift. Compared with the optimization based on area the erosion down drift is more.

When looking at the minimal width of the critical line in Section 400-675, the triangular shape gives the longest life span. If we look at the minimal width in the whole nourished area than the undulation shape has the best results. Table 7.2 present the extension of the life span of the critical section, based on a comparison with the reference situation:

	Reference	**Triangular**	**Rectangular**	**Undulations**
Life span [yr]	0.60	1.08	1.12	0.88

Table 7-2 Life span of the critical zone based on volume advancement of three cases: triangular, rectangular and 2 undulations

When looking at the development of the eroded volume in time *(Figure 7.F.2)* it is seen that the triangular and rectangular case, less volume was eroded of the nourished area in 1 yr. With the undulations case also less volume erodes in time.

7.5 Conclusions

The hypothesis was used that a better distribution of sand within the nourished area can improve the life span of the nourishment. The life span is determined by the time that it takes that at some point no dry-beach width remains. Three cases were tested with this model for optimization; an triangular, rectangular and undulation shape.

All three cases improved the critical section of 300 m near the marina, compared to the reference case (placement as originally executed). But increased the erosion further down drift. This model can not be used to predict the exact dry-beach width. And the results can not be translated in real protrusion and retreat of the waterline. So with this model it can not be said if the erosion is acceptable or not.

First the placement was redistributed based on area difference (where doubling the advancement of the waterline requires twice as much volume) and based on volume (where for deeper depths more material is required, making it profile dependent). It was seen that with the method based on area, more accretion and less erosion was computed than with the method based on volumes. This was caused by the fact that advance of the waterline requires more volume of sand the further it advances offshore.

8 Cross-shore model

8.1 Introduction

Goal of this chapter is to explain how the cross-shore effects of a profile in the nourished area can be modelled. Section 8.2 describes the objectives and Section 8.3 the model settings. In Section 8.4 a cross-shore model will be calibrated and verified. It will be subjected to a sensitivity analysis in Section 8.5. In Section 8.6 a three-day storm event at the beginning of February 2004 is modelled. Finally, in Section 8.7 the conclusions will be presented.

8.2 Objectives of the model

8.2.1 Introduction

In the former chapters the UNIBEST-CL+ package was used for Italian beach to predict longshore transports along the coast. But it was proved that the model was less effective in the prediction of the dry-beach width. Influence of cross-shore effects proved an important aspect in the determination of the life span of beach nourishment projects. In this chapter a cross-shore model will be introduced to gain further insight into the processes.

UNIBEST-TC of Delft Hydraulics is designed to predict cross-shore development of a profile and will be used in this chapter to hindcast the development of the profile. It is beyond the scope of this thesis to use this model for optimization.

8.2.2 Objectives

Simulations will be made only for profile 450. The survey data showed that the waterline retreated about 40 m and a very small volume of sand was lost in the period.

The model has the following objectives:

- Hindcast of the bottom development of profile 450 of Italian beach for the period January to August 2004
- Analysis of the UNIBEST-TC software package: Definition of its capability to make predictions for Italian beach
- Verify the estimated closure depth

8.2.3 Stages of modelling

The calibration of the model will be done through trial and error. The parameters will be adjusted until a fair result of the predicted bottom height is obtained. With this result a

sensitivity analysis will be carried out. Figure 8.1 illustrates the modelling process (number in brackets refer to the section nr.).

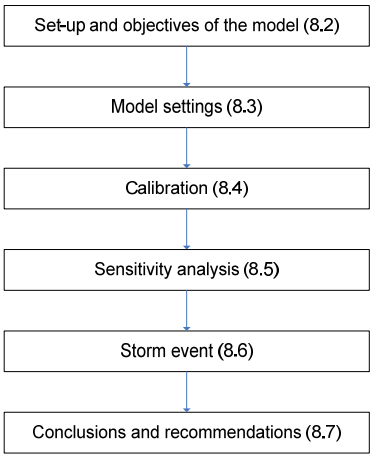

Figure 8-1 Cross-shore modelling

8.2.4 Model overview

The UNIBEST-TC model consists of 5-sub modules. Together these modules compute the bottom height changes of the profile:

- Wave propagation module
- Mean current profile module
- Wave orbital velocity module
- Bed load and suspended load transport module
- Bed level change module

Appendix D presents a full overview of the formulations and mathematical descriptions of the model. The used version is a beta-version that is still under investigation (June 2004). Changed formulations for the bed load and suspended load transport module are implemented.

8.3 Cross-shore model settings

Bottom profile
Profile 450 of Italian beach is selected for the cross-shore profile modelling. This profile is located 250 m of the Umm as Suqaym II Marina. The maximum height of this profile was CD +4.7 m and the maximum depth was CD- 8 m. Bottom profiles of 11 Feb, 4 March, 9 May and 6 August 2004 are available for verification. The last will be used for calibration.

Grain size
For the longshore computations a D_{50} of 550 μm was selected, this was obtained from sediment samples by Van Oord. Problems with stability of the program occurred, since these are very coarse particles and the wave conditions are relatively mild. In discussion with the advisors it was decided to use a D_{50} of 350 μm. This can be supported by the fact that at the waterline usually coarser particles are found than in other sections of the profile and

moreover the samples varied largely. The consequence will be further investigated in the sensitivity analysis.

Waves
Instead of UNIBEST-CL+, this model uses time records of the wave height, angle to the shore-normal and peak period at the offshore boundary. The record used for the simulations was defined in Chapter 4. It includes the effect of the 'World'. For the influence of the Marina, the wave diffraction scheme of Kamphuis (1992) is used. For stability of the model it was not possible to include all waves;

- Waves with direction offshore (wind generated) are neglected and withdrawn from the time record.
- Only waves with HRMS larger than 0.75 m are used.

Thus the one-on-one relation with the bottom profile development in time will be abandoned The total simulation time becomes 17.5 days.

Current
Current velocities were discussed in Chapter 4. No time-record of current velocity is available. It was concluded that the currents did not exceed a depth averaged velocity of 0.2 m/s. In the model current velocities are neglected in the calibration phase. The influence will be further investigated in the sensitivity analysis (Section 8.5.2).

Water levels
Water level variation occurs because of tide and wind setup, and was investigated in the boundary conditions. A sinusoidal water level variation with an amplitude of 0.7 m and 15 tides are applied. The influence will be further investigated in the sensitivity analysis (Section 8.5.1).

Wind
Wind velocity and direction can be obtained from the measurements of the DM. Since no accurate data on wind velocity is available it is not taken into account.

Parameter settings
Over 25 parameters can be adjusted for calibration of the model. After consultation with advisors from WL| Delft Hydraulics it was decided that for most parameters the default settings will be used. Calibration is carried out on the parameters from Table 7.1.

Type	Input parameter	Symbol	Name UNIBEST-TC	Value	Unit
General	Maximum relative wave period	T^*	TDRY	20	[-]
	Coefficient for interpolation of the dry beach profile	Z^*	ZDRY	2	[-]
Sediment	Median grain diameter		D_{50}	300	
	90 % grain diameter		D_{90}	450	
Transport	Tangent of angle of repose		TAN(PHI)1	0.1	

Table 8-1 Parameter settings for calibration of the cross-shore model

8.4 Calibration and verification of the cross-shore model

The calibration of the model was done by trial and error. The parameters were adjusted until a good result was obtained of the developed bottom profile at the end of the simulation period. *Figure 8.A* presents the result of the bottom change calculations. In which the blue line is the original profile from after the placement, the magenta line of the profile on 6 August and the red the computed.

Above MSL some instability of the profile was seen. This is the influence of the seawall boundary. With the default setting (ZDRY=2) the last wet part to the top of the dune is extrapolated, so that the dune changes form retaining. With a larger boundary grid than the original, a more retreated form will be obtained.

Around MSL the results are well computed by the model. Under MSL to CD -2 m the model has very good results. The slope is about equal. This shows that the model can predict the dry beach width with good results.

Below CD too much accretion is computed. This is probably because in reality part of the material was transported alongshore and to deeper depths, where accretion was observed. The slope of the bottom corresponds. Several possibilities for the found differences are listed below:

- Longshore transport
- Sediment size variation, D50 and D90
- Angle of natural repose, Tan(phi)
- Tidal amplitude and number of amplitudes
- Wave conditions

The closure depth is computed by the model around CD -5 m. This agrees with the theory (Section 4.8), but in the survey data accretion until a depth of CD -6 m was observed. This leads to the conclusion that this accretion, due to the mild wave conditions is probably not related to wave processes. It was more likely that the loosely packed sediments on the very steep slope (1:20) were transported further offshore by gravity or currents.

Conclusion of the calibration of the model is that the dry-beach part can be well modelled with the UNIBEST-TC model. Below CD too much accretion is computed and the increase at the toe was not found.

8.5 Sensitivity analysis

The goal of this analysis is to determine the influence of the model settings and parameters. Special attention is given to the under water part. Therefore (in discussion with advisors of WL| Delft Hydraulics) the following settings are subjected to a sensitivity analysis:

- Tidal amplitude and number of tides
- Tidal velocity
- Sediment size (D_{50} and D_{90})
- Tan(phi)

8.5.1 Tide and number of tides

In the calibrated model, a vertical tide of 0.7 m was imposed. In reality the amplitude of the real tide ranges between 0 and 1.0 m and is semi-diurnal. Time-series on water elevations were not available. Therefore the tide is simplified by a sinusoidal form with amplitude of 0.6 m to 1.0 m and between 3 and 19 nr. of tides (Figure 8.2 and 8.3). The number of tides is changed in order to make sure no waves were missed with large heights and low water elevations, causing some transport to the toe.

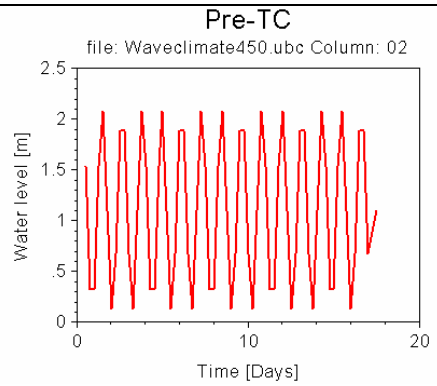

Figure 8-2 Fifteen tides and an amplitude of 1.0 m.

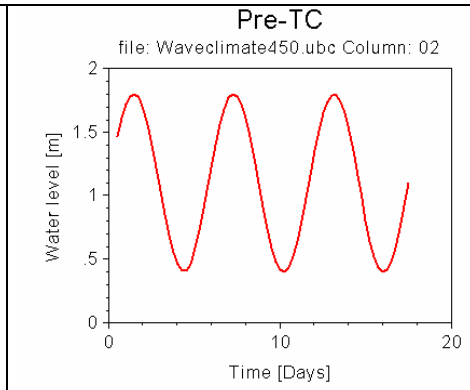

Figure 8-3 Three tides and an amplitude of 0.7 m

The results of the sensitivity analysis of the tidal amplitude are presented in *Figure 8.B*. The dry-part above MSL shows that an increase of tidal amplitude leads to more regression of the dry-beach width. Also some instability around CD is seen. Around and below CD almost no difference is seen.

Figure 8.C presents the computed bottom profiles for the nr. of tides between 3 and 19. The dry-beach part shows some minor influence and in the under water part the influence is negligible.

The influence of the water levels was further investigated in the modelling of a storm event in Section 8.6. There the water levels of a storm event of 4 days were accurately derived from the DM.

8.5.2 V_{TIDE}

The current velocity in the calibrated model was neglected, because it was very small. Here, a constant velocity between -0.2 m/s and + 0.2 m/s is imposed at a depth of 8.9 m. *Figure 8.D* shows that for these low velocities the influence is limited. In the whole profile no difference with the default values occurs. So the influence of small tidal velocity is negligible.

8.5.3 TAN(PHI)

The angle of repose was an important aspect of the calibration, it was calibrated and set on 0.1. The bed load transport is influenced by the bottom slope in two ways: First, the critical stress for a down slope movement is smaller than for an upslope movement. Secondly, the transport directly induced by gravity once the grains have been set to motion is taken into account.

Figure 8.E shows the results of a variation of tan(phi) of 0.10 and 0.30. Lower values lead to unrealistic results and are therefore not presented. This figure shows that this parameter has a large influence on the resulting bottom profile. A increased value leads to an decrease of bottom transport, while the suspended transport is not influenced. It also causes steeping under water. With the calibrated value of 0.1 m the slope around and below CD is best represented.

8.5.4 D_{50} and D_{90}

The sediment characteristics are an important aspect for the calibration. The selected median diameter was 350 μm, because problems with stability of the program occurred with the relatively mild waves for larger sediment sizes. This can be supported by the fact that at the waterline mostly coarser sediments are found than present over the whole profile.

Sensitivity of the model to the sediment characteristics is presented in *Figure 8.F*. After calibration, it shows that the sediment size has some influence on the results, but minor.

8.5.5 REF(-4)

This parameter determines the cross-shore variation of the sediment size at a selected depth. For this sensitivity analysis the sediment size at CD -4 m is varied. A finer material might lead to transports to the toe. *Figure 8.G* presents the results of variation of finer sediments with a factor ranging between 0.6 to 1.0. It shows that this has only minor influence in this model. For completeness also settings with coarser sediment at CD -4 m are computed, but not presented because the influence was negligible.

8.6 Computation of the 9 February storm

The storm of 9 February was a storm with large wave height and low water levels. It is modelled to investigate if for real-measured water level data, transport has taken place at the toe. The wave height, period, direction, and water levels are derived from the DM for every

hour. The storm with waves higher than 0.5 m lasted 3.75 days. They are presented in *Figure 8.H*.The same parameter settings are used as in the calibrated model.

The computed bottom profile is presented in *Figure 8.I* added by the profile of 11 February and the post-profile. What is seen in this figure is that a storm event has a very large impact on the development of a profile. Above CD already a large retreat has taken place. This material settles to a depth of CD -4 m.

8.7 Conclusions

Hindcast of the bottom development of profile 450 of Italian beach for the period January to August 2004

A hindcast simulation of the nourished area at Italian beach for the period January to August 2004 was performed using the software package UNIBEST-TC. With this package a model was created which was capable of predicting the dry beach width with good results.

Analysis of the UNIBEST-TC software package: Definition of its capability to make predictions for Italian beach

The model needs heavy calibration. Instability of the dune was seen for computations with grain sizes coarser than 400 μm. Also waves with H_{rms}< 0.75 m caused instability. This calibration makes the results less reliable.

Above MSL some instability of the profile was seen. This is the influence boundary (schematized by the seawall). Around MSL to CD -2 m the model has very good results. This shows that the model can predict the dry beach width with good results. Below CD too much accretion is computed. This is probably because part of the material was transported alongshore, which is not incorporated in the model and to deeper depths.

Verify the estimated closure depth

The closure depth, computed by the model was around CD -5 m. This agrees with the theory, but in the survey data accretion until a depth of CD -6 m was observed. This leads to the conclusion that this accretion, due to the mild wave conditions is probably not related to wave processes. It is more likely that the loosely packed sediments on the very steep slope (1:20) are transported further offshore by gravity or currents.

9 Conclusions and recommendations

9.1 Introduction

The location of the research is Dubai. Between Palm Island Jumeirah and Port Rashid, six beaches were nourished in 2004. Almost monthly survey data was available of some of these beaches. Part of these data was analysed in order to determine the morphologic behaviour of the nourished areas and the beaches. Based on this information a location was selected to serve as representative for the Jumeirah beaches: Italian beach. For this beach a model was created in UNIBEST –CL+, a coastline model to model the planform evolution with which a research for optimization was carried out. Ultimately the cross-shore behaviour of a representative profile of Italian beach was modelled with UNIBEST-TC.

The main objective of this thesis was presented in Section 1.4. The main objective of this thesis is to gain insight in the morphological behaviour at the nourishment locations along the Jumeirah beaches. Therefore the survey data will be analysed, and a model will be made in the morphologic package UNIBEST for a selected location on the Jumeirah beaches. Once validated with the data, this model will be used as a tool to make suggestions and optimize possible future nourishment.

Several sub-objectives were determined in order to reach this main objective. In Section 9.2 the conclusions of each sub-objective answering the main objective will be presented. In Section 9.3 recommendations for this and further research will be made.

9.2 Conclusions

Analysis of morphologic behaviour of the coast and nourished areas of the Jumeirah beaches and determination of a suitable study location

It was seen that the coastline of Dubai consists of a large number of coastal protection works and marinas. These have a large impact on the formation of the beaches and cause that each beach can be seen as a separate cell. At the beaches north of the Chicago beach area a northward directed transport takes place (Italian, Glass Palace, Jumeirah 1 and 2) causing accretion on the north side and severe erosion on the south side. Nourishments were required at these locations. South of the Chicago beach area (Madinat Jumeirah), transport was in the southern direction, due to the influence of the Palm Jumeirah.

Nourishment on all beaches was placed directly on the beach. The initial slope of the nourished profile was approx. 1:25 on the beach to a depth of CD –2 m. In general near structures, the erosion took place over the whole height between the top and the toe of the profile. On locations further down drift, the trend was that equilibrium processes cause an increase of sediments under water. Milder slopes and berm-formation was found to a depth of CD -4 m.

Based on the available data, indications of sediment transport and suitability of modelling Italian beach was selected as study location.

Analysis of the hydrodynamic conditions and sand characteristics for this location

The tide is semi-diurnal, with CD at lowest astronomical tide and MSL at CD + 1.1 m. Normal amplitude of the tide ranges between 0.1 m and 0.9 m. Currents have small velocities and are within 0.3 m/s at CD –15 m (depth averaged). The wave climate for January to August 2004 at Italian beach is derived from the program World Waves, verified with measurement by the Dubai Municipality and adjusted based on energy considerations to include the effect of the "World". A D_{50} of 550 μm was adopted for Italian beach.

Detailed analysis of the survey data of Italian beach

Sediment balances were used to compare the volume of sand in a profile with the volume directly after the placement (Post-nourishment survey). The balance of Italian beach showed that from 1 January to 11 February a large change immediately started: a reaction of the nourished area to several storm events in this period. After this in all sections erosion was slower. Between 4 March and 9 May the surveys indicated an increase of sand in the nourished area. This sand was found below CD, over the whole width of the nourished area. No indications were found to explain the increase physically. Overall an erosive trend was seen and the volume of eroded sand was about 30,000 to 40,000 m^3 in the period from January to August 2004.

The shoreline retreated in time caused by the transportation of sand from above CD to lower parts. Most severe regression was approx. 40 m. The sediment balance of this profile did not show most erosion. This leads to the conclusion that cross-shore processes were dominant for the dry-beach beach width.

Configuration, calibration and verification of a morphodynamic model in UNIBEST

A hindcast simulation of the nourished area at Italian beach for the period January to August 2004 was performed using the software package UNIBEST-CL+. A coastline model was configured and verified that predicts the behaviour of the nourishment. It was shown that a good similarity between the survey data and the model was obtained in a section of 500 m near the marina, based on the comparison of sediment balances.

The correspondence 200 m further down drift was less well. An increase of material was concluded from the surveys while the model predicted erosion in this section. Several scenarios were investigated to investigate this effect of which extending the shoreline down drift of the nourishment gave satisfactory correspondence. This leads to the conclusion that a more accurate prediction of the coastline down drift of the nourished area might improve the correspondence. A physical explanation for the surveyed accretion in this area was not found. Therefore no firm conclusion of the model performance is drawn for this section.

Less well results were obtained on the prediction of the dry-beach width and the development in time. This was according to expectations since the model is not able to simulate the cross-shore process that causes the waterline to retreat.

Analysis of the UNIBEST software package, definition of its capability to make short-term predictions

The conclusion is that with the Italian beach model volume computations can be made for Italian beach with satisfactory results. For the prediction of the position of the waterline it was less effective. This is expected since UNIBEST-CL+ does not take into account the effects of cross-shore redistribution of sand on the waterline. It is concluded that in this short period of 8 months the cross-shore processes are dominant over longshore processes for the position of the waterline for the prediction of the position of the dry-beach width at Italian beach. In general, these cross-shore effects will largely depend on the slope with which the nourishment is placed.

Optimization and suggestions for future nourishments with the UNIBEST model

The hypothesis is that better placement of sand within the nourished area can improve the life span of the nourishment. The life span is determined by the time that it takes that no dry-beach width remains at a certain area in the nourished area. Three cases were tested with this model for optimization, placement in triangular, rectangular shape near the Marina and in two undulations along the beach. All three cases improved the critical section of 300 m near the marina. But they caused more erosion further down drift. Since this model can not accurately predict the dry-beach width, it can not be stated if this is acceptable or not.

Conclusions of the cross-shore modelling

The model needs heavy calibration. Instability of the dune was seen for computations with grain sizes coarser than 400 μm. Also waves with H_{rms}< 0.75 m caused instability. This calibration makes the results less reliable.

Above MSL some instability of the profile was seen. This is the influence of the seawall boundary. Around MSL to CD -2 m the model has very good results. This shows that the model can predict the dry beach width with good results. Below CD too much accretion is computed. This is probably because part of the material was transported alongshore, which is not incorporated in the model and to deeper depths.

9.3 Recommendations

Regarding the analysis of morphologic behaviour of the coast and nourished areas

The analysis of the morphologic behaviour of the nourished areas was made based on the surveys made directly after the placement, in February and in May 2004. More surveys were probably made and analysis of all this data is recommended. This data was provided by Van Oord and based on profiles with a length of 250 m with depths between CD – 4 m and CD -6 m. It is recommended to make sediment balances using profiles which extend deeper than CD -6 m.

The analysis of the morphologic behaviour of the total beach stretch was based on satellite images made before the nourishments. With images from the period after the placements a better analysis can be made.

Regarding the surveys

Morphological studies are difficult to perform based on survey data of the nourished area only. Therefore it is recommended to survey the whole beach, because:

- It can be seen where the eroded material settled.
- More detailed information on by-pass can be obtained by survey near the updrift side of the marinas
- A better analysis and predictions of the behaviour of the whole beach can be made.

Most surveys were carried out until 400 m offshore. In some profiles this was too short and significant transport to parts of the cross-shore profile that are deeper. It is recommended to survey to a minimal depth of CD –7 m, about 650 m.

Regarding the boundary conditions

To estimate the influence of the "World" on the wave climate, simulations for the wave climate at Italian beach are recommended (and well possible) with the monthly progress of the project in the bathymetry of the World Waves program. Digital information of the measured wave climate by the Dubai Municipality could improve the accuracy of the comparison of both climates.

Information of sand-characteristics varied largely. More detailed and accurate samples would improve the reliability. To limit the variation in the results more than one sample can be made on each location and a mean of each location can be determined. Samples taken before the nourishment can be helpful to determine the native sand characteristics of the beach. For cross-shore modelling samples on different positions of the profile (also under water) can be used for more accuracy. Of particular interest are the sand characteristics at the toe at CD –7 m.

Regarding the modelling in UNIBEST-CL+

The wave climate was schematized in classes of 45^0, this is rather large. It is recommended to make smaller classes of 30^0. Along the beach different sediment characteristics were found, while only one characteristic size was used. The influence of the sand characteristics on the results is large. Modelling this might improve the results.

Verification and calibration for the whole period between January and August was carried out. Modelling on monthly basis is less straightforward but can improve the results of the model.

More state-of-the-art models such as DELFT-3D take into account more processes, such as detailed flow calculations and sediment concentrations. It is also based on time records of waves, water elevations and current. With this model better result on the prediction of the dry-beach width might be obtained.

Regarding the optimization

The optimizations were made using a lot of assumptions. Further study is required to study the effects of different placement on hydrodynamic conditions and development within the profile. Also more research has to be carried out to determine if it is physically possible to position nourishment with these shapes.

At Italian beach the life span of the nourishment was dominated by cross-shore effects over longshore effects; i.e. the dry-beach width and not the total eroded volume. Therefore a model that predicts this more accurate can predict if the coastline retreat down drift is acceptable or not.

Regarding the cross-shore modelling

The model needed heavy calibration, but for the parameter-settings mostly default values were used. More calibration of these parameters might influence the results.

References

British admiralty. 1994. “Admiralty tide tables and tidal streams tables”. Hydrographer of the navy.

CUR/RWS. 1995. “Manual on the use of rock in hydraulic engineering” Centre for Civil Engineering and Codes, Ministry of Transport, Public works and Water Management, Gouda, the Netherlands. p 4.1-4.5, 4.18-4.22, 4-46-4.49.

Dean, R.G. Dalrymple, R.A. 2002. “Coastal Processes with Engineering Applications”. Cambridge university press. p 30-32 , 162-175, 343-357.

Dean, R.G. 2002. “Beach nourishment theory and practice”. World Scientific Volume 18. USA. p 25-29.

Hellbrand, D. Fernandez, J. Stive, R. 2004. “Case study: design of Palm Island No. 1 Dubai”. Terra et Aqua-No 96. p 14-20.

Jong, R.E. de., Lindo, M.H. Saeed A., Vrijhof, J. 2003. “Execution methodology for reclamation works Palm Island 1”, Terra et Aqua, No 92. p 14-23.

Rijkswaterstaat. 1988. “Handboek zandsuppleties”. Gouda. p 83-98.

Soulsby, R. 1997. “Dynamics of Marine sands”. Thomas Telford Publications Limited.

USACE. 2003. “Coastal engineering manual part V (version 31 July 2003)”. Washington D.C. Chapter 4.

Velden, E.T.J.M. van. 2000. “ Coastal engineering Volume II”. Delft University of Technology Department of Civil Engineering. Delft. The Netherlands. p 63-95, 158-177.

Vroeg, H. de. 1999. “Pontos, diffractie”. Telefax, WL Delft | Hydraulics. pp 6.

Walstra, D.J.R. April 1999, UNIBEST-TC. User manual version 2.02. WL | Delft Hydraulics.

WL|Delft Hydraulics. 1994. “Unibest manual, theoretical reference document”. WL | Delft Hydraulics. p 4-9, 14-24. A.1-A,2.

WL | Delft Hydraulics. Rijkwaterstaat. 1987, “Manual on artificial beach nourishment”. WL | Delft Hydraulics. Rijkswaterstaat, centre for civil engineering, Research, Codes and Specifications. p 100-114, 120-121.

WL | Delft Hydraulics. Rijkswaterstaat. 1986, “Background information on artificial beach nourishment”. Rijkswaterstaat, WL | Delft Hydraulics centre for civil engineering, Research, Codes and Specifications. The Netherlands. Annex VI Coastal morphology theories. Annex VIII p 1-3.

WL | Delft Hydraulics. July 2002. “Palm Island, Dubai: Water Quality and morphology study. For Jebel Ali properties”. WL | Delft Hydraulics. p 2.21-2.5, 6.1-6.5.

Figures

M.D. van Dijk
MSc Thesis
July 12, 2005

TU Delft Van Oord WL | delft hydraulics

List of Figures

1: Palm Jumeirah
2: Palm Jebel Ali
3: The World
4: Port Rashid

Artist impression of the coastline of Dubai after the completion of the projects	Dubai	Nov 2003
WL | DELFT HYDRAULICS		Figure 1.A

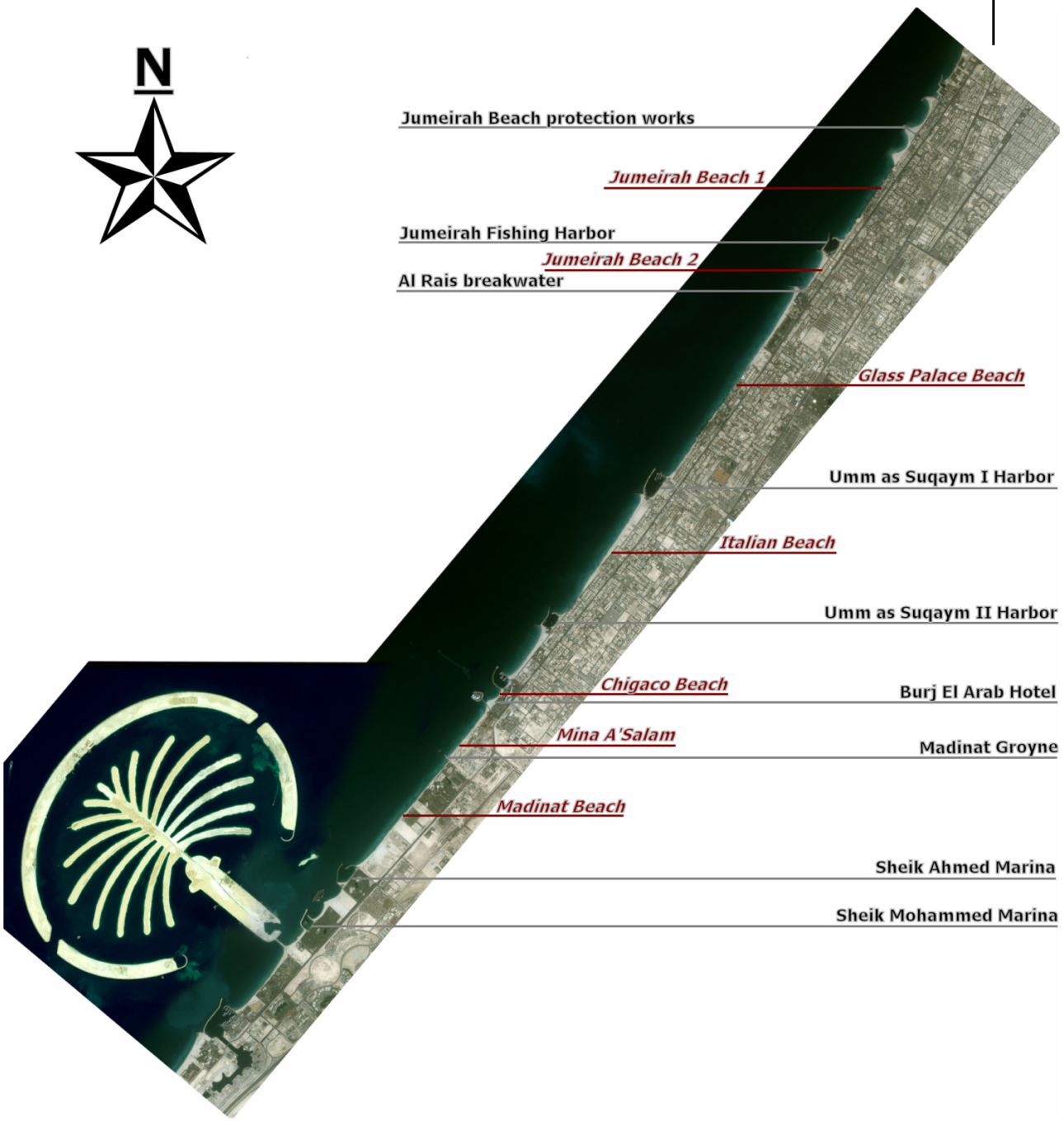

Coastline between Palm Island Jumeirah and Port Rashid.	Dubai	Oct. 2003
WL | DELFT HYDRAULICS		Figure 1.B

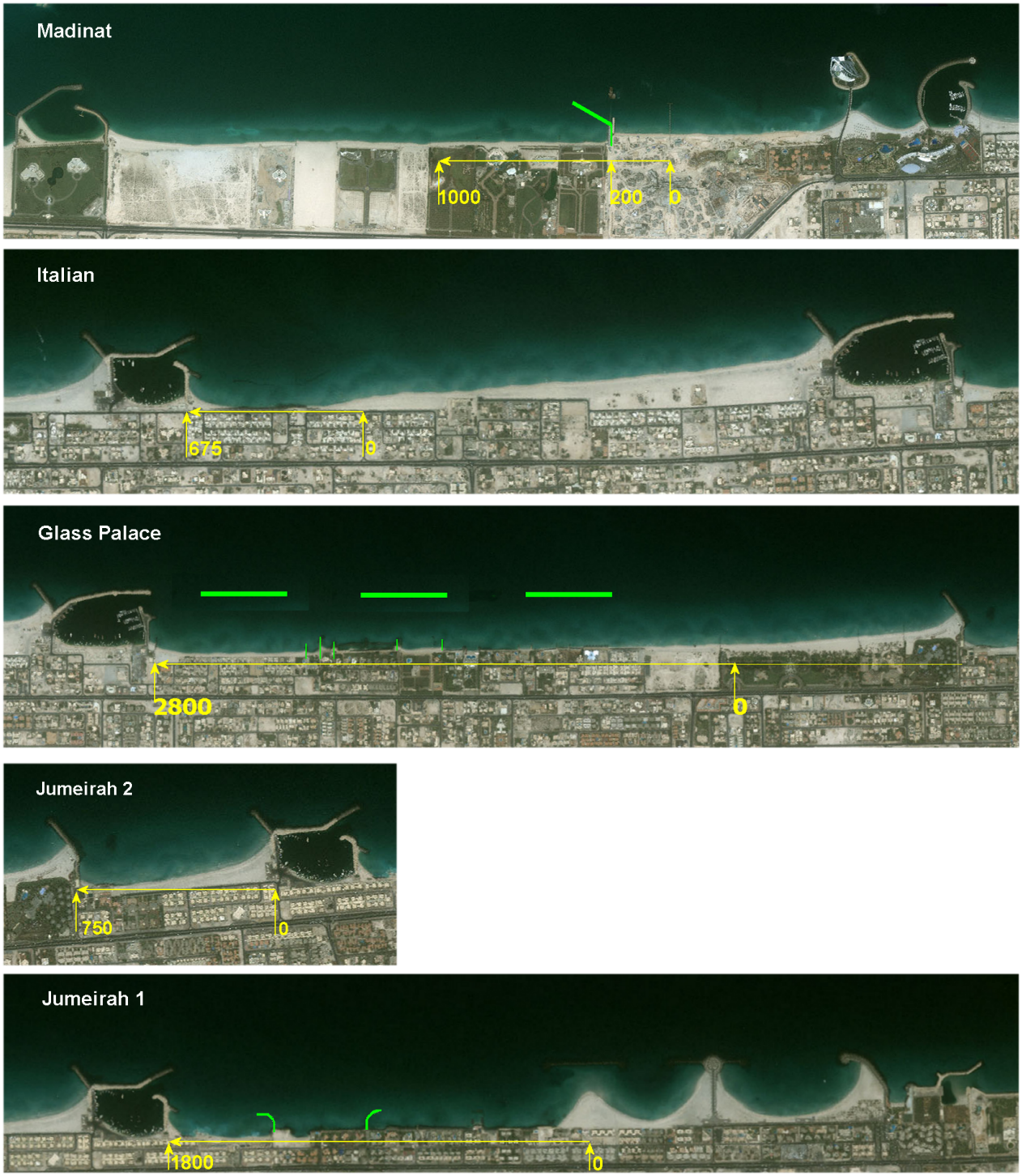

Nourished beaches in order from south to north, with reference line defined by Van Oord. (In green are the recently built coastal protection works)	Dubai	Oct. 2003
WL | DELFT HYDRAULICS		Figure 1.C

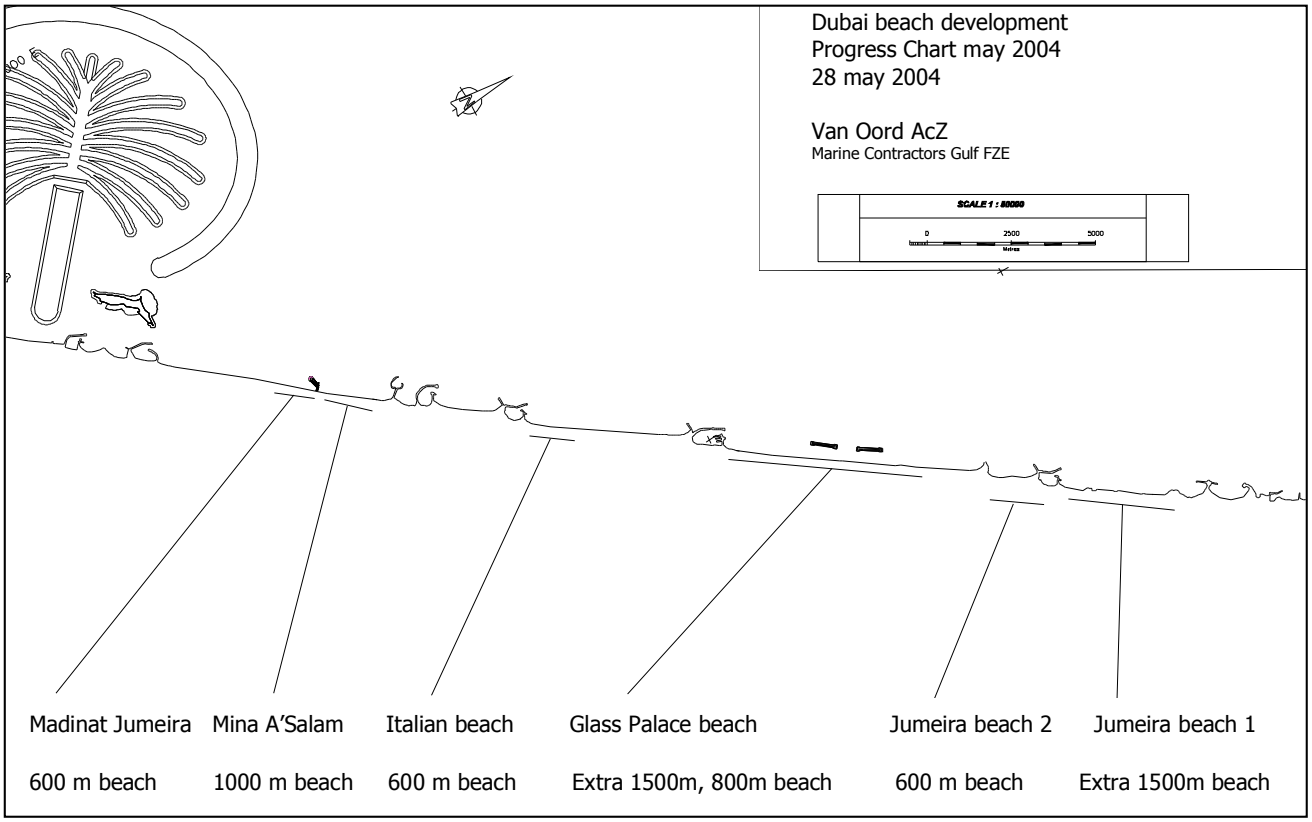

Nourishment locations (not to scale) (source: Van Oord)	Dubai	May 2004
WL | DELFT HYDRAULICS		Figure 1.D

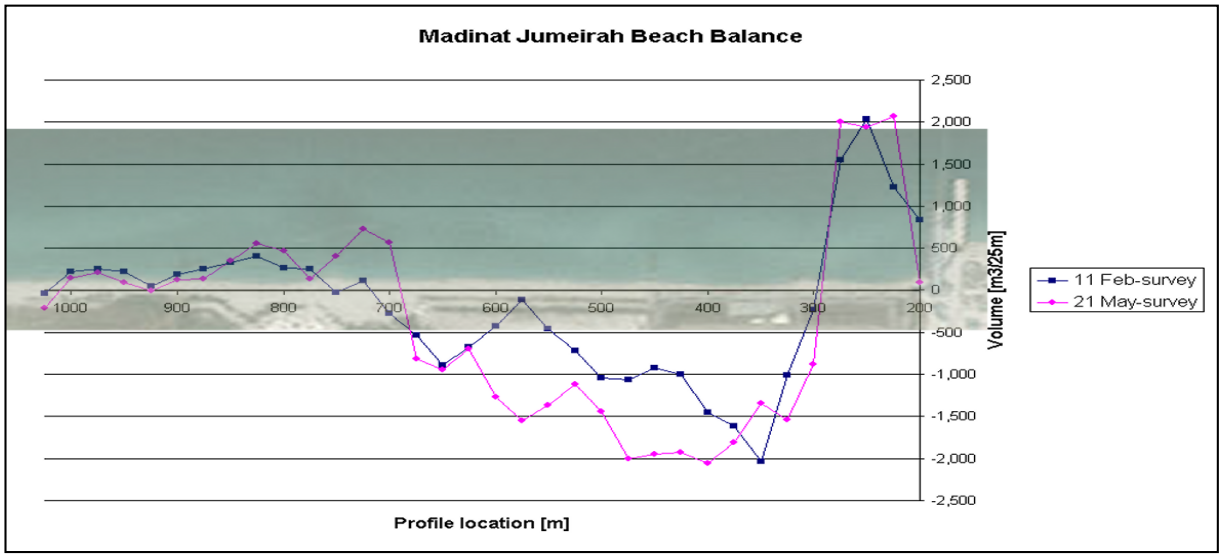

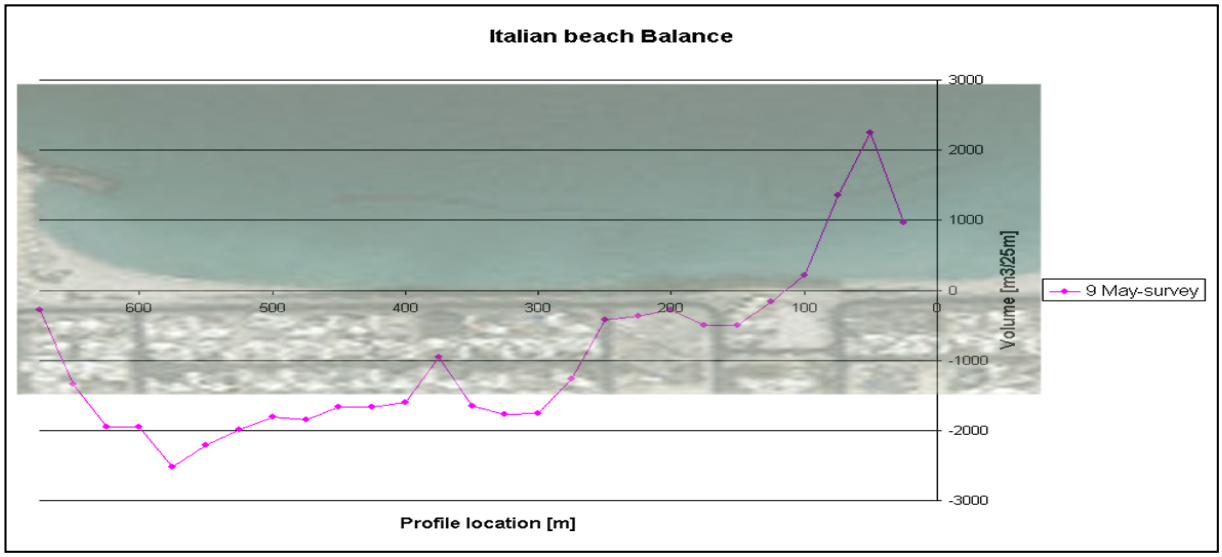

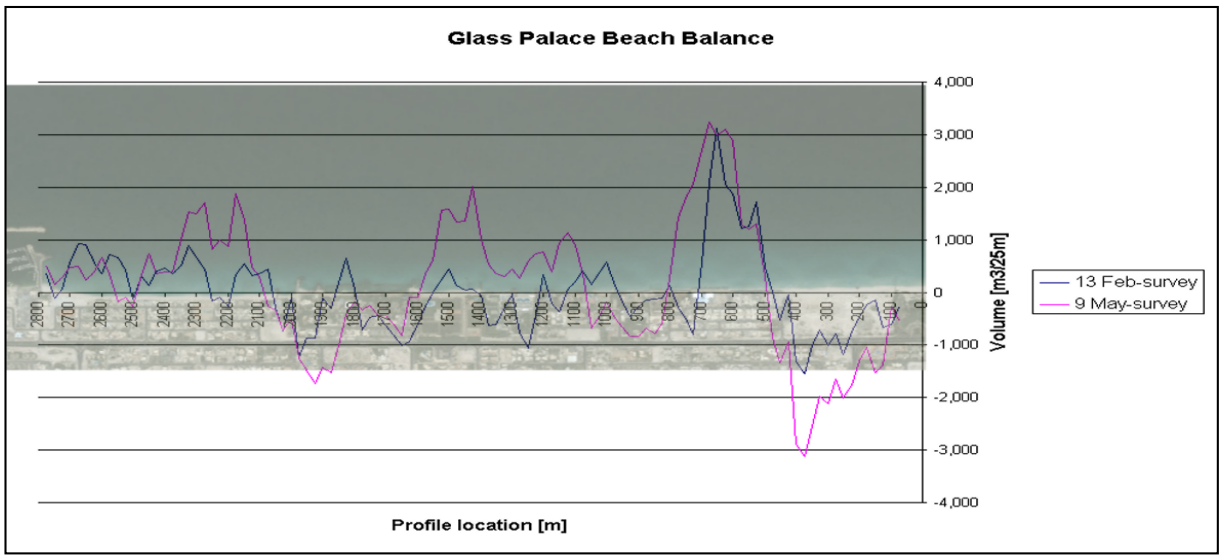

Sediment balances of Madinat, Italian and Glass Palace (Source: Van Oord)	Dubai	Oct. 2003
WL | DELFT HYDRAULICS		Figure 3.A

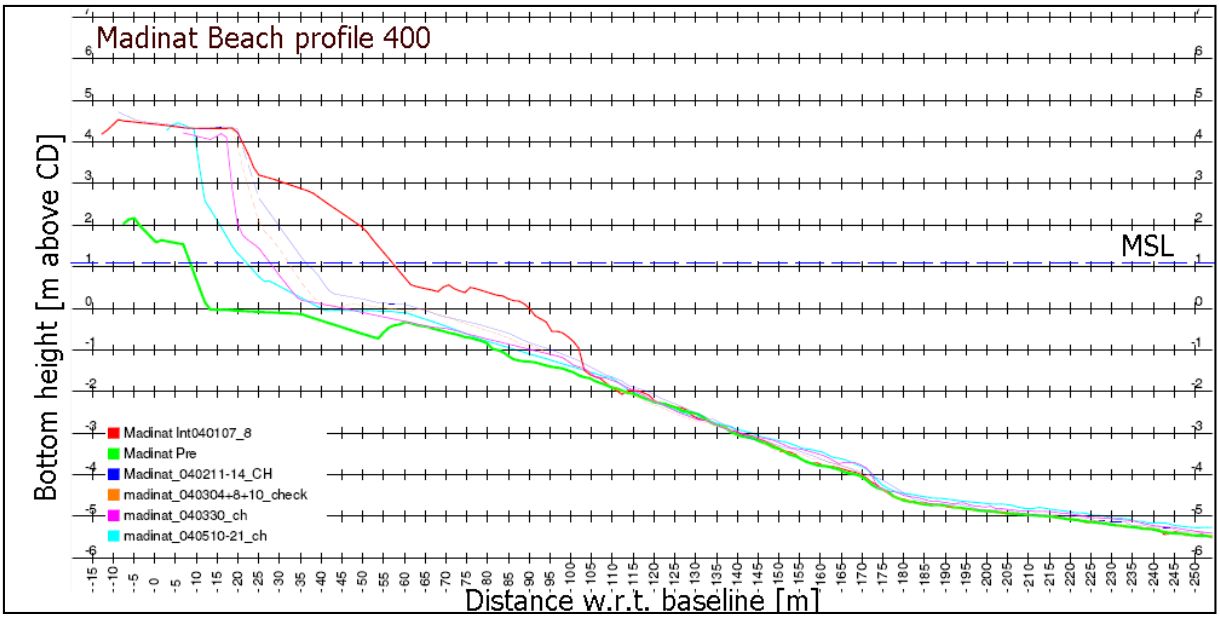

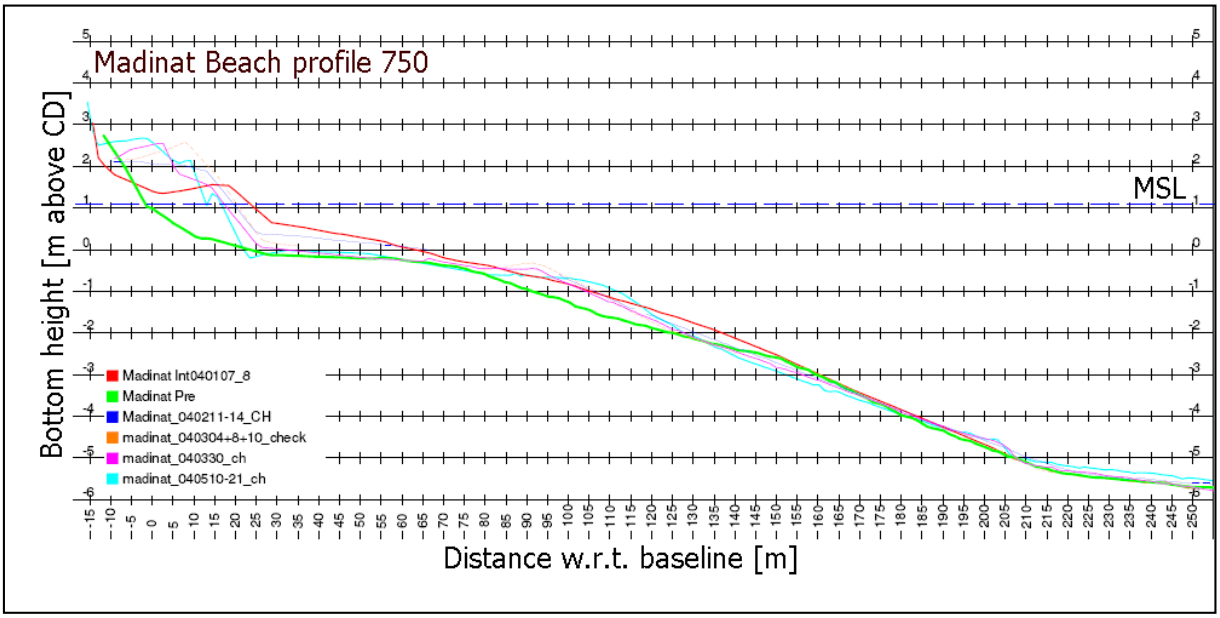

Profiles of Madinat beach (Source: Van Oord)	**Dubai**	**2004**
WL | DELFT HYDRAULICS		Figure 3.B

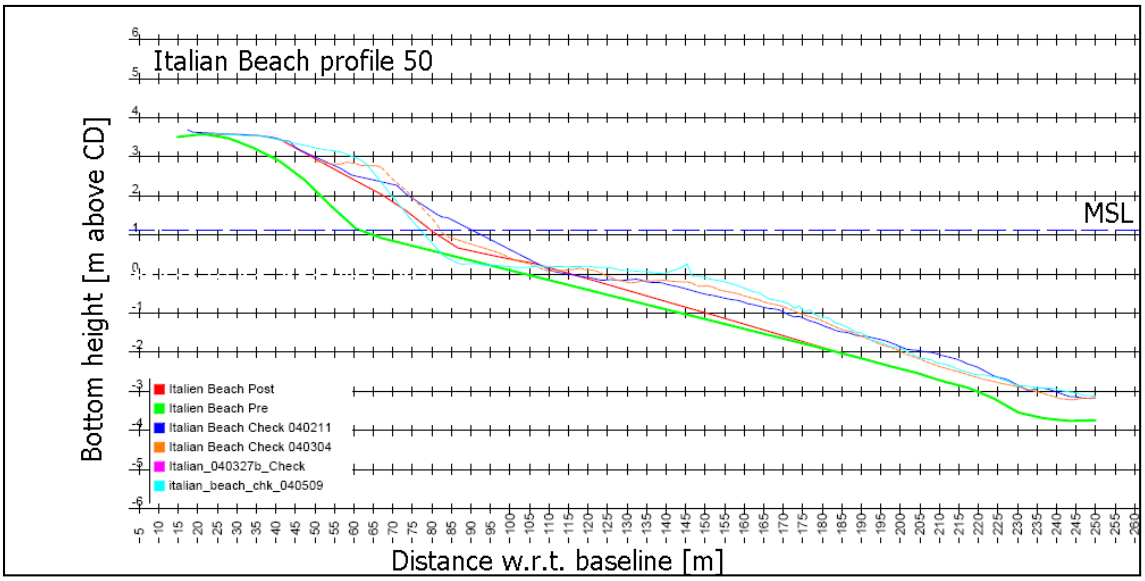

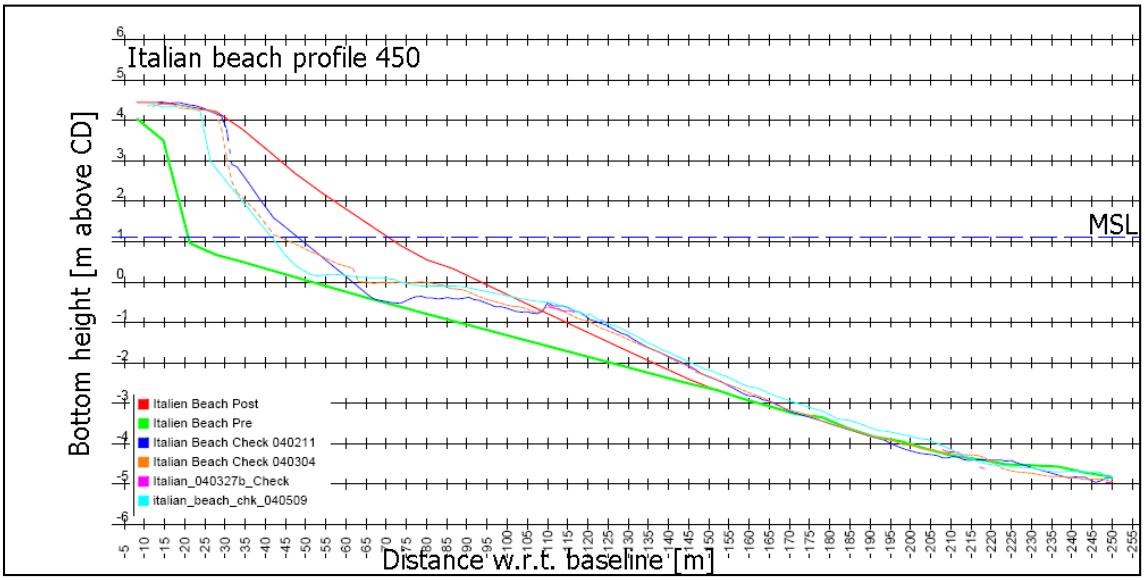

Profiles of Italian beach (Source: Van Oord)	**Dubai**	**2004**
WL | DELFT HYDRAULICS		Figure 3.C

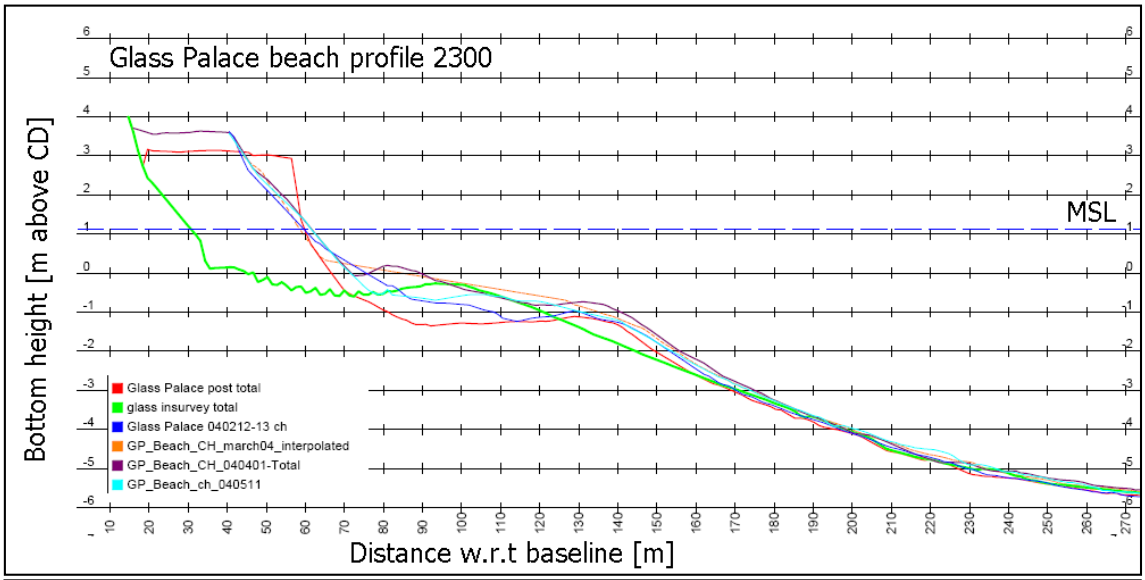

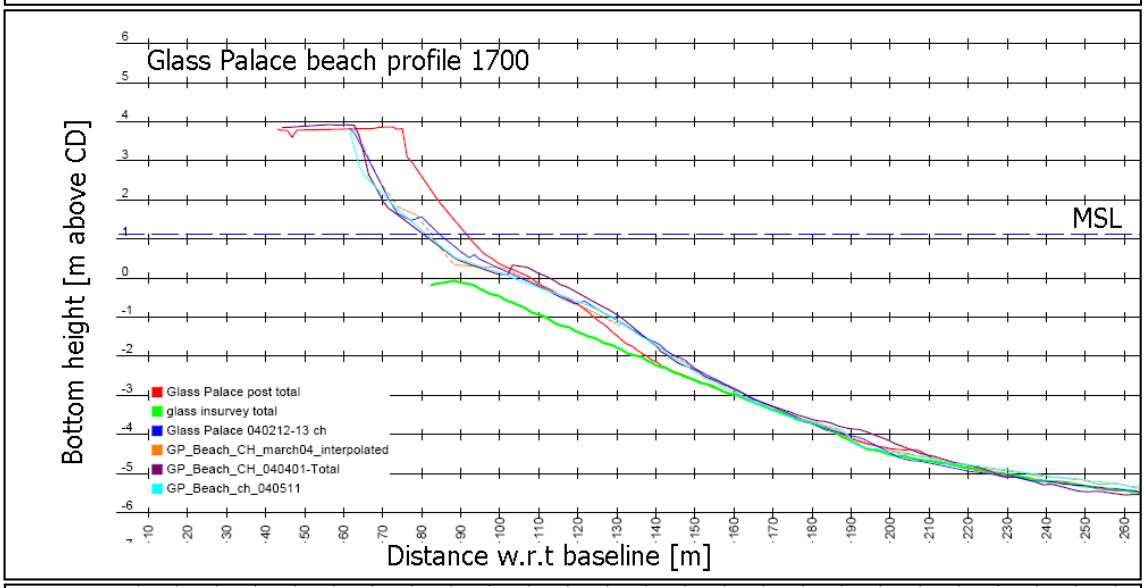

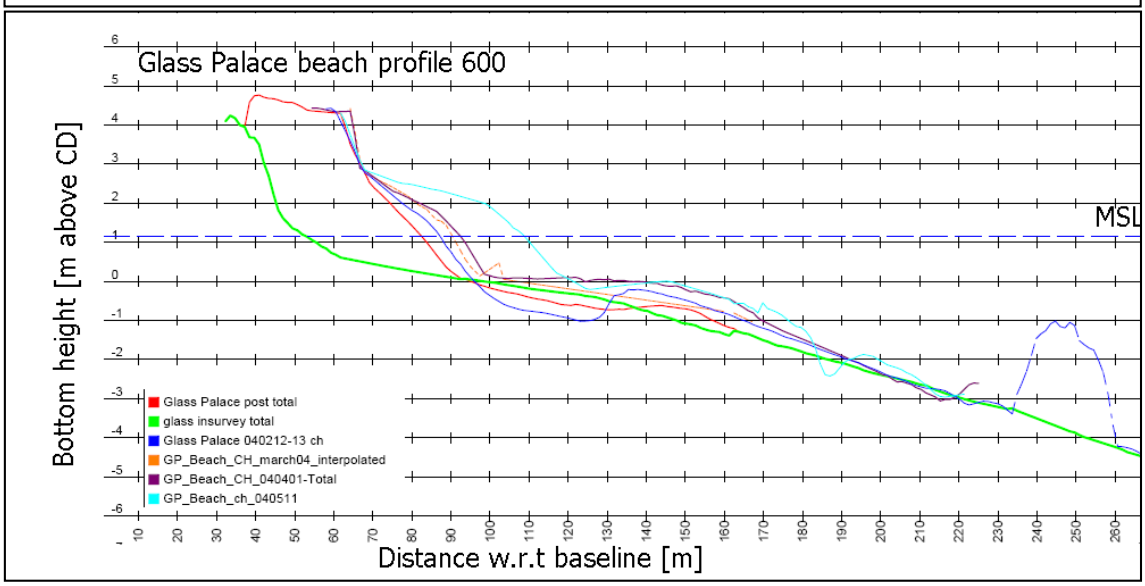

Profiles of Glass Palace beach (Source: Van Oord)	**Dubai**	**2004**
WL | DELFT HYDRAULICS		Figure 3.D

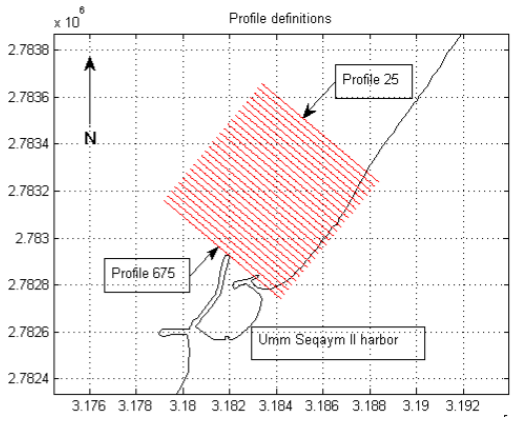

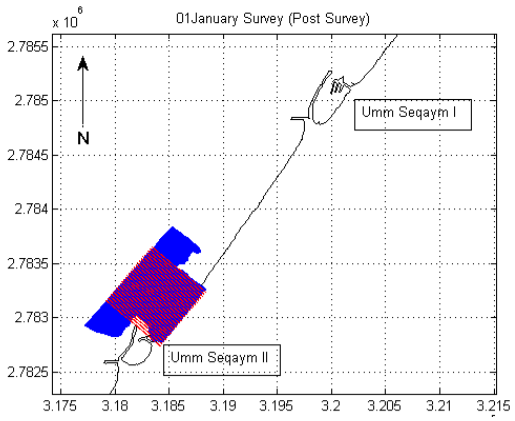

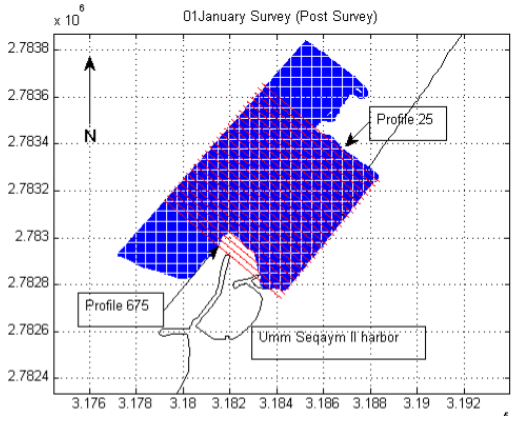

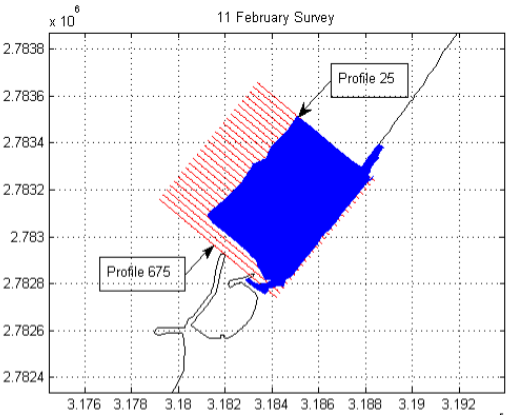

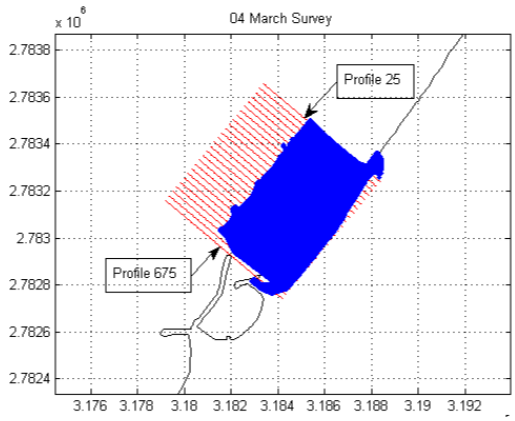

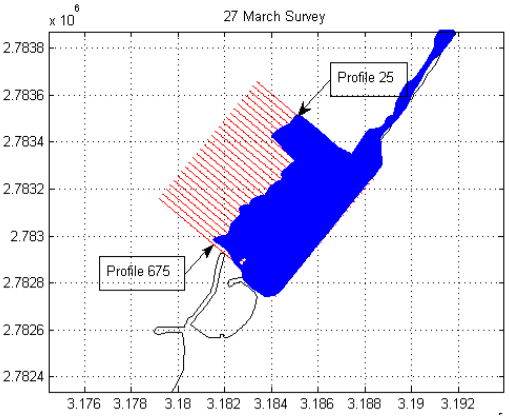

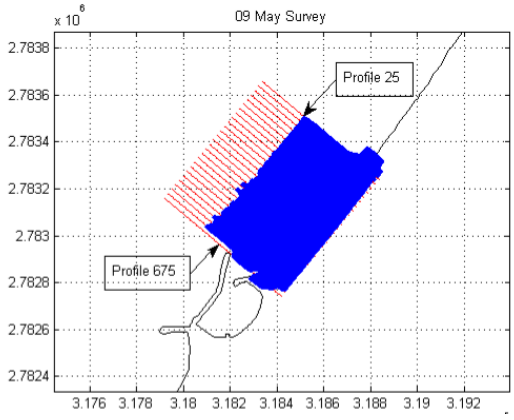

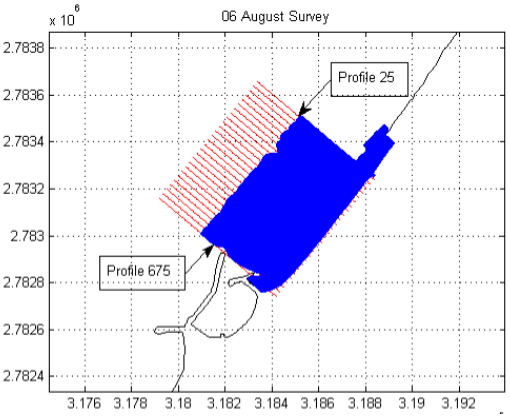

Ray definitions and survey plots for the January-August Surveys.
(Blue= survey point; Red= profile point)

Dubai | 2004

WL | DELFT HYDRAULICS | Figure 4.A

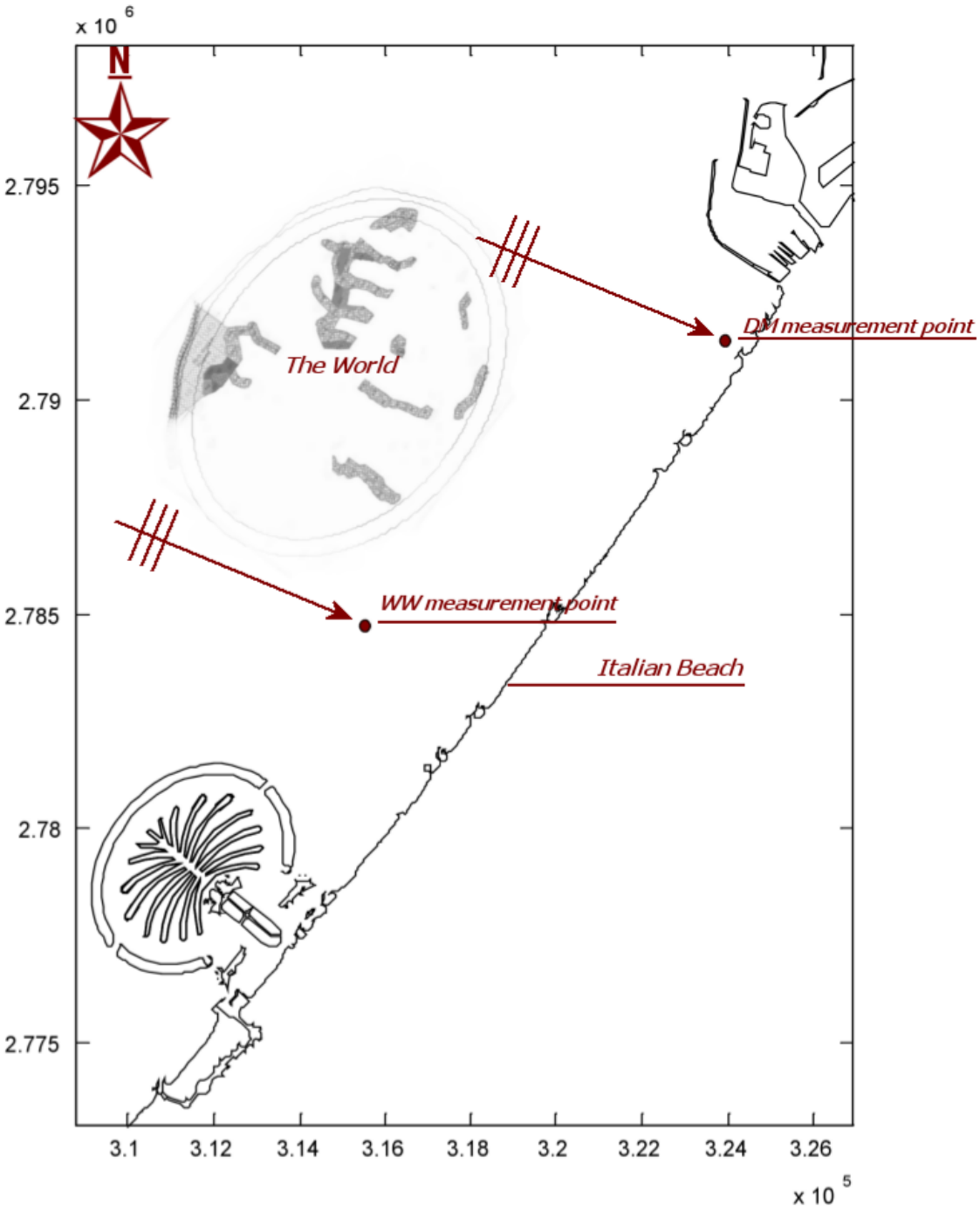

Position of the measurement points and the progress of the World in May 2004	**Dubai**	May 2004
WL | DELFT HYDRAULICS		Figure 4.B

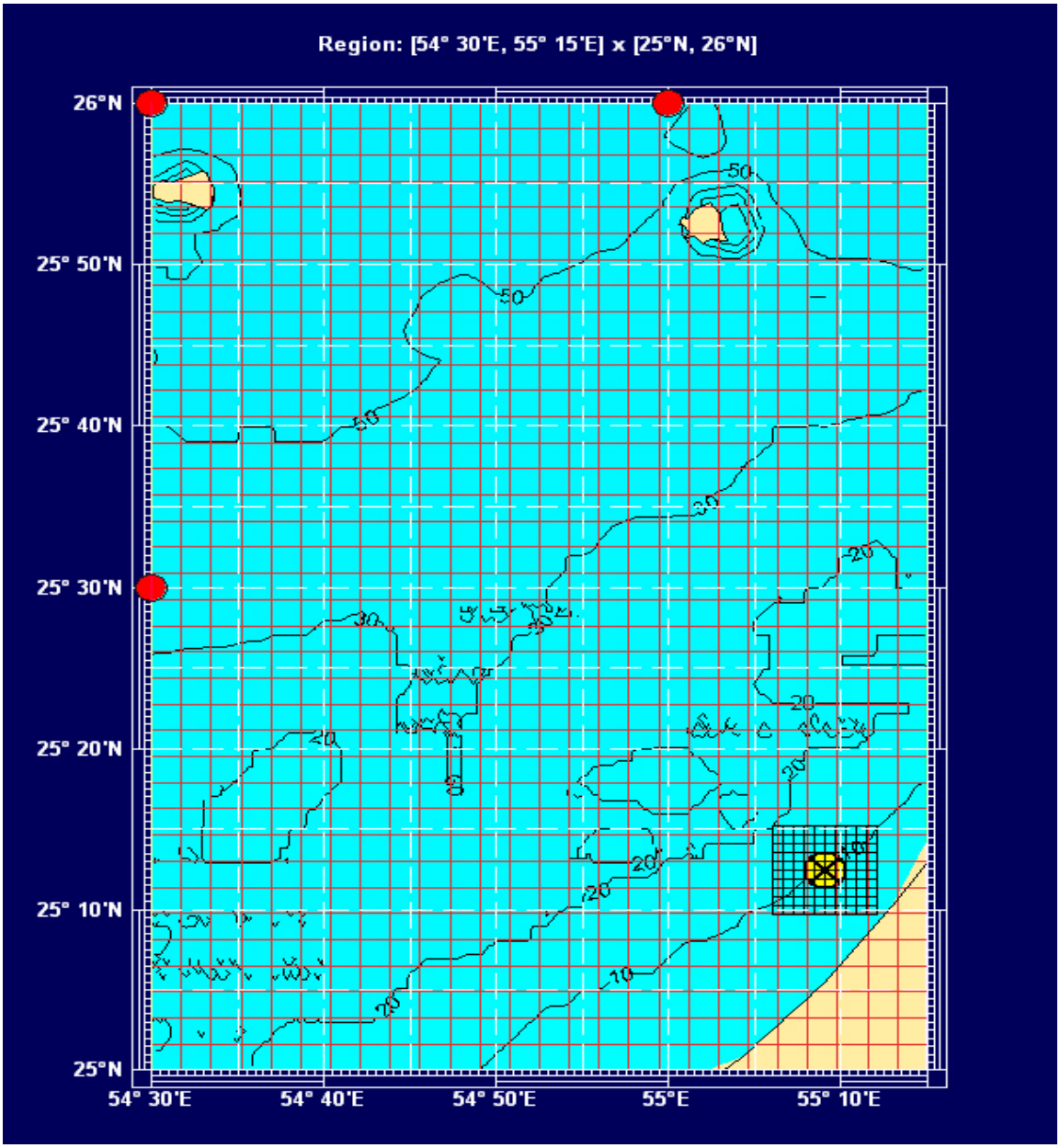

Computation area and bathymetry from the World Waves program (red dots: offshore data points)

Dubai

WL | DELFT HYDRAULICS

Figure 4.C

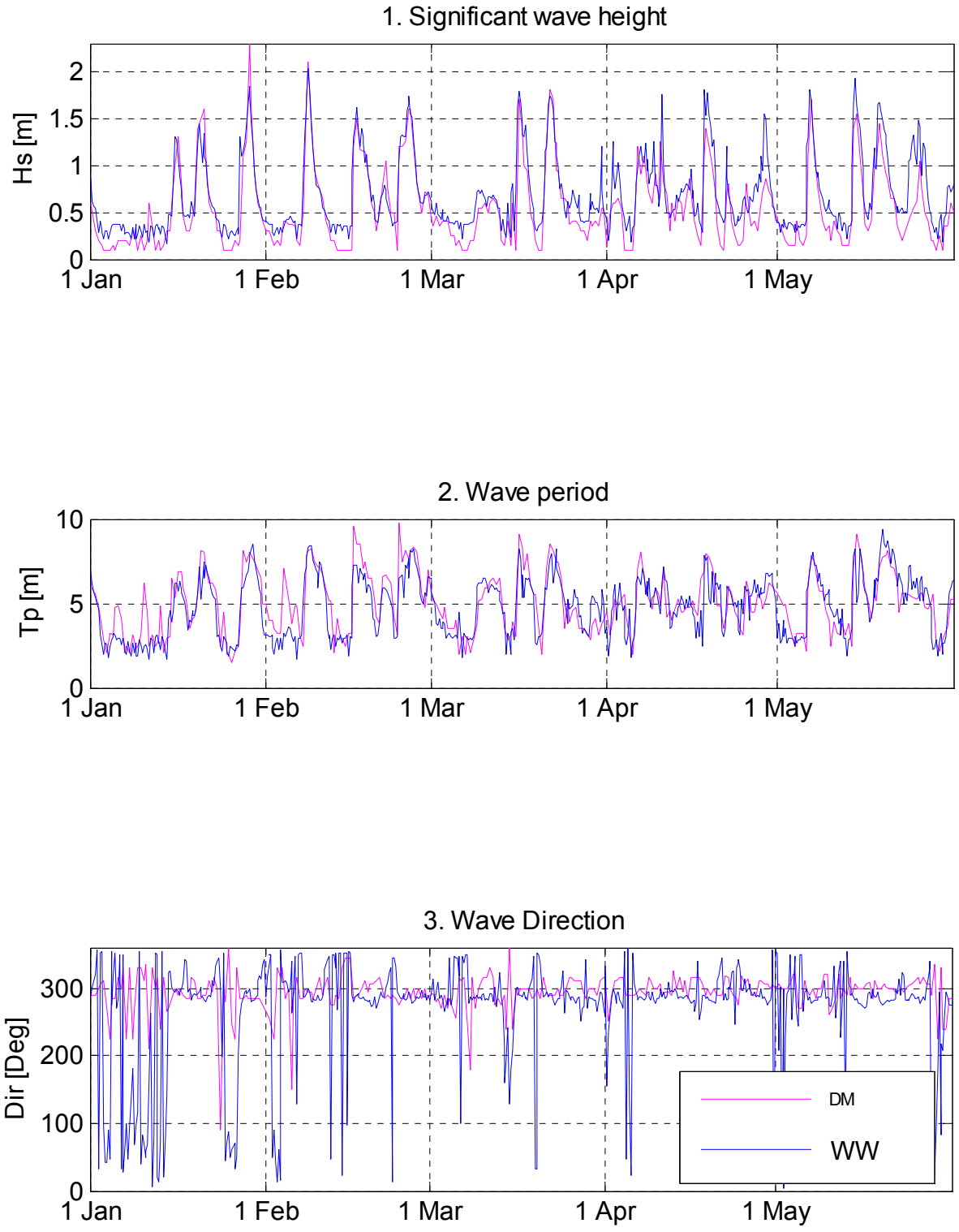

Wave record WW and DM of Hs, Tp and Direction	Dubai	2004
WL | Delft Hydraulics		Figure 4.D

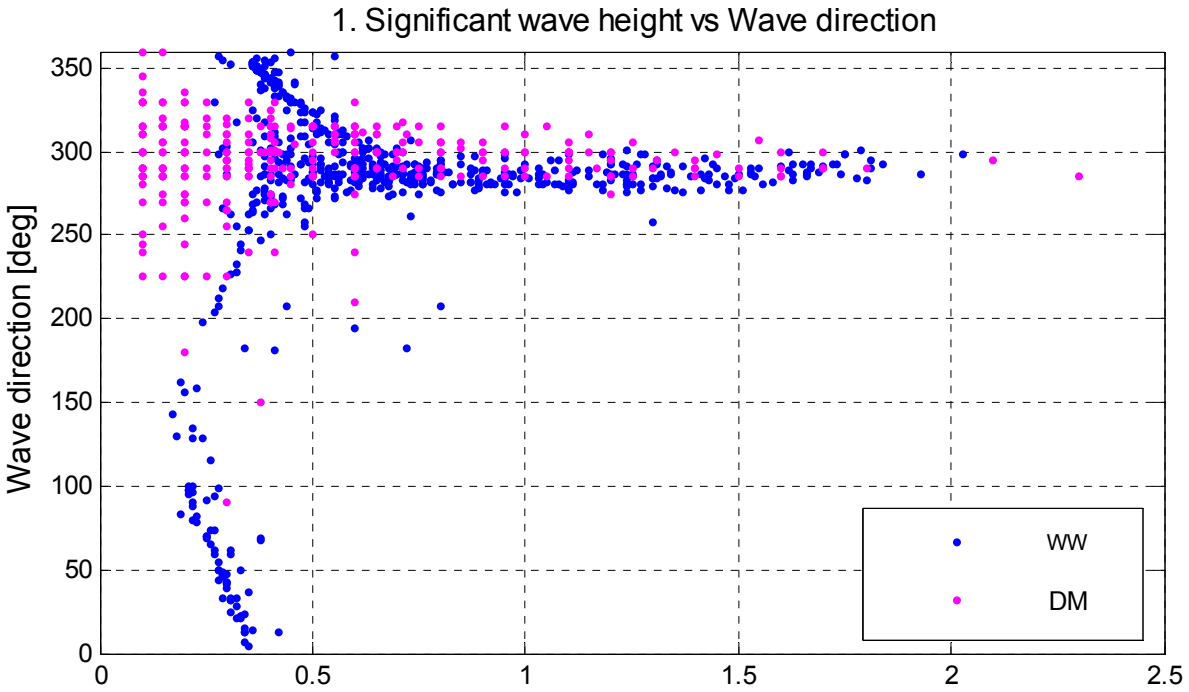

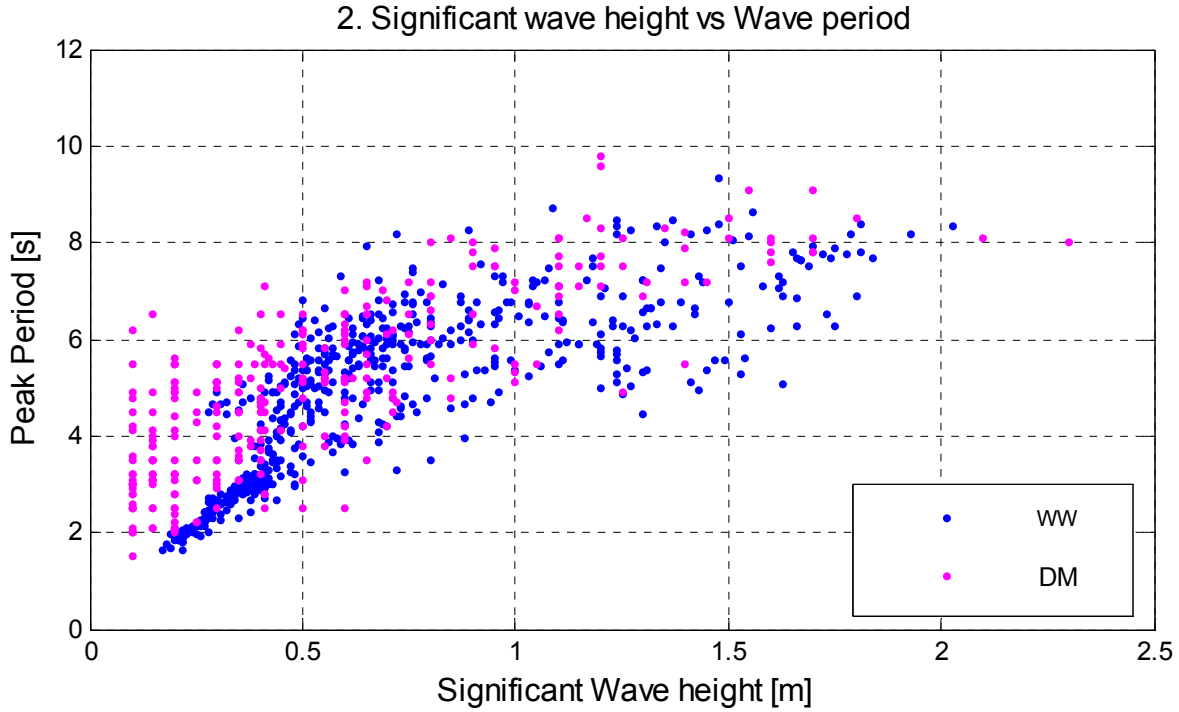

Significant wave height vs direction and period	Dubai	2004
WL | Delft Hydraulics		Figure 4.E

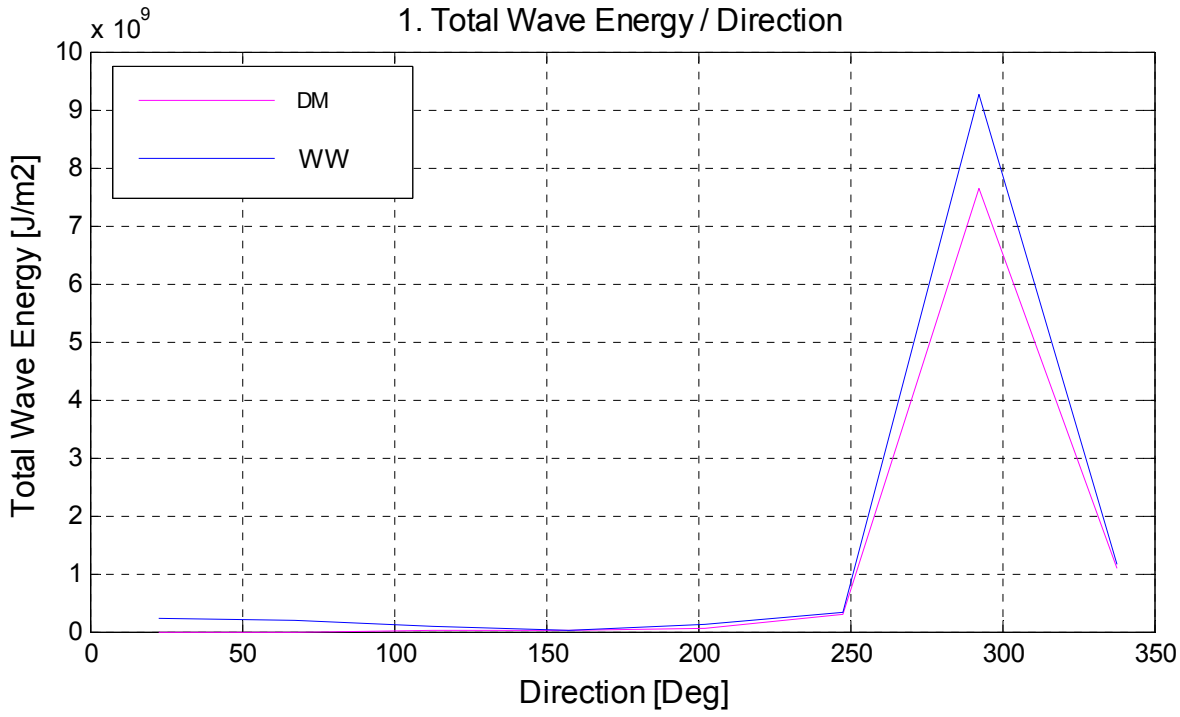

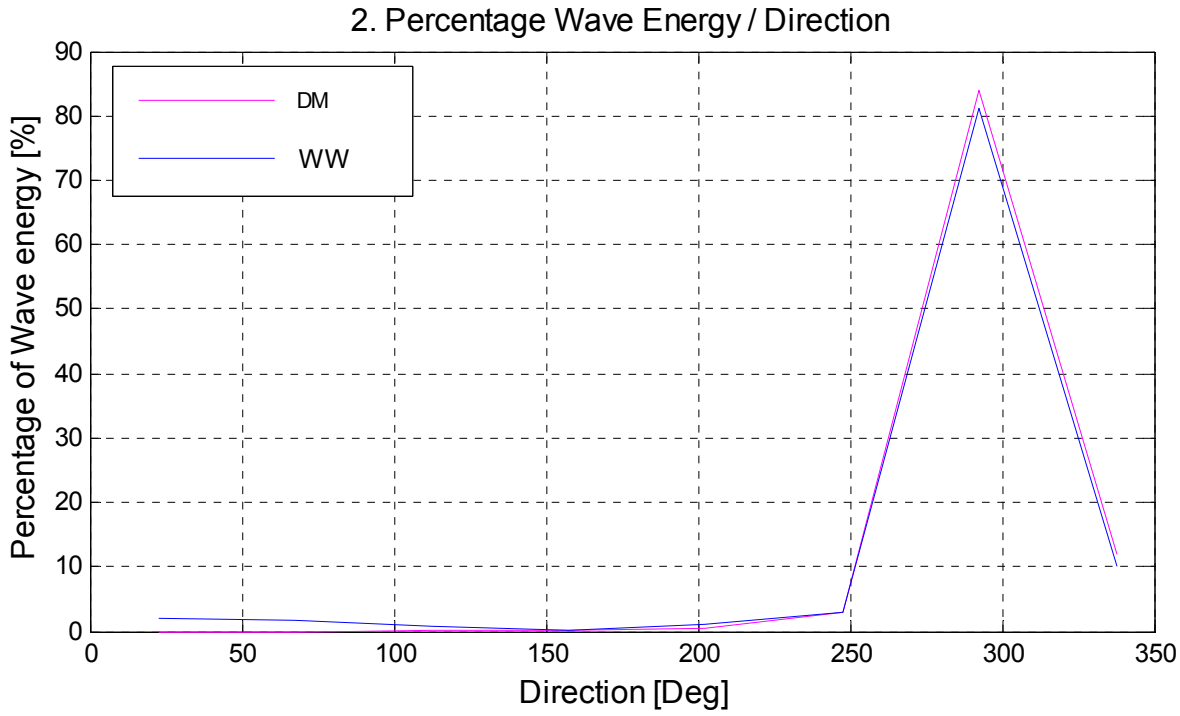

Wave Energy of WW and DM vs direction and period	Dubai	2004
WL | Delft Hydraulics		Figure 4.F

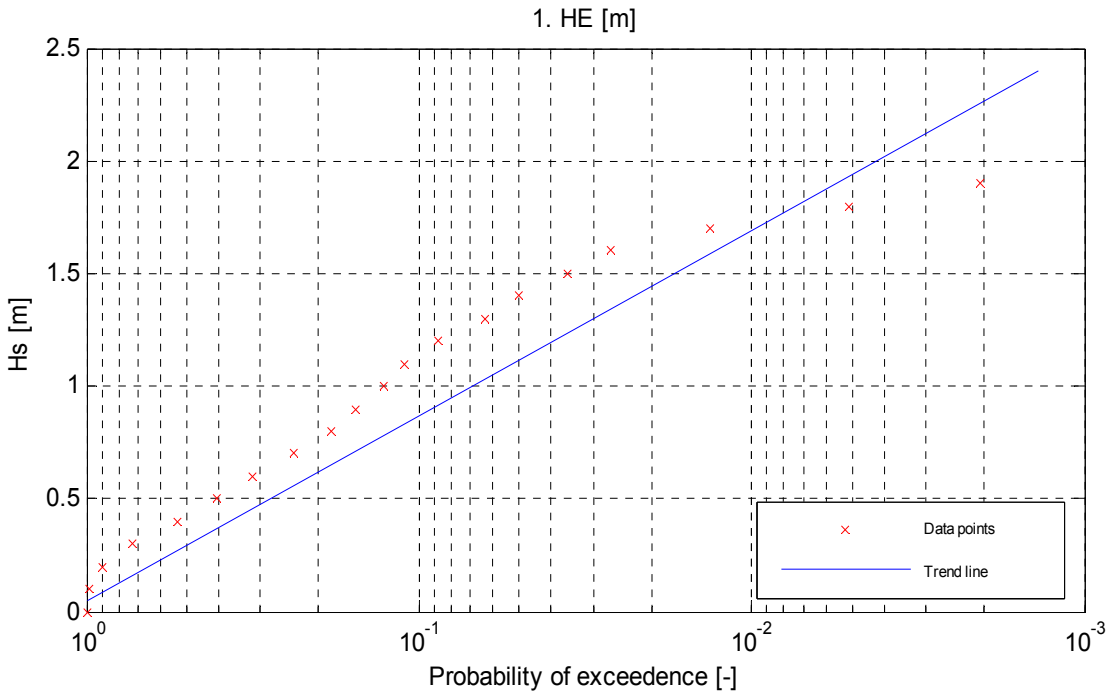

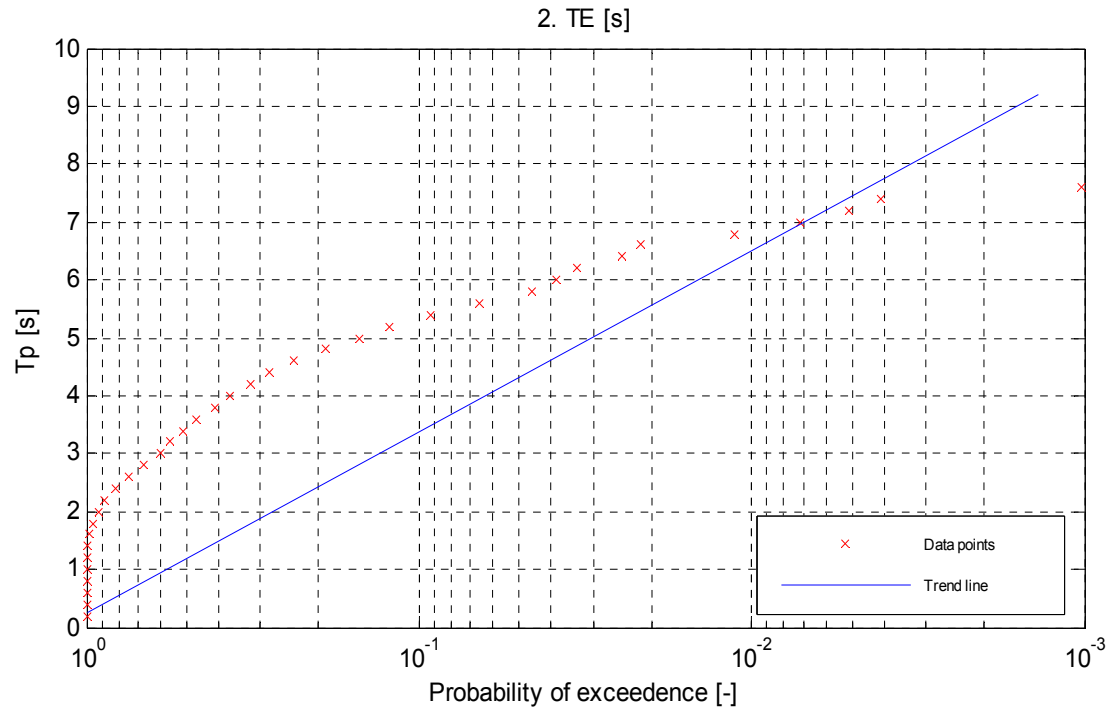

Determination of the exceedence change of the wave height and wave period	Dubai	2004
WL | Delft Hydraulics		Figure 4.G

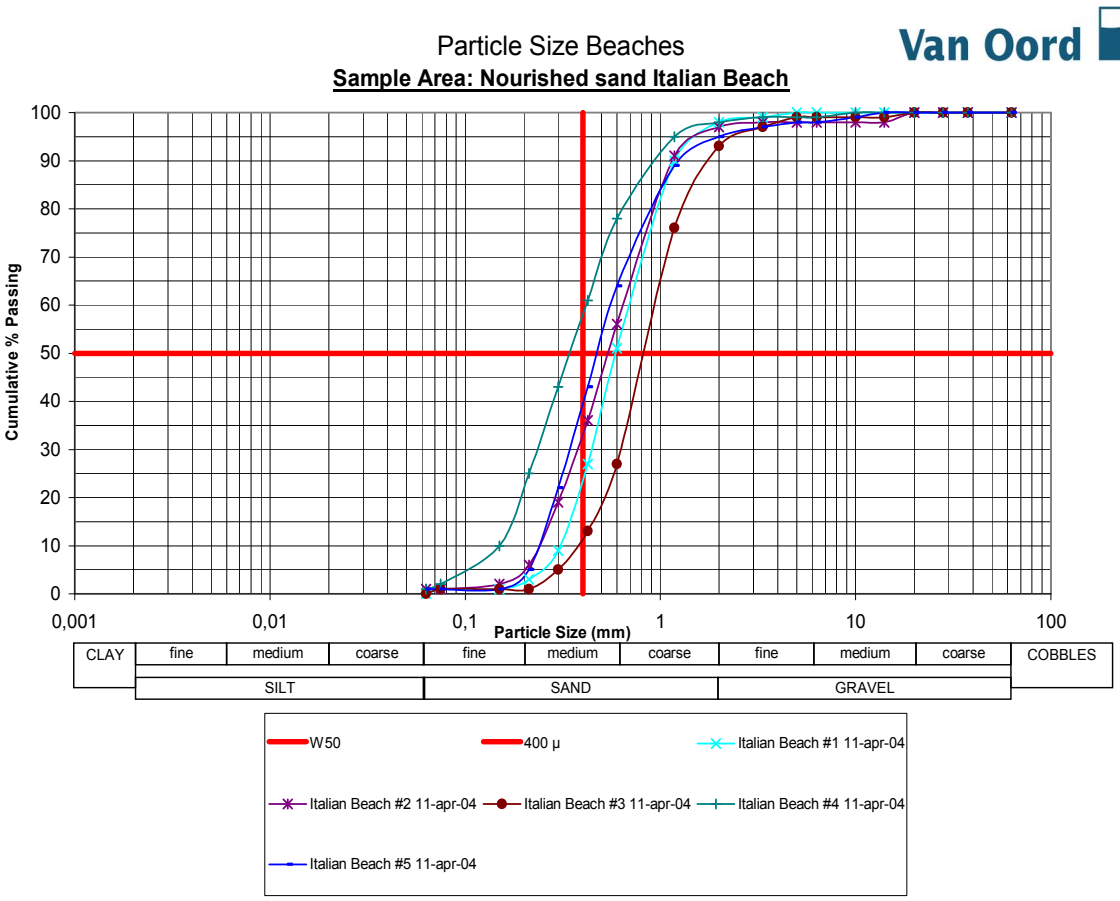

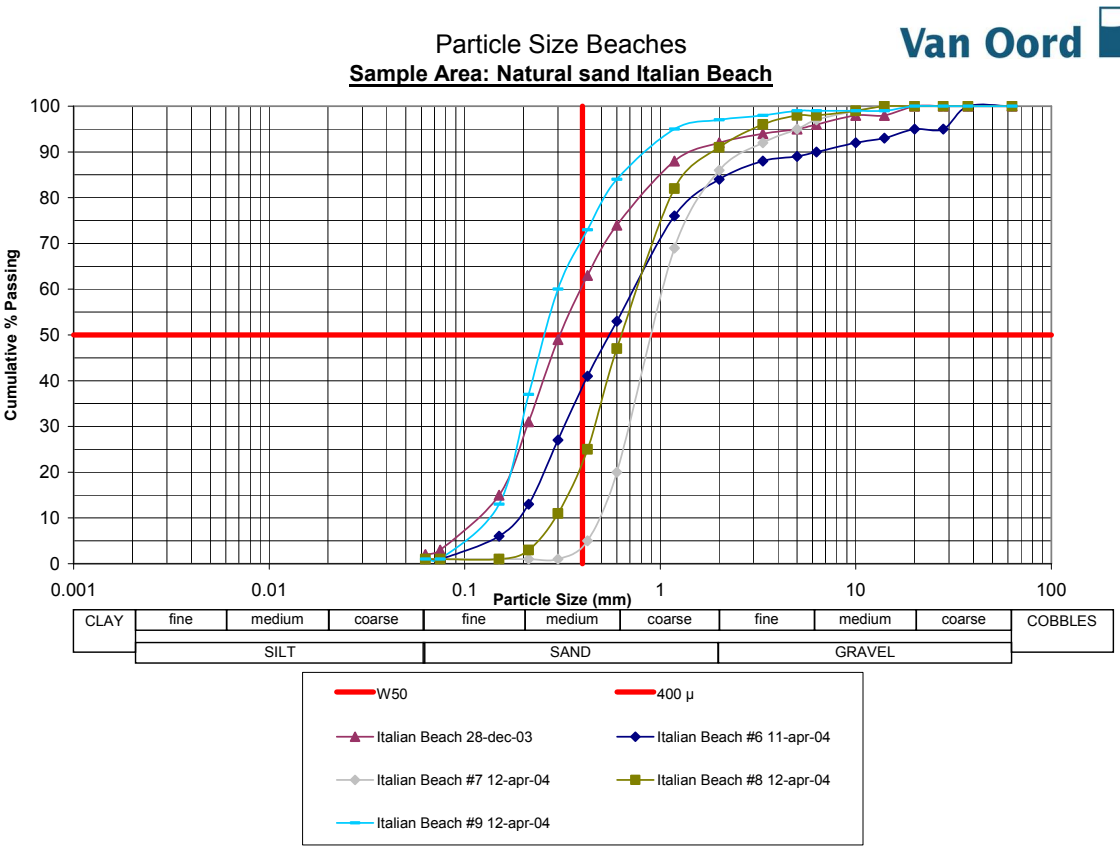

Sediment curves of Italian beach (Source: Van Oord)	Dubai	April 2004
WL | DELFT HYDRAULICS		Figure 4.H

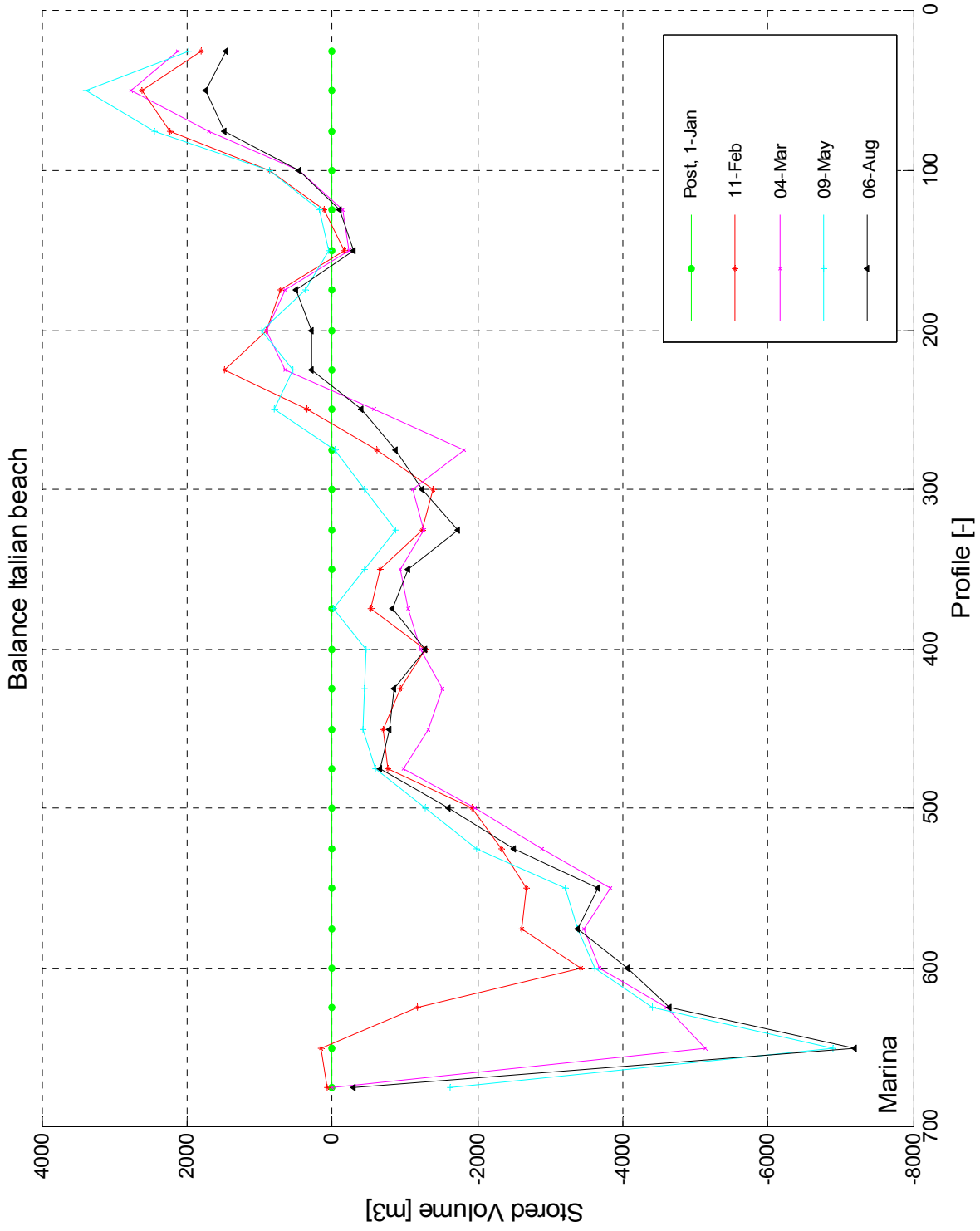

Volume difference of the Surveys with respect to the Post Survey	Dubai	2004
WL | Delft Hydraulics		Figure 5.A

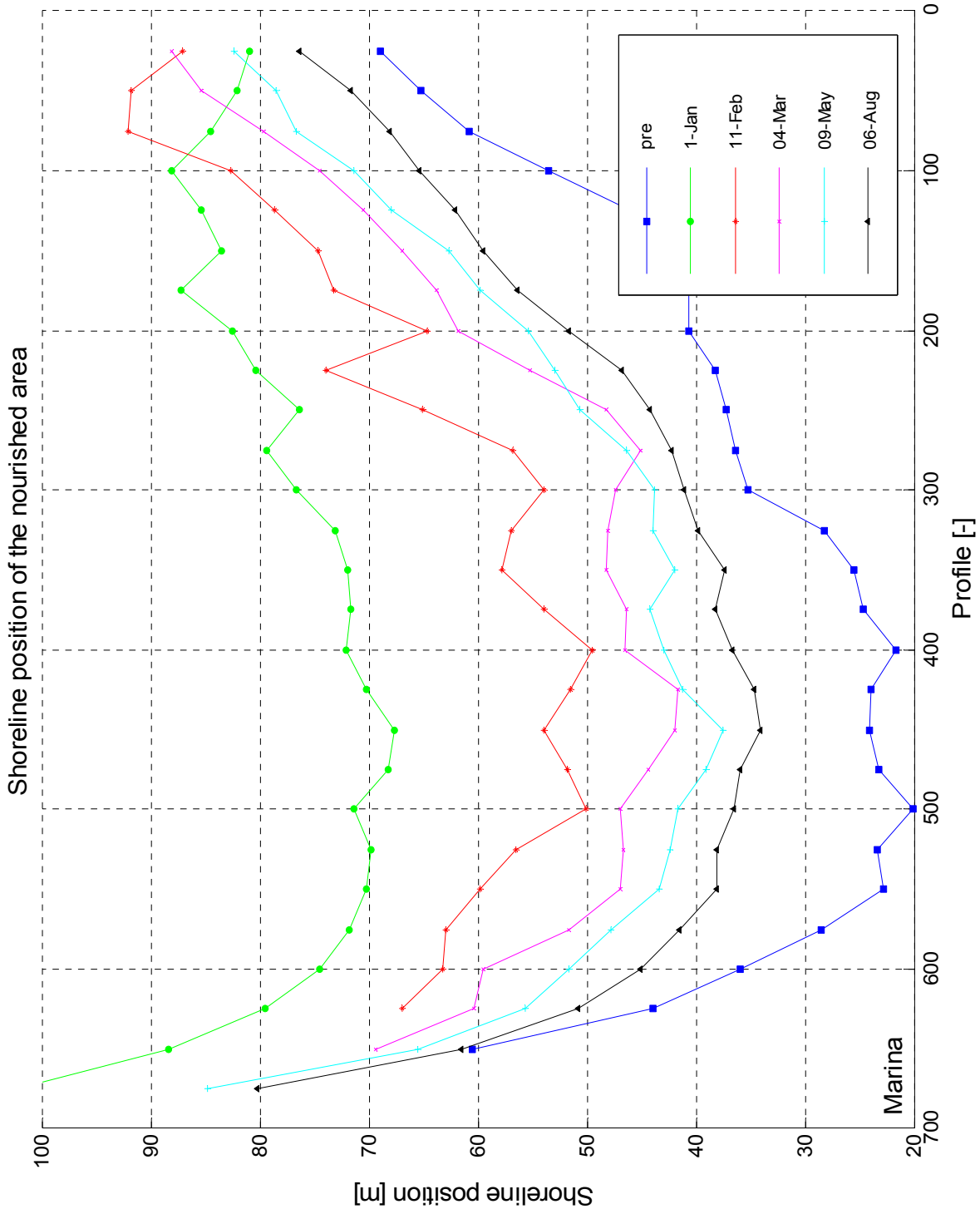

Shoreline position of the nourished area in time	Dubai	2004
WL | Delft Hydraulics		Figure 5.B

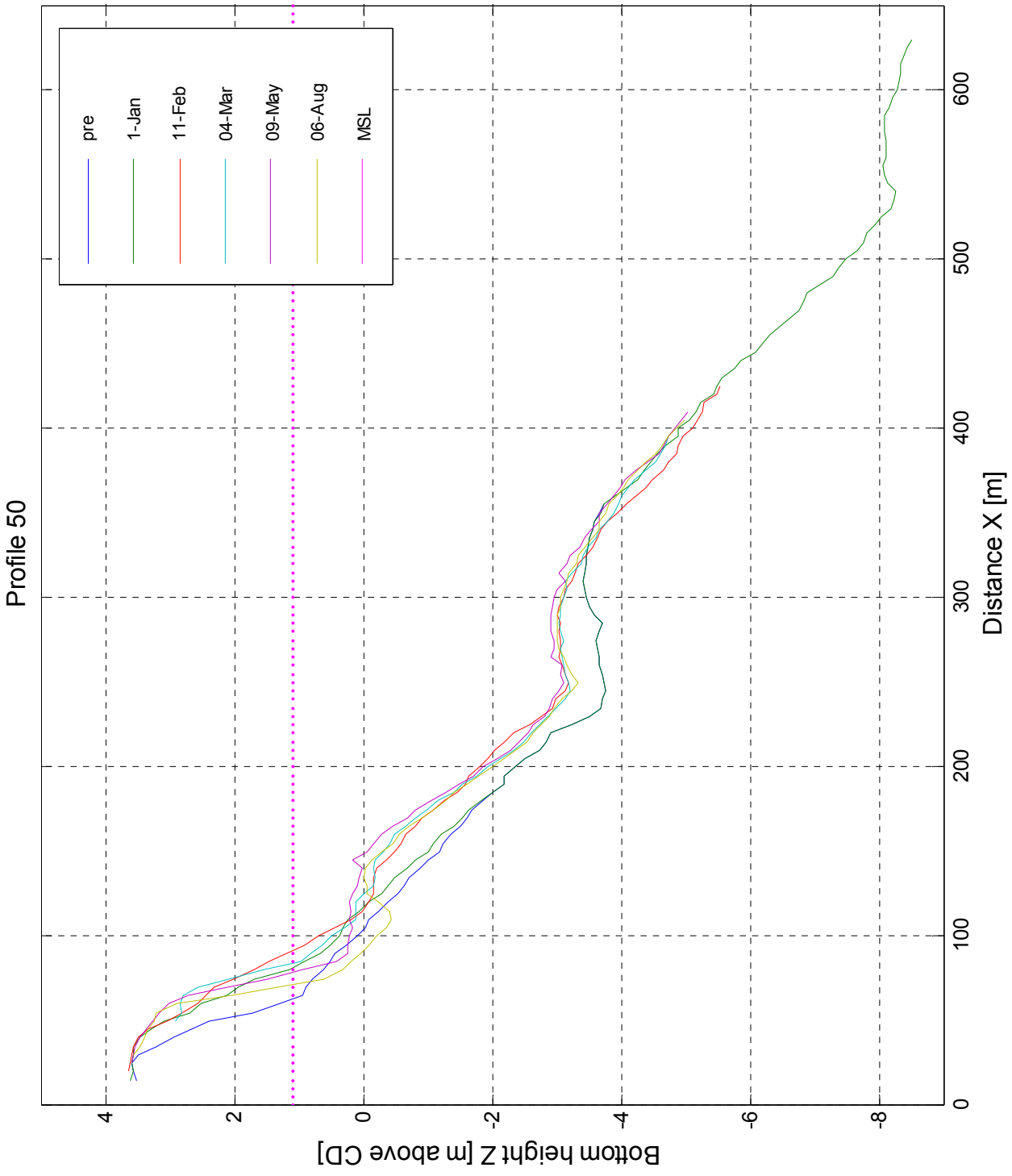

Profile 50	Dubai	2004
WL | Delft Hydraulics		Figure 5.C

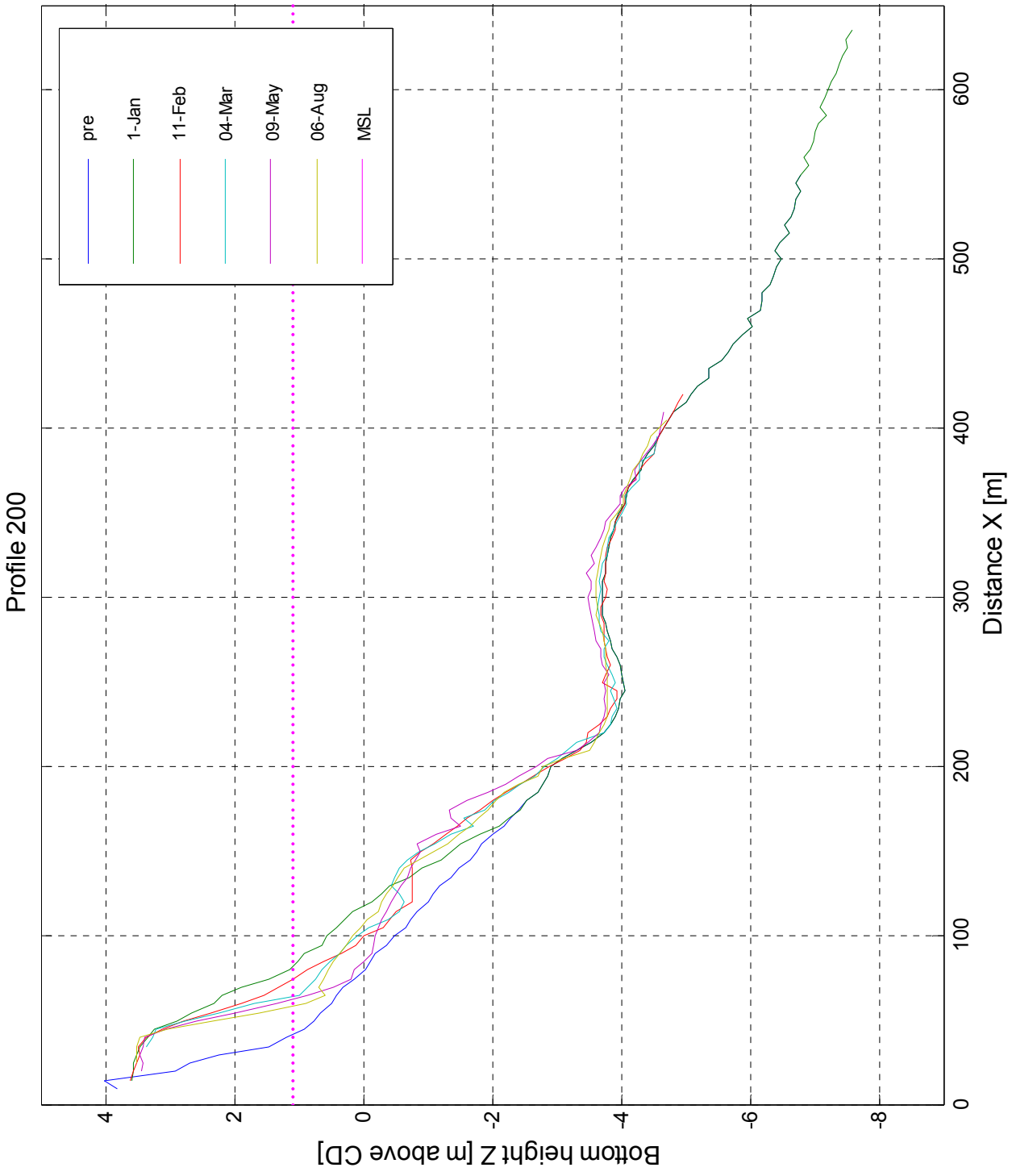

Profile 200	Dubai	2004
WL | Delft Hydraulics		Figure 5.D

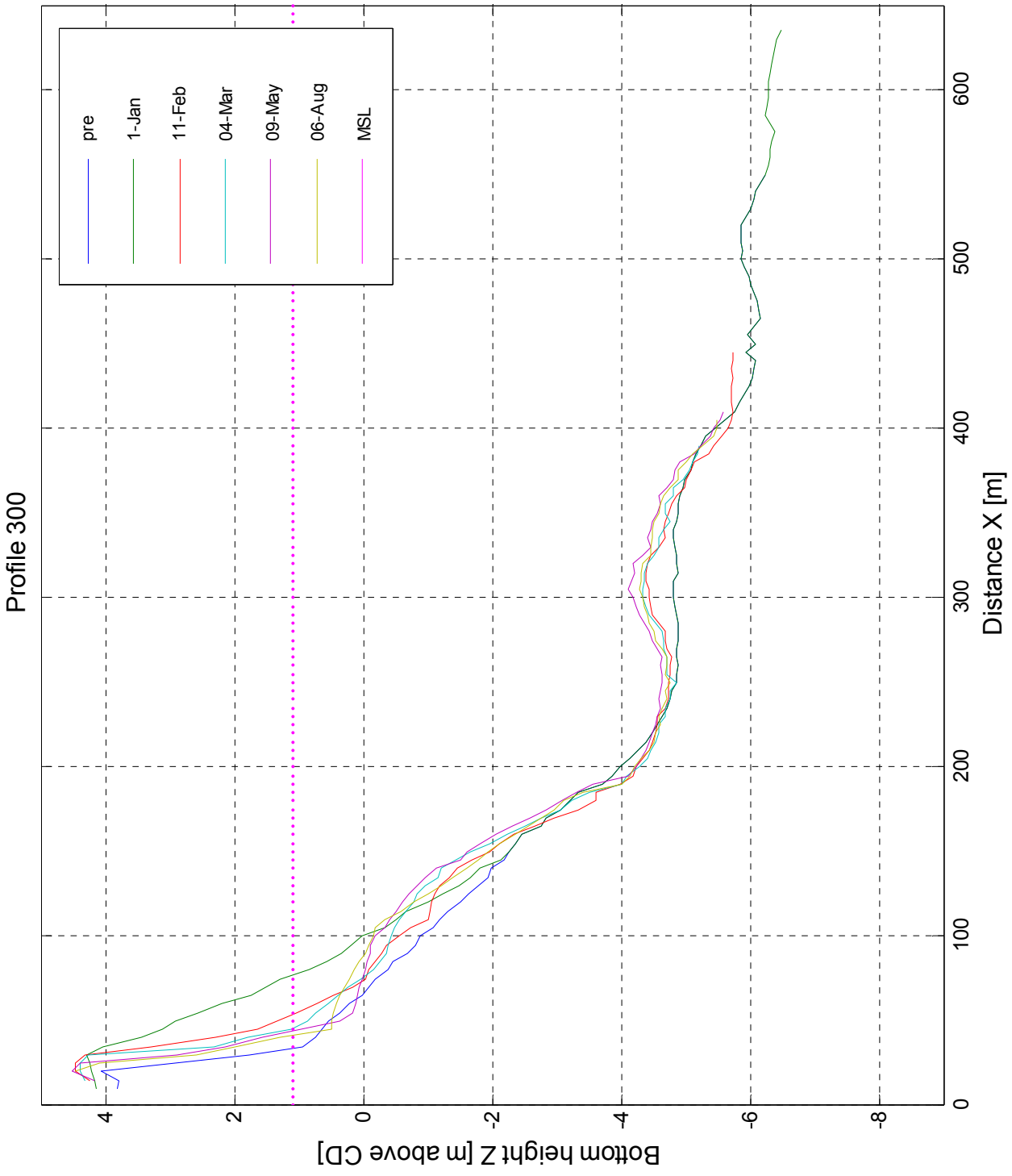

Profile 300	Dubai	2004
WL | Delft Hydraulics		Figure 5.E

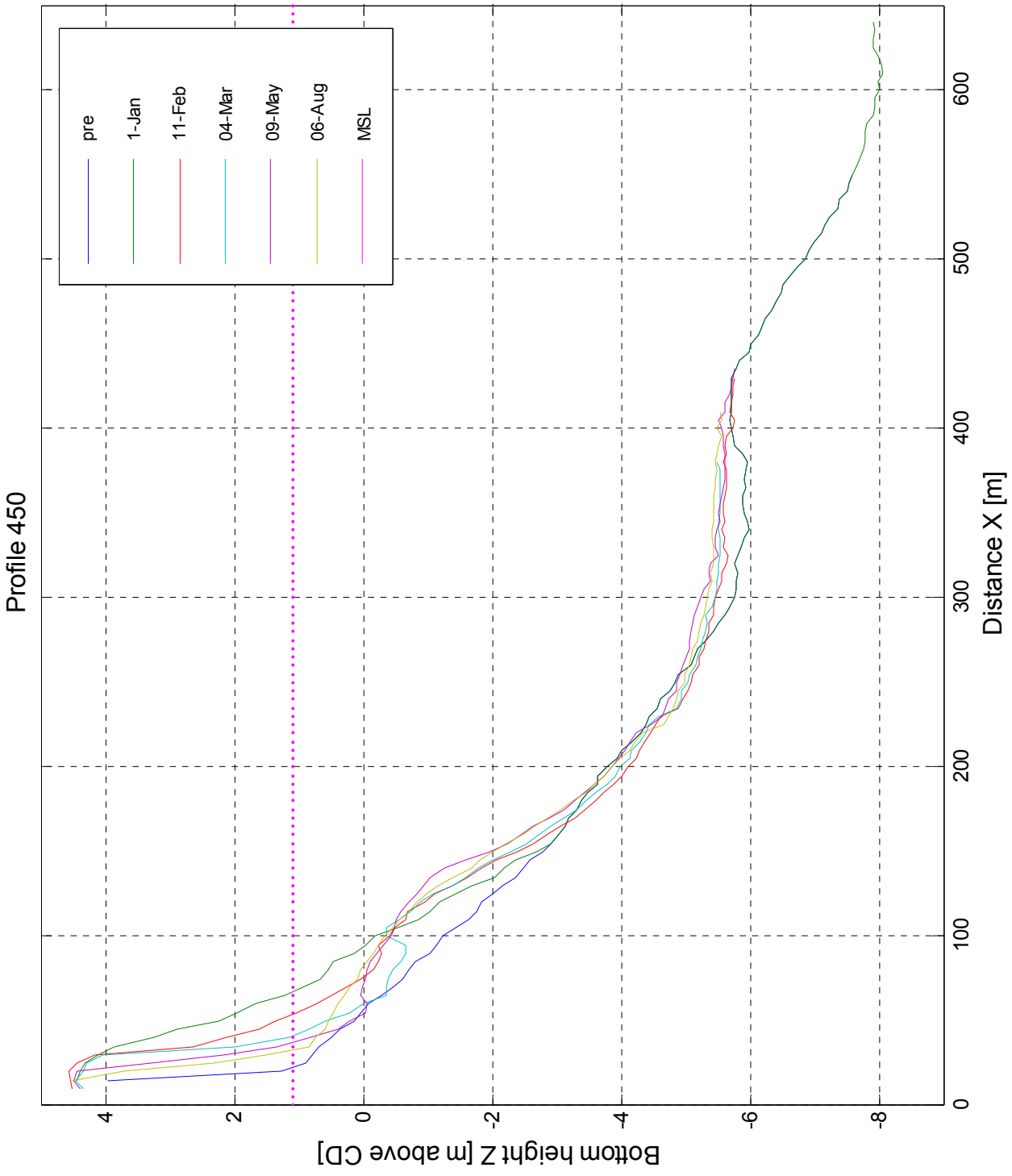

Profile 450	Dubai	2004
WL | Delft Hydraulics		Figure 5.F

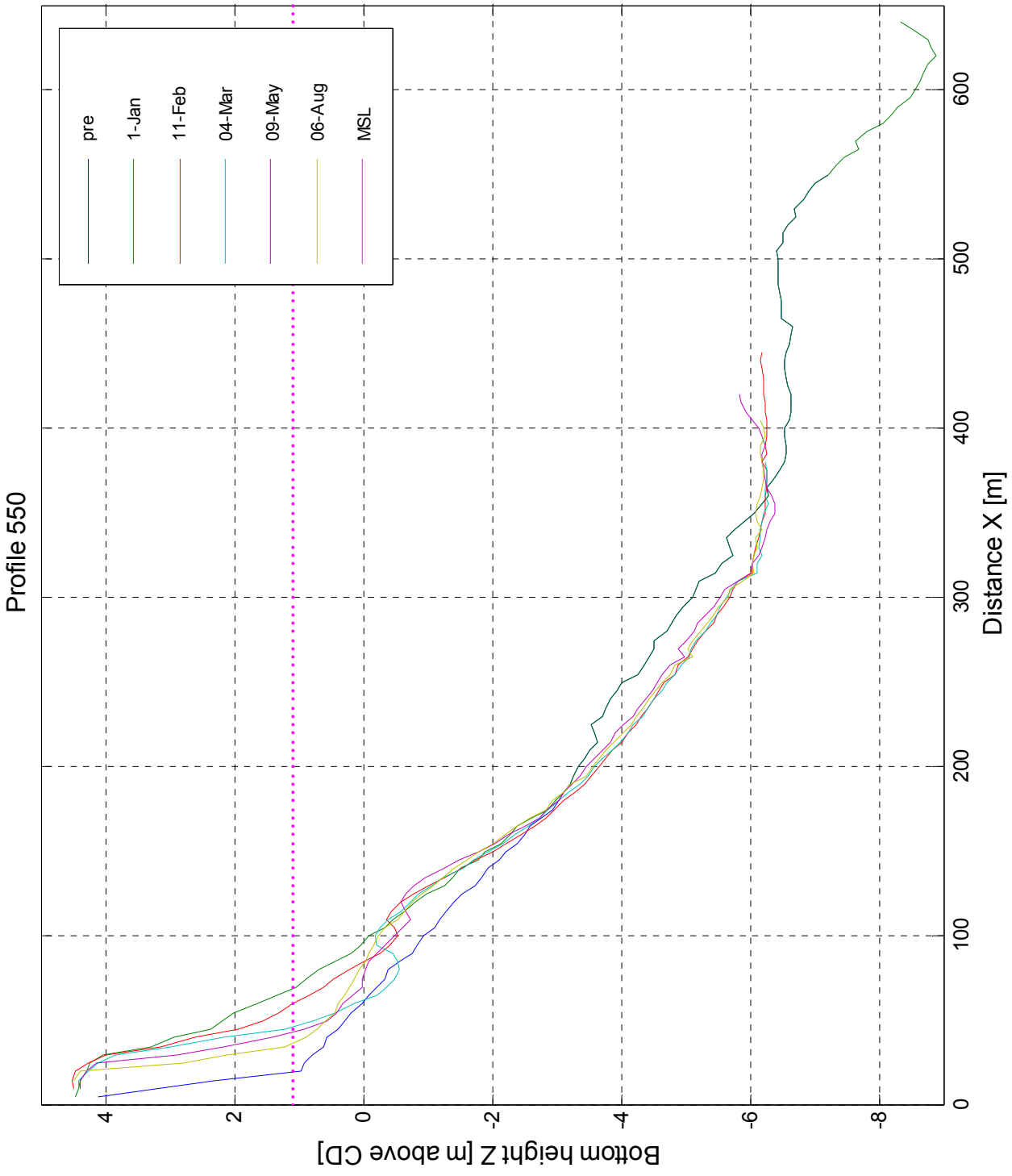

Profile 550	Dubai	2004
WL | Delft Hydraulics		Figure 5.G

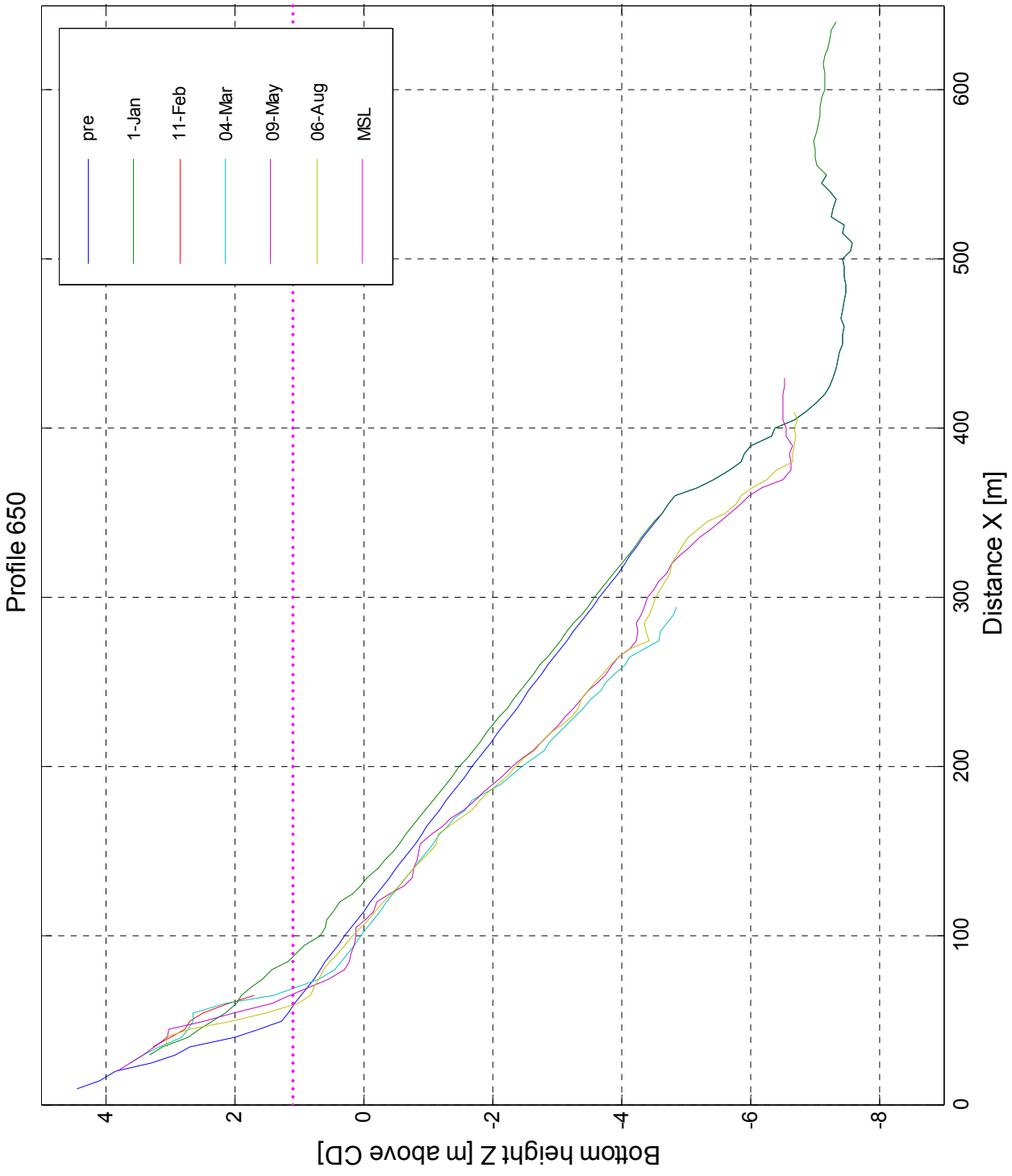

Profile 650	Dubai	2004
WL | Delft Hydraulics		Figure 5.H

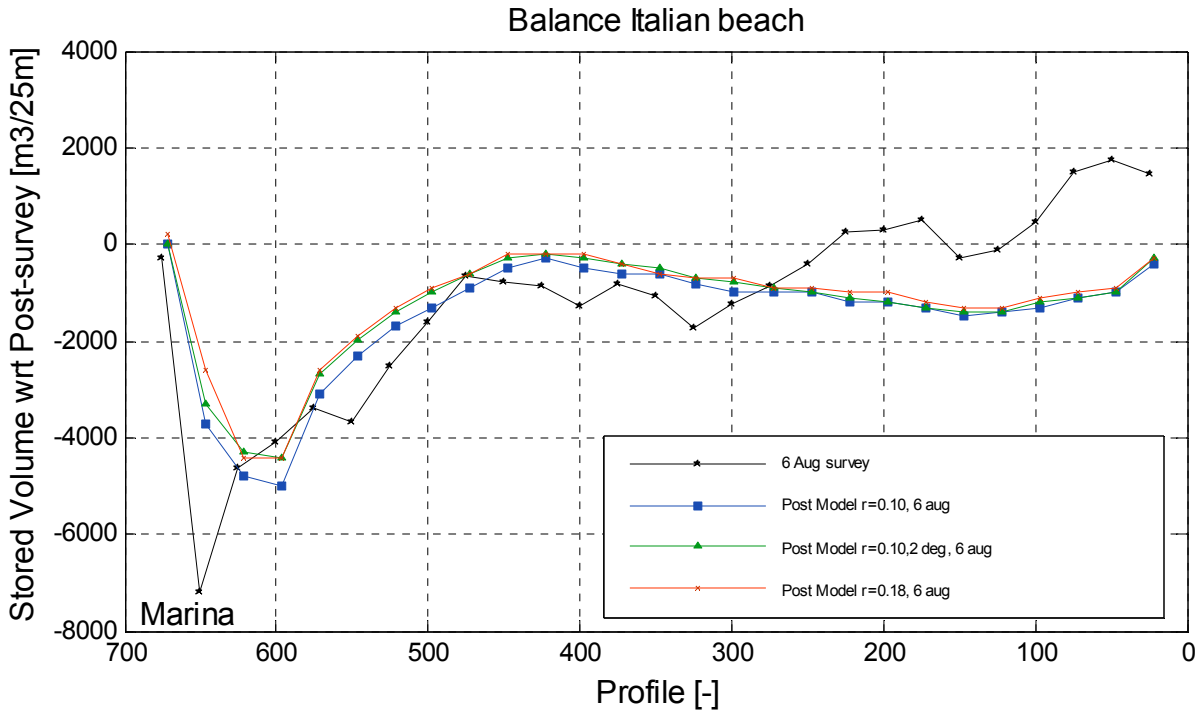

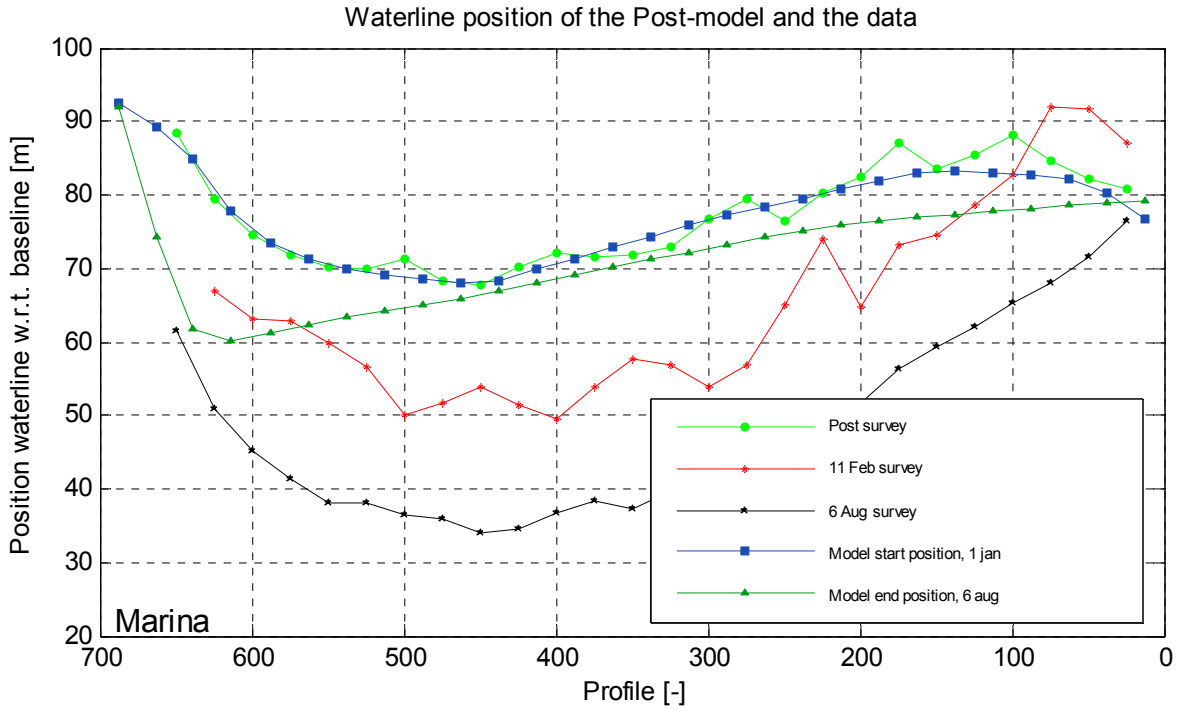

Verification of the Post model Balance, and Coastline development on 6 August 2004	Dubai	2004
WL | Delft Hydraulics		Figure 6.A

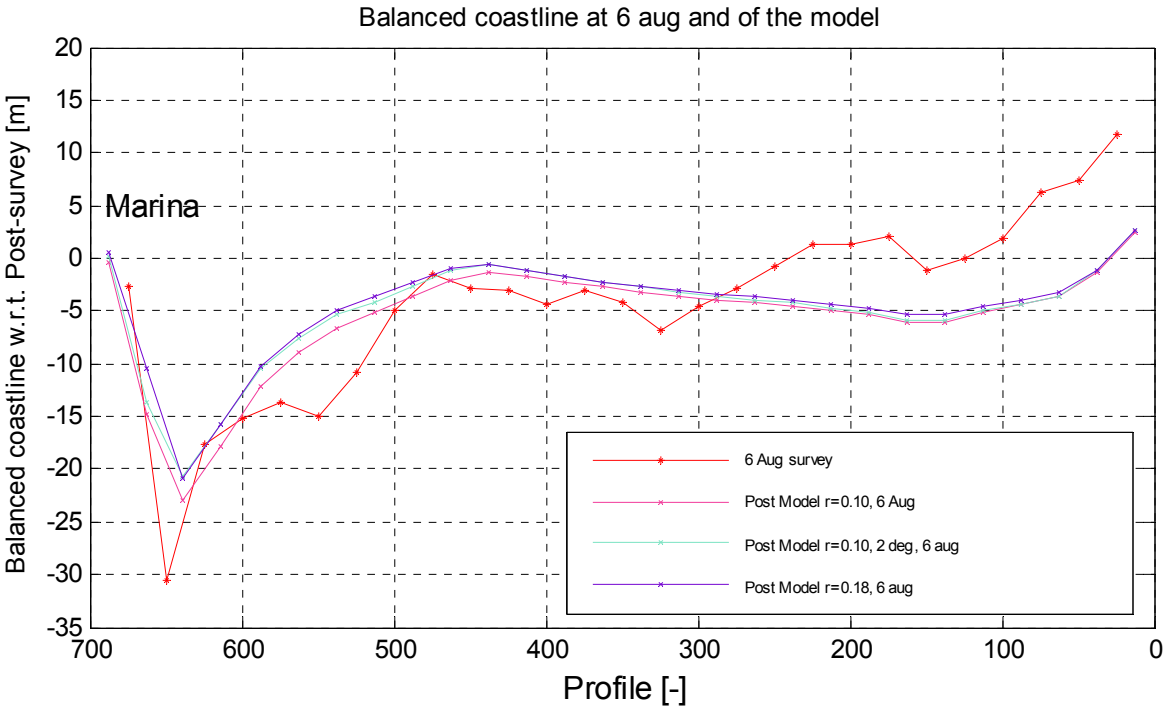

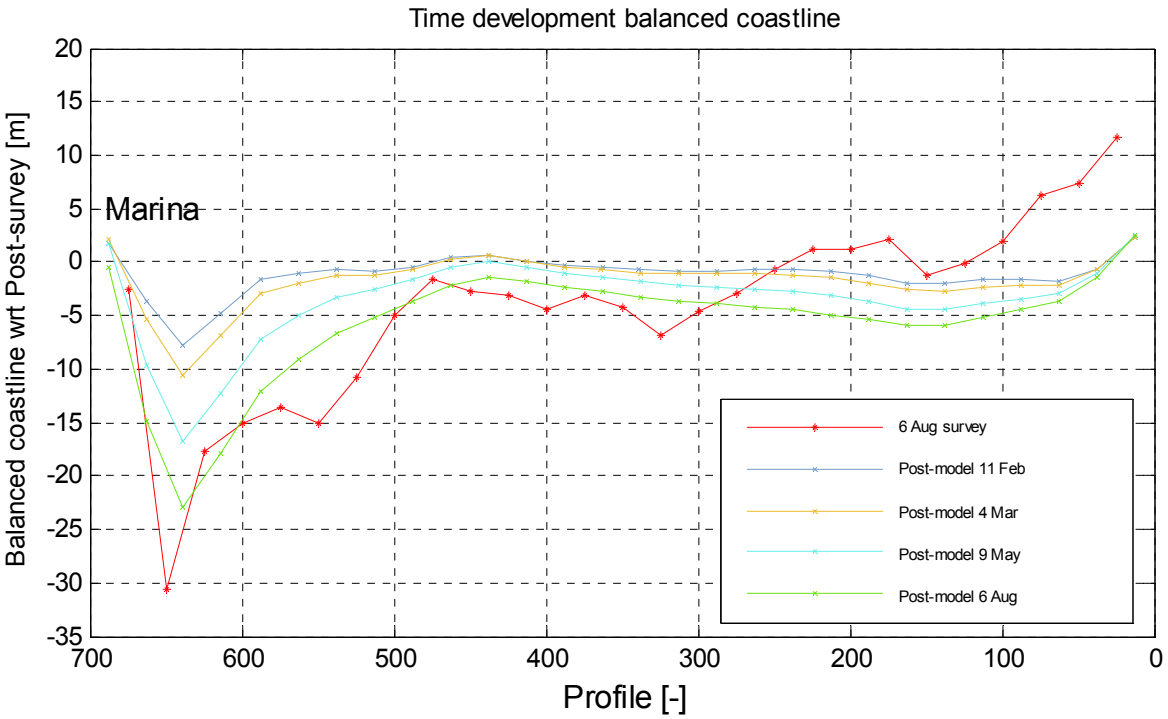

Verification of the Post-model Balanced coastline and time development	Dubai	2004
WL | Delft Hydraulics		Figure 6.B

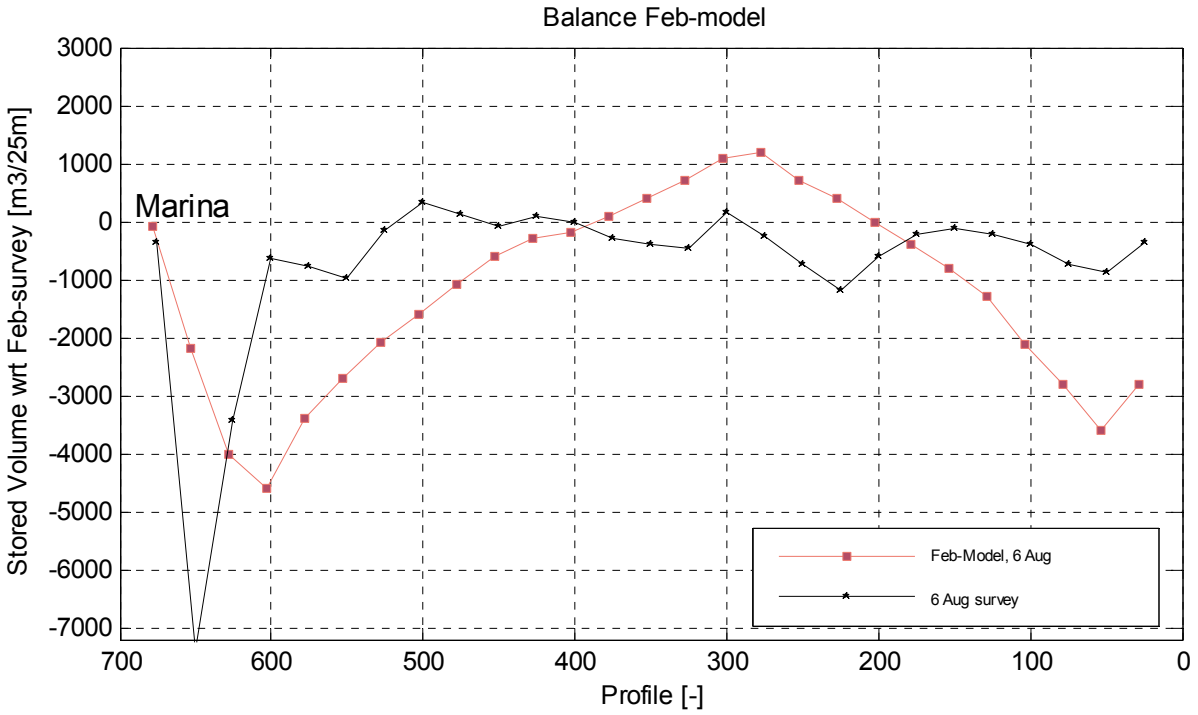

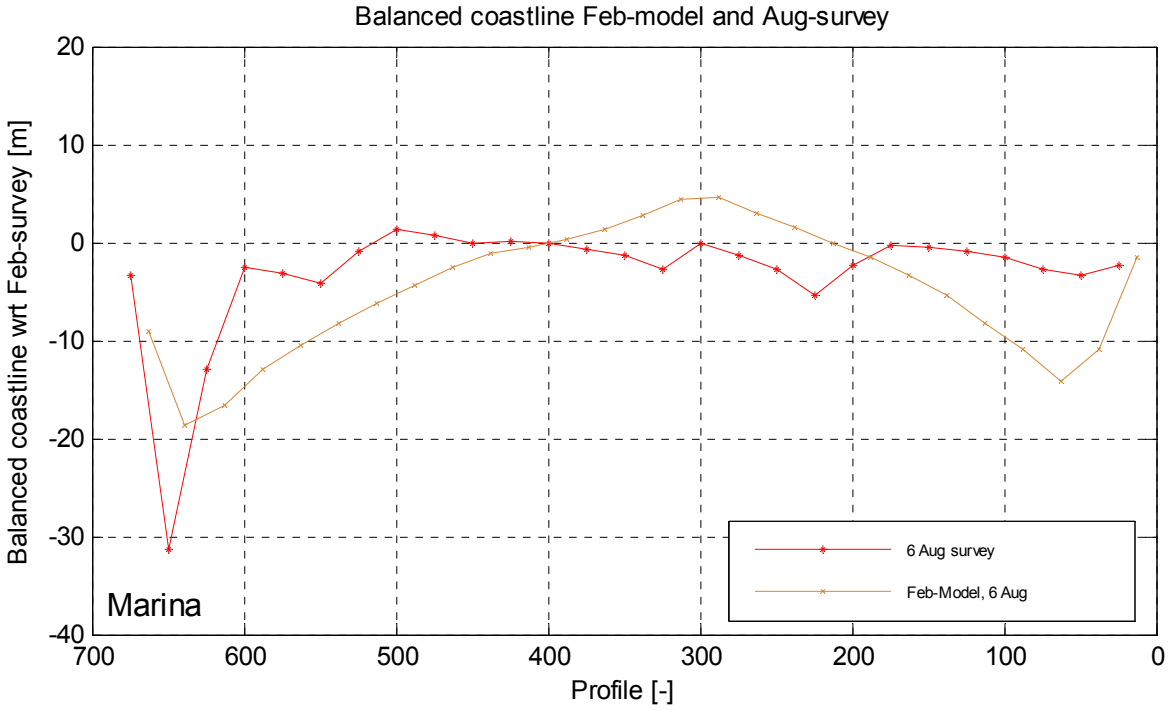

Sensitivity of the Post-model Balance, and coastline development of the Feb-model on 6 August 2004	Dubai	2004
WL | Delft Hydraulics		Figure 6.C

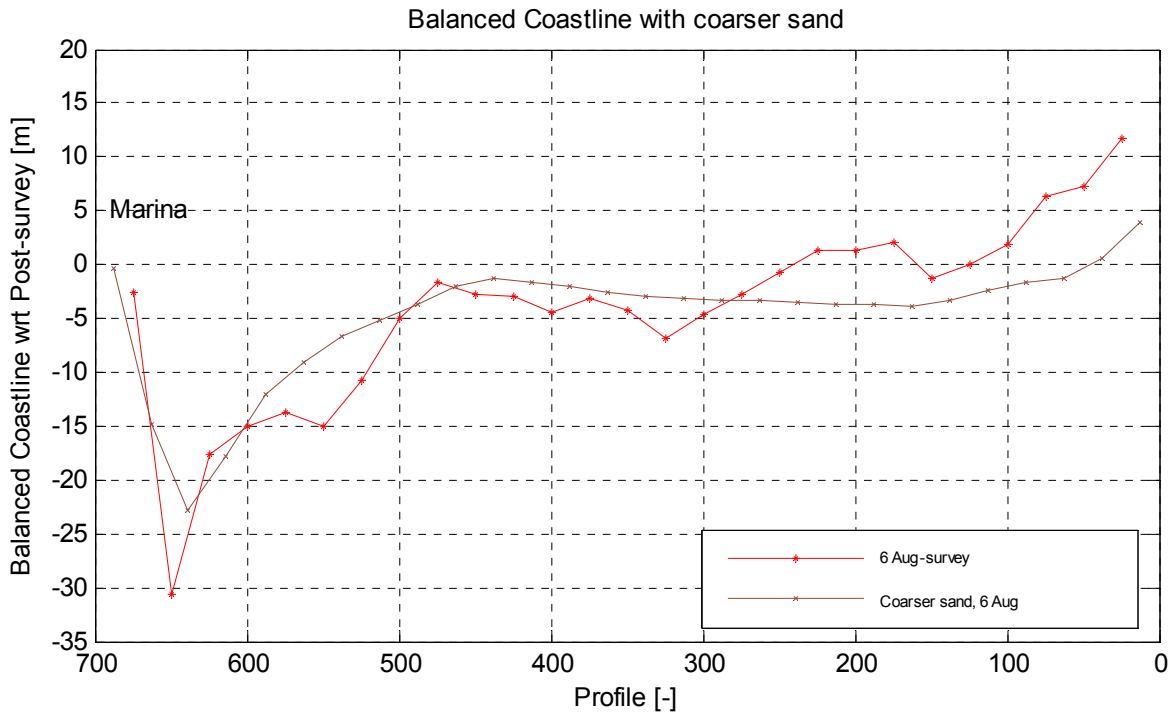

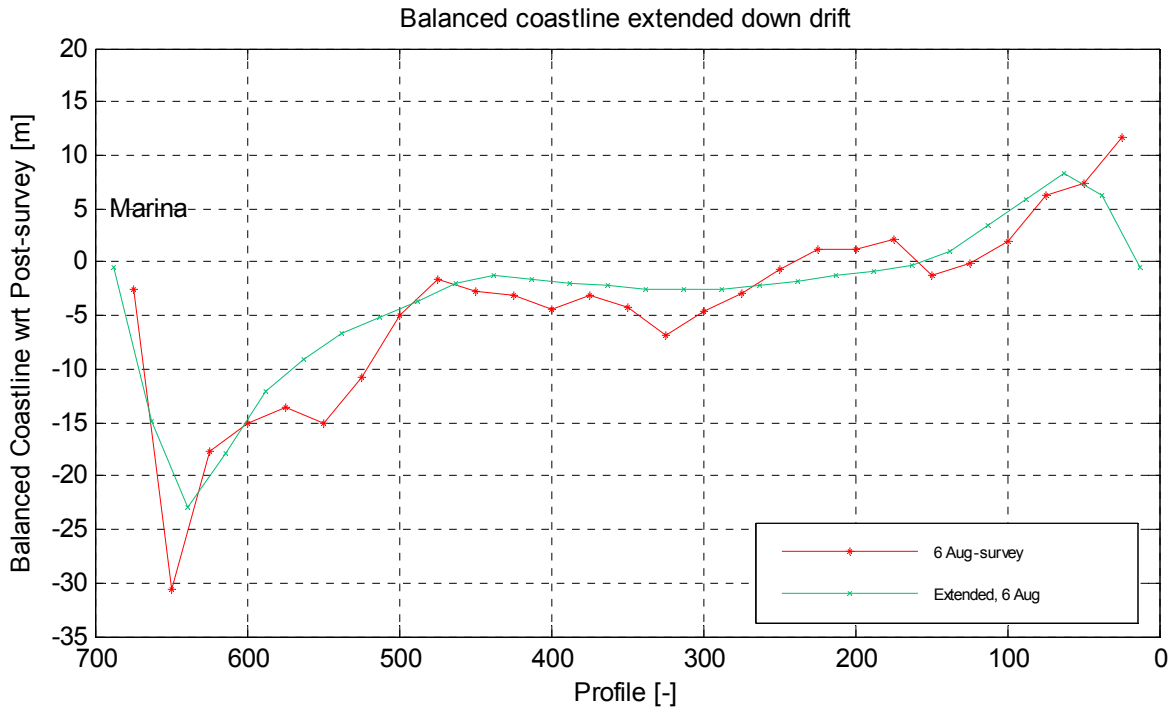

Sensitivity of the Post-model Balanced coastline with coarser sand and extended coastline down drift on 6 Aug	Dubai	2004
WL | Delft Hydraulics		Figure 6.D

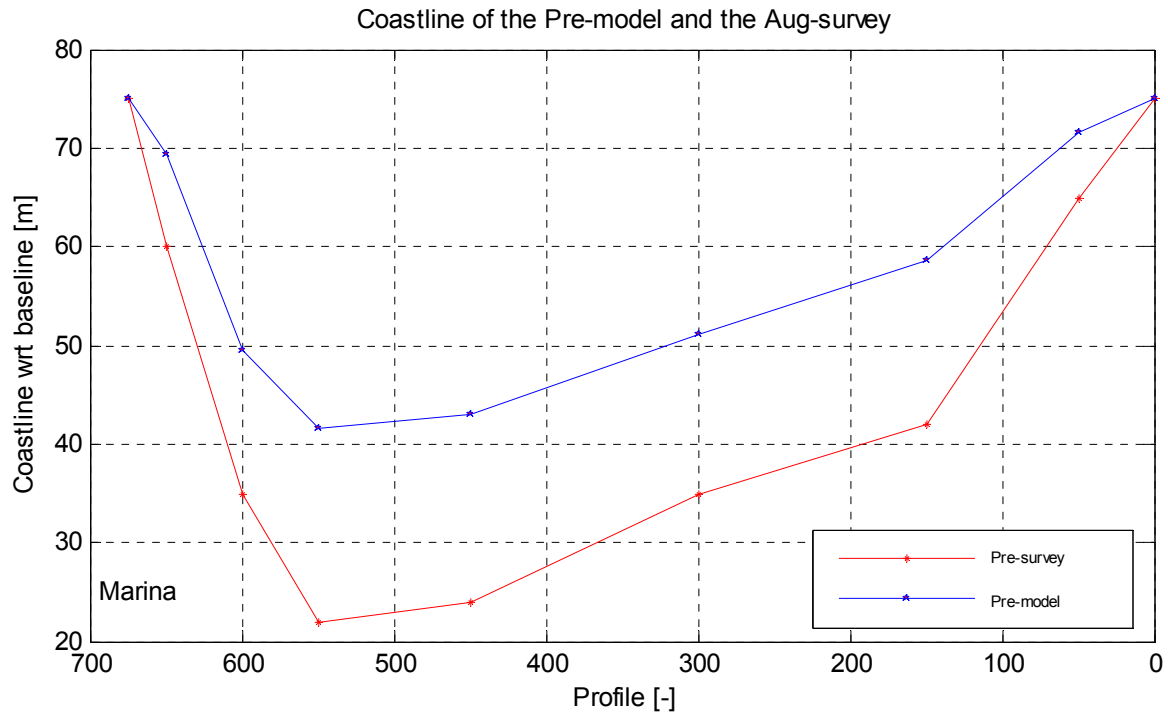

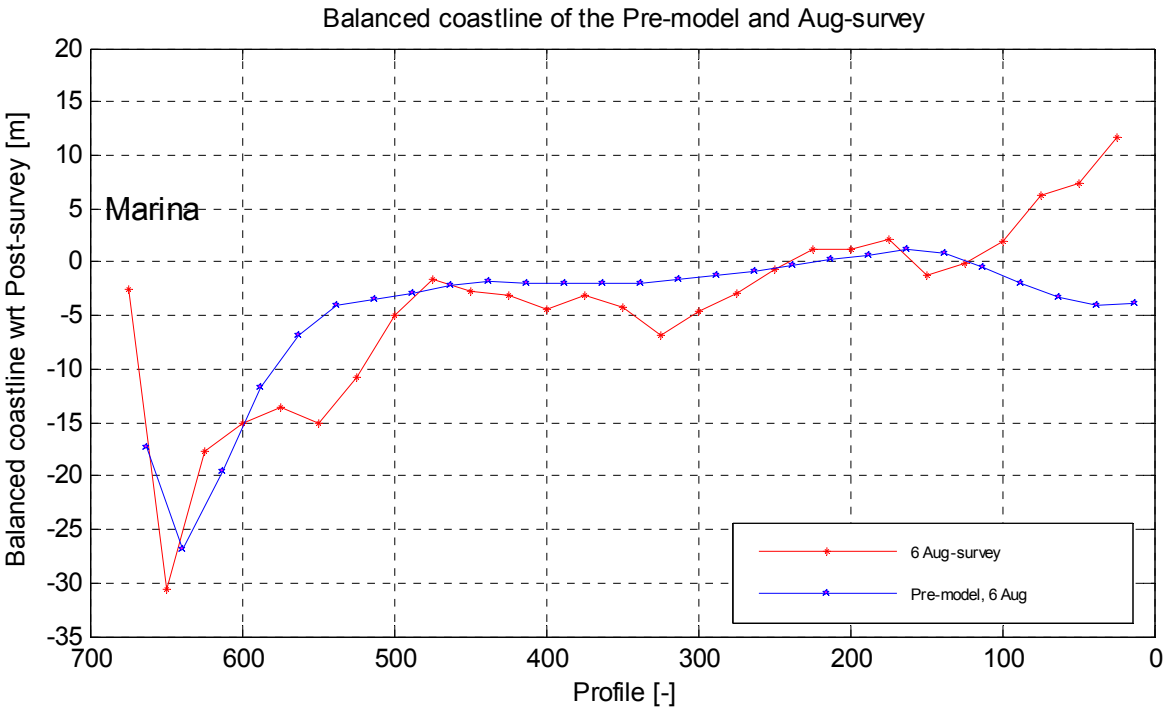

Sensitivity of the Post-model Coastline development on 6 August 2004	Dubai	2004
WL | Delft Hydraulics		Figure 6.E

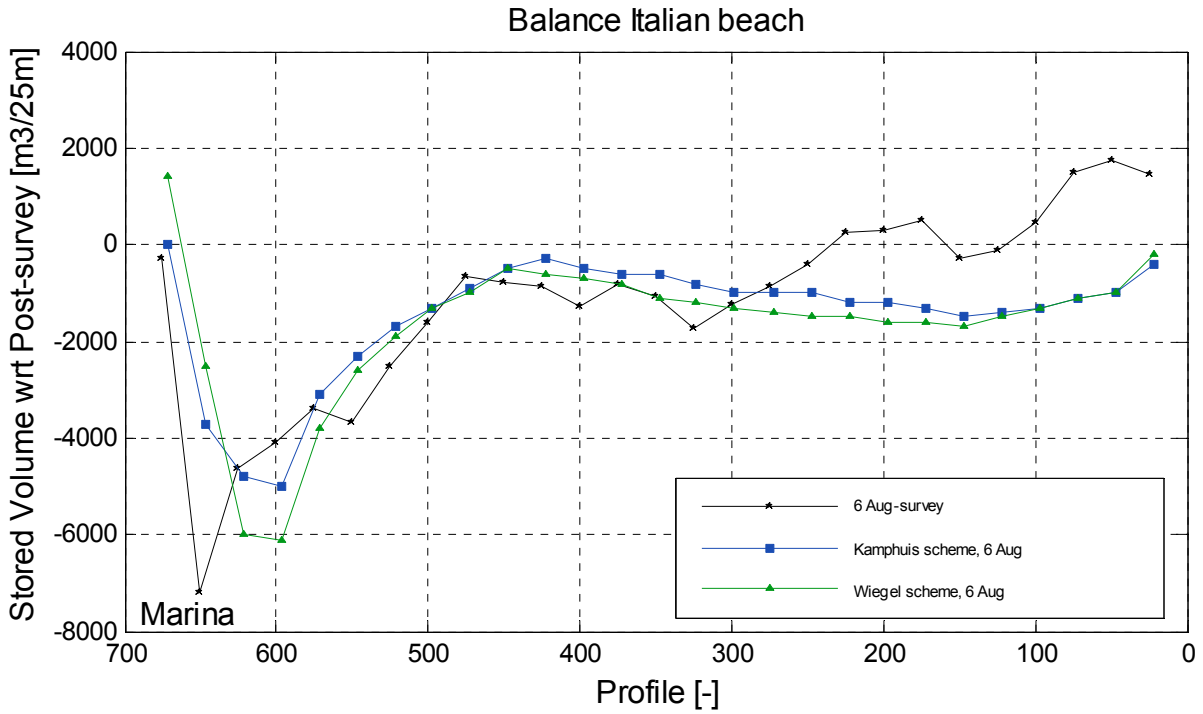

Sensitivity of the Post-model Comparison of the Kamphuis and Wiegel wave diffraction schemes	Dubai	2004
WL | Delft Hydraulics		Figure 6.F

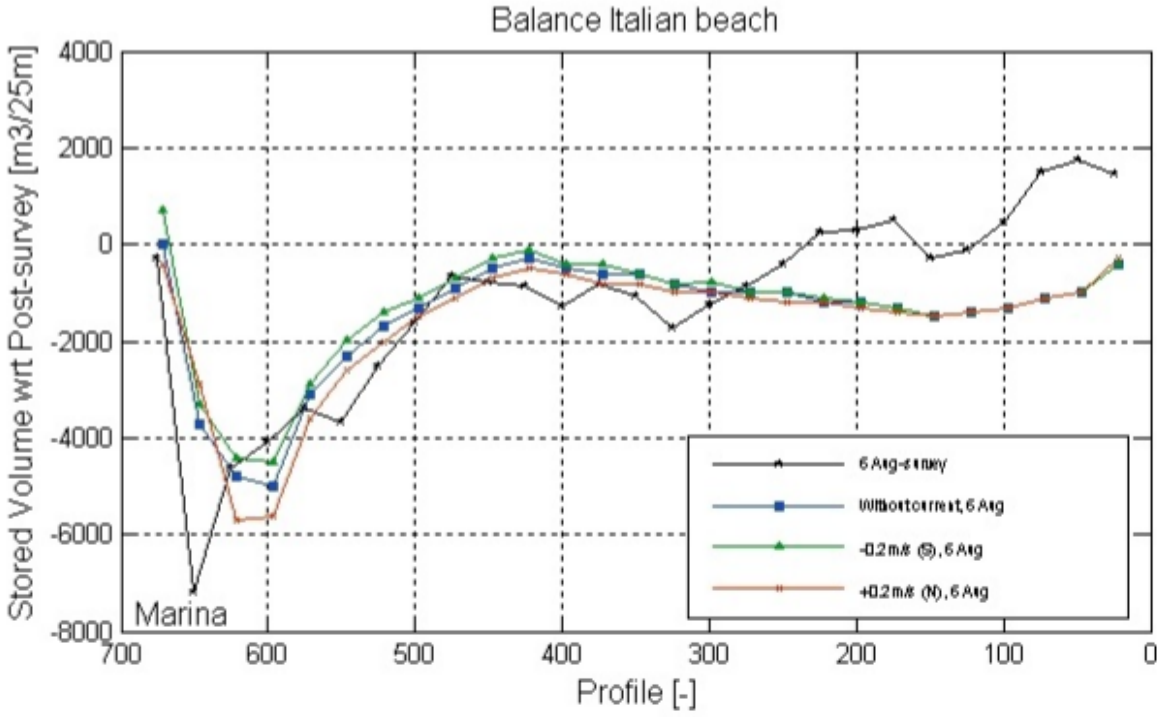

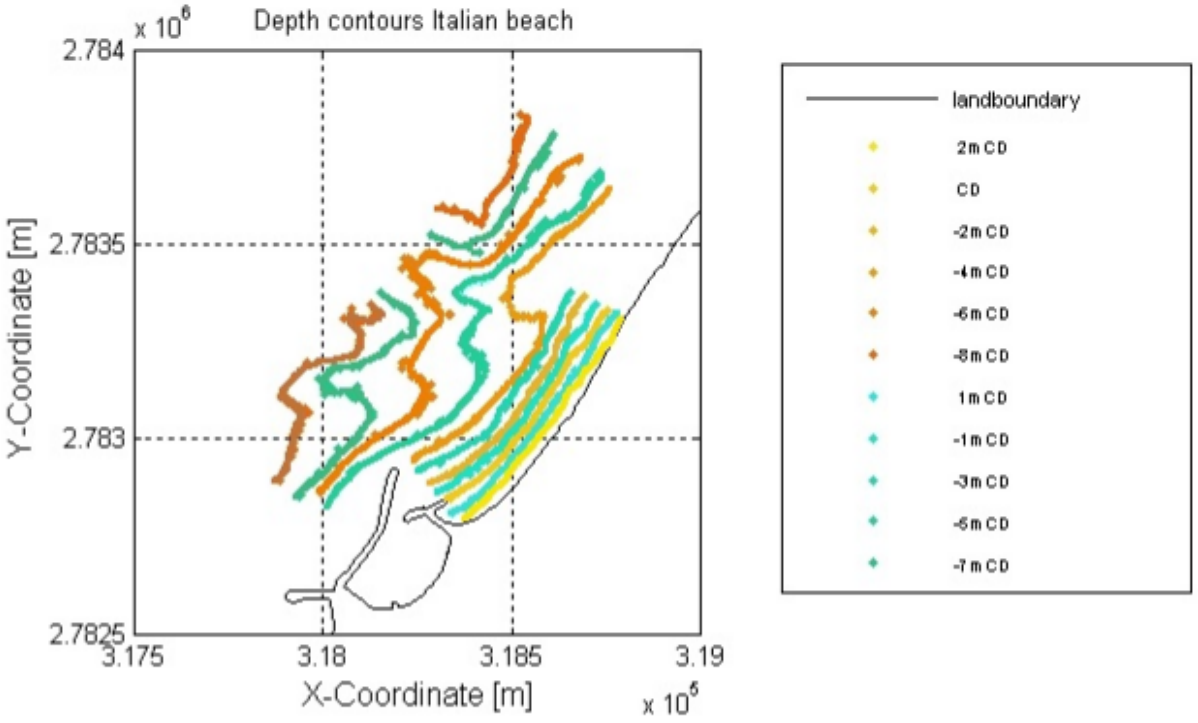

Sensitivity of the Post model Scheme with and without currents and bottom countour diffraction schemes	Dubai	2004
WL | Delft Hydraulics		Figure 6.G

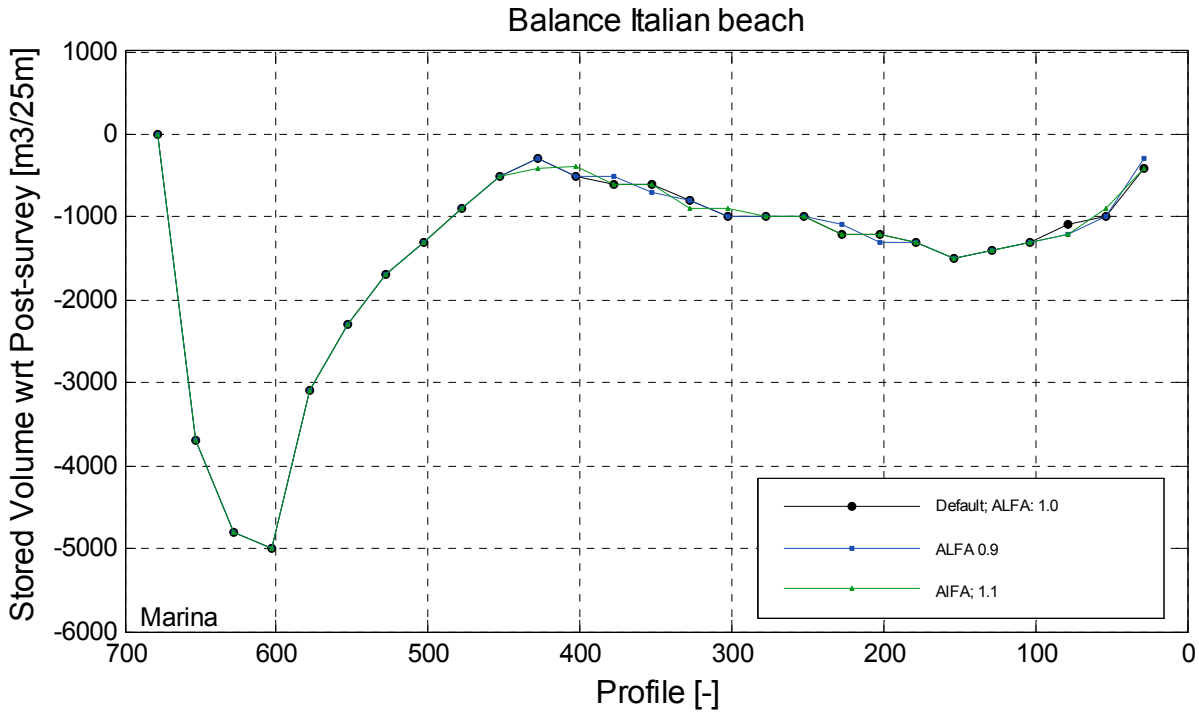

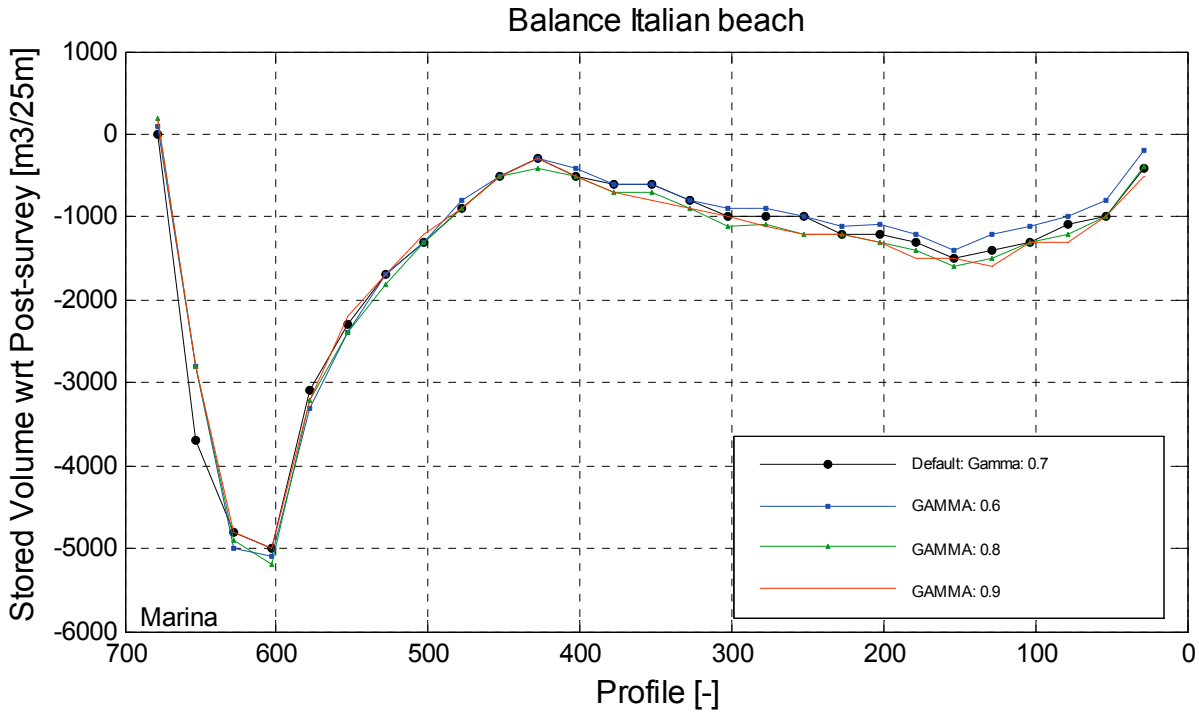

Sensitivity of the Post model To the paramaters ALFA and GAMMA	Dubai	2004
WL | Delft Hydraulics		Figure 6.H

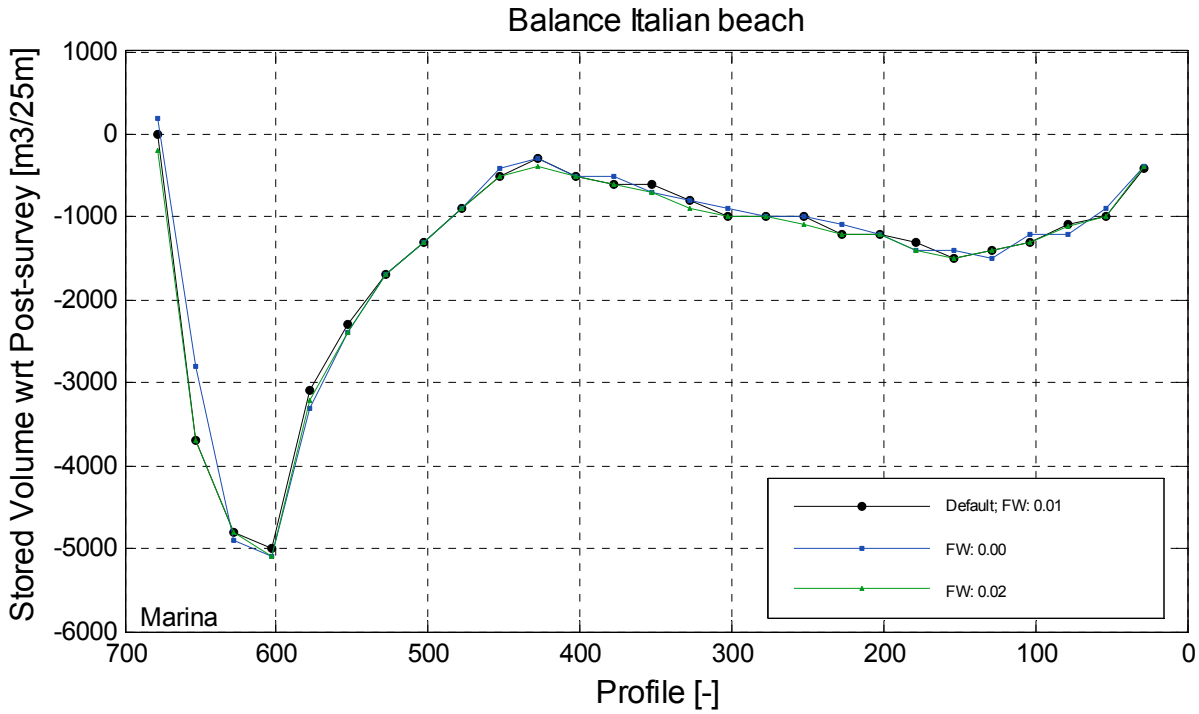

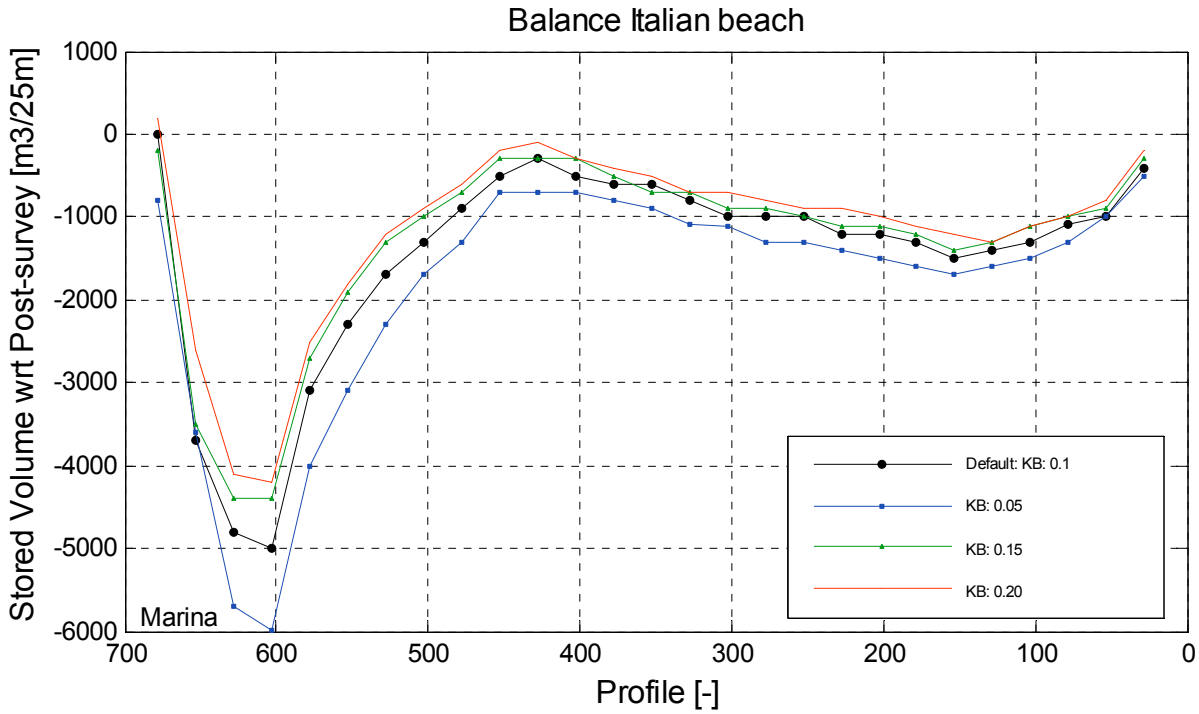

Sensitivity of the Post-model To the paramaters FW and KB	Dubai	2004
WL | Delft Hydraulics		Figure 6.I

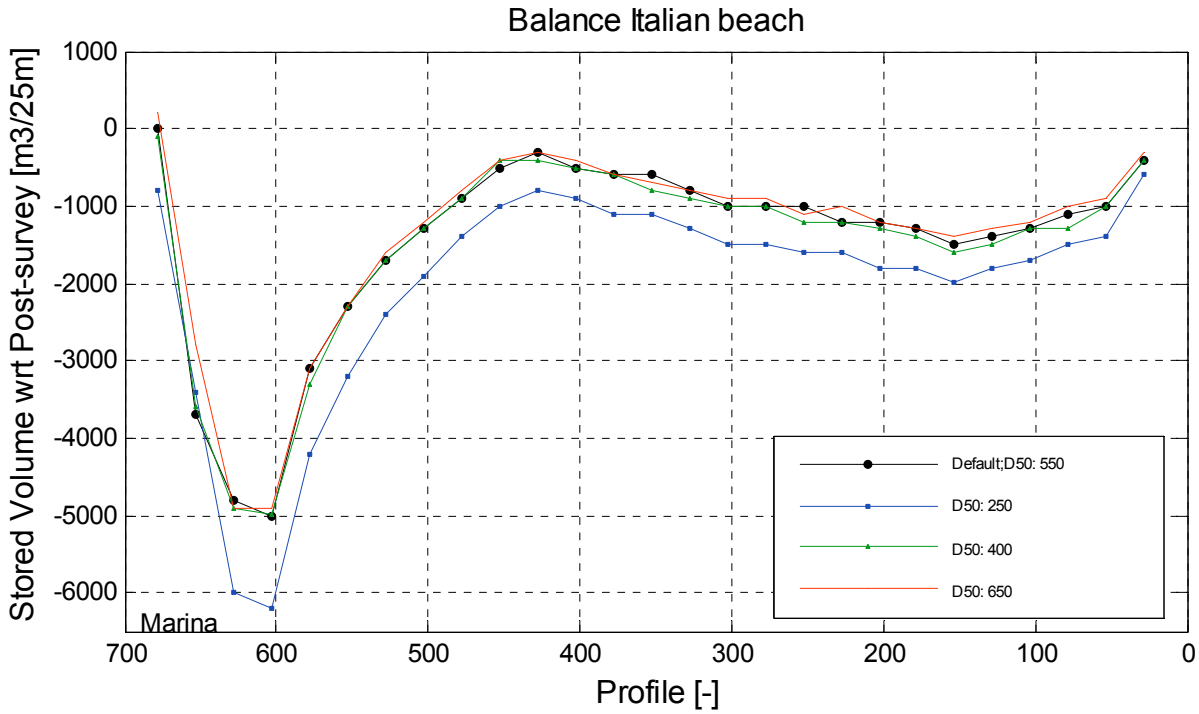

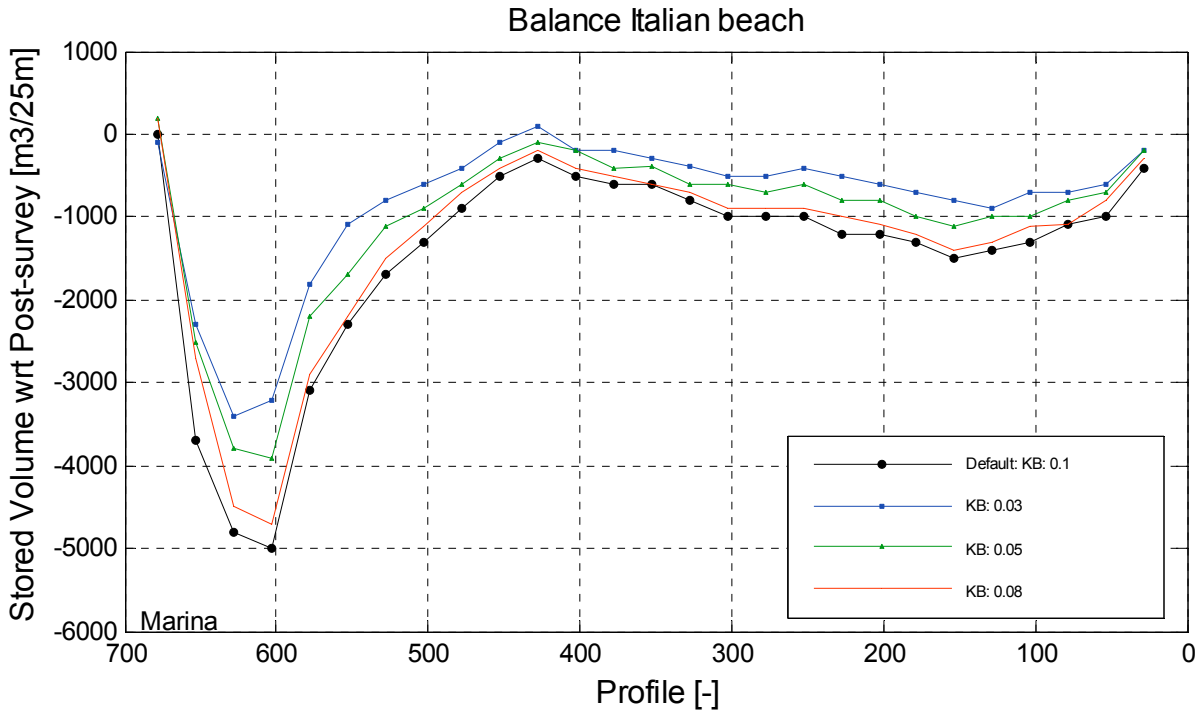

Sensitivity of the Post-model for the sediment characteristics and KB	Dubai	2004
WL | Delft Hydraulics		Figure 6.J

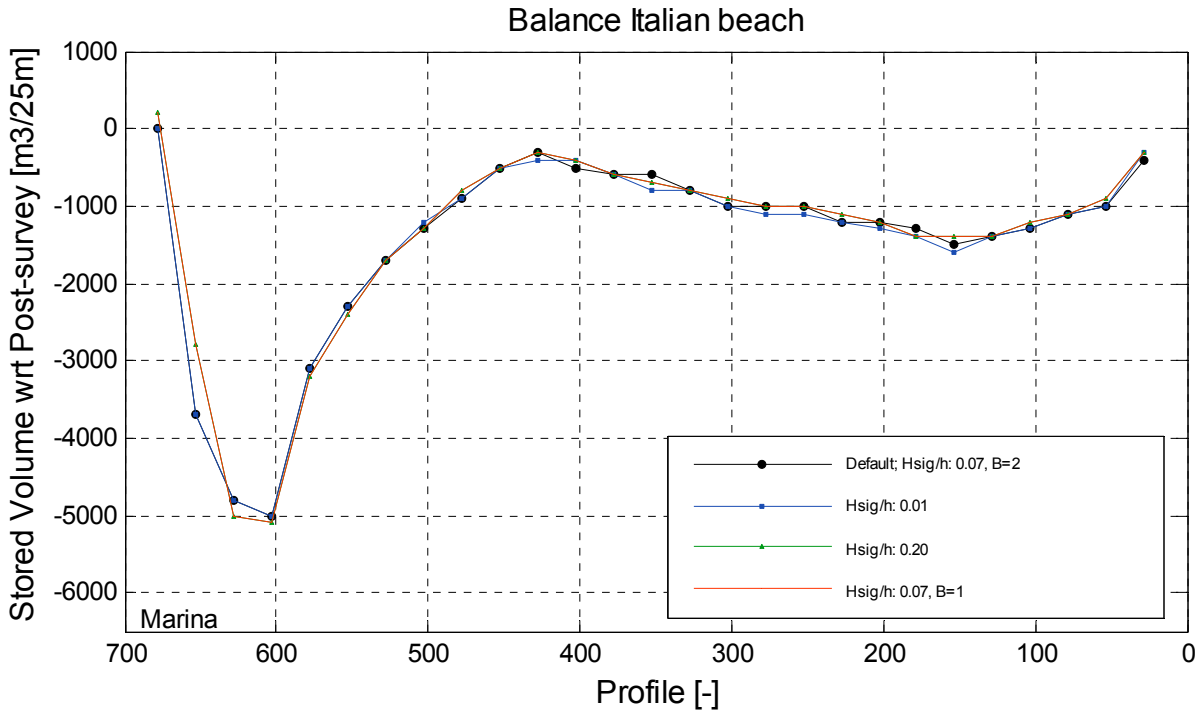

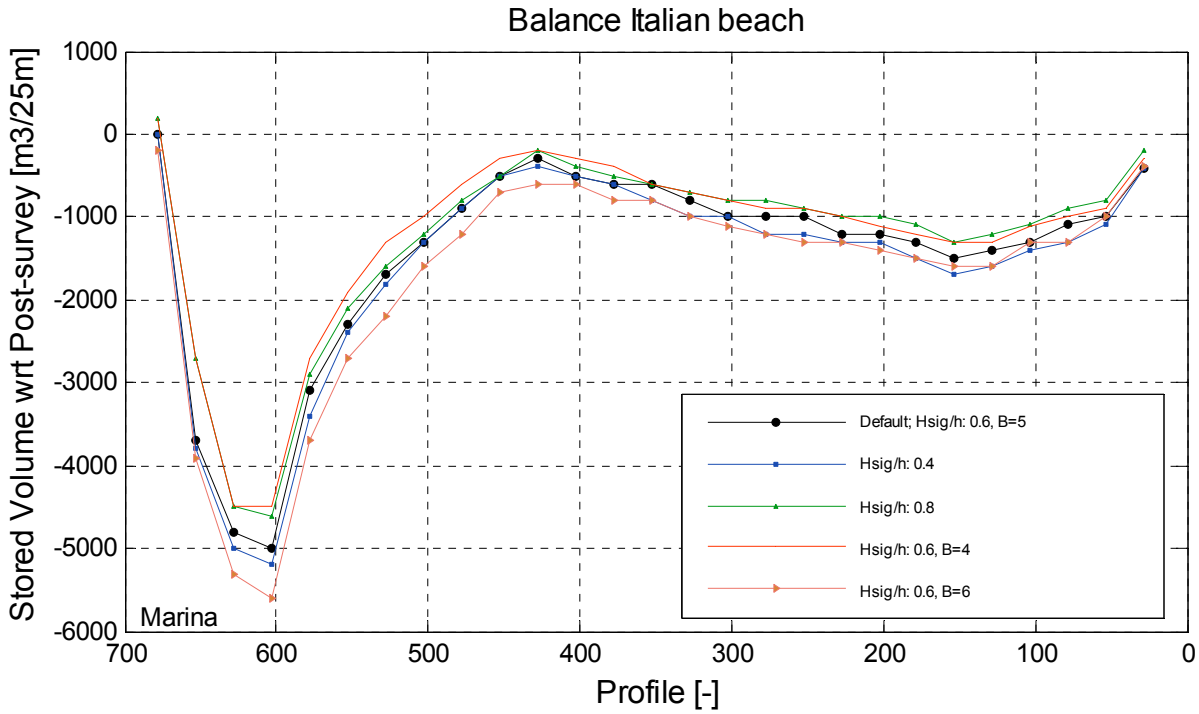

Sensitivity of the Post-model to the deep and shallow water coefficients	Dubai	2004
WL | Delft Hydraulics		Figure 6.K

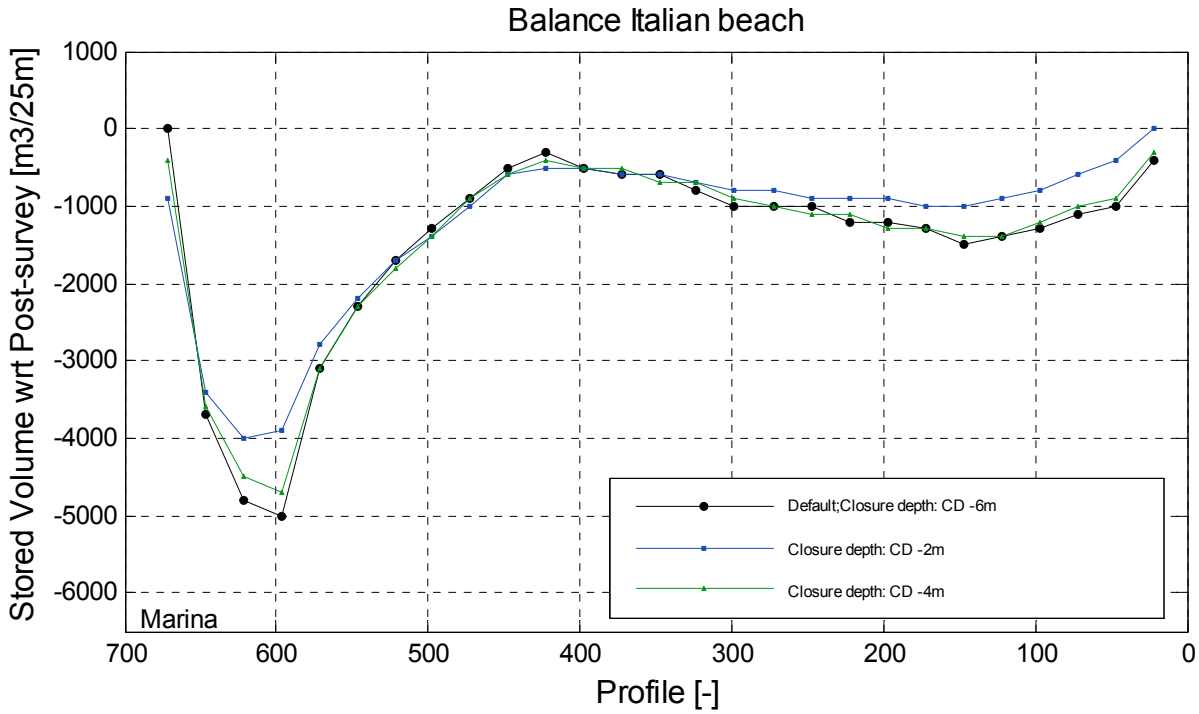

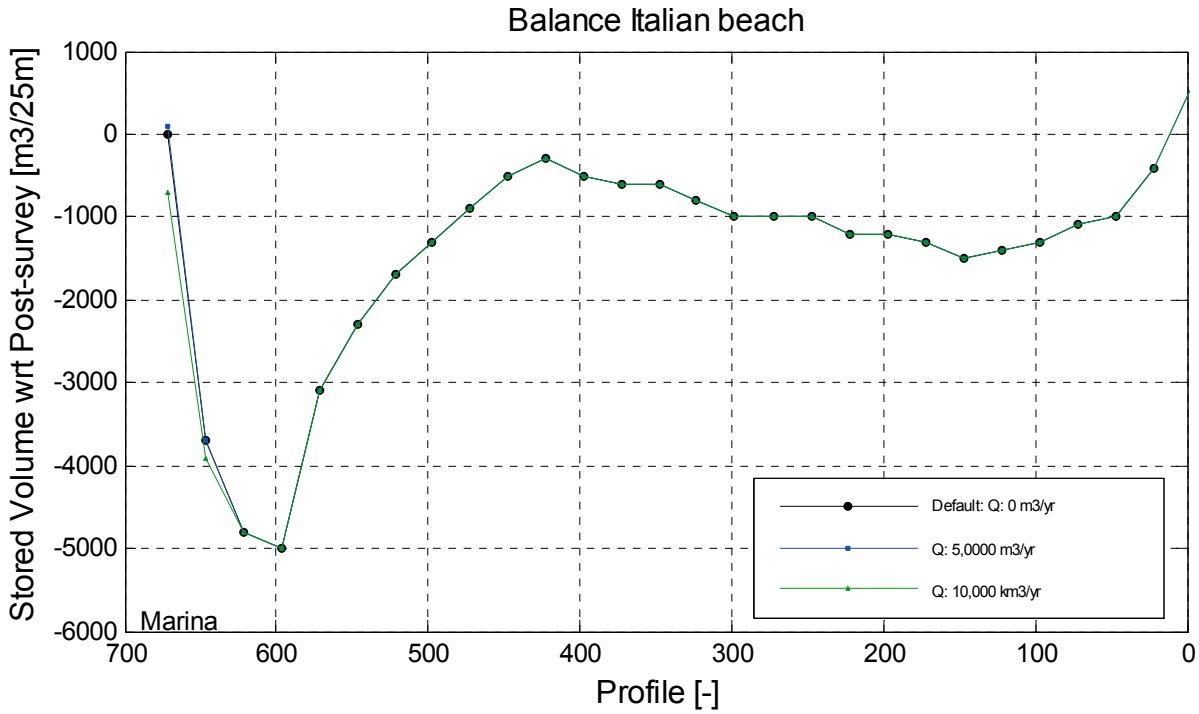

Sensitivity of the Post-model to the closure depth and boundary condition	Dubai	2004
WL | Delft Hydraulics		Figure 6.L

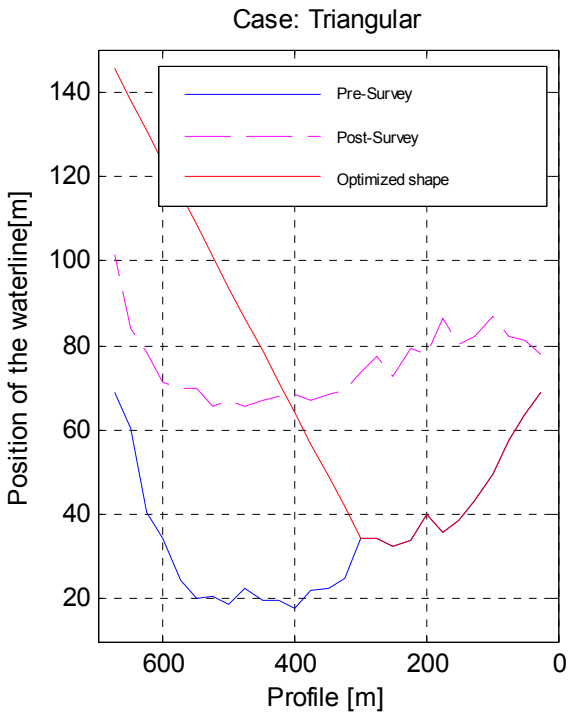

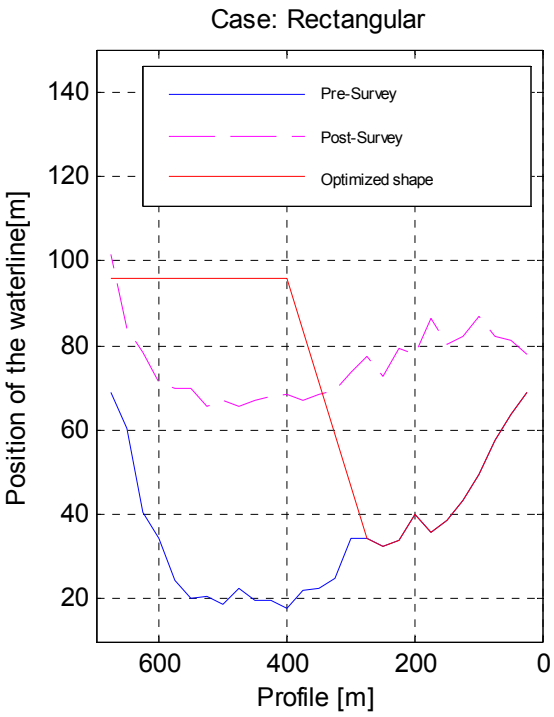

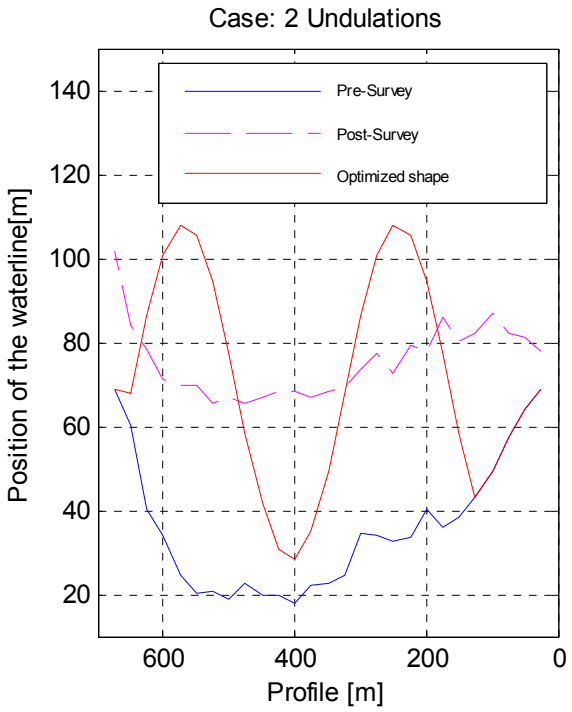

Result of the optimization based on area Coastline positions on T=0 yr	Dubai	2004
WL | Delft Hydraulics		Figure 7.A

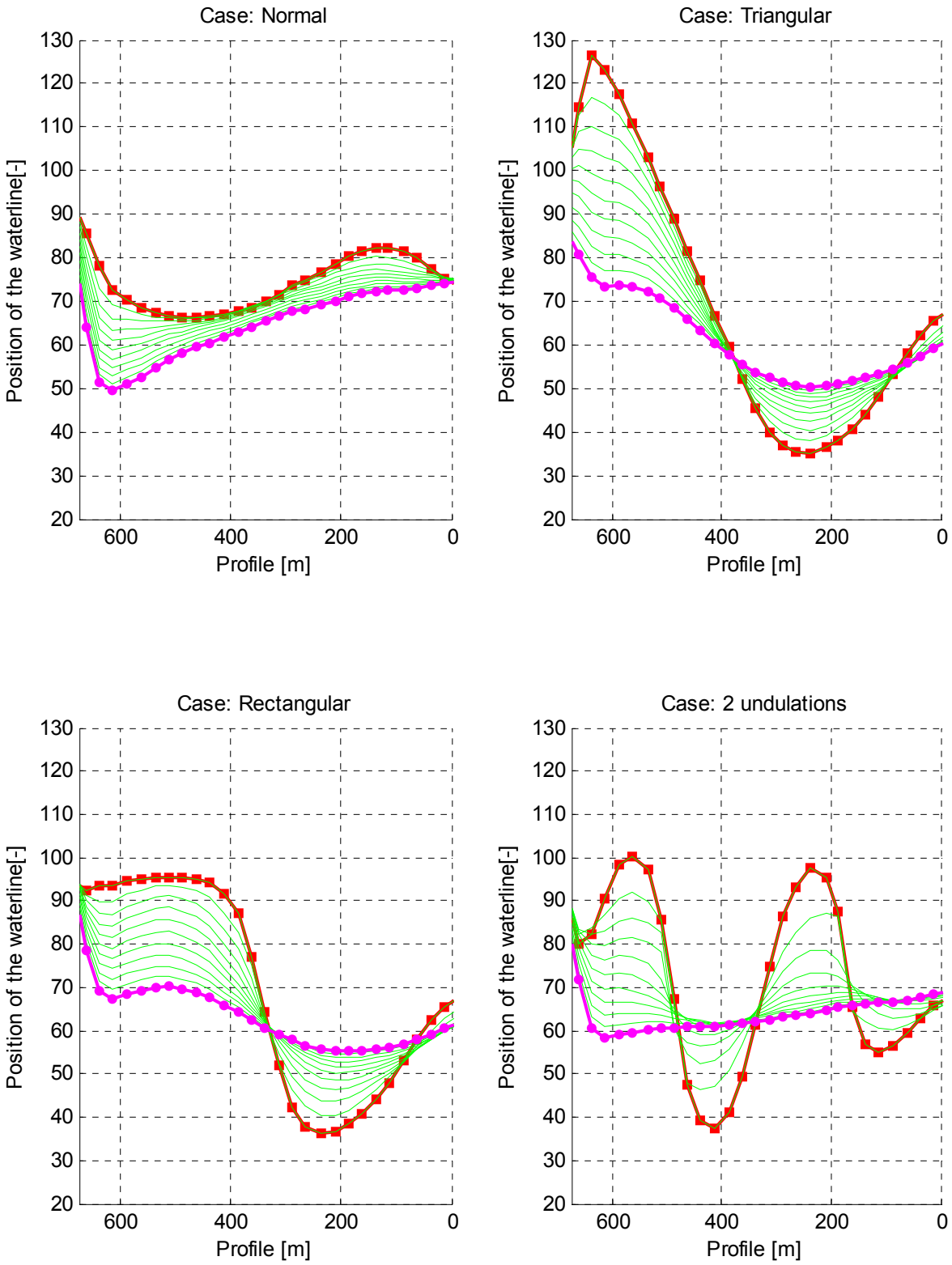

Result of the optimization based on area Coastline positions in 1 year	Dubai	2004
WL | Delft Hydraulics		Figure 7.B

1. Coastline difference w.r.t the reference case (based on area)

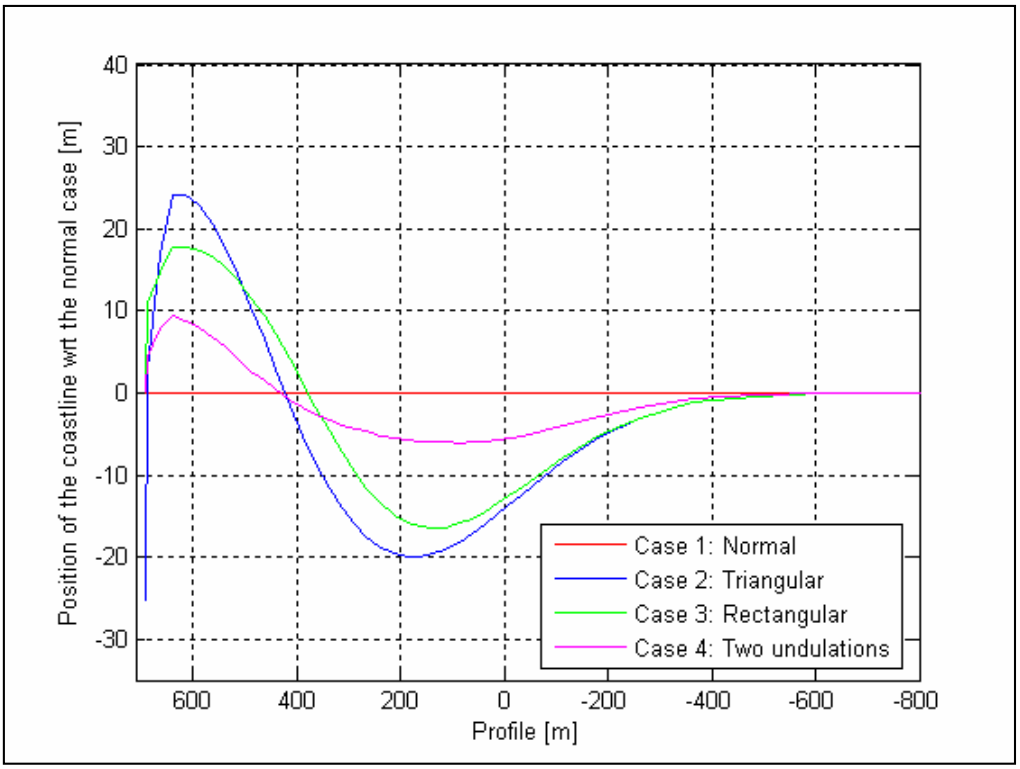

2. Eroded volume in the nourished area in time (based on area)

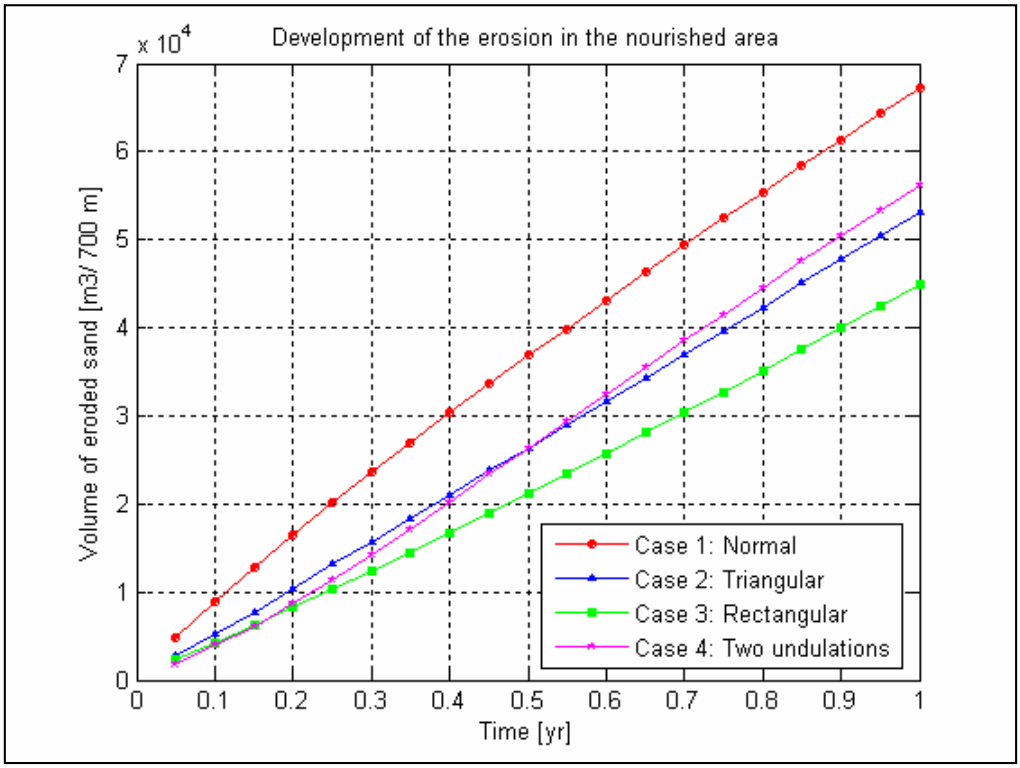

Coastline difference and eroded volume in time of the 3 cases of optimization, based on area	Dubai	2004
WL | DELFT HYDRAULICS		Figure 7.C

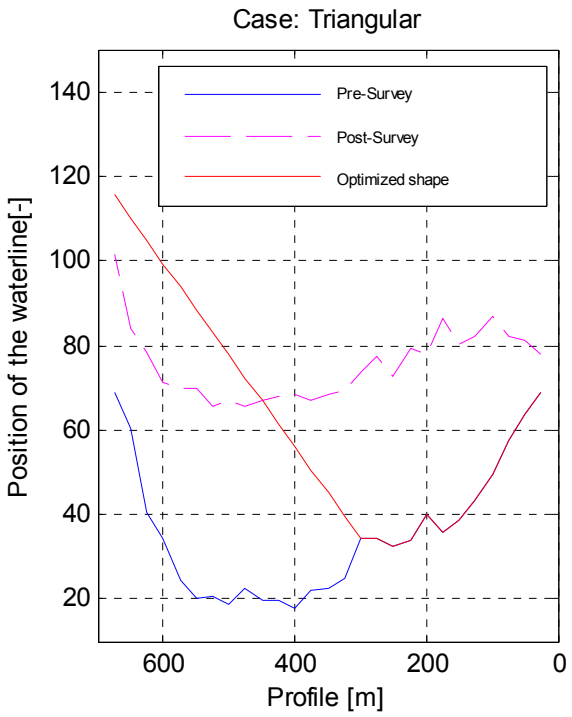

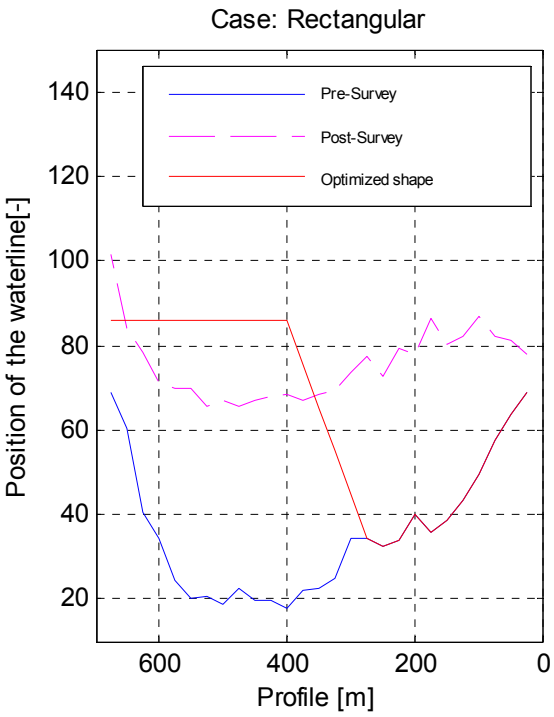

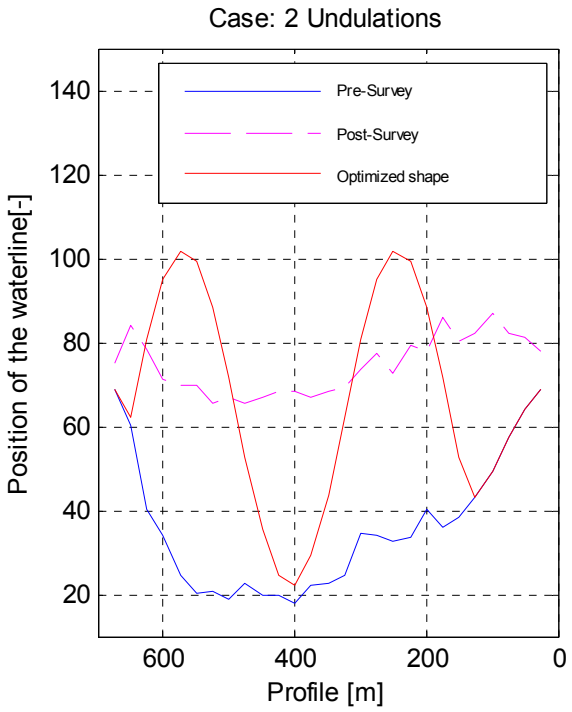

Result of the optimization based on volume Coastline positions on T=0 yr	Dubai	2004
WL | Delft Hydraulics		Figure 7.D

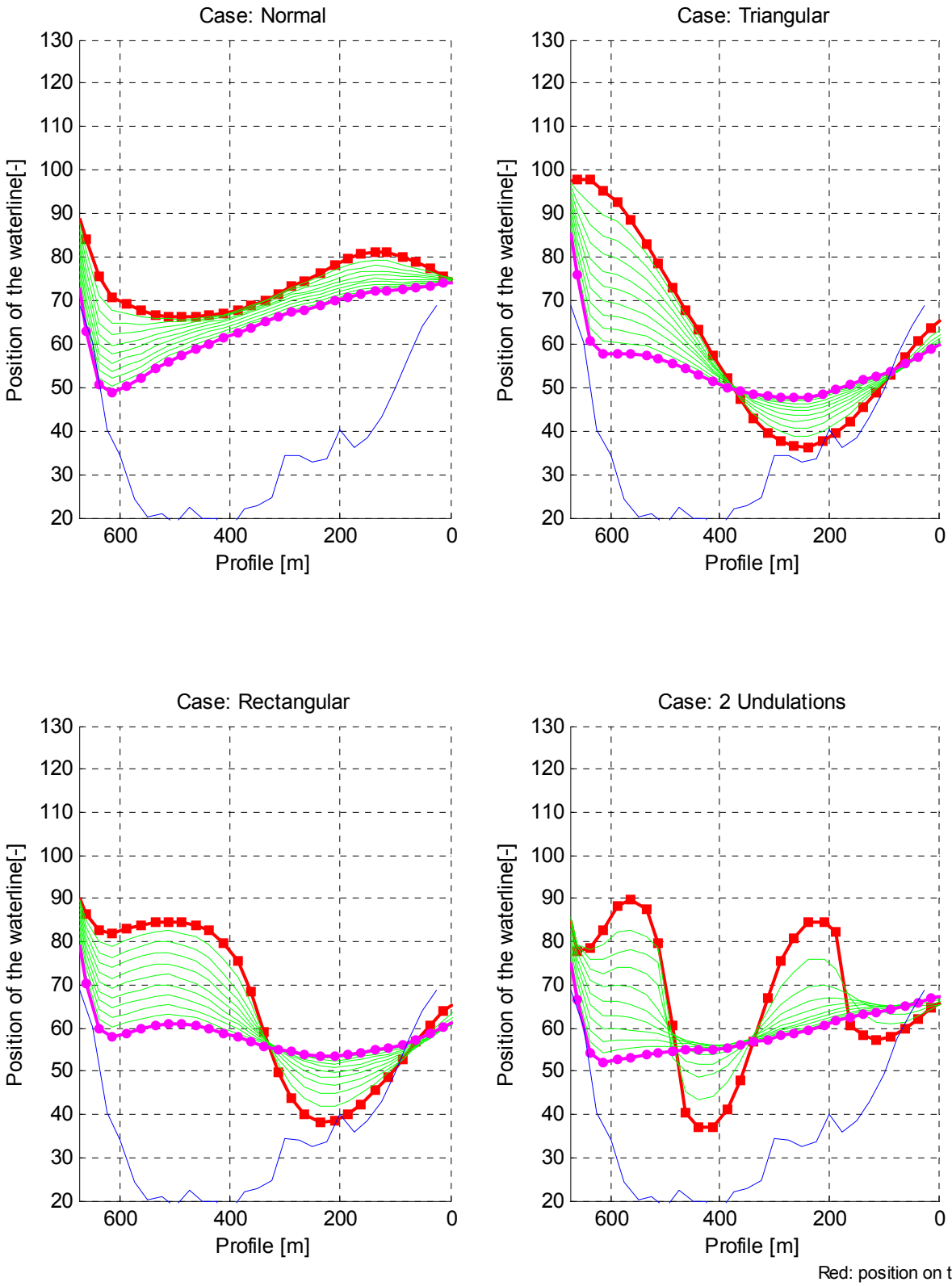

Red: position on t=0.05 yr
Green: positions of coastline
Magenta: position on t=1 yr
Blue: position pre-nourished

Result of the optimization, based on volume Coastline positions in 1 year	Dubai	2004
WL | Delft Hydraulics		Figure 7.E

1. Coastline difference w.r.t the reference case (based on volume)

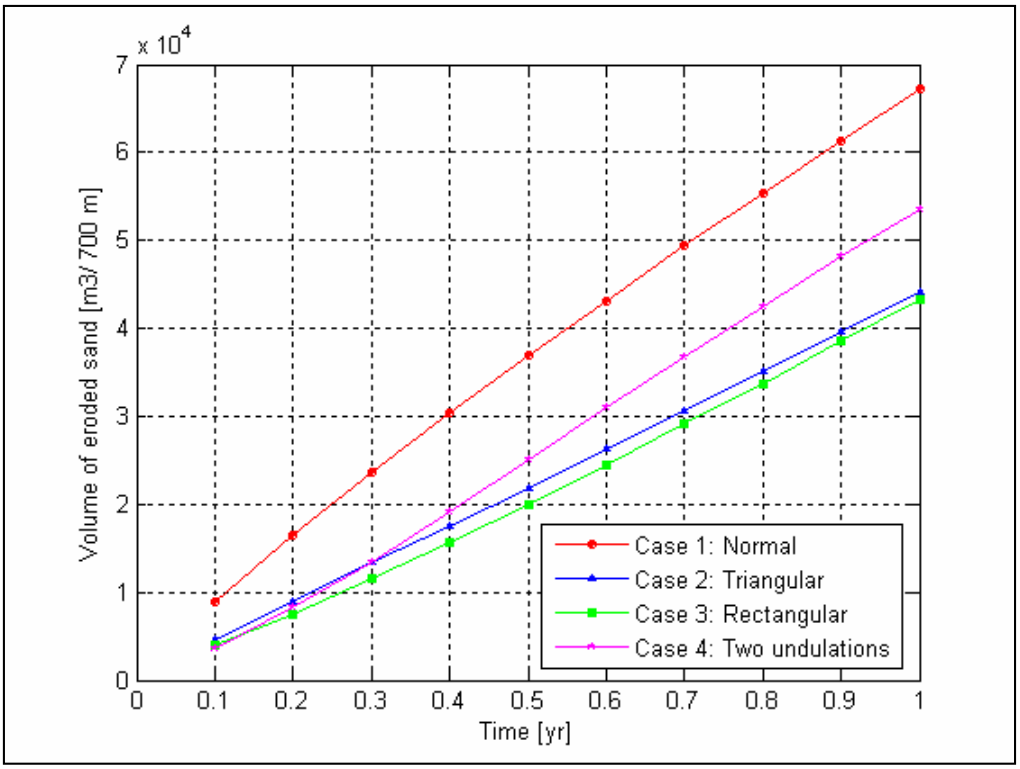

2. Eroded volume in the nourished area in time (based on volume)

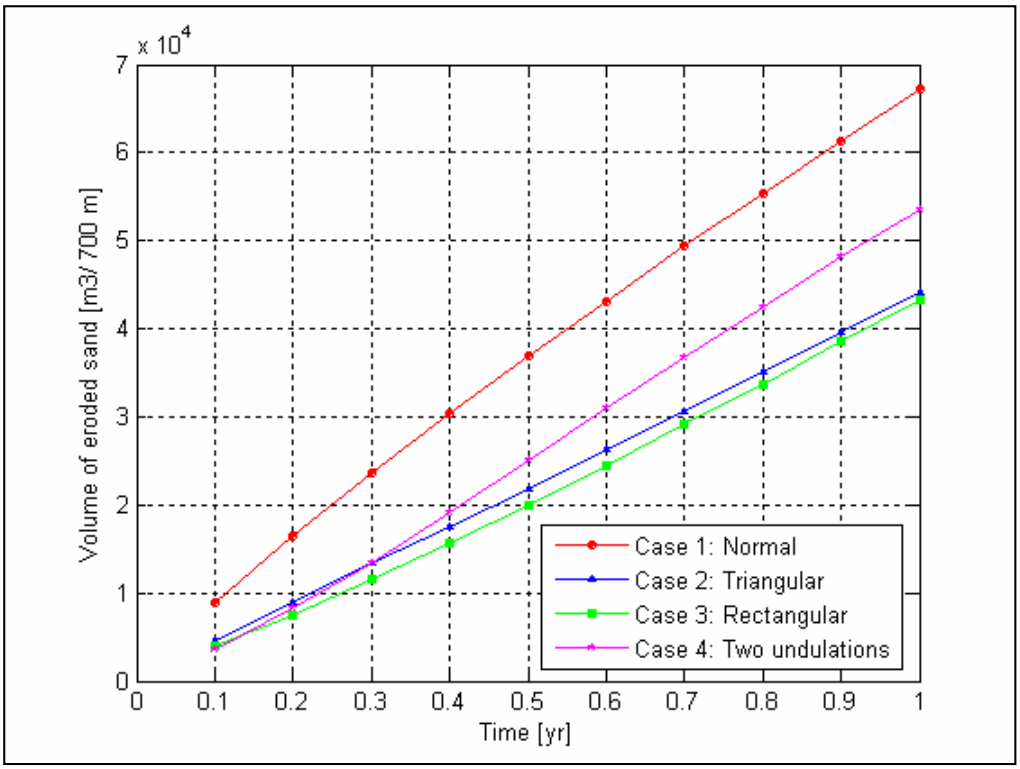

Coastline difference and eroded volume in time of the 3 cases of optimization, based on area	Dubai	2004
WL | DELFT HYDRAULICS		Figure 7.F

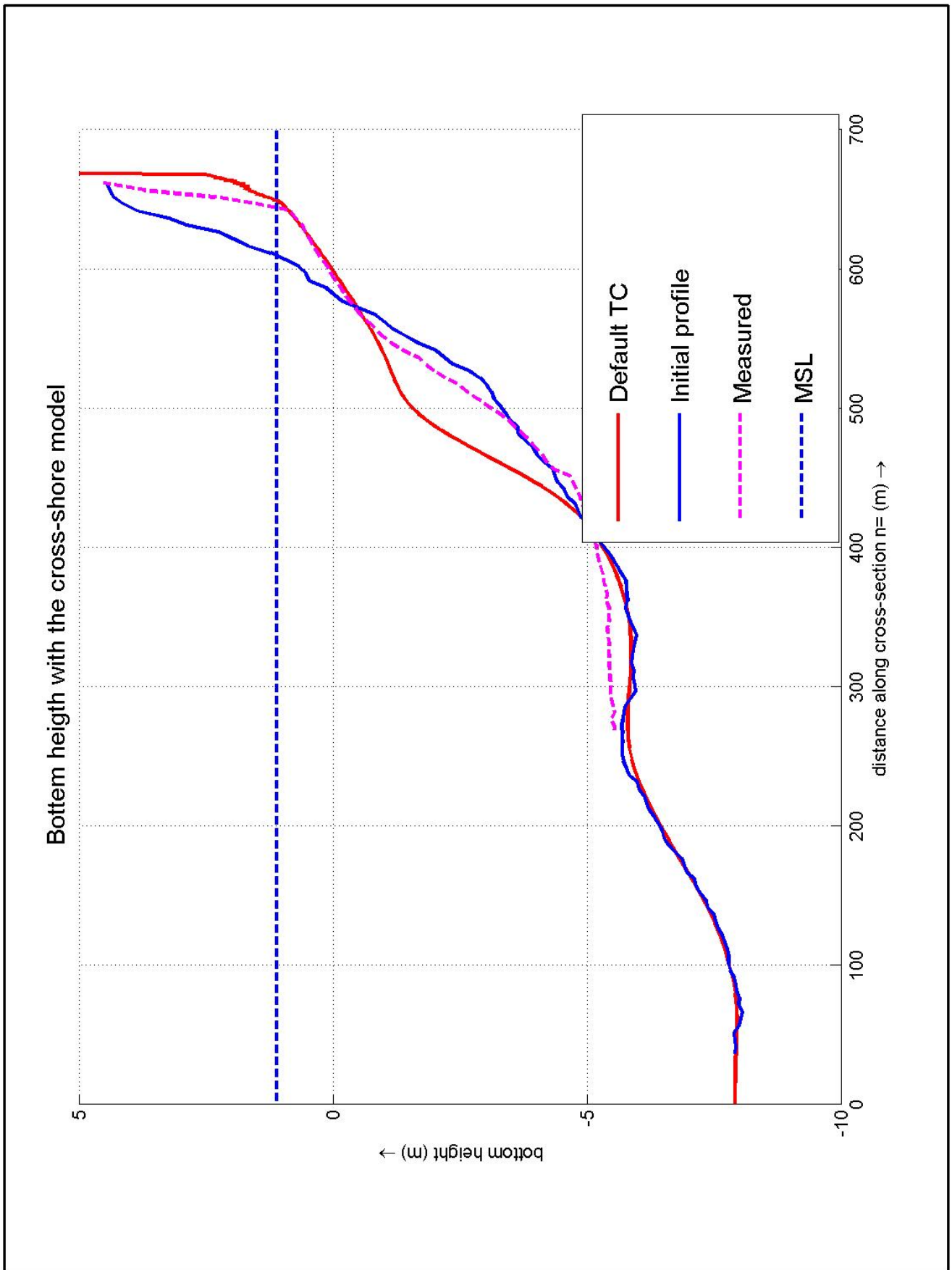

Result of the calibration and verification of the cross-shore model	Dubai	2004
WL | Delft Hydraulics		Figure 8.A

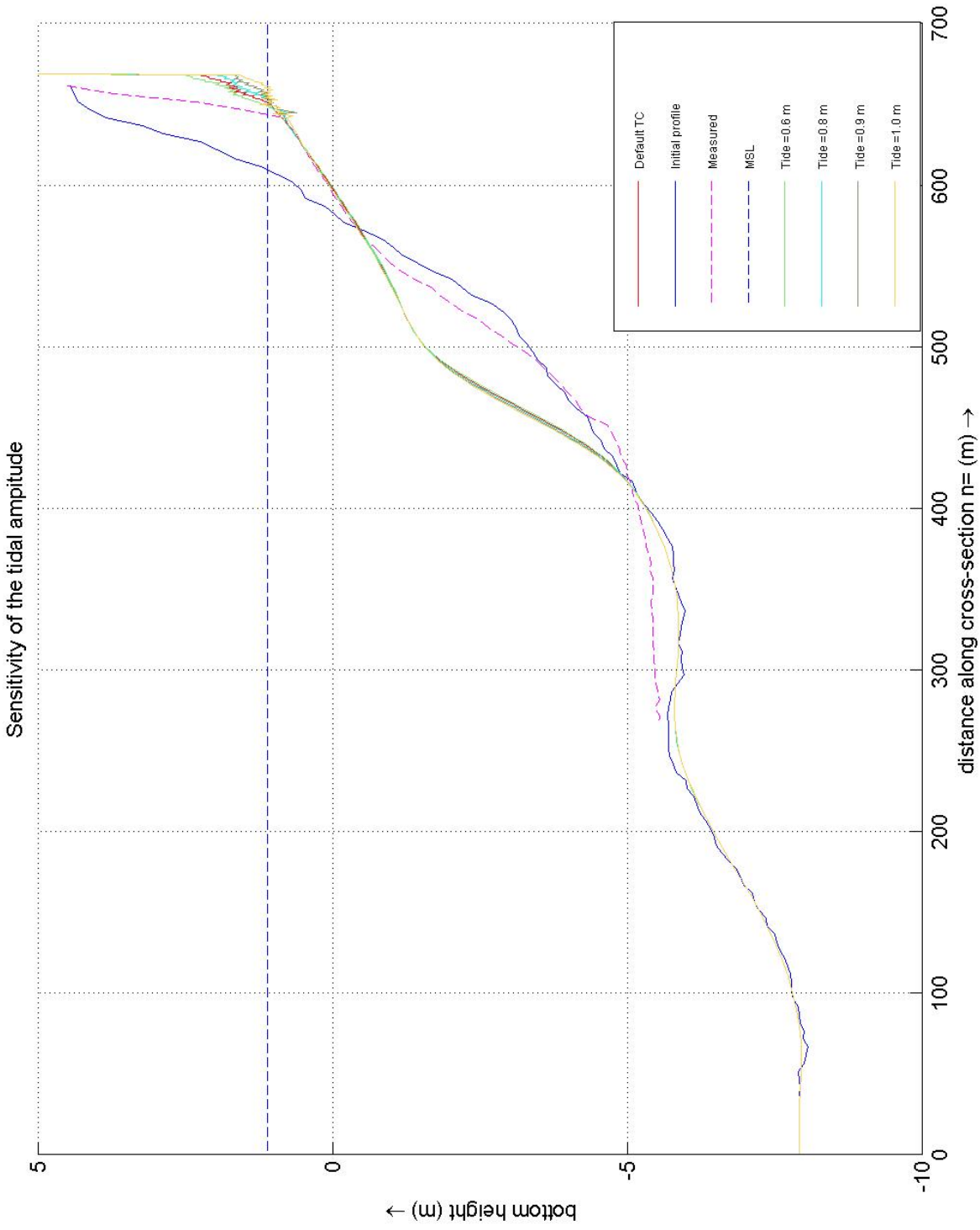

Sensitivity of the cross-shore model Tidal amplitude	Dubai	2004
WL | Delft Hydraulics		Figure 8.B

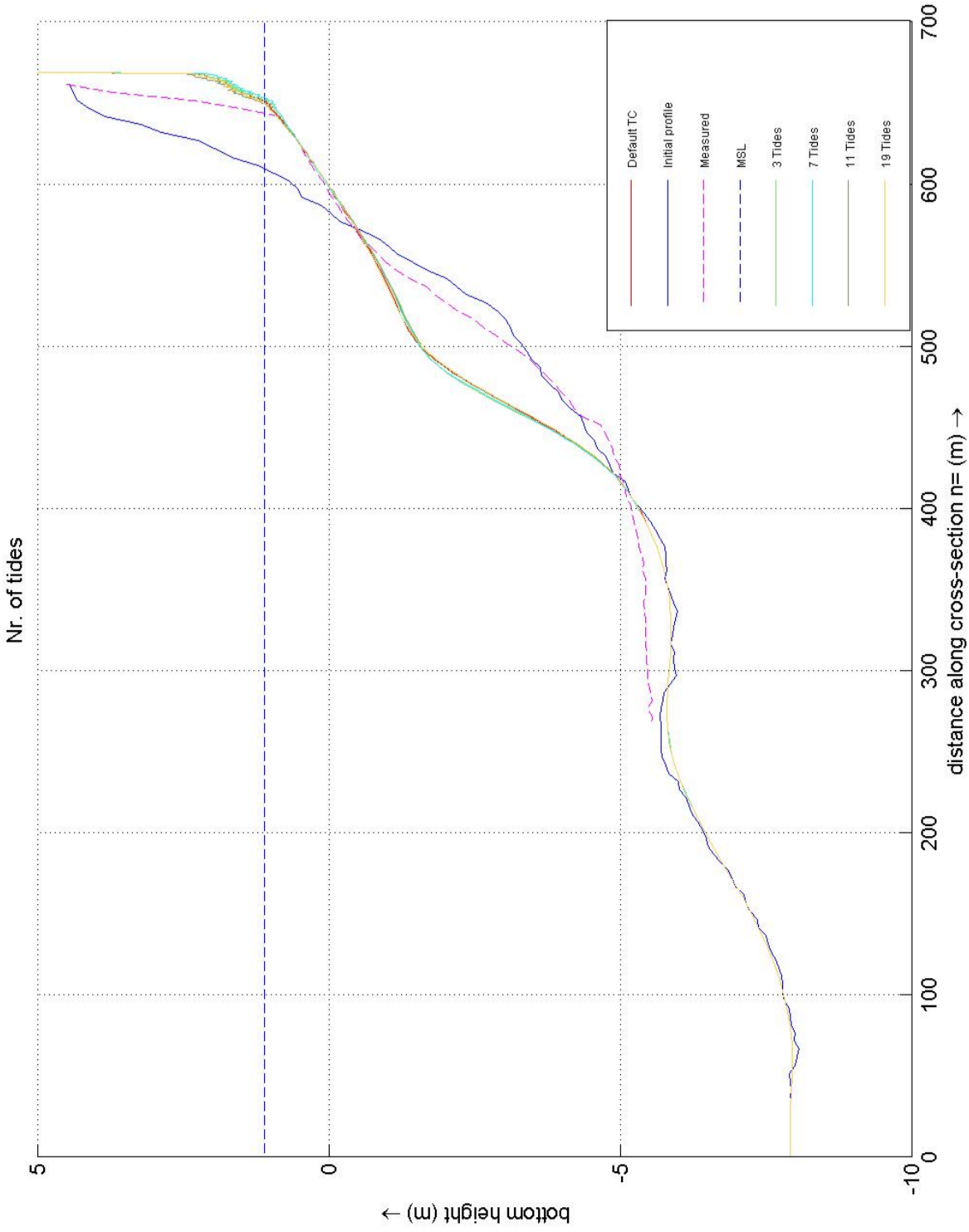

Sensitivity of the cross-shore model Nr of Tides	Dubai	2004
WL | Delft Hydraulics		Figure 8.C

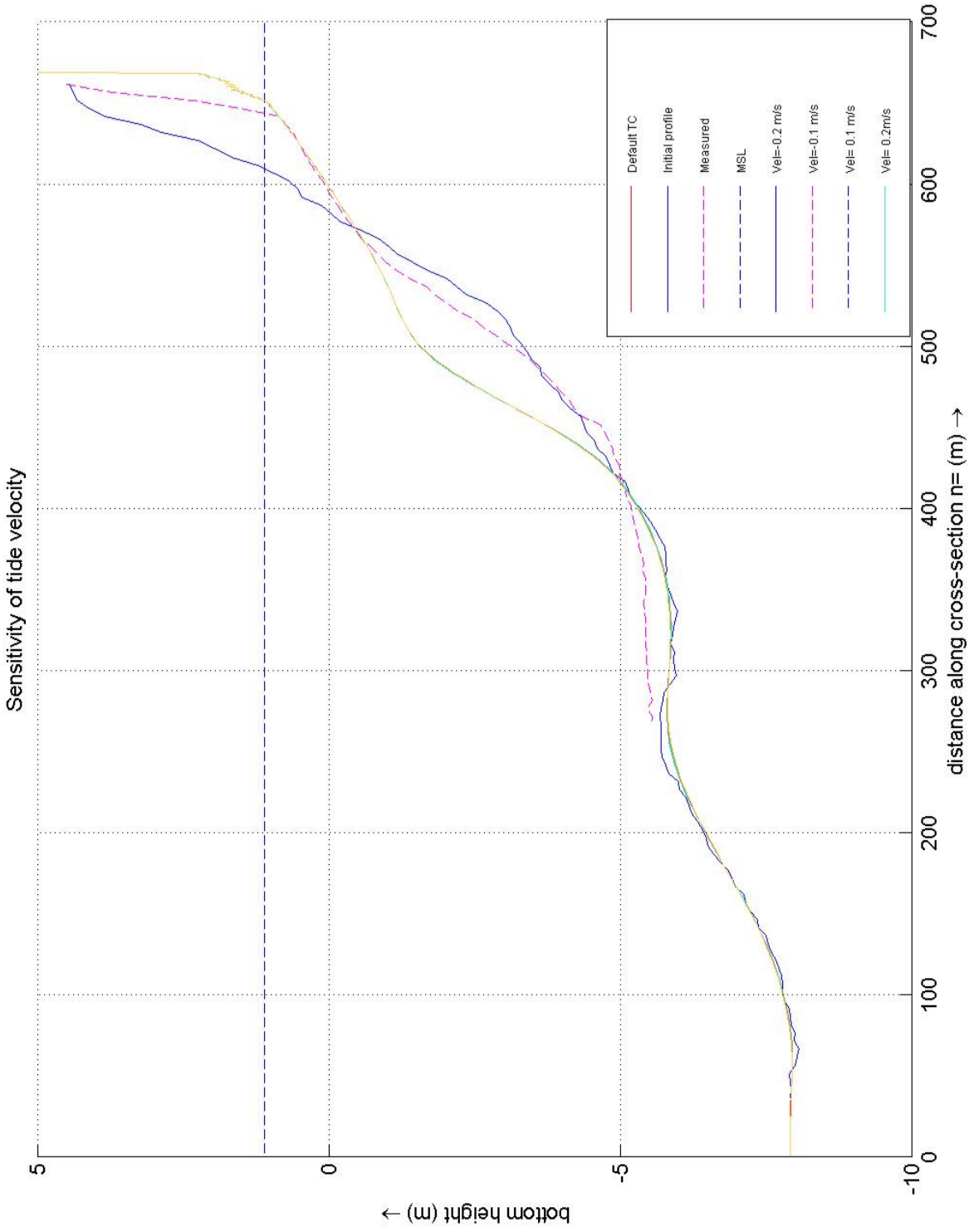

Sensitivity of the cross-shore model Velocity of the tide	Dubai	2004
WL | Delft Hydraulics		Figure 8.D

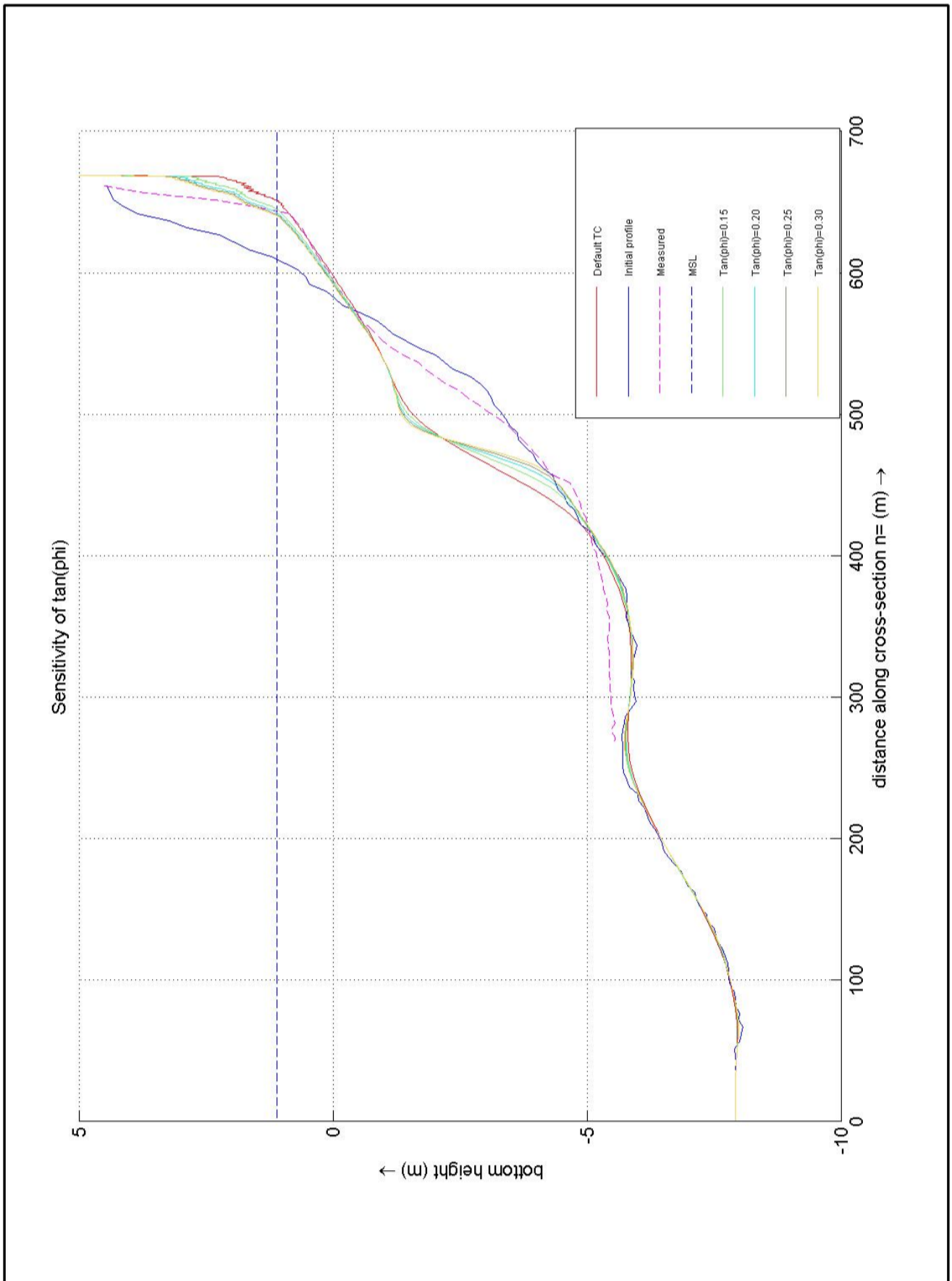

Sensitivity of the cross-shore model to the angle of natural repose	Dubai	2004
WL | Delft Hydraulics		Figure 8.E

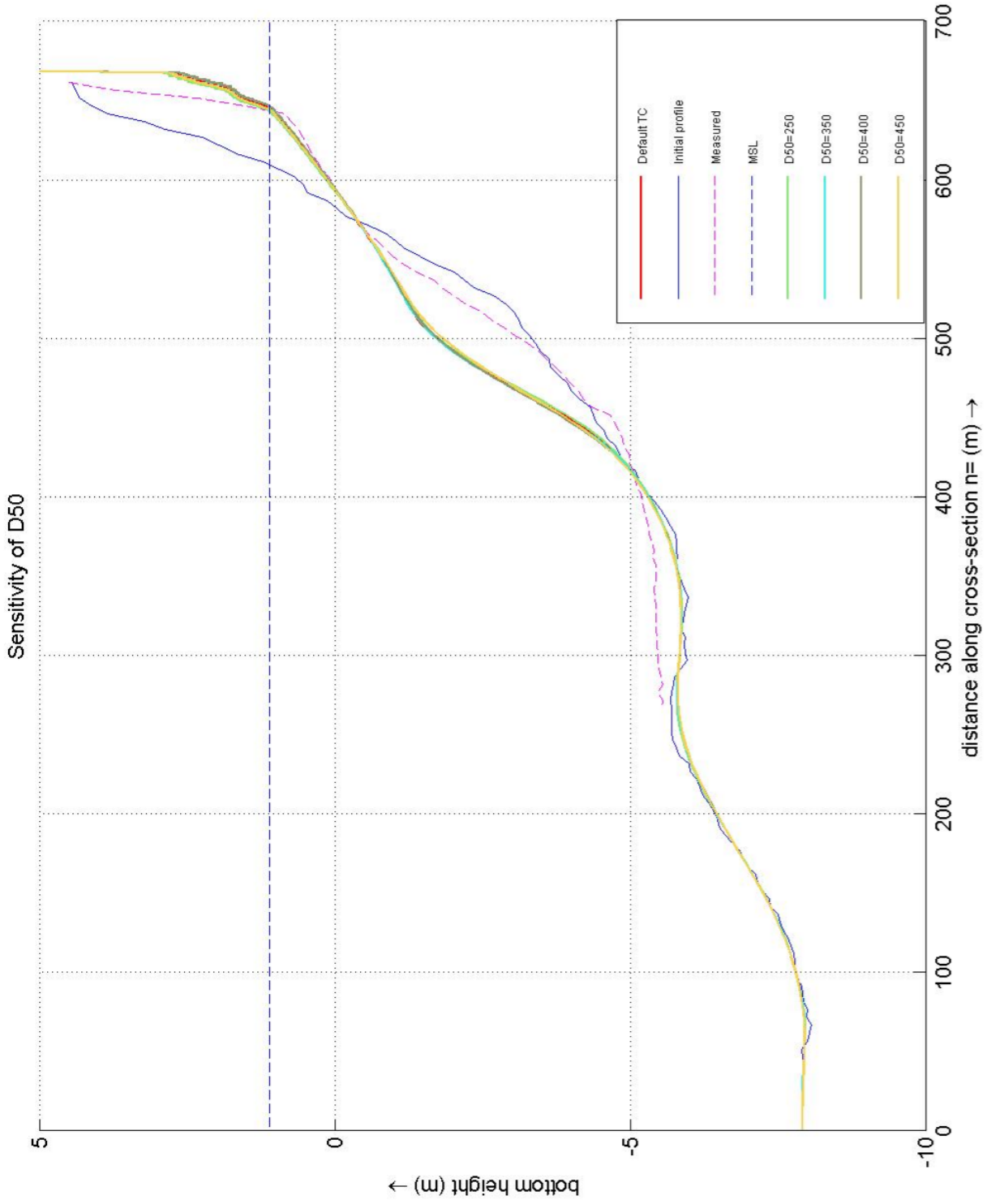

Sensitivity of the cross-shore model to the sediment characteristics	Dubai	2004
WL | Delft Hydraulics		Figure 8.F

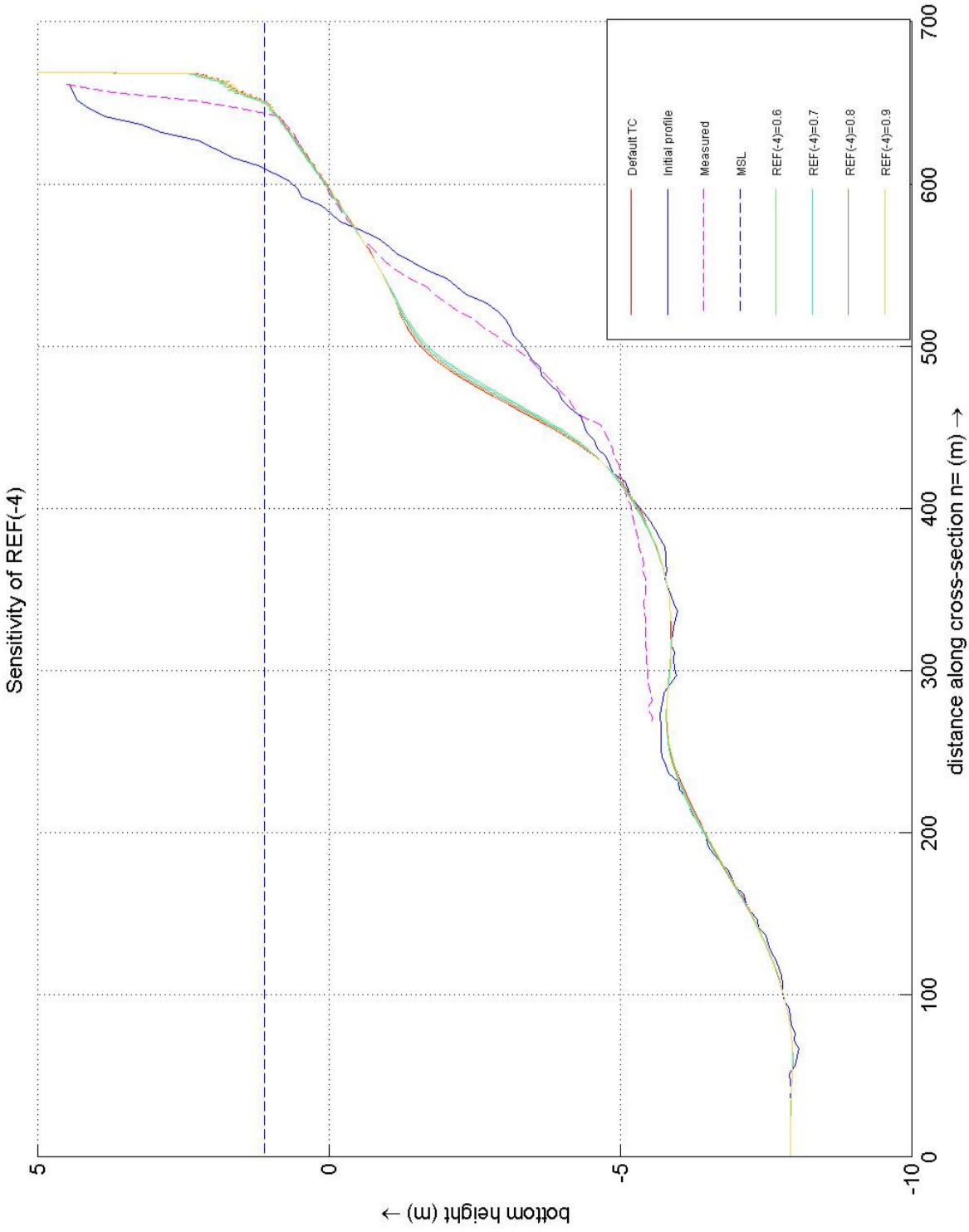

Sensitivity of the cross-shore model sediment distribution in the profile (1)	Dubai	2004
WL | Delft Hydraulics		Figure 8.G

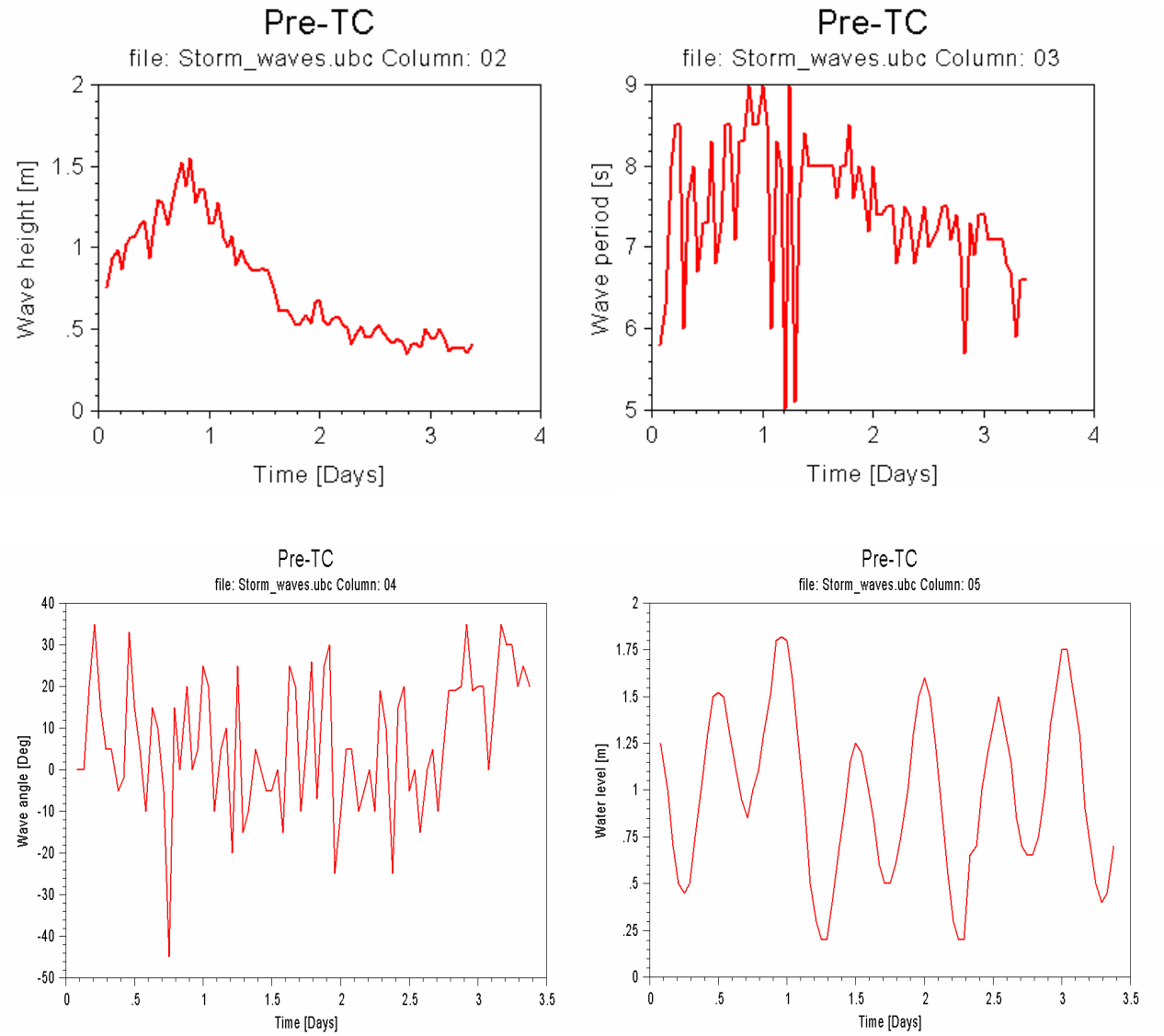

Wave climate for the input of UNIBEST-TC, of the 9 February storm.	**Dubai**	**2004**
WL | DELFT HYDRAULICS		Figure 8.H

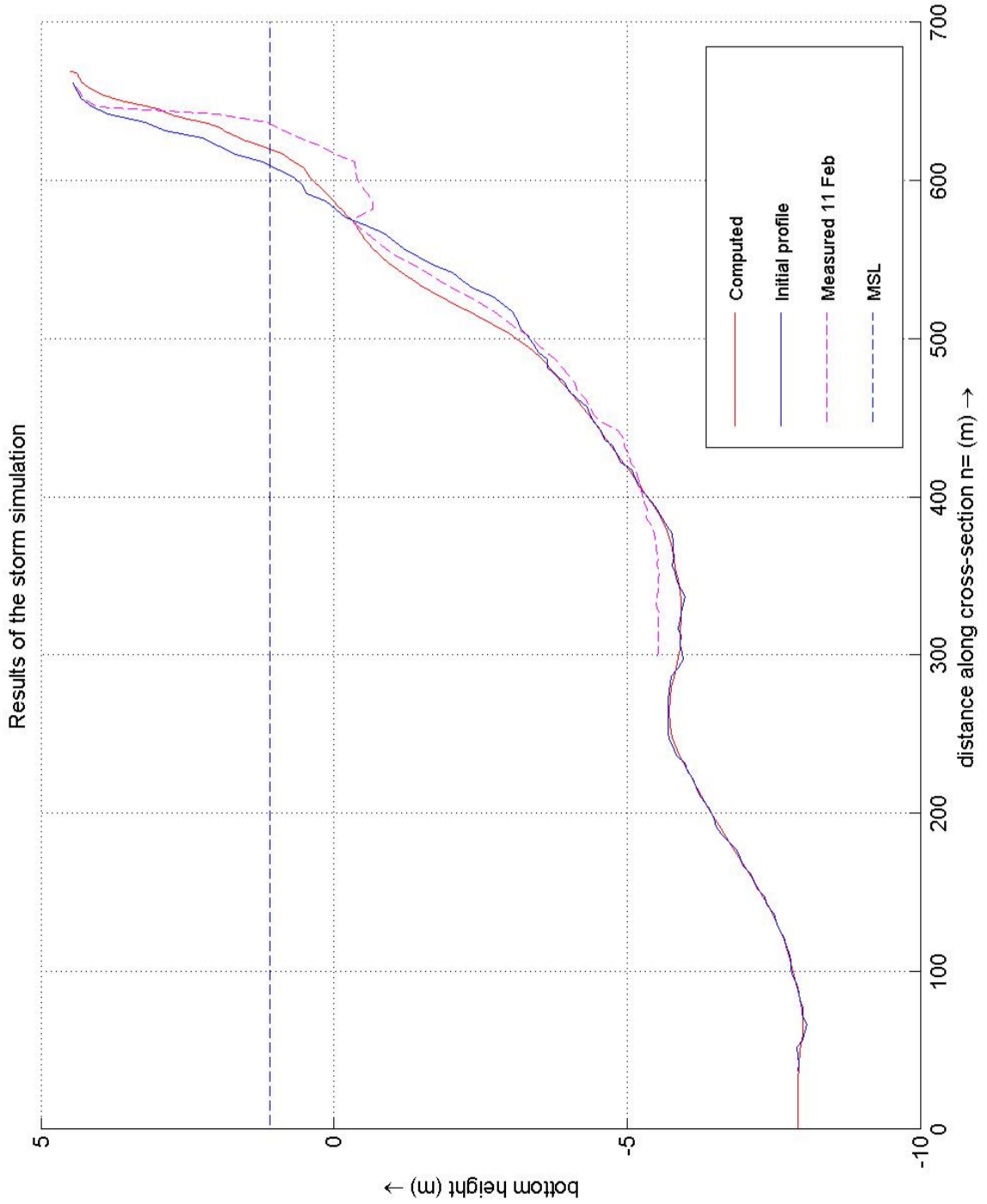

Result of the behaviour of the profile to a storm event	Dubai	2004
WL | Delft Hydraulics		Figure 8.I

Appendices

Prepared for: Van Oord, WL| Delft Hydraulics, Delft University of Technology

Morphological analysis and optimization of Dubai nourishments

M.D. van Dijk
MSc Thesis
July 14, 2005

TU Delft Van Oord WL | delft hydraulics

Prepared for: Van Oord, WL| Delft Hydraulics, Delft University of Technology

Morphological analysis and optimization of Dubai nourishments

Appendices

Graduation committee:

Prof. Dr. Ir. M.J.F. Stive	DUT
Dr. Ir. J. van de Graaff	DUT
Drs. P. Dankers	DUT
Ir. H. de Vroeg	WL | Delft Hydraulics
Dr. Ir. A. Hibma	Van Oord
Ir. G.B.H. Spaan	Van Oord

M.D. van Dijk
MSc Thesis

July 14, 2005

TU Delft Van Oord WL | delft hydraulics

Contents

A Design of beach nourishment

A.1 Using the overfill factor R_A

With the factor R_A, an estimate is obtained of the required volume of fill material to produce 1 m^3 of beach material, when the beach is in a condition with the compatible material. The overfill criteria, as developed by James (1975), are presented graphically in Figure A.1.

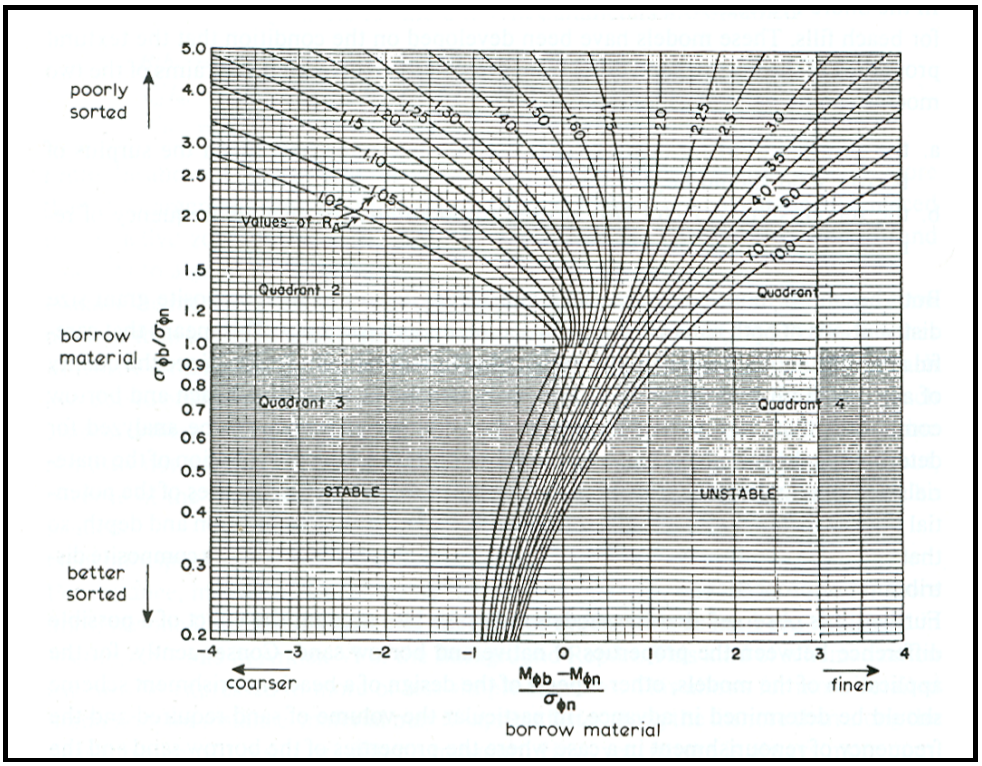

Figure A-1 Isolines of the adjusted SPM fill factor R_A (Shore Protection Manual, 1984)

In which:	M_φ	mean value of phi, = $(\varphi_{84} + \varphi_{16})/2$	[-]
	σ_φ	standard deviation of phi, = $(\varphi_{84} - \varphi_{16})/2$	[-]
	φ	phi scale, an alternative measure of sediment size. Larger values of φ denote finer material,. $\varphi = -^2\log(D)$	[-]
	φ_{84}	84^{th} percentile in phi units	[-]
	φ_{16}	16^{th} percentile in phi units	[-]
	b	subscript referred to as borrow material	[-]
	n	subscript referred to as native material	[-]

A.2 Equilibrium based design methods

A.2.1 Equilibrium beach profiles

The beach profile is the variation of water depth with distance offshore from the shoreline. The equilibrium profile is the result of the balance of destruction versus constructive forces. The destructive forces are: Gravity (making the slope horizontal), turbulence of breaking waves and the undertow. The constructive forces are; net onshore stresses at the bottom, streaming velocity due to energy dissipation, transport of particles by the wave induced crest velocities. In nature, the equilibrium profile is considered to be a dynamic concept, therefore the profile changes continuously. By averaging over a long period a mean equilibrium profile can be defined

Dean (2000) presents an equilibrium profile describe by:

$$h(y) = A(D)y^{2/3} \qquad \text{(A.1)}$$

In which:			
	h	waterdepth	[m]
	y	distance form the mean water line, in offshore direction	[m]
	A	shape parameter	[$m^{1/3}$]
	D	grain diameter	[m]

The dimensional parameter A is the profile scale factor and is a function of the energy dissipation and indirectly the grain size of the beach. This equilibrium profile is based on the assumption that turbulence is the dominant destructive force. Several other shapes have been proposed but not discussed here. Table A.1 presents values of A for sand (Dean, Walton and Kriebel, 1994)

d (mm)	**0.00**	**0.01**	**0.02**	**0.03**	**0.04**	**0.05**	**0.06**	**0.07**	**0.08**	**0.09**
0.1	0.0630	3.0672	0.0714	0.0756	0.0798	0.084	0.0872	0.0904	0.0936	0.0968
0.2	0.1000	0.1030	0.1060	0.109	0.1120	0.1150	0.1170	0.1900	0.212	0.1230
0.3	0.1250	0.1270	0.1290	0.131	0.1330	0.1350	0.1370	0.1390	0.141	0.1430
0.4	0.1450	0.1466	0.1482	0.1498	0.1514	0.1530	0.1546	0.1562	0.1578	0.1594
0.5	0.1610	0.1622	0.1634	0.1646	0.1658	0.1670	0.1682	0.1694	0.1706	0.1718
0.6	0.1730	0.1742	0.1754	0.1766	0.1778	0.1790	0.1802	0.1814	0.1826	0.1838
0.7	0.1850	0.1859	0.1868	0.1877	0.1886	0.1895	0.1904	0.1913	0.1922	0.1931
0.8	0.1940	0.1948	0.1956	0.1964	0.1972	0.1980	0.1988	0.1996	0.2004	0.2012
0.9	0.2020	0.2028	0.2036	0.2044	0.2052	0.2060	0.2068	0.2076	0.2084	0.2092
1.0	0.2100	0.2108	0.2116	0.2124	0.2132	0.214	0.2148	0.2156	0.2164	0.2172

Table A-1 Summary of Recommended A Values ($m^{1/3}$) for Particle diameters from 0.10 to 1.09 mm

A.2.2 Design

As stated, depending on the native and the borrowed sediment scale parameters A_n and A_b the nourished beach profile can be intersecting, non-intersecting, or submerged. This is shown in Figure A.2. Intersecting profile require $A_B > A_N$.

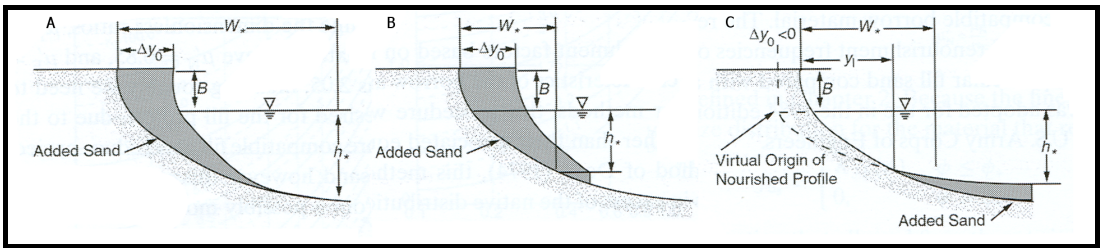

Figure A-2 Three generic types of beach profiles (Dean, 1991). (A) Intersecting profile $A_b > A_n$. (B) Non-intersecting profile. (C) Submerged profile $A_b < A_n$

The relation to determine whether the profiles are intersecting/ nonintersecting:

$$\left(\frac{\Delta y_0}{W_*}\right)_c + \left(\frac{A_n}{A_b}\right)^{3/2} - 1 \quad \text{with } W_* = \left(\frac{h_c}{A_n}\right)^{3/2} \qquad \begin{cases} < 0, \text{ intersecting profiles} \\ > 0, \text{ non intersecting profiles} \end{cases} \tag{A.2}$$

In which Δy_0 shoreline advancement [m]
h_c closure depth (on the original profile) [m]

The critical volume associated with intersecting and nonintersecting profiles is:

$$\left(V'\right)_{c1} = \left(1 + \frac{3}{5B'}\right)\left[1 - \left(\frac{A_n}{A_f}\right)^{3/2}\right] \quad \text{for } (A_f/A_n) > 1 \tag{A.3}$$

And to distinguish a non-intersecting submerged and emerged profile, with (A.4) we can determine the critical volume that will just yield a finite shoreline displacement for non-intersecting profiles.

$$\left(V^2\right)_{c2} = \frac{3}{5B'}\left(\frac{A_n}{A_b}\right)^{3/2}\left(\frac{A_n}{A_b} - 1\right) \quad \text{for } (A_b/A_n) < 1 \tag{A.4}$$

Intersecting profiles:

The volume placed per unit shoreline length V_1 that will yield a shoreline advancement Δy_0 can be calculated with equation:

$$V_1 = \Delta y_0 + \frac{3}{5} A_n \frac{\Delta y_0^{5/3}}{\left[1 - \left(\frac{A_n}{A_b}\right)^{3/2}\right]^{2/3}} \tag{A.5}$$

Or by introducing the dimensionless parameters we derive:

$$V_1' = \Delta y_0' + \frac{3}{5B'}\frac{\Delta y_0'^{5/3}}{\left[1-\left(\frac{A_n}{A_b}\right)^{3/2}\right]^{2/3}} \qquad \text{with: } V'=\frac{V}{BW_*},\ y'_0=\frac{y_0}{W_*},\ B'=\frac{B}{h_c} \tag{A.6}$$

Nonintersecting but emergent profiles

The corresponding volume V'$_2$ in non dimensional form presented in equation is:

$$V_2' = \Delta y_0' + \frac{3}{5B'}\left\{\left[\Delta y_0' + \left(\frac{A_n}{A_b}\right)^{3/2}\right]^{5/3} - \left(\frac{A_n}{A_b}\right)^{3/2}\right\} \tag{A.7}$$

Submerged profiles

For the submerged profile, where $\Delta y_0 < 0$ the corresponding non-dimensional volume of added sediment volume V' can be described by equation.

$$V' = \frac{3}{5B'}\left\{\left[\Delta y_0' + \left(\frac{A_n}{A_b}\right)^{3/2}\right]^{5/3} + \frac{\left(-\Delta y_0'\right)^{5/3}}{\left[\left(\frac{A_n}{A_b}\right)^{3/2}-1\right]^{2/3}} - \left(\frac{A_n}{A_b}\right)^{3/2}\right\} \tag{A.8}$$

A.3 Planform response

A.3.1 Single-line theory

The single-line theory was first presented by Pelnard-Considère (1956). It gives the basic equations describing the morphological processes of coastline evolution due to longshore sediment transport gradients. For the single-line theory the coastal profile is schematized (Figure A.3). The x-axis is chosen along the original coastline. The shore-normal Y–axis is chosen in a direction parallel to the original coastline, positively in offshore direction.

The basic assumption of the single-line theory is that the profile characterizing the beach is assumed to move horizontal over its entire active profile height as a result of erosion or accretion (right in Figure A.3). The beach slope therefore does not change. Beyond this active profile height the bottom does not move. The shoreward limit of the profile is located at the top of the active profile. This means that the assumptions are made that only longshore sediment transports can be taken into account and that the profile is always in equilibrium.

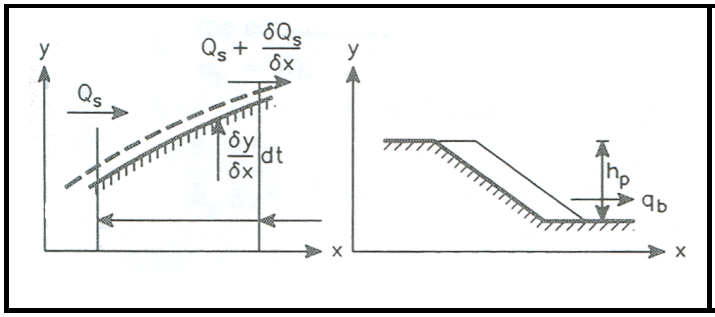

Figure A-3 Equation of continuity (left equals right Figure)

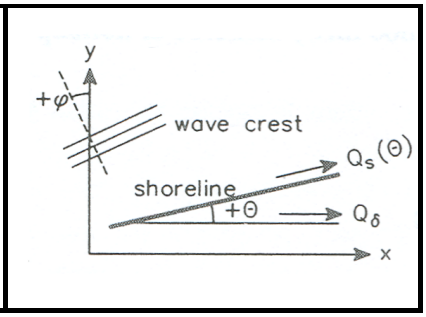

Figure A-4 Equation of motion

In order to simulate the coastal changes a continuity equation and an equation for motion are used together with initial and boundary conditions. The equation of continuity (Figure A.3) yields:

$$h_p \frac{\delta y}{\delta t} + \frac{\delta Q_s}{\delta x} + q_b = 0 \tag{A.9}$$

In which:			
	Q_s	Total longshore transport	[m^3/s]
	y	Coastline position	[m]
	h_p	Active profile height (closure depth and berm height)	[m]
	q_b	Sediment source/sink	[m^2/s]

The equation of motion (Figure A.4) is derived by assuming that the longshore transport is a (continuous) function of the coastline orientation. This leads to:

$$Q_s(\theta) = Q_{s_0} + \theta\left(\frac{\delta Q_s}{\delta \theta}\right)_{\theta=0} + \frac{1}{2}\theta^2\left(\frac{\partial^2 Q_s}{\partial \theta^2}\right)_{\theta=0} + \ldots \tag{A.10}$$

With the assumption that the second order and higher terms can be neglected this can be simplified and when defining that:

$$\theta = \tan(\theta) = \frac{\delta y}{\delta x} \text{ and } \frac{dQ_s}{d\theta} = s_1 \tag{A.11}$$

Equation (A.12) is derived, which is known as the Pelnard-Considère equation:

$$Q_s(\theta) = Q_{s_0} - s_1 \frac{dy}{dx} \tag{A.12}$$

In which:			
	$Q_s(\theta)$	longshore transport as a function of the coastline direction	[m^3/s]
	Q_{s0}	longshore transport along a straight coastline parallel to the x-axis	[m^3/s]
	s_1	variation of the transport as a function of coastline rotation	[m^3/s]
	θ	coastline orientation with respect the x-axis	[^{0}]

When the equation of motion is substituted in the equation of continuity, a so-called diffusion equation (A.13) is derived for which analytical solutions can be found (Bakker and Edelman, 1965; Bakker, 1969).

$$\frac{\partial y}{\partial t} = \frac{s_1}{h_p}\frac{\partial^2 y}{\partial x^2} \tag{A.13}$$

B Boundary conditions

B.1 Tidal levels

The Admiralty Tide tables present values for Jebel Ali Port and Port Rashid (1994). The values in Table B.1 show no large difference between the ports.

Port	Tidal levels						
	LAT	MLLW	MHLW	MSL	MLHW	MHHW	HAT
Mina Jebel Ali (height in m above CD)	0.0	0.4	0.8	1.0	1.3	1.6	2.1
Mina Rashid		0.4	0.7		1.3	1.6	

Table B-1 Tide levels (source: Admiralty Tide tables, 1994)

The real-live graphs from the Dubai municipality in the period from December 2003 to May 2004 show difference with the values from the Tide Tables. An analysis of a period of six months and of a spring-neap cycle of 14 days in February 2004 shows the results presented in Table B.2.

Location	Tidal Levels (measured in 14-day cycle)				
	LT	MLW	MSL	MHW	HT
Jumeirah beach	0.2	0.6	1.1	1.5	2.1

Table B-2 Tide levels (Dubai Municipality measurements, 2004)

Both sources data agree reasonably. Both sources present mean sea level around 1.1m above Chart Datum.

Because of the accuracy of the DM data, a raise of 0.1 m of the Mina Jebel Ali data is assumed to represent the tide at Italian beach.

B.2 Sand

B.2.1 Sand samples

From the sand curve of *Figure 4.9*, the median diameter can be derived, written as D_{50}. The definition is that by size, half of the particles in the sample will have a larger diameter and half have a smaller. D_{90} is the diameter for which 90% of the sediment has a smaller diameter. The results are listed below in Table B.3.

Sample	Date	D_{10} (µm)	D_{50} (µm)	D_{90} (µm)
	28-Dec-03	150	300	1000
1.	11-Apr-04	350	600	1100
2.	11-Apr-04	260	550	1100
3.	11-Apr-04	450	810	1400
4.	11-Apr-04	180	350	780
5.	11-Apr-04	260	470	1100
6.	11-Apr-04	230	550	2200
7.	12-Apr-04	550	900	2000
8.	12-Apr -04	350	630	1300
9.	12-Apr -04	150	250	620
Mean		290	540	1260
Median		260	550	1100

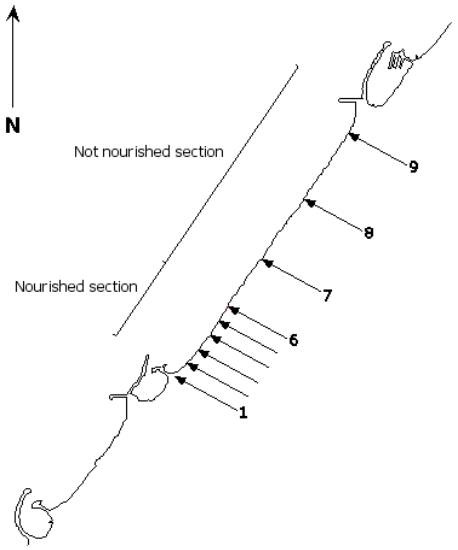

Table B-3 Distribution of the sand samples

A first estimate for a good representation of the mean sediment size is to take the median of the 10 samples. The median is the number in the middle of the sets; half have values that are greater than the median and half have values that are less.

Table B-4 Representative Sand characteristics of Italian beach (source: Van Oord, 2004) shows D_{50}, D_{10} and D_{90} of the median of the samples. The assumption is made that this sample is representative for Italian beach. Conclusion is that a relative coarse sand is used for the nourishment (D_{50}>500 µm).

	D_{10} (µm)	D_{50} (µm)	D_{90}(µm)
Mean	260	550	1100

Table B-4 Representative Sand characteristics of Italian beach (source: Van Oord, 2004)

B.2.2 Fall velocity

When a particle falls through water it accelerates until it reaches its fall or settling velocity. This is the terminal velocity that a particle reaches when the drag force on the particle just equals the (downward) gravitational force. A particle's fall velocity is a function of its size, shape and density; as well as the fluid density, viscosity and several other parameters.

The fall velocity can be calculated theoretically in still water from a force balance on a single falling grain. Where the relevant forces are the weight of the grain W, the buoyancy force and the fluid drag that the particle experiences. This gives a balance between the forces with the (B.1) as solution:

$$w_s = \sqrt{\frac{4 \cdot (\rho_s - \rho_w) \cdot g \cdot D_{50}}{3 \cdot \rho_w \cdot C_D}} \qquad \text{(B.1)}$$

In which:			
	w_s	fall velocity of sand in seawater	[m/s]
	D_{50}	median grain size	[m]
	ρ_w	density water	[kg/m^3]
	ρ_s	density sand	[kg/m^3]

For large numbers, but less than 100, Olson (1961) gives the approximation:

$$C_D = \frac{24}{\mathrm{Re}}\left(1 + \frac{3\,\mathrm{Re}}{16}\right)^{1/2} \qquad \text{(B.2)}$$

In which:			
	C_D	Drag coefficient	[-]
	RE	Reynolds number	[-]

Another approach is to calculate the fall velocity with Equation (B.3) and is derived for seawater at a temperature of 5 ^{0}C (Basis rapport zandige kust, 1995).

$$^{10}\log(1/w_s) = 0.476 \cdot (^{10}\log D_{50})^2 + 2.180 \cdot {}^{10}\log(D_{50}) + 3.226 \qquad \text{(B.3)}$$

CEM (2003) presents a chart, which relates the fall velocity of quartz spheres in air and water to the grain size and the temperature of the water (Vanoni, 1975).

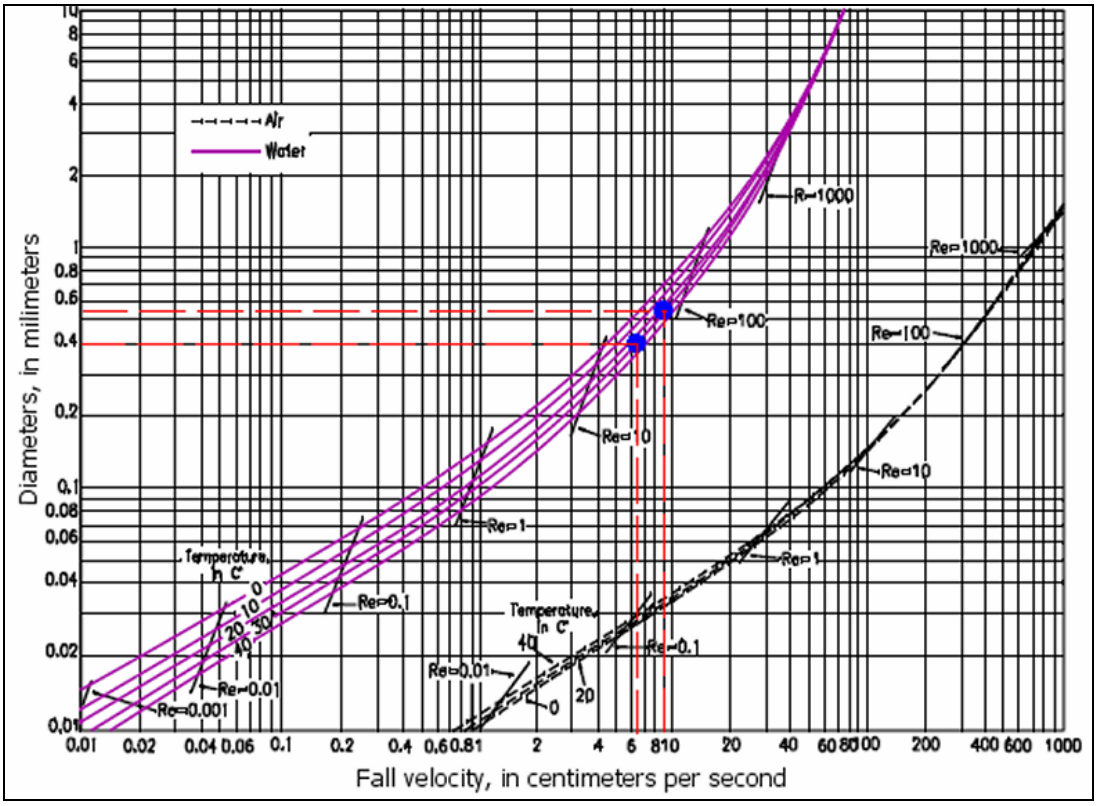

Figure B-1 Fall velocity of quartz spheres in air and water (Vanoni, CEM, 2003)

These three approaches lead to a fall velocity presented in Table B-5.

Approach	**Source**	**w_s (m/s)**
Theoretic	Equation (B.1)	0.09
Basisrapport zandige kust	Equation (B.3)	0.07
Vanoni	CEM, 2003	0.09

Table B-5 Results fall velocities computations (for D_{50} is 550 μm)

The water in Dubai has a higher temperature than for which equation B.3 is derived. So the assumption is made that 0.09 m/s is a good representative for the fall velocity of a grain with a median diameter of 550 μm.

C UNIBEST-CL+ model

C.1 Introduction

This appendix describes the formulation of the UNIBEST-CL+ model. It describes the basic modelling concepts in Section C.2. This information is obtained from the user manual of December 2000. Section C.3 gives the mathematical descriptions of the model and transport formula. In Section C.4 the used formulations for the modelling of the wave diffraction around the Umm as Suqaym II marina is presented. Section C.5 presents relations to determine the breaker index.

C.2 Basic modelling concepts

The UNIBEST-CL+ consists of two integrated sub-modules:
- The Longshore Transport module (LT-module)
- The CoastLine module (CL-module)

The CL-module simulates the coastline evolution based on the longshore transport gradients that are present along the considered coast. These longshore gradients are derived from longshore transport calculations performed with the LT-module. The results of LT-calculations have been transformed to a function that describes the integrated longshore transports as a function of the coastline orientation.

During a coastline simulation with the CL-module the actual transport rates are derived from the transport functions based on the actual coastline orientation. If due to accretion or erosion the coastline orientation changes with time, the longshore transports also change.

C.2.1 The basic model

The basic model which defines the actual coastline consists of:

- The curved x,y-system (with the x-axis shore parallel and the y-axis perpendicular to the x-axis)
- The y(x) initial coastline
- The grid points along the curved x-axis (with y(x)=0)

The x-axis is a curved line, and the y-direction is defined perpendicular to it. The x-axis is created by defining a number of basic points. The program fits a curved line through the basic points using a local third-degree interpolation with continuous first derivatives at the basic points. At these points the coastline position y(x) is defined, which are the basic y-points. At the basic point and at a user-defined number in between, *x*-grid points (*x-points*) are created. At x-points the transport rate Q_s is defined by the transport rays from the LT-module (Section C.3.1).

Halfway these x-points, the xy-points are located (points where the coastline y is defined). The y-value is obtained by linear interpolation between the basic Y-points, assuming the x,y-system to be a rectangular coordinate system.

C.2.2 LT-Run specifications

C.2.2.1 Transport rays

A transport ray is the result of a longshore sediment transport calculation with the LT-module based on coastline orientation, a prescribed wave- and current-climate and a bottom profile. Basically it is a transport function that defines the longshore sediment transport as a function of the coastline orientation. Transport rays are used in the CL-module to determine the actual longshore transports based in the calculated coastline orientation.

More specific a Transport Ray is defined by the following transport properties.

- The angle of coastal orientation upon which the cross-ray is defined. In the model the coastal orientation is expressed as the direction of the seaward directed coast-normal, measured clockwise relatively to the north
- Coefficients defining the transport rate as a function of the actual coastline orientation, $Q_s=f(\alpha_e, c_1, c_2)$
- The characteristic points x^r_b, $x^r_{2\%}$... $x^r_{100\%}$ with respect to the coastal point x^r_c. These points define the cross-shore integrated transport percentages which are used to determine the sediment by-pass in case of groynes. The x^r_c point in the coastal profile determines the location in the coastal profile and thus the depth contour that corresponds with the y-values in the shoreline model
- The profile height as defined by the user. This is the height within the transport takes place
- The profile shape factor

The input for an LT-Run calculation step is:

- A wave-and current-scenario (definition wave angles with respect to the north)
- The coastal orientation angle (direction of the seaward directed coast normal, measured clockwise relative to the north)
- A cross-section
- A selected transport formula and the required coefficients
- Coefficients for the energy decay calculation

A LT-calculation runs as follows:

- It makes an estimate of the equilibrium angle (the rotation of the coast, where the resultant sediment drift is zero), based in a simplified method
- For a number of angles around the equilibrium angle (-60^0 and $+60^0$) the total transport $Q_s(\theta)$ is calculated for all wave-current combinations
- Draws a Q_s-θ curve

The equilibrium angle is the coast angle for which the transport is zero. By using the least-square method this function can be approximated by the analytical solution presented by Equation(C.1).

$$Q(\theta) = c_1 \cdot \theta_r \cdot \exp\left[-\left(c_2 \cdot \theta_r\right)^2\right] \quad \text{(C.1)}$$

In which:			
	θ_r	resultant of θ-θ_e	[^{0}]
	θ	actual coast orientation	[^{0}]
	θ_e	equilibrium angle for which $Q_s(\theta)$ is zero	[^{0}]
	c_1, c_2	coefficients, determined from the $Q_s(\theta)$ function	[-]

For each combination of wave-and current a 'one-wave' approximation is made by Equation(C.2).

$$Q_s = c_{1i} \cdot \frac{90}{\pi \sin\theta_n} + c_{2i}\sqrt{\cos\theta_n} \quad \text{(C.2)}$$

In which:			
	θ_n	wave normal (resultant of θ-θ_w)	[^{0}]
	θ_w	the wave angle with respect to the coastal normal	[^{0}]

C.2.2.2 Wave- and current scenario

The wave scenario is defined by a sequence of wave conditions. The current scenario is defined by a sequence of flow conditions.

Wave scenario input:
- Significant wave height
- Water level
- Peak period
- Wave angle with respect to the North
- Duration

Current scenario input:
- Tidal surge
- Tidal flow velocity
- Reference depth
- Percentage of duration

Each condition from the wave scenario is combined with all the conditions in the current scenario. The wave conditions are used as boundary condition at the sea boundary of a cross-shore profile defined along the normal of a coast section. The current conditions are translated via a Chézy-relation to a surface slope term in the longshore velocity equation.

C.2.2.3 Cross-shore profile

A cross-shore profile is defined by a sequence of bottom heights. It is divided in two parts: The static part (outside the transport zone) and a dynamic part. The dynamic part is supposed to rotate in the same way as the coastline. A point within the dynamic area can be selected to cut-off the area in which sediment transport takes place (by setting the truncation transport within the dynamic area).

C.2.2.4 Global and local transport

The global transports define transport properties at each x-gridpoint along the model axis (transport rays). Additional conditions (e.g. a groyne) often involve the description of local transports.

C.2.3 Boundary condition

The boundary conditions describe the model behaviour at the two model boundaries in terms of the coastline position y, the transports Q_s, or the coast angle. There are three options:

- The coastline position remains constant
- The coastal angle remains constant
- The transport is a user-defined constant value or function of time

C.3 Mathematical description

C.3.1 Wave propagation and breaking model

The wave propagation and breaking model is used in the LT-module to use for the sediment transport computations. The wave propagation and decay and the wave induced cross-shore water level set-up are based on three basic equations.

The first basic equation is for the wave energy balance:

$$\frac{d}{dx}\left(C_g \cdot \cos\theta_n \cdot \frac{E}{\omega_r}\right) + \frac{D_b}{\omega_r} + \frac{D_f}{\omega_r} = 0 \qquad \text{(C.3)}$$

In which:			
	C_g	group velocity of waves	[m/s]
	θ_n	angle between wave direction and shore normal	[^{0})
	E	wave energy	[J/m^2]
	ω_r	relative wave peak frequency	[m^{-1}]
	D_b	dissipation of wave energy due to wave breaking	[W/m^2]
	D_f	dissipation of wave energy due to bottom friction	[W/m^2]

The second basic equation is for the wave-induced cross shore water level set-up and yields (C.4):

$$\frac{d}{dx}S_{xx} + \rho g\left(h_0 + \eta\right)\frac{d\eta}{dx} \qquad \text{(C.4)}$$

In which:			
	S_{xx}	cross-shore radiation stress component	[N/m]
	h_0	still water depth	[m]
	η	wave set up	[m]

The third basic equation is Snellius' law:

$$k\sin\left(\theta_n\right) = \text{constant} \qquad \text{(C.5)}$$

The wave energy per unit surface area is defined according to linear wave theory:

$$E = \frac{1}{8}\rho g H_{RMS}^2 \tag{C.6}$$

In which:			
	ρ	density of water	[kg/m^3]
	g	acceleration of gravity	[m/s^2]
	H_{RMS}	root mean square wave height	[m]

The relative wave peak frequency is defined as:

$$\omega_r = \omega - k \cdot \sin(\theta_n) \cdot V \tag{C.7}$$

In which:			
	ω	peak frequency	[m^{-1}]
	k	wave number	[m^{-1}]
	V	alongshore velocity (from basic equation from current)	[m/s]

The dissipation of wave energy due to wave breaking is defined as:

$$D_b = \frac{1}{4}\rho g \cdot \alpha_c \cdot Q_b \left(\frac{\omega_r}{2\pi}\right) \cdot H_m^2 \tag{C.8}$$

In which:			
	α_c	coefficient of wave breaking (*ALFA)*	[-]
	D_b	dissipation of wave energy due to wave breaking	[W/m2]
	Q_b	local fraction of breaking waves	[-]
	H_m	depth limited wave height	[m/s]

The local fraction of breaking waves is defined as:

$$\frac{1-Q_b}{-\ln Q_b} = \left(\frac{H_{RMS}}{H_m}\right)^2 \tag{C.9}$$

The depth limited wave height is defined as:

$$H_m = \frac{0.88}{k}\tanh\left(\frac{\gamma \cdot kd}{0.88}\right) \tag{C.10}$$

In which:			
	γ	coefficient of wave breaking (*GAMMA)*	[-]
	d	water depth (defined as: d = h_0+η-z)	[m]

The dissipation of wave energy due to bottom friction is defined as:

$$D_f = \frac{1}{8}\rho \cdot f_w \cdot \pi^{-\frac{1}{2}} \left(\frac{\omega_r H_{rms}}{\sinh(kd)}\right)^3 \tag{C.11}$$

In which:			
	f_w	coefficient for the bottom friction (*FW)*	[-]

With given boundary conditions of waves H_{rms}, T_p and θ_n, and wave parameters, the bottom profile z(x) and bottom related parameter, and the alongshore current distribution; the equation system can be solved.

S_{xx} is the radiation stress component in cross-shore direction and is defined as:

$$S_{xx} = E\left[n\left(1+\cos^2\theta_n\right) - 1/2\right] \tag{C.12}$$

In which: n group velocity/ wave propagation speed *(C_g/C)* [-]

C.3.2 Currents

The basic equation describing the longshore current distribution is the momentum equation alongshore and is presented in equation C.13.

$$\frac{d}{dx}S_{xy} + \rho g d \frac{dh_0}{dy} + \rho \frac{g}{C^2} V |V_{tot}| = 0 \qquad \text{(C.13)}$$

In which:
- S_{xy} longshore radiation stress component [N/m]
- V Alongshore current velocity [m/s]
- V_{tot} velocity function in shear stress term [m/s]
- C Chézy friction coefficient [$m^{1/2}/s$]

The longshore radiation stress component is defined as:

$$S_{xy} = S_{yx} = E \cdot n \cdot \cos\theta_n \cdot \sin\theta_n \qquad \text{(C.14)}$$

The velocity function in shear stress term is defined as:

$$V_{tot} = \sqrt{V^2 + U_{RMS}^2} \qquad \text{(C.15)}$$

In which: U_{RMS} amplitude of the wave orbital velocity based on linear wave theory and H_{RMS} [-]

The Chézy friction coefficient is defined as:

$$C = 18 \log\left(\frac{12d}{k_b}\right) \qquad \text{(C.16)}$$

In which: k_b bottom roughness *(KB)* [m]

The tidal surface slope alongshore dh_0/dy is implicitly defined by the tidal current velocity V_{tidal} at a reference depth d_{ref} as follows:

$$V_{tidal} = C\sqrt{d_{ref}\frac{dh_0}{dy}} \qquad \text{(C.17)}$$

With given boundary conditions of waves (H_{rms}, T_p and θ), the bottom profile z(x), and bottom related parameter, the equation system can be solved and the alongshore current distribution can be computed.

C.3.3 Sediment transport with the Bijker formula

The sediment transport along the cross-rays can be calculated by using one of the available formulae for sediment transport. For this thesis the Bijker (1971) method was selected, based on experience and reliability.

Bijker (1971) proposed a formula for bed load due to waves and currents, which was based upon the formula of Kalinske-Frijlink (1952) for bed load due to currents only. For that a formulation for the increase of the bottom shear stress by waves was developed. Afterwards Bijker added a distribution of the suspended load to the bed load, which was based upon the Einstein-Rouse concentration vertical.

$$S = S_b + S_s \tag{C.18}$$

In which:			
	S_b	bottom sediment transport	[m^3/m/s]
	S_s	suspended sediment transport	[m^3/m/s]

The formulation of S_b reads:

$$S_b = B \cdot D_{50} \cdot \frac{V}{C} g^{1/2} \exp\left(\frac{-0.27\Delta \cdot D_{50} \cdot C^2}{\mu \cdot \overline{\tau_{cw}}} \right) \tag{C.19}$$

In which:			
	B	coefficient deep (1) or shallow water (5)	[-)
	D_{50}	median grain diameter	[m]
	V	alongshore current velocity	[m/s]
	C	Chézy coefficient	[$m^{1/2}$/s]
	Δ	relative density, defined as: $(\rho_s-\rho)/\rho$	[-]
	μ	ripple factor, ratio of the grain roughness to the total roughness (defined as $(C/C_{90})^{3/2}$)	[-]
	-0.27	experimental coefficient	[-]
	$\overline{\tau_{cw}}$	bed shear stress due to waves and currents (time averaged)	[N/m^2]

$$\overline{\tau_{cw}} = V^2 \left(1 + \frac{1}{2} \left(\xi \frac{u_b}{V} \right)^2 \right) \tag{C.20}$$

u_b	Orbital velocity near the bottom	[m/s]
ξ	Bijker parameter: $C\sqrt{FW/2g}$	[-]
S_s	suspended sediment transport	[m^3/sm]

The coefficient for the wave related bottom roughness r_c defined as:

$$f_w = \exp\left[-5.977 + 5.213 \left(\frac{u_b}{\omega r_c} \right)^{-0.194} \right] \tag{C.21}$$

In which:			
	r_c	bottom roughness	[m]

The formulation of S_s reads:

$$S_s = 1.83 S_b \left[I_1 \ln(33d / r_c) + I_2 \right] \tag{C.22}$$

In which: I_1, I_2 Einstein Integrals

$$I_1 = R \int_{r_c/d}^{1} \left[(1-y)/y \right]^{z_*} dy \qquad \text{y=z/h} \qquad \text{(C.23)}$$

$$I_2 = R \int_{r_c/d}^{1} \ln y \left[(1-y)/y \right]^{z_*} dy \qquad \text{(C.24)}$$

$$R = \frac{0.216 \left(r_c/d \right)^{z_*-1}}{1 - \left(r_c/d \right)^{z_*}} \qquad \text{(C.25)}$$

$$z_* = w/(\kappa \cdot V_*) \qquad \kappa\text{; Von Karman constant} \qquad \text{(C.26)}$$

$$V_* = \frac{V}{C} \sqrt{g \cdot \left(1 + \frac{1}{2} \left(\xi \frac{u_b}{V} \right)^2 \right)} \qquad \text{(C.27)}$$

C.4 Wave diffraction scheme of Kamphuis (1992)

The wave diffraction is expressed in the diffraction coefficient K_d which is defined as:

$$K_d = H_d / H_i \qquad \text{(C.28)}$$

In which:			
	K_d	diffraction coefficient	[-]
	H_d	diffracted wave height	[m]
	H_i	incident wave height	[m]

The applied formulations for diffraction around a structure have been derived by Kamphuis (1992). The equations presented by Kamphuis are:

$$\begin{aligned} K_d &= 0.69 + 0.008\theta && \text{for } -90 \le \theta \le 0 \\ K_d &= 0.71 + 0.37 \sin(\theta) && \text{for } 0 \le \theta \le 40 \\ K_d &= 0.83 + 0.17 \sin(\theta) && \text{for } 40 \le \theta \le 90 \end{aligned} \qquad \text{(C.29)}$$

In which: θ angle between the point of interest and the diffraction point (α_d) and the incident wave direction (α_i) [^{0}]

C.5 Breaker Index

Wave breaking occurs due to two criteria, depth and wave steepness. While depth induced breaking is usually the determining factor in shallow water, the limit of steepness should

also be considered. The steepness criterion (Miche, 1944) is calculated for regular waves where the water is not deep with relation (C.30)

$$H / L \le \left[H / L\right]_{\max} = 0.14 \tanh(2\pi h / L) \qquad \text{(C.30)}$$

The breaking criterion due to the water depth is given by a non-dimensional parameter called the breaker index (γ_{br}), defined as the maximum wave height to depth ration (H/h) limited to depth:

$$H / h \le \left[H / h\right]_{\max} = \gamma_{br} \qquad \text{(C.31)}$$

The breaking parameter has values for regular waves ranging between 0.5 and 1.5. While for irregular waves typical values are found to be 0.5-0.6.

Design curves for the combined effect of wave shoaling and wave breaking, obtained from an energy based wave model (ENDEC) presents Equation (C.32)

$$\gamma_{br} = 0.5 + 0.4 \tanh(33 \cdot s_0) \qquad \text{(C.32)}$$

In which: γ_{br} Breaking parameter [-]

s_0 deep water wave steepness: $H \Big/ \left(gT^2 \Big/ 2\pi \right)$ [-]

The UNIBEST manual presents relations for wave breaking as a function of the steepness (Table C.1).

H_{rms}/λ	**0**	**0.01**	**0.02**	**0.03**	**0.04**
γ	0.5	0.63	0.73	0.81	0.85

Table C-1 Relation for wave breaking (UNIBEST Manual, 1994)

If we assume the waves to be Rayleigh distributed then relation (C.33) holds.

$$H_s \approx \sqrt{2} H_{RMS} \qquad \text{(C.33)}$$

For both wave climates the breaker index is calculated and presented in Table C.2.

	DM	**WW**
ENDEC (D.4)	0.67	0.68
UNIBEST	(-)	0.63

Table C-2 Results for breaker index

D Appendix UNIBEST-TC

D.1 Introduction

This appendix is derived from the UNIBEST-TC manual (WL| Delft Hydraulics, 2000). It describes how the model computes bottom changes in a cross-shore profile.

D.2 General set-up of UNIBEST-TC

UNIBEST-TC (Time-dependent Cross-shore) is the cross-shore sediment transport module of the UNIBEST Coastal Software package. It is designed to compute cross-shore sediment transport and the resulting profile changes along a coastal profile under the combined action of waves, longshore tidal currents and wind.

The UNIBEST-TC model consists of five sub-models:

- Wave propagation model (Appendix D.3.1)
- Mean current profile model (Appendix D.3.2)
- Wave orbital velocity model (Appendix D.3.3)
- Bed load and suspended load transport model (Appendix D.3.4)
- Bed level change model (Appendix D.3.5)

A schematic representation of the various sub-models is given in Figure D.1.

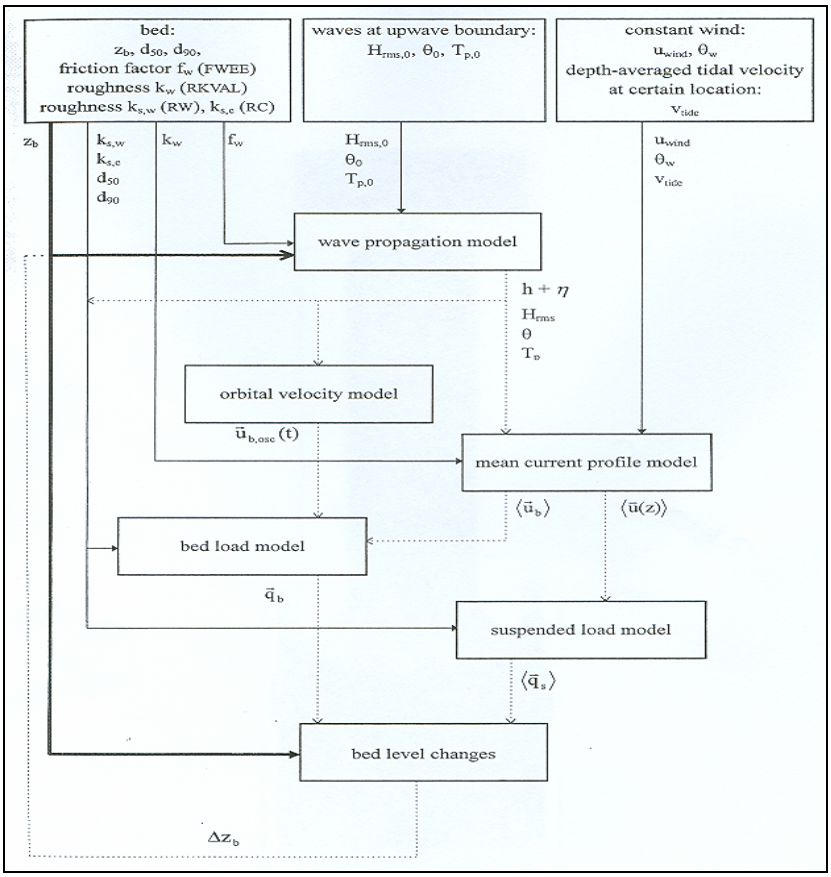

Figure D-1 Overview of UNIBEST-TC sub models (Source: UNIBEST-TC; overview of model formulations, 2000)

D.3 Model formulations

D.3.1 Wave model

The wave model computes the wave energy decay along a cross-ray including effects of shoaling, refraction and energy dissipation. The model consists of three first-order differential equations. The time-averaged wave energy balance (Battjes and Janssen, 1978), the balance equation for the energy contained in surface rollers in breaking waves (Nairn et al.,1990) and the horizontal momentum balance from which the mean water level set-up is computed. The refraction of the waves is computed using Snellius' law. These three coupled equations are solved by numerical integration over the cross-shore profile.

These equations generate the input required by the local models for the vertical velocity profile, the concentration vertical and the bed-load transport.

The energy balance equation for organised wave energy '*E*' is the same as used in the UNIBEST-CL+ model (Equation C.3 to C.11).

The balance equation for the energy contained in surface rollers in breaking waves reads:

$$\frac{\delta}{\delta x} 2E_r \cdot C \cdot \cos(\theta) = D_W - DISS;\ E_r = \frac{1}{2}\rho \cdot C^2 \cdot \frac{A}{L};\ DISS = 2\beta g \frac{E_r}{C} \quad \text{(D.1)}$$

In which:			
	2	factor from additional dissipation of roller energy due to a net transfer of water from the wave to the roller	[-]
	E_r	roller energy	[J/m^2]
	C	wave propagation speed	[m/s]
	DW	dissipation of organised wave energy	[W/m^2]
	$DISS$	Dissipation of roller energy	[W/m^2]
	β	Slope of the face of the wave (BETD)	[-]
	A	Area of the roller	[m]
	L	Length of the roller	[m]

The third differential equation is the cross-shore momentum equation, which reads:

$$\frac{\delta\eta}{\delta x} = -\frac{1}{\rho g h} \cdot \frac{\delta S_{xx}}{\delta x}, \text{ with } S_{xx} = ((n + n\cos^2\theta - 0.5)E + 2E_r \cos^2\theta) \quad \text{(D.2)}$$

In which:			
	η	mean wave set up, $h=\eta-z_b$	[-]
	x	position along the profile	[-]
	S_{xx}	cross-shore radiation stress	[-]
	n	group velocity/ wave propagation speed (C_g/C)	[-]

In order to solve the system for the three unknown, E, E_r and η boundary conditions for H_{RMS}, T_p, and θ at the upwave boundary and a given bottom height z_b are needed.

D.3.2 Mean current profile model

The mean current profile model computes the vertical distribution of the wave-avaraged mean current in both longshore and cross-shore direction, accounting for the vertical non-uniform driving forces: wind shear stress, wave breaking, bottom dissipation in the wave boundary layer and the slope of the free surface due to a longshore (tidal) current.

In order to calculate this velocity distribution, the horizontal momentum balance needs to be solved. This is done using a quasi 3-D model which consists of three layers (De Vriend, Stive, 1987):

- The surface or trough-to-crest layer, which is represented by boundary conditions on the middle layer
- The middle layer, from top of the bottom (wave) boundary layer to the mean water level
- The bottom boundary layer

The total shear stress can be calculated by integrating a momentum balance of the following form:

$$\frac{\partial \tau_i}{\partial \sigma} = R_i \quad \text{, for } \sigma > \delta \quad \text{(D.3)}$$

$$\frac{\partial \tau_i}{\partial \sigma} = R_i + \frac{\partial}{\partial \sigma}\left(\rho \tilde{u}_i \tilde{w}\right) \quad \text{, for } \sigma < \delta \tag{D.4}$$

In which:			
	τ_i	horizontal shear stress	[N/m^2]
	σ	dimensionless depth (z/h)	[-]
	R_i	pressure gradient forcing, assumed to be depth independent	[N/m^2]
	$\tilde{u}_i \tilde{w}$	oscillating velocity components in i-direction and vertical direction respectively	[m/s]
	δ	thickness of the wave boundary layer	[-]
	i	i-direction with i = x or y	[-]

The non-dimensional thickness of the wave boundary layer reads:

$$\delta = 0.09\alpha\left(\frac{A}{k_s}\right)^{0.82}\frac{k_s}{h}, \quad \text{with } \delta_{max} = 0.5 \text{ and } \delta_{min} = \alpha\frac{ez_0}{h} \quad , z_0 = k_s/33 \tag{D.5}$$

In which:			
	A	wave orbital excursion parameter	[-]
	α	factor for irregular waves *(ALFAC)*	[-]
	k_s	user defined roughness height *(RKVAL*	[m]

Integrating of Equation D-3 and D-4 from the surface downwards leads to:

$$\tau_i = \tau_{s,i} - R_i(1-\sigma) \quad \text{,for } \sigma > \delta \tag{D.6}$$

$$\tau_i = \tau_{s,i} - R_i(1-\sigma) + \frac{D_f k_i}{\omega}\frac{\delta-\sigma}{\delta} \quad \text{, for } \sigma < \delta \tag{D.7}$$

In which:			
	$\tau_{s,i}$	surface shear stress applied at MSL, which account for wind stress and shear stress by the dissipation in the surface rollers	[N/m^2]
	k_i	wave number in i-direction	[m^{-1}]
	D_f	dissipation due to bottom friction	[W/m^2]

The formulation of the dissipation due to bottom friction is computed as:

$$D_f = \frac{1}{2\sqrt{\pi}}\rho f_w u_{orb}^3 \quad \text{,with } f_w = 1.39\left(\frac{A}{z_0}\right)^{-0.52} \text{ and } f_{w,max} = 0.3 \tag{D.8}$$

In which:			
	f_w	friction factor	[-]
	u_{orb}	orbital velocity near the bed	[m/s]

The shear stress is related to the velocity gradients by:

$$\tau_i = \frac{\rho \nu_t}{h}\frac{\partial u_i}{\partial \sigma} \tag{D.9}$$

In which:			
	υ_t	eddy viscosity	[-]

The vertical structure of the eddy viscosity is calculated separately for the middle and the bottom layer. It is written as the product of the depth-averaged viscosity and a parabolic shape function. The depth-averaged viscosity is defined as the root-mean-square of the depth-averaged viscosity contributions due to braking, wind and the slope-driven current. In the boundary layer, the eddy velocity is increased to account for the increased turbulence due to the wave orbital motion.

Integrating Equation C-9 gives an expression for the vertical velocity profile as a function of the eddy viscosity. Integrating once more gives the depth-mean velocity in x- and y-direction as a function of the forcing: wind shear stress, the roller shear stress, the streaming function and the depth-independent pressure gradient.

The depth mean velocity in x-direction follows from the mass flux in the surface layer:

$$\overline{u_x} = -\frac{q_{drift,x}}{h} = -\frac{q_{drift}\cos(\theta)}{h} \qquad \text{with } q_{drift} = q_{non-breaking} + q_{roller} = \frac{E + 2E_r}{c} \tag{D.10}$$

The depth independent pressure gradient in y-direction R_Y follows from the Chézy equation:

$$V = C\sqrt{h\frac{\partial h}{\partial y}} \qquad \text{with } C = 18\log\left(\frac{12h}{k_b}\right) \tag{D.11}$$

In which:

	V	(tidal) velocity at a reference depth	[m/s]
	k_b	roughness height (RKVAL)	[m]

The remaining unknowns are the depth-mean velocity in y-direction and the pressure gradient R_x in x-direction. These values depend on the depth-averaged velocity, which itself depends on R_x (via the slope-driven current). Therefore an iterative procedure is followed to solve the equations, leading to a solution for the depth-mean current and the current profile in x- and y-direction.

D.3.3 Near-bed orbital velocity model

The near –bed velocity computes the time-variation of the near bed velocity (orbital motion) due to non-linear short and long waves related to wave groups. Starting point is a time series in the case of regular waves, based on Rienecker and Fenton (1981).

$$U_1(t) = \sum_{j=1}^{n} B_j \cos(j\omega t) \tag{D.12}$$

In which:

	Bj	amplitudes numerically determined such that the difference between the min and max velocity of the asymmetric waves equals the difference in case of monochromatic waves	[-]
	U_1	near bed velocity	[-]

Next step is to add a second velocity time series which is slightly out of phase with the first, the amplitude modulation on the time scale of a wave group is introduced yielding a time series $U_2(t)$:

$$U_2(t) = \sum_{j=1}^{n} B_j \cos(j\omega t)[0.5(1+\cos(\Delta t))]^j \tag{D.13}$$

In which:

	$\Delta\omega$	= ω/m, m being the number of waves in one wave group (default is 7)	[-]
	U_1	near bed velocity	[-]

The magnitude of U_2 is corrected to U'_2 in such a way that the third moment of U'_2 equals the third moment of U_1.

$$U_t^{'}(t) = \left[\frac{\frac{1}{T}\int_0^T U_1^3 dt}{\frac{1}{mT}\int_0^{mT} U_2^3 dt} \right]^{1/3} U_2(t) \qquad \text{(D.14)}$$

In which: T wave period [s]

The long wave velocity is computed according to Roelvink and Stive (1989) who assume that the wave train with equal features of a random wave field may be represented by a bichromatic wave train with equal amplitudes a_m and a_n, and a accompanying bound long wave with amplitude ξ_a and reads:

$$U_3(t) = \zeta_a \frac{\sqrt{gh}}{h} \cos(\frac{\omega}{m} t + \varphi), \text{ with } \zeta_a = -G_{nm} \frac{a_n a_m}{h} \text{ and}$$
$$\mathrm{m}_0 = \frac{1}{8} H_{rms}^2 = \tfrac{1}{2} a_n^2 + \tfrac{1}{2} a_m^2 + \tfrac{1}{2} \zeta_a^2 \qquad \text{(D.15)}$$

In which:

ξ_a	long wave amplitude	[m]
φ	phase shift	[rad]
G_{nm}	transfer function according to Sand (1982)	[-]
a_m, a_n,	amplitudes of the bichromatic wave train	[m]
m_0	total surface variance	[m^2]

The phase shift is calculated according to Roelvink and Stive (1989) by:

$$\cos(\varphi) = C_r \left[1 - 2 \left(\frac{H_{rms}}{H_{rms,0}} \right)^2 \right] \qquad \text{(D.16)}$$

In which:

C_r	a correlation coefficient (C_R)	[-]
$H_{rms,0}$	the incoming wave height at the seaward boundary	[m]

Final step is the computations of the times series $U_4(t)$ of the total orbital velocity, by simply adding the effects due to the short-wave envelope and the bound long wave:

$$U_4 = U_2^{'}(t) + U_3(t) \qquad \text{(D.17)}$$

D.3.4 Bed load transport and suspended load model

Bed load transport formulation

The net bed-load transport rate in conditions with uniform bed material is obtained by time-averaging (over the wave period T) of the instantaneous transport rate using the bed-load transport model (quasi-steady approach), as follows:

$$q_b = \left(\frac{1}{T}\right)\int q_{b,t}\,dt \qquad \text{(D.18)}$$

In which: $q_{b,t}$ F(instantaneous hydrodynamic and sediment transport parameters). [m^3/m/s]

The formula applied, reads as:

$$q_{b,t} = 0.5\rho_s d_{50} D_*^{-0.3}\left(\frac{\tau'_{b,cw,t}}{\rho}\right)^{0.5}\left(\frac{\max\left(0,\tau'_{b,cw,t}-\tau_{b,cr}\right)}{\tau_{b,cr}}\right) \qquad \text{(D.19)}$$

In which:

$\tau'_{b,cw,t}$	instantaneous grain-related bed-shear stress due to both current and wave motion = 0.5 ρ f'_{cw} $(U_{\delta,cw,t})^2$	[N/m^2]
$U_{\delta,cw,t}$	instantaneous velocity due to current and wave motion at reference height *a*	[m/s]
f'_c	current-related grain friction coefficient =0.24$(\log(12h/k_{s,grain}))^{-2}$	[-]
f'_w	wave-related grain friction coefficient=Exp[-6+5.2$(A_\delta/k_{s,grain})^{-0.19}$],	[-]
$\hat{U}_\delta$	the peak orbital velocity, v_R is the equivalent current velocity calculated at reference height *a*	[m/s]
β_f	coefficient related to vertical structure of velocity profile	[-]
A_δ	peak orbital excursion	[m]
$\tau_{b,cr}$	critical bed-shear stress according to Shields,	[N/m^2]

The two most influential parameters of Eq. (D.19) are: f'_{cw} and $k_{s,grain}$. Various field data sets from the literature and new data sets (laboratory and field) collected within the SANDPIT project have been used to verify/improve these parameters of the bed-load transport formulations (see Van Rijn and Walstra, 2003).

Based on the findings of Van Rijn and Walstra (2003), the following expressions have been implemented:

$$f'_{cw} = \alpha^{0.5}\beta_f f'_c + \left(1-\alpha^{0.5}\right) f'_w \qquad \text{(D.20)}$$

$$k_{s,grain} = d_{90} \qquad \text{(D.21)}$$

Suspended load transport formulation

The wave-related suspended transport component is modelled as follows:

$$q_{s,w} = \gamma\left(\frac{U^4_{\delta,for}-U^4_{\delta,back}}{U^3_{\delta,for}+U^3_{\delta,back}}+u_\delta\right)\int c\,dz \qquad \text{(D.22)}$$

In which:	$U_{\delta,for}$	near-bed peak orbital velocity in onshore direction (in wave direction)	[m/s]
	$U_{\delta,back}$	near-bed peak orbital velocity in offshore direction (against wave direction)	[m/s]
	u_δ	wave-induced streaming velocity near the bed	[m/s]
	γ	phase lag function (0.2)	[-]

The mixing coefficient near the bed is modelled as:

$$\varepsilon_{w,bed} = 0.018\beta_w \delta_s U_{\delta,r} \tag{D.23}$$

The reference level is described by:

$$a = \min\left(0.2h, \max\left(0.5k_{s,c,r}, 0.5\,k_{s,w,r}, 0.01\right)\right) \tag{D.24}$$

In which:	$k_{s,c,r}$	current-related bed roughness height due to small-scale ripples	[m]
	$k_{s,w,r}$	wave-related bed roughness height due to small-scale ripples	[m]

The reference concentration (single fraction approach) is described by:

$$c_a = 0.015\,\rho_s \frac{d_{50}\left(T_a\right)^{1.5}}{a\left(D_*\right)^{0.3}} \quad with\ c_{a,MAX} = 0.05\rho_s$$

D.3.5 Bed level change model

The bed level changes are computed from the depth-averaged mass balance that reads:

$$\frac{\partial z}{\partial t} + \frac{\partial q_{bot+sus}}{\partial x} = 0 \tag{D.25}$$

It is possible to introduce a longshore gradient in this equation leading to:

$$\begin{aligned} &\frac{\partial z}{\partial t} + \frac{\partial q_{bot+sus}}{\partial x} + FL\_POS \cdot q_y = 0 \qquad \text{for } q_y > 0 \\ &\frac{\partial z}{\partial t} + \frac{\partial q_{bot+sus}}{\partial x} + FL\_MIN \cdot q_y = 0 \qquad \text{for } q_y < 0 \end{aligned} \tag{D.26}$$

In which:	q_{ya}	longshore transport rate	[-]
	FL_POS	coefficient to introduce longshore transport gradient	[m^{-1}]
	FL_MIN	coefficient to introduce longshore transport gradient	[m^{-1}]

Approaching the water line the calculations stop when the water becomes shallow. This depth is calculated from the user-defined relative wave period:

$$T^* = T_p\sqrt{g/h} \tag{D.27}$$

In which:	T^*	relative wave period (TDRY)	[m^3/m/s]
	T_p	peak wave period	[m^{-1}]

Landward of the depth calculated with this equation the sediment transport is interpolated over the profile. The cross-shore sediment transport q_{tot} varies linearly between the last calculation point and the user defined transport (USTRA) as the most landward point.